INLAND WATERS BRANCH

Theoretical Analysis of Regional Groundwater Flow

R. A. FREEZE

SCIENTIFIC SERIES No. 3

DEPARTMENT OF ENERGY,
MINES AND RESOURCES

THEORETICAL ANALYSIS OF REGIONAL GROUNDWATER FLOW

SCIENTIFIC SERIES No. 3

Theoretical Analysis of Regional Groundwater Flow

R. A. FREEZE

INLAND WATERS BRANCH
DEPARTMENT OF ENERGY, MINES AND RESOURCES
OTTAWA, CANADA

Cat. No.: M26-502/3

Contents

Contents (cont'd)

Illustrations

Acknowledgments

The helpful suggestions and prodding encouragement of Professor P.A. Witherspoon of the University of California at Berkeley contributed significantly to the success of this study. The author is particularly indebted to Professor Witherspoon for his initial suggestion pointing out the potential power of the mathematical model method and the use of the high-speed digital computer in the solution of hydrogeological problems.

The author also received guidance and encouragement from Joe Tóth of the Alberta Research Council, and Peter Meyboom of the Geological Survey of Canada (now with Hydrological Sciences Division of the Inland Waters Branch).

The author would like to express his gratitude to the staff of the University of California Computer Center, whose efficiency made possible the large number of computer runs necessary in a study such as this.

This work was carried out while on educational leave from the Geological Survey of Canada and the author would like to thank G.S.C. for this opportunity to undertake graduate research.

Abstract

A mathematical model representing steady-state regional groundwater flow in a three-dimensional, non-homogeneous, anisotropic groundwater basin is developed. Two independent methods of solution are presented: the analytical separation of variables technique is used to solve the two-dimensional, three-layer case; the numerical finite-difference approach is used to solve the general case. The numerical method is more versatile, mathematically simpler, and well-suited to computer-oriented methods of data storage. Computer programs have been written for both methods; the output consists of plotted potential nets from which flow patterns can be constructed.

The potential patterns for over 70 hypothetical cases are presented to illustrate the qualitative and quantitative control exerted on the flow system by:

(a) the "depth/lateral extent" ratio of the ground-water basin.

(b) the configuration of the water table.

(c) the geologic configuration and resultant permeability contrasts.

The concept of "natural basin yield" is introduced.

The mathematical model approach using numerical solutions and the digital computer can be used both as a reconnaissance tool preceding field investigation and as an interpretive tool following the field program. The results of mathematical model analyses on two actual groundwater basins in the Canadian prairies are presented.

CHAPTER 1

Introduction

PREVIOUS WORK; MOTIVATION AND OBJECTIVES OF PRESENT STUDY

In 1940, M. King Hubbert published his classic paper "The Theory of Ground-Water Motion". In this paper the physical laws governing the *steady-state* flow of groundwater were presented for the first time in their exact mathematical framework. At the same time a parallel course, in which formal mathematics was used to describe and predict *transient* hydrological phenomena, was being followed by many other hydrologists and applied mathematicians. The fundamental difference between the two approaches, apart from the time factor, was one of scale; while Hubbert concerned himself mainly with the large-scale regional effects of his theory, workers in the transient field used the individual well as their unit of study. The immediate applicability of the latter studies in the determination of local aquifer conditions resulted in a preoccupation with the well and well field throughout the period 1935-1960 and led to the mathematical solution of almost all the meaningful problems in well hydraulics.

In the 1960's, attention has again turned to the regional picture and the groundwater basin has been re-established as an acceptable unit of hydrological study. The first significant additions to Hubbert's original work were published in 1962 and 1963 by J. Tóth. The most important contribution of these two papers is the basic concept that exact groundwater flow patterns can be obtained mathematically as solutions to formal boundary value problems. This method offers a theoretical approach to complement the usual field techniques.

Tóth's papers also opened the investigation of the factors affecting regional groundwater flow systems. Tóth considered the case of a two-dimensional section through a homogeneous basin and developed the flow patterns resulting from two separate water-table configurations. While the method used by Tóth is reasonably general, the actual formulae and quantitative results are restricted to the specific cases considered.

The literature of the soil physics and land drainage fields provides another source of background material. The works of Luthin and Day (1955), Luthin (1957), Kirkham (1958), and Wesseling (1964) provide a source of solutions to flow problems similar to those considered in this study. As with Tóth's work, the solutions are limited to homogeneous media and apply only to the specific cases treated.

The desire to extend the available solutions to more general cases provided the primary motivation for the present study. In addition, there is the obvious need to continue the investigation of the factors controlling groundwater flow systems.

The two objectives of this study can therefore be stated:

1. To develop a suitable mathematical model such that theoretical solutions can be obtained, in the form of flow patterns for a general three-dimensional non-homogeneous groundwater basin with any water-table configuration.
2. To investigate, using the mathematical model, the qualitative and quantitative effects of the configuration of the water table and the underlying geological configuration on the groundwater flow system.

The practical significance of such a study is confirmed by a statement from the initial News Bulletin of the Canadian National Committee of the International Hydrologic Decade: "The problem of finding water for man's needs is not a new one. What is new is the magnitude and extent of the accelerating demand. A question urgently requiring an answer is therefore: Is sufficient known about

the processes associated with fresh water resources of the inhabited or inhabitable parts of the world to determine if these resources are adequate to meet the growing demand? "

Apart from the obvious application to basin-wide development of groundwater resources, an understanding of the regional groundwater flow regime is prerequisite to the undertaking of many engineering projects, among them underground nuclear waste disposal and the impounding of a reservoir behind a large dam.

The development of a suitable model led the author down two separate mathematical paths: first, toward the formal analytical methods used by Tóth; and second, toward a more powerful method using numerical solutions.

Numerical methods were introduced to the groundwater hydrology literature by Stallman (1956) for the analysis of regional water levels. Fayers and Sheldon (1962) and Tyson and Weber (1964) were the first to employ numerical solutions in connection with mathematical models of groundwater basins and aquifers. In the land drainage field, Luthin and Gaskell (1950) and Kirkham and Gaskell (1951) used numerical solutions to assist in design. Shaw and Southwell (1941) have described a numerical procedure for deriving flow nets for seepage through earth dams. The general use of mathematical models using a digital computer has been recommended by many authors, notably Walton (1962).

A number of texts proved so valuable in the development of this work, and the fundamental concepts they contain are so intertwined with the new aspects of this study that further individual reference to them throughout the text is practically impossible. For the development of the mathematics involved in the analytical solutions, reference was made to Wylie (1960), Sneddon (1957), Sokolnikoff and Redheffer (1958), Byerly (1959), Kellogg (1953), Carslaw and Jaeger (1959), and Moon and Spencer (1961). For the special application of such solutions to hydrological settings, Muskat (1946), Luthin (1957), Scheidegger (1960), and Polubarinova Kochina (1962) proved valuable.

Of the many available texts on numerical analysis, Forsythe and Wasow (1960), and McCracken and Dorn (1964) proved most useful. Others of note are Ralston and Wilf (1960), Salvadori and Baron (1961), Todd, J. (1962), Thom and Appelt (1961), and Panov (1963). Todd, D.K. (1959), and Harr (1962) were used as general references for groundwater hydrology.

An abridged version of this study is published in a series of three papers in Water Resources Research (Freeze and Witherspoon, 1966, Freeze and Witherspoon, 1967, Freeze and Witherspoon, 1968). The papers emphasize the mathematical development of the method and present the essential qualitative and quantitative interpretations.

DEFINITIONS

Throughout the literature of groundwater hydrology, the terminology tends to be inconsistent. It is necessary therefore, to define the author's concept of some of the terms which appear in this study.

Recharge refers to that water which percolates down through the unsaturated zone to the water-table and actually enters the dynamic groundwater flow system. This definition excludes that portion of the moisture surplus which enters the ground and increases the soil moisture content, but does not enter the flow pattern itself. The term is not to be confused with the actual areal precipitation which may, in some cases or some areas of the basin, lead to groundwater recharge and in other cases or in other areas may not.

Discharge is that water which is discharged from the dynamic groundwater flow system by means of stream baseflow, springs, seepage areas, and evapotranspiration.

A *discharge area* is an area where the direction of groundwater flow is toward the water table.

A *recharge area* is an area where the direction of groundwater flow is away from or parallel to the water table.

A *groundwater basin* is a three-dimensional, closed system which contains the entire flow paths followed by all the water recharging the basin. The flow pattern within a given basin may be simple

involving only one recharge area and one discharge area, or complex involving many.

These definitions do not deny the existence of groundwater "recharge" to a "discharge area". Water which percolates down to the saturated zone in a discharge area will encounter upward rising groundwater, and the "dynamic groundwater flow pattern" that such water will enter is one of upward motion. The result of the recharge must therefore be a rise in the water table, and the only possible route which such water can subsequently follow is the return to the surface via one of the agents of discharge, when conditions permit. In a recharge area, on the other hand, a certain amount of recharge is required just to maintain the water table. In periods of no recharge, the water table will fall. Any water which does enter the dynamic flow system in a recharge area will be transmitted away from its point of entry along some flow path within the groundwater basin toward an area of discharge.

The use of the term "water table" can lead to confusion. In this report the water table is considered to be an imaginary surface beneath the surface of the ground at which the pressure is atmospheric. The water table does not coincide with the surface separating the zone of saturation from the unsaturated zone. Such a surface, sometimes known as the air-water interface, will occur at the top of the zone of capillary saturation, somewhat above the water table. As has been shown by Hubbert (1940), the "conception of the water table as a surface of discontinuity between a zone of saturation and a capillary fringe having fundamentally different physical characteristics is a misleading fiction . . . . . The equipotential surfaces cross this isobaric surface without interruption and extend to the air-water interface. . . . . The fluid flow obeys precisely the same laws in the region where $p < 1$ atmosphere as in that characterized by $p > 1$ atmosphere". To be entirely rigorous, therefore, one should consider the air-water interface as the upper boundary of the flow system. There are advantages, however, in the construction of the mathematical model, to considering the water table, i.e., the surface where $p = 1$ atmosphere, as the upper boundary of flow, and in this study, as in Tóth (1962, 1963b,c), this slight inaccuracy has been allowed. This point is discussed further under the heading "Assumptions of Study".

In the construction of a regional groundwater flow net, should one consider the upper boundary of the system (in our case, the water table) as a flow line or as an equipotential? It is neither. Considering a groundwater basin as a three-dimensional closed system, if the water table were a flow line, all the percolating water attempting to enter the flow system would be transmitted down the flow line along the water table. This single flow line would thus carry increasing quantities of water from the groundwater divide to the sink and no alternative routes would be possible, as a single flow line cannot split. The assumption of the water table as a flow line would thus preclude the existence of any three-dimensional flow system.

The suggestion that the water table is an equipotential line is equally invalid, for in this case, groundwater flow would have to be perpendicularly toward or perpendicularly away from the water table. As we know that both situations exist within a single groundwater basin and as it is obvious that this cannot be true if the water table has a single potential value, this concept is also incorrect.

On review it can be seen that the definition of the water table has an *equipressure* (isobaric) line does not infer it to be an *equipotential* line. This will be clarified after the introduction of the concept of hydraulic potential.

The misconception that the water table is a flow line has probably arisen from the considerable body of work on seepage through earth dams. Here, the assumption that there will be no "recharge" from above through the dam to the "water table" within the dam is a realistic assumption and such a "water table" is indeed a flow line. The water table on a regional scale, however, is much more analogous to the seepage face which may occur at the lower end of an earth dam. The seepage face is in fact a situation identical to a regional water table in a discharge area.

To complete this argument, suffice it to say that, in general, one would expect both flow lines and equipotentials to meet the water table obliquely. The water table becomes a flow line only in regions where there is no groundwater recharge from above and lateral flow exists, and it becomes an equipotential only when the groundwater motion is perpendicular to it, as is often the case in the region around a groundwater divide or where wide flat valley sinks exist.

BASIS OF MATHEMATICAL MODEL

Hydraulic Potential

The existence of a three-dimensional groundwater flow system implies the existence of a corresponding three-dimensional potential field. A field, by definition, is a region, at every point of which there corresponds a value of a physical quantity. The field in this case is the groundwater basin. The physical quantity, "which must be capable of measurement at every point in the field and whose properties must be such that the flow always occurs from regions in which the quantity has higher values to those in which it has lower, regardless of the direction in space" (Hubbert, 1940), is the hydraulic potential. Hubbert (1940) has shown that the hydraulic potential can be obtained as a generalization of the Bernoulli theorem relating the elevation, pressure and velocity along a given flow line of a fluid in frictionless flow. In groundwater flow, the velocity term is negligible and the hydraulic potential is the sum of the gravitational and pressure potentials. It can be written:

$$(1.1) \quad \Phi = gz + \int_{p_o}^{p} \frac{dp}{\rho}$$

For liquids, this reduces to:

$$(1.2) \quad \Phi = gz + \frac{p - p_o}{\rho}$$

where:

Φ = hydraulic potential at any point P in the field.
g = acceleration due to gravity.
z = elevation of P above a standard horizontal datum.
p = pressure at the point P.
p_o = atmospheric pressure
ρ = density of water.

If a piezometer is placed at point P, the liquid will rise to a height h above the standard datum. Applying the identity:

$$(1.3) \quad p = \rho g(h-z) + p_o$$

to equation (1.2):

$$(1.4) \quad \Phi = gz + \frac{[\rho g(h - z) + p_o] - p_o}{\rho} = gh$$

The magnitude of the fluid potential is thus indicated by the height h of the piezometer and is numerically equal to h multiplied by the acceleration due to gravity.

Considering (1.1), we see that the potential of a fluid at point P is the work required to transmit a unit of mass of the fluid from zero elevation and a pressure of 1 atmosphere to point P at elevation z and pressure p. The units of hydraulic potential in the dynamical c.g.s. system are ergs/gm; in the gravitational c.g.s. system, gm/cm/gm. Hubbert (1940) has noted that the hydraulic potential is a force potential.

The quantity $h = \frac{\phi}{g}$ is known as the hydraulic head. It is measured in units of centimeters of water or feet of water above standard datum. As the hydraulic head equals the hydraulic potential divided by a constant, it too is a potential quantity and will consequently obey all the laws of potential theory. Since it is measured in units which are simple and which have geometrical significance in regional groundwater flow, the hydraulic head will be used as the potential function throughout this study. For this reason, the hydraulic head is denoted from this point on by ϕ, a Greek letter commonly used for quantities having the properties of potential functions. We note that:

$$(1.5) \quad \phi = h$$

where:

ϕ = hydraulic head at point P, a potential function
h = elevation above standard datum of the liquid level in a piezometer inserted at P.

Returning to our discussion of the previous section, it is now clear, by reference to (1.2), that an isobaric line is not an equipotential.

Darcy's Law

Having defined the hydraulic potential and the hydraulic head we can proceed to state Darcy's law for the flow of water through a porous medium. For flow in the x-direction of an x,y,z coordinate system in a homogeneous medium, Darcy's law states:

$$(1.6)\quad v_x = K \frac{\delta \phi}{\delta x}$$

where:

v_x = velocity in the x-direction
K = permeability
ϕ = hydraulic head

Similar expressions can be written for flow in the other two coordinate directions.

Throughout this study, the viscosity and temperature of groundwater are assumed to remain constant so that the coefficient of permeability is a function of the medium alone. The permeability can be measured in velocity units (ft/min,cm/sec) or as the rate of flow through a cross-sectional area (gpm/ft^2).

For non-homogeneous media where the permeability varies continuously with the space variables, the permeability must be written K(x,y,z). For anisotropic media, the permeability is no longer a scalar but becomes a second order symmetric tensor.

For further discussion of Darcy's law and the permeability tensor, the reader is directed to Scheidegger (1960, 1963), Liakopoulos (1965) and Fayers and Sheldon (1962).

Equation of Continuity

The law of conservation of matter is expressed by the equation of continuity which, for fluid flow through a porous media, takes the form (Muskat, 1946):

$$(1.7)\quad \frac{\delta(\rho v_x)}{\delta x} + \frac{\delta(\rho v_y)}{\delta y} + \frac{\delta(\rho v_z)}{\delta z} = -f \frac{\delta \rho}{\delta t}$$

where:

v_x, v_y, v_z = velocities in the three coordinate directions
ρ = density of water
f = porosity of porous medium
t = time

At any given time, ρ is assumed to be constant with respect to the space variables and we can remove it from within the partial derivatives. Transposing it to the right-hand side, we are left with:

$$(1.8)\quad \frac{\delta v_x}{\delta x} + \frac{\delta v_y}{\delta y} + \frac{\delta v_z}{\delta z} = -\frac{f}{\rho} \frac{\delta \rho}{\delta t}$$

It will be shown, and indeed it is one of the basic assumptions of this study, that regional groundwater flow can be represented as a *steady-state* boundary value problem. For steady flow, there is no change in conditions with time and the right-hand side of (1.8) becomes zero. We are left with:

$$(1.9)\quad \frac{\delta v_x}{\delta x} + \frac{\delta v_y}{\delta y} + \frac{\delta v_z}{\delta z} = 0$$

Laplace's Equation and Richards' Equation

We can now combine the appropriate form of Darcy's law (1.6) with the equation of continuity (1.9). For a homogeneous medium we have:

$$(1.10)\quad \frac{\delta}{\delta x}\left(K\frac{\delta\phi}{\delta x}\right)+\frac{\delta}{\delta y}\left(K\frac{\delta\phi}{\delta y}\right)+\frac{\delta}{\delta z}\left(K\frac{\delta\phi}{\delta z}\right)=0 \quad \therefore K\frac{\delta^2\phi}{\delta x^2}+K\frac{\delta^2\phi}{\delta y^2}+K\frac{\delta^2\phi}{\delta z^2}=0$$

$$(1.11)\quad \frac{\delta^2\phi}{\delta x^2}+\frac{\delta^2\phi}{\delta y^2}+\frac{\delta^2\phi}{\delta z^2}=0$$

which is Laplace's equation. In two dimensions, (1.11) becomes:

$$(1.12)\quad \frac{\delta^2\phi}{\delta x^2}+\frac{\delta^2\phi}{\delta z^2}=0$$

For a non-homogeneous medium, (1.9) becomes:

$$(1.13)\quad \frac{\delta}{\delta x}\left[K(x,y,z)\frac{\delta\phi}{\delta x}\right]+\frac{\delta}{\delta y}\left[K(x,y,z)\frac{\delta\phi}{\delta y}\right]+\frac{\delta}{\delta z}\left[K(x,y,z)\frac{\delta\phi}{\delta z}\right]=0$$

or, in two dimensions:

$$(1.14)\quad \frac{\delta}{\delta x}\left[K(x,z)\frac{\delta\phi}{\delta x}\right]+\frac{\delta}{\delta z}\left[K(x,z)\frac{\delta\phi}{\delta z}\right]=0$$

In soil science literature, this equation is known as Richards' equation and it will be referred to by that name throughout this report.

The subscript notation for partial derivatives will be used interchangeably with the standard notation used above. With the subscript notation, (1.12) and (1.14) become:

$$(1.12)\quad \phi_{xx}+\phi_{zz}=0$$

$$(1.14)\quad [K(x,z)\phi_x]_x+[K(x,z)\phi_z]_z=0$$

Boundary Conditions

We have defined the partial differential equations which describe the steady-state regional flow of groundwater: Laplace's equation for a homogeneous medium, Richards' equation for the non-homogeneous case. It is now necessary to define the region in which we wish to solve the appropriate equation, and to note the boundary conditions which exist along the boundaries of the region. For the sake of convenience we shall restrict ourselves in this section to a two-dimensional vertical section.

Hubbert (1940) was the first to consider this problem, although he did so only qualitatively. Figure 1a shows his "approximate flow pattern in uniformly permeable material between the sources distributed over the air-water interface and the valley sinks". It can be seen that the diagram is symmetric, and it is sufficient to consider one half the flow system.

For the more general case of a non-homogeneous medium and a less regular water table, the physical model might look like Figure 1b. Such a model assumes a horizontal impermeable boundary at some depth and imaginary vertical impermeable boundaries representing the major groundwater divides.

It is now possible to put this physical model into mathematical terms. Figure 1c shows such a mathematical model for the homogeneous case. The equation which must be solved is Laplace's equation and the region in which it must be solved is that shown cross-hatched in the diagram. An x-z coordinate system has been set up with the origin at the lower left-hand corner such that at any point P(x,z) within the region there is a corresponding value of the potential ϕ.

Since there is no flow across the impermeable boundaries, the gradient across such boundaries must be zero. This is represented by the boundary condition $\frac{\delta\phi}{\delta x}=0$ along the vertical impermeable boundaries and $\frac{\delta\phi}{\delta z}=0$ along the horizontal base.

(a)
AFTER
HUBBERT
(1940)

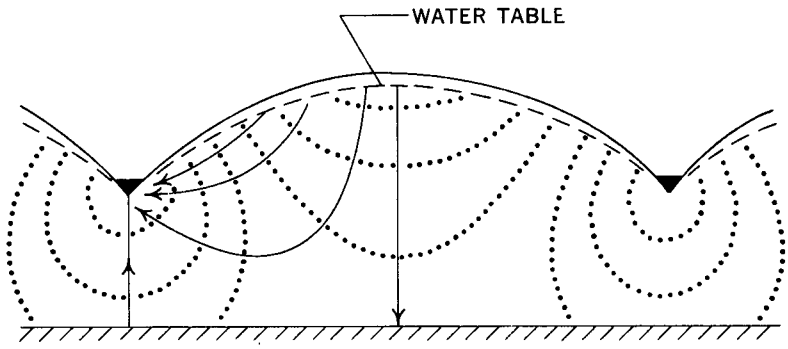

(b)

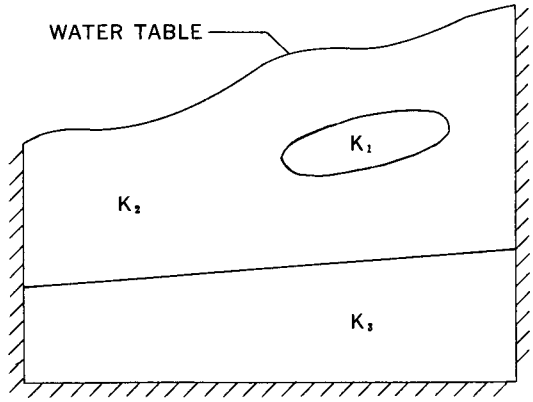

(c)

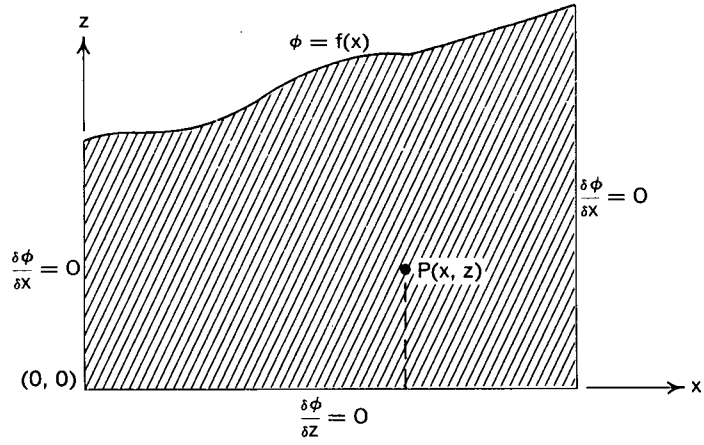

E.G. HOMOGENEOUS CASE—EQUATION: $\frac{\delta^2\phi}{\delta X^2} + \frac{\delta^2\phi}{\delta Z^2} = 0$

Figure 1. A suitable physical and mathematical model

To develop the boundary condition along the water table it is necessary to return to the expression for the hydraulic potential:

$$(1.2)\quad \Phi = gz + \frac{p - p_o}{\rho}$$

At any point on the water table, the pressure is atmospheric so that the second term disappears. Therefore: $\Phi = gz$ or in terms of the hydraulic head: $\phi = z$. The hydraulic head (our potential function) at any point on the water table is thus equal to the elevation of the point above the standard datum, i.e., above the basal impermeable boundary denoted by $z = 0$. The values of z, and thus ϕ, along the water table are a function of x, so that the boundary condition along the water table can be represented by $\phi = f(x)$ where $f(x)$ is the equation of the water-table configuration.

Similar mathematical models may be developed for the non-homogeneous case and for three-dimensional problems. The approach, however, varies with the method of solution and a more detailed account of the mathematical model (including, for example, the applicable boundary condition between layers of different permeability) must await the choice of suitable methods of solution. It should be noted that the first sections of both Chapters 2 and 3 involve a further discussion of the appropriate mathematical models.

Methods of Solution

There are several methods of solution for boundary value problems involving partial differential equations. These methods can be divided into two broad fields: analytical solutions involving classic formal mathematics; and numerical solutions using the finite difference approach.

For Laplace's equation, three separate analytical methods can be listed:

1. Separation of Variables
2. Green's Functions
3. Conformal Mapping

The first of these results in solutions in the form of converging infinite series; the second provides closed solutions but is limited to boundary value problems of a very regular nature; the third, conformal mapping, is a branch of the theory of complex variables and, rather than being a direct method of solution, is a tool which may be used to reduce a complicated problem to one which is amenable to one of the first two methods of solution.

In Chapter 2, the separation of variables technique is used to obtain analytical solutions to Laplace's equation. There are no advantages to be gained by using Green's functions so this method has not been applied. The possible applications of conformal mapping are investigated, but with little success.

The general form of Richards' equation is non-linear and satisfactory analytical solutions are not available.

Both Laplace's equation and Richards' equation are easily solved using the finite-difference approach and in Chapter 3 the numerical solutions are fully developed.

A high-speed digital computer is used in both the analytical and numerical techniques but the nature of the usage is different in the two cases. In the analytical method, the solution is obtained without the aid of the computer and is in the form of a long algebraic expression representing the potential at any point (x,z) in the field. The computer is then used to obtain the numerical values of ϕ independently at many points in the region, thereby defining the potential field. In the numerical technique, a network of nodes representing the groundwater basin is set up and the method of solution involves the computation of ϕ at each point of the nodal array.

ASSUMPTIONS OF STUDY

1. There exists an impermeable basement at some depth above which all rock is permeable, if only to the slightest degree.

2. The Concept of a groundwater basin is a valid one, that is, there exists a three-dimensional closed hydrologic unit bounded on the bottom by a horizontal impermeable basement, on the top by the ground surface and on all sides by imaginary, vertical, impermeable boundaries representing the major groundwater divides.

3. The upper boundary of the flow system is the water table.

4. The configuration of the water table is known, and a reasonable estimate of the subsurface permeability contrasts can be made.

5. The position of the water table is steady, that is, it does not fluctuate with time. This corresponds to what is referred to in soil science literature as the "steady rainfall" case, a better term for which might be the "steady recharge" case. The recharge *to* the water table (or discharge *from* the water table) is the amount necessary to maintain it in its equilibrium position at every point along its length at all times. It is thus a case of dynamic equilibrium. This assumption of a steady water table enables us to treat regional groundwater flow as a steady-state problem.

In defence of these assumptions, a few comments and amplifications are necessary. First, it should be noted that the initial assumption implies that one can discard the terminology of "confined" and "unconfined" aquifers. All the geological formations within the basin have some permeability, no matter how small. As shown by the results, to be presented later, the *conditions* inferred by the term "confined aquifer" *will* arise when we have a high permeability formation underlying one with a permeability many magnitudes lower.

While the second assumption specifies a horizontal impermeable basement, it is possible to consider the case of a sloping impermeable basement by introducing a wedge-shaped formation of very low permeability at the base of the model.

It should also be pointed out that vertical impermeable boundaries need not exist under every topographic high; indeed, this is one of the questions this study is designed to investigate. It has been found in the field, however, that the extent of a groundwater basin is controlled by *major* topographic features. This comment leads us to the fourth assumption which is that the configuration of the water table is known. In many locations, but not all, it is valid to assume that the water table will follow the topographic configuration. This fact, emphasized by Tóth (1962, 1963b), has subsequently been criticized by many workers whose experience has not led them to the same conclusion. It is reasonable, however, to assume that the water table will have its highs beneath the major regional topographic highs and its lows contiguous to the major topographic lows. Whether the water table reflects every hummock in the topography is a moot point and one which must be investigated in the field in any area in which the methods outlined in this report are to be employed. In areas where the water table follows the topography, setting up the mathematical model is simple, requiring only topographic information; in areas where the relationship is doubtful, the configuration of the water-table must be obtained independently. It is, of course, realized that the water table will be closer to the surface in a discharge area than in a recharge area.

The fifth assumption, that of a steady-state water table, is the assumption most basic to the study and is also the one most liable to criticism. It can be defended on the basis of the following:

1. The zone of fluctuation of the water table is only a very small percentage of the total saturated depth of the groundwater basin. For the regional scale of this investigation the difference of a few feet between the high water and low water positions of the water table will have little effect on the flow patterns.

2. The relative configuration of the water table usually remains the same throughout the cycle of fluctuations, that is, the high points remain the highest and the low points remain the lowest.

If either (1) or (2) is not true, then the methods of this study must be adapted. It may be necessary to run several models of a single basin, each with a different water-table configuration, representing the fluctuating position of the water table at various periods in time. As an example, consider a small prairie pothole in a hummocky terrain. Meyboom (1966) has suggested that the water table in the

vicinity of such potholes is liable to reverses in slope such that the pothole is a discharge area through part of the year and a recharge area in the remainder. This is truly a transient behaviour and cannot be represented by a steady-state assumption. Flat water tables which accept irregular recharge due to local irregularities in rainfall patterns are also conductive to major changes in flow pattern with time.

Tóth (1963a), in reply to the objections of Davis (1963) states: ". . .the theory gives the *long term average* of the potential distribution. The theory does not yield quantitatively-transient configurations of the flow pattern. . . . . ." He recommends using "the mean position of the water table, the average of that of many dry and wet seasons" as the upper boundary of flow.

The third assumption is one of convenience. It would be more rigorous to assume the upper boundary of the saturated flow system to be the air-water interface at the top of the capillary zone, but there are two distinct advantages to using the water table. First, it is convenient in establishing the upper boundary condition of the mathematical model and second, it is easily measured in the field. This assumption can be validated on the same grounds as the fifth: the configuration of the water table is similar to that of the air-water interface and the vertical distance between the two is negligible in comparison with the total depth of the groundwater basin.

Perhaps an even more logical approach would be to consider the entire saturated-unsaturated system as continuous, which it is (Luthin and Day, 1955), and use the ground surface as the upper boundary of flow. The numerical solution presented in this paper is, in fact, applicable to such a system but the high variability of permeability contrasts which result from the existing soil moisture profiles places a serious strain on the capacity of the digital computer to handle such problems on a regional scale.

The five basic assumptions listed above hold throughout this study regardless of whether analytical or numerical solutions are being employed. For the numerical method, they constitute the only assumptions. The analytical method, on the other hand, is limited by further restrictions which will become apparent in the first section of Chapter 2 dealing with the analytical mathematical model.

CHAPTER 2

Analytical Solutions

MATHEMATICAL MODEL FOR ANALYTICAL METHOD

The use of the formal analytical method of solution results in three further restrictions to the mathematical model:

1. The analytical method is restricted to two dimensions. The mathematical theory for the solution of boundary value problems in three dimensions is available, but in the case of regional groundwater flow it would necessitate the representation of the water table, an irregular two-dimensional surface, by an algebraic expression f(x,y). This would be impossible for any realistic water-table configuration. If, on the other hand, we consider a two-dimensional vertical section through the basin, the problem is reduced to finding an algebraic expression for the line representing the water table. This is a much simpler task and one which is considered under the heading "Generalized water-table configuration". In order that a two-dimensional section be considered representative of the basin, it must be taken perpendicular to the contours of the water-table surface, i.e., parallel to the direction of slope of the water table.

2. Since analytical solutions to Richards' equation are unknown, we are restricted to the use of Laplace's equation. This means we cannot consider the general non-homogeneous case of a permeability which varies continuously with the space variables. We can, however, treat layered cases where the basin consists of two or more horizontal geologic formations having different permeabilities. Each geological unit, however, must be homogeneous and isotropic with respect to permeability. The boundary conditions which must be satisfied between the layers are listed under a separate heading.

3. We must use the rectangular approximation described below.

Rectangular Approximation

The available analytical methods of solution to Laplace's equation are limited to regions of a very regular shape. We cannot solve the problem in the region shown crosshatched in Figure 2a so we must approximate the cross-hatched region by a rectangle. This is accomplished by applying the boundary condition $\phi = f(x)$ along the upper surface of a rectangle instead of along the line representing the position of the water table. This "rectangular approximation" is shown in Figure 2b. The boundary value problem which we originally wished to solve (Figure 2a) is a special one in that the boundary condition $\phi = f(x)$ also defines the region in which we wish to solve the problem. By transferring the potential distribution $\phi = f(x)$ onto the upper surface of the rectangle, we have in effect made the region of solution constant but we may still represent any water-table configuration by varying f(x). We are, however, ignoring the small wedge of area which exists between the horizontal upper edge of the rectangle and the true position of the water table. The method is thus limited to regional slopes of a few degrees. The range of validity of the rectangular approximation is investigated in Chapter 4 using the numerical method of solution as a check.

Generalized Water-Table Configuration

Tóth (1962, 1963b) solved the problem of regional groundwater flow for a homogeneous medium and two specific water-table configurations. The two configurations are:

(2.1a) $f(x) = z_o + cx$

(2.1b) $f(x) = z_o + c'x + a'\sin b'x$

The first represents a water table whose elevation increases linearly from the valley bottom to the

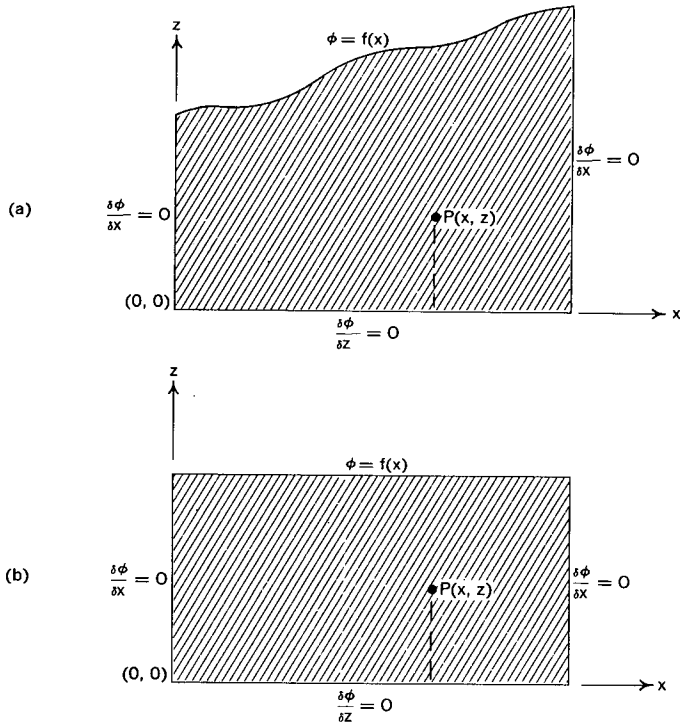

Figure 2. Rectangular approximation

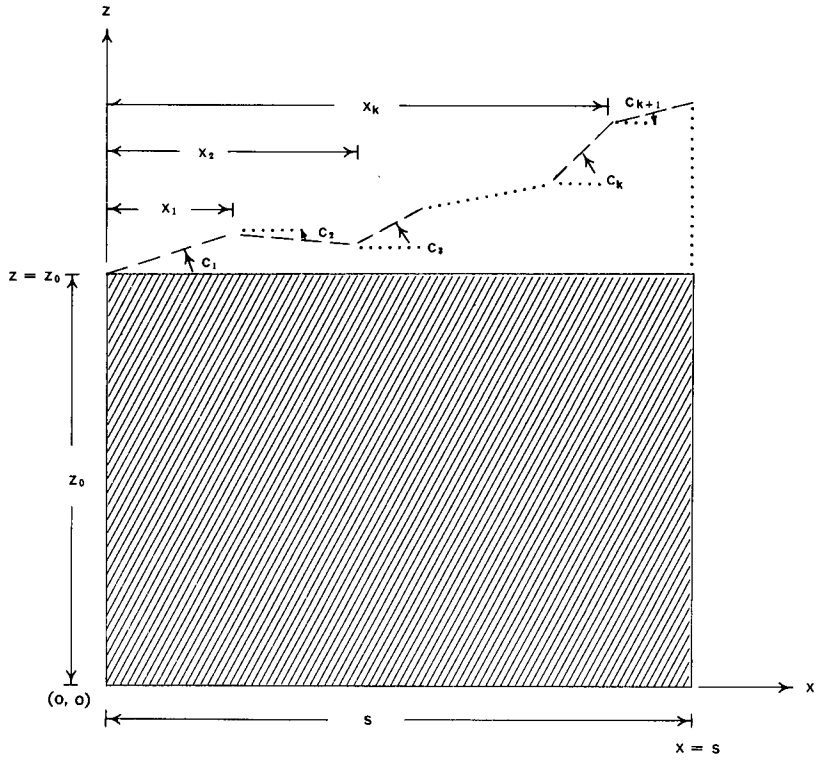

Figure 3. Generalized water-table configuration

water divide. The second has a sine curve imposed upon this regional slope. The parameters are:

z_o = elevation of the water table above datum at the valley bottom
α = angle of slope of water table
c = tan α
a′ = a/cos
b′ = b/cos
a = amplitude of sine curve
b = $2\pi/\lambda$
λ = wave length of the sine curve

It is the author's desire to obtain a mathematical expression for a generalized water-table configuration, one which would include those treated by Tóth as well as any other realistic water-table configurations. Such an expression is:

$$(2.2)\quad f(x) = z_o + c_1 x \qquad (\text{for } 0 \leq x \leq x_1)$$

$$= z_o + c_1 x_1 + c_2(x - x_1) \qquad (\text{for } x_1 < x \leq x_2)$$

$$= z_o + c_1 x_1 + c_2(x_2 - x_1) + c_3(x - x_2) \qquad (\text{for } x_2 < x \leq x_3)$$

$$\vdots$$

$$= z_o + c_1 x_1 + c_2(x_2 - x_1) + \ldots\ldots\ldots\ldots + c_k(x_k - x_{k-1}) + c_{k+1}(x - x_k)$$

$$(\text{for } x_k < x \leq s)$$

As shown in Figure 3, this represents a series of straight-line segments. The slopes $c_1, c_2, \ldots\ldots c_{k+1}$ and the positions of x_1, x_2 ..... x_k are arbitrary so that any configuration of straight line segments can be represented. To prove the generality of this expression, it will be shown in a later section of this chapter that, by choosing the appropriate series of straight-line segments, one can obtain the identical potential pattern as that produced using Tóth's sine curve.

Interlayer Boundary Conditions

There are two boundary conditions which must be satisfied at the surface of discontinuity separating two horizontal layers of differing permeability:

$$(2.3)\quad \phi_1 = \phi_2$$

$$(2.4)\quad K_1 \frac{\delta\phi_1}{\delta z} = K_2 \frac{\delta\phi_2}{\delta z}$$

The first condition (2.3) expresses the requirement that the potential be continuous across the surface of discontinuity. Equation (2.4) states that the normal component of velocity must be continuous at the surface of discontinuity. This is merely another way of stating the tangent law for the refraction of flow lines across a permeability boundary.

We are now in a position to obtain an analytical solution to our mathematical problem, using the separation of variables technique and the rectangular approximation described above.

ANALYTICAL SOLUTION TO TWO-DIMENSIONAL THREE-LAYER PROBLEM WITH GENERALIZED WATER-TABLE CONFIGURATION

The mathematical model is a two-dimensional, vertical section through a groundwater basin, with a generalized water-table configuration and three geologic layers. The following terminology is used:

x = horizontal coordinate direction
z = vertical coordinate direction

(x,z) = coordinates of any point P in field
s = lateral extent of basin
z_o = depth of basin
r_1 = vertical distance from z = O axis (basal impermeable boundary) to contact between layer 1 and layer 2
r_2 = vertical distance from z = O axis to contact between layer 2 and layer 3
K_1 = permeability of Layer 1
K_2 = permeability of Layer 2
K_3 = permeability of Layer 3
$\phi_1(x,z)$ = hydraulic head at any point (x,z) in Layer 1
$\phi_2(x,z)$ = hydraulic head at any point (x,z) in Layer 2
$\phi_3(x,z)$ = hydraulic head at any point (x,z) in Layer 3
$x_1 x_2, \ldots x_k$ = horizontal distance from x = O axis (left-hand vertical impermeable boundary) to each break in slope in the generalized water-table configuration
$c_1 c_2, \ldots c_{k+1}$ = slopes of various straight-line segments in generalized water-table configuration.

The boundary value problem which we wish to solve is, in actuality, three interrelated boundary value problems (Figure 4). It is necessary to obtain three separate expressions for ϕ_1, ϕ_2 and ϕ_3 representing the hydraulic head, i.e., the hydraulic potential expressed as the head of water above the basal datum plane, in each of the three layers. For layer 1, where the permeability is K_1, ϕ_1 must satisfy the Laplace equation:

$$(2.5)\quad \frac{\delta_2 \phi_1}{\delta x^2} + \frac{\delta^2 \phi_1}{\delta z^2} = 0 \qquad (\text{where } r_1 \leq z \leq z_o)$$

and the boundary conditions:

$$(2.6a)\quad \frac{\delta \phi_1}{\delta x}(0,z) = 0$$

$$(2.6b)\quad \frac{\delta \phi_1}{\delta x}(s,z) = 0$$

$$(2.6c)\quad K_1 \frac{\delta \phi_1}{\delta z}(x,r_1) = K_2 \frac{\delta \phi_2}{\delta z}(x,r_1)$$

$$(2.6d)\quad \phi_1(x,r_1) = \phi_2(x,r_1)$$

$$(2.6e)\quad \phi_1(x,z_o) = f(x)$$

where:

$$(2.6f)\quad f(x) = z_o + c_1 x \qquad (\text{for } 0 \leq x \leq x_1)$$

$$= z_o + c_1 x_1 + c_2(x - x_1) \qquad (\text{for } x_1 \leq x \leq x_2)$$

$$\vdots$$

$$= z_o + c_1 x_1 + c_2(x_2 - x_1) + \ldots + c_k(x_k - x_{k-1}) + c_{k+1}(x - x_k)$$

$$(\text{for } x_k < x \leq s)$$

In layer 2, with permeability K_2, we have:

$$(2.7)\quad \frac{\delta^2 \phi_2}{\delta x^2} + \frac{\delta^2 \phi_2}{\delta z^2} = 0 \qquad (\text{where } r_2 \leq z \leq r_1)$$

and the boundary conditions:

$$(2.8a)\quad \frac{\delta \phi_2}{\delta x}(0,z) = 0$$

(a)

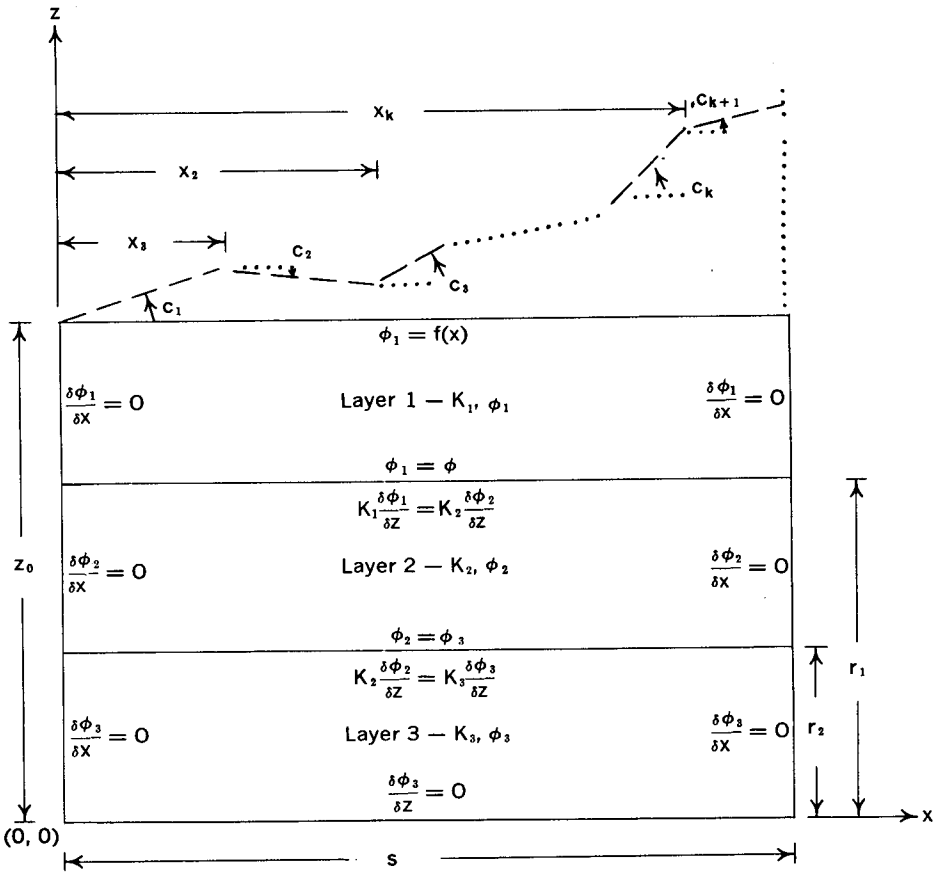

(b)

LAYER 1

$\phi_1 = f(x)$

$\frac{\delta\phi_1}{\delta X} = 0$ $\qquad$ $\frac{\delta\phi_1}{\delta X} = 0$

$\phi_1 = \phi_2$, $K_1\frac{\delta\phi_1}{\delta Z} = K_2\frac{\delta\phi_2}{\delta Z}$

LAYER 2

$\phi = \phi_2$, $K_1\frac{\delta\phi_1}{\delta Z} = K_2\frac{\delta\phi_2}{\delta Z}$

$\frac{\delta\phi_2}{\delta X} = 0$ $\qquad$ $\frac{\delta\phi_2}{\delta X} = 0$

$\phi_2 = \phi_3$, $K_2\frac{\delta\phi_2}{\delta Z} = K_3\frac{\delta\phi_3}{\delta Z}$

LAYER 3

$\phi_2 = \phi_3$, $K_2\frac{\delta\phi_2}{\delta Z} = K_3\frac{\delta\phi_3}{\delta Z}$

$\frac{\delta\phi_3}{\delta X} = 0$ $\qquad$ $\frac{\delta\phi_3}{\delta X} = 0$

$\frac{\delta\phi_3}{\delta Z} = 0$

Figure 4. Mathematical model for analytical method

(2.8b) $\frac{\delta \phi_2}{\delta x}(s,z) = 0$

(2.8c) $K_1 \frac{\delta \phi_1}{\delta z}(x,r_1) = K_2 \frac{\delta \phi_2}{\delta z}(x,r_1)$

(2.8d) $\phi_1(x,r_1) = \phi_2(x,r_1)$

(2.8e) $K_2 \frac{\delta \phi_2}{\delta z}(x,r_2) = K_3 \frac{\delta \phi_3}{\delta z}(x,r_2)$

(2.8f) $\phi_2(x,r_2) = \phi_3(x,r_2)$

In layer 3, with permeability k_3, ϕ_3 must satisfy:

(2.9) $\frac{\delta^2 \phi_3}{\delta x^2} + \frac{\delta^2 \phi_3}{\delta z^2} = 0$ (where $0 \leq z \leq r_2$)

and the boundary conditions:

(2.10a) $\frac{\delta \phi_3}{\delta x}(0,z) = 0$

(2.10b) $\frac{\delta \phi_3}{\delta x}(s,z) = 0$

(2.10c) $\frac{\delta \phi_3}{\delta z}(x,0) = 0$

(2.10d) $K_2 \frac{\delta \phi_2}{\delta z}(x,r_2) = K_3 \frac{\delta \phi_3}{\delta z}(x,r_2)$

(2.10e) $\phi_2(x,r_2) = \phi_3(x,r_2)$

Having defined the problem, we may proceed to solve it using the method of separation of variables. Consider first layer 3, and assume a product solution:

(2.11) $\phi_3(x,z) = X_3(x)Z_3(z)$

Substituting this expression into (2.9) yields:

(2.12) $Z_3(z)\frac{d^2X_3(x)}{dx^2} + X_3(x)\frac{d^2Z_3(z)}{dz^2} = 0$

Using the notation:

(2.13) $\frac{dX_3(x)}{dx} = X_3'$, $\frac{dZ_3(z)}{dz} = Z_3'$, $\frac{d^2X_3(x)}{dx^2} = X_3''$, $\frac{d^2Z_3(z)}{dz^2} = Z_3''$

(2.12) becomes:

(2.14) $Z_3X_3'' + X_3Z_3'' = 0$

Dividing through by X_3Z_3 then gives:

(2.15) $\frac{X_3''}{X_3} + \frac{Z_3''}{Z_3} = 0$

or

(2.16) $\frac{X_3''}{X_3} = -\frac{Z_3''}{Z_3} = \text{a constant} = \beta$

Since the left-hand side is a function of x alone and the right-hand side is a function of z alone, both

sides must be equal to a constant β. We must investigate the sign of β:

Case 1: $\beta > 0$. Then (2.16) yields two ordinary differential equations:

(2.17) $X_3'' - \beta X_3 = 0$

(2.18) $Z_3'' + \beta Z_3 = 0$

The solution to (2.17) is:

(2.19) $X_3 = F \cosh \sqrt{\beta}\, x + G \sinh \sqrt{\beta}\, x$ (where F and G are constants)

and therefore

(2.20) $X_3' = F \sqrt{\beta} \sinh \sqrt{\beta}\, x + G \sqrt{\beta} \cosh \sqrt{\beta}\, x$

The solution to (2.18) is:

(2.21) $Z_3 = H \sin \sqrt{\beta}\, z + J \cos \sqrt{\beta}\, z$ (where H and J are constants)

By (2.11), $\phi_3(x,z) = X_3(x)Z_3(z)$; therefore

(2.22) $\dfrac{\delta \phi_3(x,z)}{\delta x} = X_3'(x)Z_3(z)$

Boundary condition (2.10a) then implies:

$$\frac{\delta \phi_3}{\delta x}(0,z) = 0 = X_3'(0)Z_3(z) \Rightarrow X_3'(0) = 0 \Rightarrow G = 0$$

and boundary condition (2.10b) becomes:

$$\frac{\delta \phi_3}{\delta x}(s,z) = 0 = X_3'(s)Z_3(z) \Rightarrow X_3'(s) = 0 \Rightarrow F = 0$$

Therefore F = G = 0 and we have no solution. Therefore $\beta \not> 0$

Case 2: $\beta = 0$. Then (2.16) yields:

(2.23) $X_3'' = 0$

(2.24) $Z_3'' = 0$

The solution to (2.23) is:

(2.25) $X_3 = F_X + G$ (where F and G are constants)

Therefore:

(2.26) $X_3' = F$

The solution to (2.24) is:

(2.27) $Z_3 = H_Z + J$ (where H and J are constants)

and hence

(2.28) $Z_3' = H$

Boundary condition (2.10a) then implies, using equation (2.22):

$$\frac{\delta \phi_3}{\delta z}(0,z) = 0 = X_3'(0)Z_3(z) \Rightarrow X_3'(0) = 0 \Rightarrow F = 0$$

Boundary condition (2.10c) becomes:

$$\frac{\delta \phi_3}{\delta z}(x,0) = 0 = X_3(x)Z_3'(0) \Rightarrow Z_3'(0) = 0 \Rightarrow H = 0$$

Therefore F = H = 0 and $\phi_3 = X_3 Z_3 = GJ$ = a constant, which is not a solution. Therefore $\beta \neq 0$.

Case 3: Since $\beta \not> 0$ and $\beta \neq 0$, then $\beta < 0$. Let $\beta = -\lambda^2$ (2.16) becomes:

$$(2.29)\quad \frac{X_3''}{X_3} = -\frac{Z_3''}{Z_3} = -\lambda^2$$

The two resulting ordinary differential equations are:

$$(2.30)\quad X_3'' + \lambda^2 X_3 = 0$$

$$(2.31)\quad Z_3'' - \lambda^2 Z_3 = 0$$

Considering (2.30) first; the solution is:

$$(2.32)\quad X_3 = F\cos\lambda x + G\sin\lambda x \qquad \text{(where F and G are constants)}$$

and consequently:

$$(2.33)\quad X_3' = -\lambda F\sin\lambda x + \lambda G\cos\lambda x$$

Since $\phi_3 = X_3(x)Z_3(z)$, boundary condition (2.10a) becomes:

$$\frac{\delta\phi_3}{\delta x}(0,z) = 0 = X_3'(0)Z_3(z) \Rightarrow X_3'(0) = 0$$

Therefore from (2.33);

$$0 = \lambda G \Rightarrow G = 0$$

and (2.33) becomes

$$(2.34)\quad X_3' = -\lambda F\sin\lambda x$$

Applying boundary condition (2.10b) yields:

$$\frac{\delta\phi_3}{\delta x}(s,z) = 0 \Rightarrow X_3'(s) = 0$$

Therefore from (2.34):

$$0 = -\lambda F\sin\lambda s$$

If $\lambda F = 0$, there is no solution. Therefore

$$\sin\lambda s = 0$$

$$\therefore \lambda s = m\pi \qquad m = 0,1,2,\ldots.$$

$$(2.35)\quad \lambda = \frac{m\pi}{s} \qquad m = 0,1,2,\ldots.$$

These values of λ represent the eigenvalues of the problem. Since $G = 0$ and $\lambda = \frac{m\pi}{s}$ we have, from (2.32):

$$(2.36)\quad X_3 = F\cos\frac{m\pi x}{s} \qquad m = 0,1,2,\ldots.$$

The solution to (2.31) is:

$$(2.37)\quad Z_3 = H\cosh\lambda z = J\sinh\lambda z$$

Applying boundary condition (2.10c) we find $J = 0$ and therefore

$$(2.38)\quad Z_3 = H\cosh\frac{m\pi z}{s} \qquad m = 0,1,2,\ldots.$$

The product solution is therefore:

$$\phi_3 = X_3Z_3 = F\cos\frac{m\pi x}{s}\cdot H\cosh\frac{m\pi z}{s} \qquad m = 0,1,2,\ldots.$$

Combining the constants F and H into one constant, we have:

(2.39) $\phi_3(x,z) = A \cos \frac{m\pi x}{s} \cosh \frac{m\pi z}{s}$ $\qquad m = 0,1,2, \ldots$

Before applying the upper boundary conditions (2.10d) and (2.10e) which describe the interrelationship of ϕ_2 and ϕ_3, we must develop an analogous expression to (2.39) for ϕ_2.

Once again we assume a product solution:

(2.40) $\phi_2 = X_2(x)Z_2(z)$

Therefore,

(2.41) $\frac{\delta^2\phi_2}{\delta x^2} = X_2'' Z_2$

(2.42) $\frac{\delta^2\phi_2}{\delta z^2} = X_2 Z_2''$

and (2.7) becomes:

(2.43) $X_2'' Z_2 + X_2 Z_2'' = 0$

Dividing through by $X_2 Z_2$ and transposing yields:

(2.44) $\frac{X_2''}{X_2} = - \frac{Z_2''}{Z_2} = \text{a constant} = - a^2$

where the constant must be less than zero by the same reasoning as for β in the development of the expression for layer 3.

The ordinary differential equations corresponding to (2.44) are:

(2.45) $X_2'' + a^2 X_2 = 0$

(2.46) $Z_2'' - a^2 Z_2 = 0$

The solution to (2.45) is:

(2.47) $X_2 = K \cos ax + L \sin ax$ $\qquad$ (where K and L are constants)

Therefore,

(2.48) $X_2' = - aK \sin ax + aL \cos ax$

From boundary conditions (2.8a):

(2.49) $\frac{\delta\phi_2}{\delta x}(0,z) = 0 \Rightarrow X_2'(0) = 0$

Therefore, from (2.48), L = 0. From boundary condition (2.8b).

(2.50) $\frac{\delta\phi_2}{\delta x}(s,z) = 0 \Rightarrow X_2'(s) = 0$

From which we deduce

$\sin as = 0$ $\qquad n = 0,1,2, \ldots$

$as = n\pi$ $\qquad n = 0,1,2, \ldots$

$a = \frac{m\pi}{s}$

Recall that:

$\lambda = \frac{m\pi}{s}$ $\qquad m = 0,1,2, \ldots$

We thus have two infinite sets of identical eigenvalues

(i.e., $a_0 = 0 = \lambda_0$, $a_1 = \frac{\pi}{s} = \lambda_1$, $a_2 - \frac{2\pi}{s} = \lambda_2$, etc.),

one set for the solution of ϕ_3 in layer 3, the other for the solution of ϕ_2 in layer 2.

We cannot choose n and m independently because the two solutions for ϕ_2 and ϕ_3, thus far independent of one another, will subsequently be related (see below) by means of the interlayer boundary conditions (2.10d) and (2.10e). In effect, we have only one boundary value problem and it must have a single unique set of eigenvalues. It is this property of the uniqueness of the eigenvalues which allows us to obtain three independent series solutions, one for each layer, which contain a *single* Fourier constant A_m, which is a function of m (page 24).

Therefore we can write:

$$a = \frac{m\pi}{s} = \lambda \qquad m = 0,1,2, \ldots\ldots\ldots$$

Since L = 0 and $a = \frac{m\pi}{s}$ we have, from (2.47):

$$(2.51)\quad X_2 = K \cos \frac{m\pi x}{s} \qquad m = 0,1,2, \ldots\ldots\ldots$$

The solution to (2.46) is

$$(2.52)\quad Z_2 = M \cosh az = N \sinh az$$

or substituting for a:

$$(2.53)\quad Z_2 = M \cosh \frac{m\pi z}{s} + N \sinh \frac{m\pi z}{s} \qquad m = 0,1,2, \ldots\ldots$$

The product solution, from (2.51) and (2.53) is:

$$\phi_2 = X_2 Z_2 = K \cos \frac{m\pi x}{s} \left[M \cosh \frac{m\pi z}{s} + N \sinh \frac{m\pi z}{s} \right] \qquad m = 0,1,2, \ldots\ldots$$

or combining constants:

$$(2.54)\quad \phi_2(x,z) = \cos \frac{m\pi x}{s} \left[B \cosh \frac{m\pi z}{s} + C \sinh \frac{m\pi z}{s} \right] \qquad m = 0,1,2, \ldots\ldots$$

Using equation (2.5) and boundary conditions (2.6a) and (2.6b) we can arrive at an identical expression to (2.54) for layer 1. It is:

$$(2.55)\quad \phi_1(x,z) = \cos \frac{m\pi x}{s} \left[D \cosh \frac{m\pi z}{s} + E \sinh \frac{m\pi z}{s} \right] \qquad m = 0,1,2, \ldots\ldots$$

Equations (2.39), (2.54) and (2.55) give us solutions for ϕ_1, ϕ_2, and ϕ_3 in terms of 5 arbitrary constants, A, B, C, D and E. We can reduce the number of arbitrary constants to one by considering the interlayer boundary conditions. Let us first consider (2.39) and (2.54) and the boundary conditions (2.10d) and (2.10e):

$$(2.39)\quad \phi_3(x,z) = A \cos \frac{m\pi x}{s} \cosh \frac{m\pi z}{s} \qquad m = 0,1,2, \ldots\ldots$$

$$(2.54)\quad \phi_2(x,z) = \cos \frac{m\pi x}{s} \left[B \cosh \frac{m\pi z}{s} + C \sinh \frac{m\pi z}{s} \right] \qquad m = 0,1,2, \ldots\ldots$$

$$(2.10d)\quad K_2 \frac{\delta \phi_2}{\delta z} (x,r_2) = K_3 \frac{\delta \phi_3}{\delta z} (x,r_2)$$

$$(2.10e)\quad \phi_2(x,r_2) = \phi_3(x,r_2)$$

Applying (2.10e) to (2.39) and (2.54) yields

$$(2.56)\quad A\cos\frac{m\pi x}{s}\cosh\frac{m\pi r_2}{s} = \left[B\cos\frac{m\pi x}{s}\cosh\frac{m\pi r_2}{s} + C\cos\frac{m\pi x}{s}\sinh\frac{m\pi r_2}{s}\right]$$

Transposing:

$$(2.57)\quad (A - B)\cos\frac{m\pi x}{s}\cosh\frac{m\pi r_2}{s} = C\cos\frac{m\pi x}{s}\sinh\frac{m\pi r_2}{s}$$

Therefore:

$$(2.58)\quad C = \frac{A - B}{\tanh\frac{m\pi r_2}{s}}$$

We may now substitute (2.58) into (2.54) to eliminate C:

$$(2.59)\quad \phi_2(x,z) = B\cos\frac{m\pi x}{s}\cosh\frac{m\pi z}{s} + \frac{A\cos\frac{m\pi x}{s}\sinh\frac{m\pi z}{s}}{\tanh\frac{m\pi r_2}{s}} - \frac{B\cos\frac{m\pi x}{s}\sinh\frac{m\pi z}{s}}{\tanh\frac{m\pi r_2}{s}}$$

To eliminate B from (2.59) we must apply boundary condition (2.10d) to (2.39) and (2.54). This yields:

$$(2.60)\quad A\left[\cos\frac{m\pi x}{s}\sinh\frac{m\pi r_2}{s}\right]\frac{m\pi}{s} = \frac{K_2}{K_3}\left\{\left[B\cos\frac{m\pi x}{s}\sinh\frac{m\pi r_2}{s}\right]\frac{m\pi}{s} + \left[C\cos\frac{m\pi x}{s}\cosh\frac{m\pi r_2}{s}\right]\frac{m\pi}{s}\right\}$$

Substituting (2.58) for C yields:

$$(2.61)\quad \left[A\cos\frac{m\pi x}{s}\sinh\frac{m\pi r_2}{s}\right]\frac{m\pi}{s} - \frac{\left[A\cos\frac{m\pi x}{s}\cosh^2\frac{m\pi r_2}{s}\right]\frac{m\pi}{s}\cdot\frac{K_2}{K_3}}{\sinh\frac{m\pi r_2}{s}}$$
$$= \frac{K_2}{K_3}\left\{\left[B\cos\frac{m\pi x}{s}\sinh\frac{m\pi r_2}{s}\right]\frac{m\pi}{s} - \frac{\left[B\cos\frac{m\pi x}{s}\cosh^2\frac{m\pi r_2}{s}\right]\frac{m\pi}{s}}{\sinh\frac{m\pi r_2}{s}}\right\}$$

from which:

$$(2.62)\quad A\left[\sinh^2\frac{m\pi r_2}{s} - \frac{K_2}{K_3}\cosh^2\frac{m\pi r_2}{s}\right] = \frac{K_2}{K_3}B(-1)$$

Therefore:

$$(2.63)\quad B = A\left[\cosh^2\frac{m\pi r_2}{s} - \frac{K_3}{K_2}\sinh^2\frac{m\pi r_2}{s}\right]$$

Substituting this expression for B into (2.59) gives:

$$(2.64)\quad \psi_2(x,z) = A\cos\frac{m\pi x}{s}\cosh\frac{m\pi z}{s}\left(\cosh^2\frac{m\pi r_2}{s} - \frac{K_3}{K_2}\sinh^2\frac{m\pi r_2}{s}\right)$$

$$+\ \frac{A\cos\frac{m\pi x}{s}\sinh\frac{m\pi z}{s}\left(1-\cosh^2\frac{m\pi r_2}{s}+\frac{K_3}{K_2}\sinh^2\frac{m\pi r_2}{s}\right)}{\tanh\frac{m\pi r_2}{s}}$$

Introducing the notation:

$$(2.65)\quad W(m,r_2,K_2,K_3,s) = \cosh^2\frac{m\pi r_2}{s} - \frac{K_3}{K_2}\sinh^2\frac{m\pi r_2}{s}$$

$$(2.66)\quad V(m,r_2,K_2,K_3,s) = \frac{1-W}{\tanh\frac{m\pi r_2}{s}}$$

we are left with the following expressions for ϕ_2 and ϕ_3 in terms of the single constant A:

$$(2.67)\quad \phi_2(x,z) = A\cos\frac{m\pi x}{s}\left[\cosh\frac{m\pi z}{s}(W) + \sinh\frac{m\pi z}{s}(V)\right] \qquad m = 0,1,2,\ldots.$$

$$(2.39)\quad \psi_3(x,z) = A\cos\frac{m\pi x}{s}\cosh\frac{m\pi z}{s} \qquad m = 0,1,2,\ldots.$$

We must now examine the effect of the interlayer boundary conditions (2.6c) and (2.6d) on equations (2.55) and (2.67) above:

$$(2.55)\quad \phi_1(x,z) = \cos\frac{m\pi x}{s}\left[D\cosh\frac{m\pi z}{s} + E\sinh\frac{m\pi z}{s}\right] \qquad m = 0,1,2,\ldots.$$

$$(2.6c)\quad K_1\frac{\delta\psi_1}{\delta z}(x,r_1) = K_2\frac{\delta\phi_2}{\delta z}(x,r_1)$$

$$(2.6d)\quad \phi_1(x,r_1) = \phi_2(x,r_1)$$

Applying (2.6d) to (2.55) and (2.67) yields:

$$(2.68)\quad [A(W) - D]\cos\frac{m\pi x}{s}\cosh\frac{m\pi r_1}{s} + A(V)\sinh\frac{m\pi r_1}{s}\cos\frac{m\pi x}{s}$$

$$= E\cos\frac{m\pi x}{s}\sinh\frac{m\pi r_1}{s}$$

from which

$$(2.69)\quad E = \frac{[A(W) - D]}{\tanh\frac{m\pi r_1}{s}} + A(V)$$

Substituting (2.69) into (2.55) eliminates E:

$$(2.70)\quad \phi_1(x,z) = D\cos\frac{m\pi x}{s}\cosh\frac{m\pi z}{s} + A(V)\sinh\frac{m\pi z}{s}\cos\frac{m\pi x}{s}$$

$$+\ \frac{[A(W) - D]\cos\frac{m\pi x}{s}\sinh\frac{m\pi z}{s}}{\tanh\frac{m\pi r_1}{s}} \qquad m = 0,1,2,\ldots.$$

Now applying (2.6c) to (2.70) and (2.67), we obtain:

$$(2.71)\quad \left(D\cos\frac{m\pi x}{s}\sinh\frac{m\pi r_1}{s}\right)\frac{m\pi}{s} + A(V)\left(\cos\frac{m\pi x}{s}\cosh\frac{m\pi r_1}{s}\right)\frac{m\pi}{s} + \frac{[A(W) - D]\left(\cos\frac{m\pi x}{s}\cosh\frac{m\pi r_1}{s}\right)\frac{m\pi}{s}}{\tanh\frac{m\pi r_1}{s}} = \frac{K_2}{K_1}A\cos\frac{m\pi x}{s}\left[\left(\sinh\frac{m\pi r_1}{s}\right)\frac{m\pi}{s}(W) + \left(\cosh\frac{m\pi r_1}{s}\right)\frac{m\pi}{s}(V)\right]$$

Bringing A terms to the left-hand side and D terms to the right-hand side, we get:

$$(2.72)\quad \left(A\cos\frac{m\pi x}{s}\right)\frac{m\pi}{s}\left\{\left[\frac{(W)\left(\cosh^2\frac{m\pi r_1}{s} - \frac{K_2}{K_1}\sinh^2\frac{m\pi r_1}{x}\right)}{\sinh\frac{m\pi r_1}{s}}\right] + \left[\cosh\frac{m\pi r_1}{s}(V)\left(1 - \frac{K_2}{K_1}\right)\right]\right\} = \frac{\left(D\cos\frac{m\pi x}{s}\right)\frac{m\pi}{s}}{\sinh\frac{m\pi r_1}{s}}$$

Therefore:

$$(2.73)\quad D = A\left[(W)\left(\cosh^2\frac{m\pi r_1}{s} - \frac{K_2}{K_1}\sinh^2\frac{m\pi r_1}{s}\right) + \cosh\frac{m\pi r_1}{s}\sinh\frac{m\pi r_1}{s}(V)\left(1 - \frac{K_2}{K_1}\right)\right]$$

Substituting (2.73) into (2.70) for D yields:

$$(2.74)\quad \phi_1(x,z) = A\cos\frac{m\pi x}{s}\cosh\frac{m\pi z}{s}\left[(W)\left(\cosh^2\frac{m\pi r_1}{s} - \frac{K_2}{K_1}\sinh^2\frac{m\pi r_1}{s}\right) + \cosh\frac{m\pi r_1}{s}\sinh\frac{m\pi r_1}{s}(V)\left(1 - \frac{K_2}{K_1}\right)\right] + A(V)\sinh\frac{m\pi z}{s}\cos\frac{m\pi x}{s} + \frac{A(W)\cos\frac{m\pi x}{s}\sinh\frac{m\pi z}{s}}{\tanh\frac{m\pi r_1}{s}} - \frac{A\cos\frac{m\pi x}{s}\sinh\frac{m\pi z}{s}}{\tanh\frac{m\pi r_1}{s}}\left[(W)\left(\cosh^2\frac{m\pi r_1}{s} - \frac{K_2}{K_1}\sinh^2\frac{m\pi r_1}{s}\right) + \cosh\frac{m\pi r_1}{s}\sinh\frac{m\pi r_1}{s}(V)\left(1 - \frac{K_2}{K_1}\right)\right]$$

$$m = 0,1,2,\ldots..$$

Let:

$$(2.75)\quad T(m,r_1,K_1,K_2,s) = \cosh^2\frac{m\pi r_1}{s} \quad \frac{K_2}{K_1}\sinh^2\frac{m\pi r_1}{s}$$

and:

$$(2.76)\quad U(m,r_1,r_2,K_1,K_2,K_3,s) = (W)(T) + \cosh\frac{m\pi r_1}{s}\sinh\frac{m\pi r_1}{s}(V)\left(1 - \frac{K_2}{K_1}\right)$$

The expression (2.74) for ϕ_1 then becomes:

$$(2.77)\quad \phi_1(x,z) = A\cos\frac{m\pi x}{s}\cosh\frac{m\pi z}{s}\,(U) + A\cos\frac{m\pi x}{s}\sinh\frac{m\pi z}{s}\left[(V) + \frac{(W)-(U)}{\tanh\frac{m\pi r_1}{s}}\right] \qquad m = 0,1,2,\ldots..$$

Further, defining:

$$(2.78)\quad R(m,r_1,K_1,K_2,s) = \frac{1-(T)}{\tanh\frac{m\pi r_1}{s}}$$

$$(2.79)\quad Y(m,r_1,r_2,K_1,K_2,K_3,s) = (W)(R) + (V)\left[1 + \frac{K_2}{K_1} - T\right]$$

gives:

$$(2.80)\quad \phi_1(x,z) = A\cos\frac{m\pi x}{s}\left[\cosh\frac{m\pi z}{s}\,(U) + \sinh\frac{m\pi z}{s}\,(Y)\right] \qquad m = 0,1,2,\ldots..$$

We now have expressions for ϕ_1 (2.80), ϕ_2 (2.67), and ϕ_3 (2.39) in terms of the single arbitrary constant A. Each expression represents an infinite number of solutions corresponding to the values of m = 0,1,2,..... Since Laplace's equation is linear, we may sum these solutions to give

$$(2.81a)\quad \phi_1(x,z) = \sum_{m=0}^{\infty} A_m\cos\frac{m\pi x}{s}\left[\cosh\frac{m\pi z}{s}\,(U) + \sinh\frac{m\pi z}{s}\,(Y)\right]$$

$$(2.81b)\quad \phi_2(x,z) = \sum_{m=0}^{\infty} A_m\cos\frac{m\pi x}{s}\left[\cosh\frac{m\pi z}{s}\,(W) + \sinh\frac{m\pi z}{s}\,(V)\right]$$

$$(2.81c)\quad \phi_3(x,z) = \sum_{m=0}^{\infty} A_m\cos\frac{m\pi x}{s}\cosh\frac{m\pi z}{s}$$

We have now applied all the boundary conditions to all three layers except the upper water table configuration:

$$(2.82)\quad \phi_1(x,z_0) = f(x)$$

Therefore from (2.81a)

$$(2.83)\quad f(x) = \sum_{m=0}^{\infty} A_m\cos\frac{m\pi x}{s}\left[\cosh\frac{m\pi z_0}{s}\,(U) + \sinh\frac{m\pi z_0}{s}\,(Y)\right]$$

Let:

$$(2.84)\quad Q(m,r_1,r_2,K_1,K_2,K_3,s,z_0) = \cosh\frac{m\pi z_0}{s}\,(U) + \sinh\frac{m\pi z_0}{s}\,(Y)$$

Then (2.83) becomes:

$$(2.85)\quad f(x) = \sum_{m=0}^{\infty} A_m\cos\frac{m\pi x}{s}\cdot Q$$

But this represents a half-range Fourier cosine expansion over the interval (o,s) and we know from the theory of Fourier series (Wylie, 1960; Byerly, 1959) that:

$$(2.86)\quad A_m = \frac{2}{sQ}\int_0^s f(x)\cos\frac{m\pi x}{s}\,dx$$

$$(2.87)\quad A_0 = \frac{2}{s}\int_0^s f(x)\,dx \qquad \text{(since } Q = 1 \text{ for } m = 0)$$

and the expressions for ϕ_1, ϕ_2, and ϕ_3 become, from (2.81):

$$(2.88)\quad \phi_1(x,z) = \frac{A_0}{2} + \sum_{m=1}^{\infty} A_m \cos\frac{m\pi x}{s}\left[\cosh\frac{m\pi z}{s}(U) + \sinh\frac{m\pi z}{s}(Y)\right]$$

$$(2.89)\quad \phi_2(x,z) = \frac{A_0}{2} + \sum_{m=1}^{\infty} A_m \cos\frac{m\pi x}{s}\left[\cosh\frac{m\pi z}{s}(W) + \sinh\frac{m\pi z}{s}(V)\right]$$

$$(2.90)\quad \phi_3(x,z) = \frac{A_0}{2} + \sum_{m=1}^{\infty} A_m \cos\frac{m\pi x}{s}\cosh\frac{m\pi z}{s}$$

To determine A_m and A_0, we must evaluate the integrals in (2.86) and (2.87) for the expression (2.6f) for f(x) representing the generalized topographic configuration. Considering the integral in (2.83) first, we have:

$$(2.91)\quad \int_0^s f(x)\cos\frac{m\pi x}{s}\,dx = \int_0^{x_1} f(x)\cos\frac{m\pi x}{s}\,dx + \int_{x_1}^{x_2} f(x)\cos\frac{m\pi x}{s}\,dx$$

$$+ \int_{x_2}^{x_3} f(x)\cos\frac{m\pi x}{s}\,dx + \cdots\cdots + \int_{x_k}^{s} f(x)\cos\frac{m\pi x}{s}\,dx$$

We will evaluate the integrals on the right-hand side in turn:

$$(2.92)\quad \int_0^{x_1} f(x)\cos\frac{m\pi x}{s}\,dx = \int_0^{x_1} (z_0 + c_1 x)\cos\frac{m\pi x}{s}\,dx$$

$$= z_0\int_0^{x_1}\cos\frac{m\pi x}{s}\,dx + c_1\int_0^{x_1} x\cos\frac{m\pi x}{s}\,dx$$

$$= \frac{z_0 s}{m\pi}\sin\frac{m\pi x_1}{s} + c_1\left(\frac{s}{m\pi}\right)^2\left[\cos\frac{m\pi x}{s} + \frac{m\pi x}{s}\sin\frac{m\pi x}{s}\right]_0^{x_1}$$

$$= \frac{z_0 s}{m\pi}\sin\frac{m\pi x_1}{s} + c_1\left(\frac{s}{m\pi}\right)^2\left[\cos\frac{m\pi x_1}{s} + \frac{m\pi x_1}{s}\sin\frac{m\pi x_1}{s} - 1\right]$$

$$(2.93)\quad \int_{x_1}^{x_2} f(x)\cos\frac{m\pi x}{s}\,dx = \int_{x_1}^{x_2} (z_0 + c_1 x_1 + c_2 x - c_2 x_1)\cos\frac{m\pi x}{s}\,dx$$

$$= (z_0 + c_1 x_1 - c_2 x_1)\int_{x_1}^{x_2}\cos\frac{m\pi x}{s}\,dx + c_2\int_{x_1}^{x_2} x\cos\frac{m\pi x}{s}\,dx$$

$$= [z_0 + x_1(c_1 - c_2)]\left[\frac{s}{m\pi}\right]\left[\sin\frac{m\pi x_2}{s} - \sin\frac{m\pi x_1}{s}\right]$$

$$+ c_2\left(\frac{s}{m\pi}\right)^2\left[\cos\frac{m\pi x_2}{s} - \cos\frac{m\pi x_1}{s} + \frac{m\pi x_2}{s}\sin\frac{m\pi x_2}{s} - \frac{m\pi x_1}{s}\sin\frac{m\pi x_1}{s}\right]$$

$$(2.94)\quad \int_{x_2}^{x_3} f(x)\cos\frac{m\pi x}{s}\,dx = \int_{x_2}^{x_3} [z_0 + c_1 x_1 + c_2(x_2 - x_1) + c_3 x - c_3 x_2]\cdot\cos\frac{m\pi x}{s}\,dx$$

$$= [z_0 + x_1(c_1 - c_2) + x_2(c_2 - c_3)]\left[\left(\frac{s}{m\pi}\right)\right]\left[\sin\frac{m\pi x_3}{s} - \sin\frac{m\pi x_2}{s}\right]$$

$$+ c_3\left(\frac{s}{m\pi}\right)^2\left[\cos\frac{m\pi x_3}{s} - \cos\frac{m\pi x_2}{s} + \frac{m\pi x_3}{s}\sin\frac{m\pi x_3}{s} - \frac{m\pi x_2}{s}\sin\frac{m\pi x_2}{s}\right]$$

$$(2.95)\quad \int_{x_k}^{s} f(x)\cos\frac{m\pi x}{s}\,dx = \int_{x_k}^{s}\left[z_0 + c_1x_1 + c_2(x_2 - x_1) + \cdots\cdots + c_k(x_k - x_{k-1}) + c_{k+1}(x - x_k)\right]\cos\frac{m\pi x}{s}\,dx$$

$$= \left[z_0 + x_1(c_1 - c_2) + x_2(c_2 - c_3) + \cdots\cdots + x_k(c_k - c_{k+1})\right]\left[\frac{s}{m\pi}\right]\left[-\sin\frac{m\pi x_k}{s}\right]$$

$$+ c_{k+1}\left(\frac{s}{m\pi}\right)^2\left[\cos m\pi - \cos\frac{m\pi x_k}{s}\quad \frac{m\pi x_k}{s}\sin\frac{m\pi x_k}{s}\right]$$

Summing (2.92) through (2.95):

$$(2.96)\quad \int_0^s f(x)\cos\frac{m\pi x}{s}\,dx = \left(\frac{s}{m\pi}\right)\left\{[-x_1(c_1 - c_2)]\sin\frac{m\pi x_1}{s}\right.$$

$$+ [-x_2(c_2 - c_3)]\sin\frac{m\pi x_2}{s}$$

$$\vdots$$

$$\left. + [-x_n(c_k - c_{k+1})]\sin\frac{m\pi x_k}{s}\right\} + \left(\frac{s}{m\pi}\right)^2\left\{[c_1 - c_2]\cos\frac{m\pi x_1}{s}\right.$$

$$+ [c_2 - c_3]\cos\frac{m\pi x_2}{s}$$

$$\vdots$$

$$\left. + [c_k - c_{k+1}]\cos\frac{m\pi x_k}{s} + c_{k+1}\cos m\pi\right\} + \left(\frac{s}{m\pi}\right)^2\left\{[c_1 - c_2]\frac{m\pi x_1}{s}\sin\frac{m\pi x_1}{s}\right.$$

$$+ [c_2 - c_3]\frac{m\pi x_2}{s}\sin\frac{m\pi x_2}{s}$$

$$\vdots$$

$$\left. + [c_k - c_{k+1}]\frac{m\pi x_k}{s}\sin\frac{m\pi x_k}{s} - c_1\right\}$$

Simplifying:

$$(2.97)\quad \int_0^s f(x)\cos\frac{m\pi x}{s}\,dx = \left(\frac{s}{m\pi}\right)^2[(c_1 - c_2)\cos\frac{m\pi x_1}{s} + \cdots\cdots + (c_k - c_{k+1})\cos\frac{m\pi x_k}{s}$$

$$+ c_{k+1}\cos m\pi - c_1] = \left(\frac{s}{m\pi}\right)^2\left[c_{k+1}\cos m\pi - c_1 + \sum_{\ell=1}^{k}(c_\ell - c_{\ell+1})\cos\frac{m\pi x_\ell}{s}\right]$$

Therefore, from (2.86) and (2.97):

$$(2.98)\quad A_m = \frac{2}{sQ}\left[\left(\frac{s}{m\pi}\right)^2\left\{c_{k+1}\cos m\pi - c_1 + \sum_{\ell=1}^{k}(c_\ell - c_{\ell+1})\cos\frac{m\pi x_\ell}{s}\right\}\right]$$

Now to get an expression for A_0, we must expand:

$$(2.99)\quad \int_0^s f(x)dx = \int_0^{x_1} f(x)dx + \int_{x_1}^{x_2} f(x)dx + \cdots\cdots + \int_{x_k}^{s} f(x)dx$$

Evaluating these integrals separately:

$$(2.100)\quad \int_0^{x_1} f(x)dx = \int_0^{x_1} (z_0 + c_1 x)dx = z_0 x + \frac{c_1 x_1^2}{2}$$

$$(2.101)\quad \int_{x_1}^{x_2} f(x)dx = \int_{x_1}^{x_2} (z_0 + c_1 x_1 + c_2 x - c_2 x_1)dx = (z_0 x + c_1 x_1 x - c_2 x_1 x + \frac{c_2 x^2}{2}) \int_{x_1}^{x_2}$$

Therefore:

$$(2.102)\quad \int_{x_1}^{x_2} f(x)dx = z_0 x_2 + c_1 x_1 x_2 - c_2 x_1 x_2 + \frac{c_2 x_2^2}{2} - z_0 x_1 - c_1 x_1^2 + c_2 x_1^2 - \frac{c_2 x_1^2}{2}$$

$$(2.103)\quad \int_{x_2}^{x_3} f(x)dx = \int_{x_2}^{x_3} [z_0 + c_1 x_1 + c_2(x_2 - x_1) + c_3 x - c_3 x_2]dx$$

$$= z_0 x_3 - z_0 x_2 + (c_1 - c_2)x_1 x_3 + (c_2 - c_3)x_2 x_3$$

$$- (c_1 - c_2)x_1 x_2 + (\frac{c_3}{2} - c_2)x_2^2 + \frac{c_3 x_3^2}{2}$$

$$(2.104)\quad \int_{x_k}^{s} f(x)dx = \int_{x_k}^{s} [z_0 + c_1 x_1 + c_2(x_2 - x_1) + \ldots\ldots + c_k(x_k - x_{k-1})$$

$$+ c_{k+1}(x - x_k)]dx = z_0 s - z_0 x_k - (c_k - \frac{c_{k+1}}{2})x_k^2 + \frac{c_{k+1} s^2}{2}$$

$$+ (c_1 - c_2)(x_1 s - x_1 x_k) + (c_2 - c_3)(x_2 s - x_2 x_k)$$

$$+ \ldots\ldots + (c_{k-1} - c_k)(x_{k-1} s - x_{k-1} x_k) + (c_k - c_{k+1})x_k s$$

Summing (2.100) through (2.104):

$$(2.105)\quad \int_0^s f(x)dx = z_0 s + (c_2 - c_1)(\frac{x_1^2}{2} - x_1 s) + (c_3 - c_2)(\frac{x_2^2}{2} - x_2 s)$$

$$+ \ldots\ldots + (c_{k+1} - c_k)(\frac{x_k^2}{2} - x_k s) + \frac{c_{k+1}}{2} s^2$$

$$= z_0 s + \sum_{\ell=1}^{k} (c_{\ell+1} - c_\ell)(\frac{x_\ell^2}{2} - x_\ell s) + \frac{c_{k+1}}{2} s^2$$

Therefore from (2.87 and 2.105):

$$(2.106)\quad \frac{A_0}{2} = \frac{1}{s}\left[z_0 s + \frac{c_{k+1}}{2} s^2 + \sum_{\ell=1}^{k} (c_{\ell+1} - c_\ell)(\frac{x_\ell^2}{2} - x_\ell s)\right]$$

We have now completely solved the boundary value problem shown in Figure 2. The solution is:

$$(2.107a)\quad \phi_1(x,z) = \frac{A_0}{2} + \sum_{m=1}^{\infty} A_m \cos\frac{m\pi x}{s}\left[\cosh\frac{m\pi z}{s}(U) + \sinh\frac{m\pi z}{s}(Y)\right]$$

$$(2.107b)\quad \phi_2(x,z) = \frac{A_0}{2} + \sum_{m=1}^{\infty} A_m \cos\frac{m\pi x}{s}\left[\cosh\frac{m\pi z}{s}(W) + \sinh\frac{m\pi z}{s}(V)\right]$$

$$(2.107c)\quad \phi_3(x,z) = \frac{A_0}{2} + \sum_{m=1}^{\infty} A_m \cos\frac{m\pi x}{s}\cosh\frac{m\pi z}{s}$$

where

$$(2.107d)\quad \frac{A_0}{2} = \frac{1}{s}\left[z_0 s + \frac{c_{k+1}}{2} s^2 + \sum_{\ell=1}^{k} (c_{\ell+1} - c_\ell)\left(\frac{x_\ell^2}{2} - x_\ell s\right)\right]$$

$$(2.107e)\quad A_m = \frac{2}{sQ}\left[\left(\frac{s}{m\pi}\right)^2 \left\{c_{k+1} \cos m\pi - c_1 + \sum_{\ell=1}^{k} (c_\ell - c_{\ell+1}) \cos \frac{m\pi x_\ell}{s}\right\}\right]$$

$$(2.107f)\quad W = \cosh^2 \frac{m\pi r_2}{s} - \frac{K_3}{K_2} \sinh^2 \frac{m\pi r_2}{s}$$

$$(2.107g)\quad V = \frac{1 - W}{\tanh \frac{m\pi r_2}{s}}$$

$$(2.107h\quad T = \cosh^2 \frac{m\pi r_1}{s} - \frac{K_2}{K_1} \sinh^2 \frac{m\pi r_1}{s}$$

$$(2.107j)\quad R = \frac{1 = T}{\tanh \frac{m\pi r_1}{s}}$$

$$(2.107k)\quad U = (W)(T) + \cosh \frac{m\pi r_1}{s} \sinh \frac{m\pi r_1}{s} (V)\left(1 - \frac{K_2}{K_1}\right)$$

$$(2.107m)\quad Y = (W)(R) + (V)\left(1 + \frac{K_2}{K_1} - T\right)$$

$$(2.107n)\quad Q = \cosh \frac{m\pi z_0}{s} (U) + \sinh \frac{m\pi z_0}{s} (Y)$$

We may confirm this solution by showing that Laplace's equation is satisfied in each of the three layers and that each of the boundary conditions shown in Figure 4 is satisfied.

Consider first, the expression (2.107a) for ϕ_1:

$$(2.108)\quad \frac{\delta \phi_1}{\delta x}(x,z) = \sum_{m=1}^{\infty} A_m \left(\sin \frac{m\pi x}{s}\right) \frac{m\pi}{s}\left[\cosh \frac{m\pi z}{s} (U) + \sinh \frac{m\pi z}{s} (Y)\right]$$

and therefore:

$$(2.6a)\quad \frac{\delta \phi_1}{\delta x}(0,z) = 0$$

$$(2.6b)\quad \frac{\delta \phi_1}{\delta x}(s,z) = 0$$

Now from (2.107a) and (2.108):

$$\frac{\delta^2 \phi_1}{\delta x^2} = -\sum_{m=1}^{\infty} A_m \cos \frac{m\pi x}{s} \left(\frac{m\pi}{s}\right)^2 \left[\cosh \frac{m\pi z}{s} (U) + \sinh \frac{m\pi z}{s} (Y)\right]$$

and

$$\frac{\delta^2 \phi_1}{\delta z^2} = \sum_{m=1}^{\infty} A_m \cos \frac{m\pi x}{s} \left(\frac{m\pi}{s}\right)^2 \left[\cosh \frac{m\pi z}{s} (U) + \sinh \frac{m\pi z}{s} (Y)\right]$$

and Laplace's equation (2.5) is satisfied.

We can show, in exactly the same manner, that equations (2.7) and (2.9) for ϕ_2 and ϕ_3, and boundary conditions (2.8a), (2.8b), (2.10a) and (2.10b) are satisfied. To show (2.10c), we differentiate (2.107c) with respect to z to obtain:

$$\frac{\delta\phi_3}{\delta z} = \sum_{m=1}^{\infty}\left[A_m \cos\frac{m\pi x}{s}\sinh\frac{m\pi z}{s}\right]\frac{m\pi}{s}$$

Then

(2.10c) $$\frac{\delta\phi_3}{\delta z}(x,0) = 0$$

To check the interlayer boundary conditions, consider first (2.6d):

(2.109) $$\phi_1(x,r_1) = \frac{A_0}{2} + \sum_{m=1}^{\infty} A_m \cos\frac{m\pi x}{s}\left[\cosh\frac{m\pi r_1}{s}(U) + \sinh\frac{m\pi r_1}{s}(Y)\right]$$

(2.110) $$\phi_2(x,r_1) = \frac{A_0}{2} + \sum_{m=1}^{\infty} A_m \cos\frac{m\pi x}{s}\left[\cosh\frac{m\pi r_1}{s}(W) + \sinh\frac{m\pi r_1}{s}(V)\right]$$

We must show that the bracketed term of (2.109) is equal to the bracketed term of (2.110). Expanding this term by means of (2.107k and m):

$$\left[\cosh\frac{m\pi r_1}{s}(U) + \sinh\frac{m\pi r_1}{s}(Y)\right] = \cosh\frac{m\pi r_1}{s}(W)\left[\cosh^2\frac{m\pi r_1}{s} - \frac{K_2}{K_1}\sinh^2\frac{m\pi r_1}{s}\right]$$

$$+ \cosh^2\frac{m\pi r_1}{s}\sinh\frac{m\pi r_1}{s}(V)\left(1 - \frac{K_2}{K_1}\right)$$

$$+ \sinh\frac{m\pi r_1}{s}(W)\frac{\left(1 - \cosh^2\frac{m\pi r_1}{s} + \frac{K_2}{K_1}\sinh^2\frac{m\pi r_1}{s}\right)}{\tanh\frac{m\pi r_1}{s}}$$

$$+ \sinh\frac{m\pi r_1}{s}(V)\left(1 + \frac{K_2}{K_1} - \cosh^2\frac{m\pi r_1}{s} + \frac{K_2}{K_1}\sinh^2\frac{m\pi r_1}{s}\right)$$

$$= \cosh\frac{m\pi r_1}{s}(W) + \sinh\frac{m\pi r_1}{s}\left[\cosh^2\frac{m\pi r_1}{s}(V)\left(1 - \frac{K_2}{K_1}\right)\right.$$

$$\left. + (V)\left(1 - \cosh^2\frac{m\pi r_1}{s} + \frac{K_2}{K_1}\cosh^2\frac{m\pi r_1}{s}\right)\right] = \left[\cosh\frac{m\pi r_1}{s}(W) + \sinh\frac{m\pi r_1}{s}(V)\right]$$

Similarly, to check (2.8f):

(2.111) $$\phi_2(x,r_2) = \frac{A_0}{2} + \sum_{m=1}^{\infty} A_m \cos\frac{m\pi x}{s}\left[\cosh\frac{m\pi r_2}{s}(W) + \sinh\frac{m\pi r_2}{s}(V)\right]$$

(2.112) $$\phi_3(x,r_2) = \frac{A_0}{2} + \sum_{m=1}^{\infty} A_m \cos\frac{m\pi x}{s}\left[\cosh\frac{m\pi r_2}{s}\right]$$

and using (2.10f and g):

$$\left[\cosh\frac{m\pi r_2}{s}(W) + \sinh\frac{m\pi r_2}{s}(V)\right]$$

$$= \cosh^3\frac{m\pi r_2}{s} - \frac{K_3}{K_2}\cosh\frac{m\pi r_2}{s}\sinh\frac{m\pi r_2}{s} + \cosh\frac{m\pi r_2}{s}(1-W)$$

$$= \cosh\frac{m\pi r_2}{s}(W) + \cosh\frac{m\pi r_2}{s}(1-W)$$

$$= \left[\cosh\frac{m\pi r_2}{s}\right]$$

For boundary condition (2.6c) we have:

$$(2.113)\quad K_1 \frac{\delta\phi_1}{\delta z}(x,r_1) = \sum_{m=1}^{\infty} A_m \cos\frac{m\pi x}{s}\left[\sinh\frac{m\pi r_1}{s}(U) + \cosh\frac{m\pi r_1}{s}(Y)\right]\left(\frac{m\pi}{s}\right)K_1$$

$$(2.114)\quad K_2 \frac{\delta\phi_2}{\delta z}(x,r_1) = \sum_{m=1}^{\infty} A_m \cos\frac{m\pi x}{s}\left[\sinh\frac{m\pi r_1}{s}(W) + \cosh\frac{m\pi r_1}{s}(V)\right]\left(\frac{m\pi}{s}\right)K_2$$

Considering the portion of the summation in (2.113) which is not common to (2.114) we have, upon expansion:

$$K_1\left[\sinh\frac{m\pi r_1}{s}(U) + \cosh\frac{m\pi r_1}{s}(Y)\right]$$

$$= K_1\left[\sinh\frac{m\pi r_1}{s}(W)\left(\cosh^2\frac{m\pi r_1}{s} - \frac{K_2}{K_1}\sinh^2\frac{m\pi r_1}{s}\right) + \sinh^2\frac{m\pi r_1}{s}\cosh\frac{m\pi r_1}{s}(V)\left(1 - \frac{K_2}{K_1}\right)\right.$$

$$+ \cosh^2\frac{m\pi r_1}{s}(W)\frac{\left(1 - \cosh^2\frac{m\pi r_1}{s} + \frac{K_2}{K_1}\sinh^2\frac{m\pi r_1}{s}\right)}{\sinh\frac{m\pi r_1}{s}}$$

$$\left. + \cosh\frac{m\pi r_1}{s}(V)\left(1 + \frac{K_2}{K_1} - \cosh^2\frac{m\pi r_1}{s} + \frac{K_2}{K_1}\sinh^2\frac{m\pi r_1}{s}\right)\right]$$

$$= K_1\left[(W)\sinh\frac{m\pi r_1}{s}\cosh^2\frac{m\pi r_1}{s} - (W)\frac{K_2}{K_1}\sinh^3\frac{m\pi r_1}{s}\right.$$

$$+ (V)\sinh^2\frac{m\pi r_1}{s}\cosh\frac{m\pi r_1}{s} - (V)\frac{K_2}{K_1}\sinh^2\frac{m\pi r_1}{s}\cosh\frac{m\pi r_1}{s}$$

$$+ \frac{(W)\cosh^2\frac{m\pi r_1}{s}}{\sinh\frac{m\pi r_1}{s}} - \frac{(W)\cosh^4\frac{m\pi r_1}{s}}{\sinh\frac{m\pi r_1}{s}} + (W)\frac{K_2}{K_1}\cosh^2\frac{m\pi r_1}{s}\sinh\frac{m\pi r_1}{s}$$

$$\left. + (V)\cosh\frac{m\pi r_1}{s} + (V)\frac{K_2}{K_1}\cosh\frac{m\pi r_1}{s} - (V)\cosh^3\frac{m\pi r_1}{s} + (V)\frac{K_2}{K_1}\cosh\frac{m\pi r_1}{s}\sinh^2\frac{m\pi r_1}{s}\right]$$

$$= K_1\left[\frac{K_2}{K_1}(W)\sinh\frac{m\pi r_1}{s} + \frac{K_2}{K_1}(V)\cosh\frac{m\pi r_1}{s}\right]$$

$$= K_2\left[\sinh\frac{m\pi r_1}{s}(W) + \cosh\frac{m\pi r_1}{s}(V)\right]$$

and (2.6c) is satisfied. The final interlayer condition is (2.8e) and:

$$(2.115)\quad K_2 \frac{\delta\phi_2}{\delta z}(x,r_2) = \sum_{m=1}^{\infty} A_m \cos\frac{m\pi x}{s}\left[\sinh\frac{m\pi r_2}{s}(W) + \cosh\frac{m\pi r_2}{s}(V)\right]\left(\frac{m\pi}{s}\right)K_2$$

$$(2.116)\quad K_3 \frac{\delta\phi_3}{\delta z}(x,r_2) = \sum_{m=1}^{\infty} A_m \cos\frac{m\pi x}{s}\left[\sinh\frac{m\pi r_2}{s}\right]\left(\frac{m\pi}{s}\right)K_3$$

Expanding the non-common portion of the summation in (2.115):

$$K_2\left[\sinh\frac{m\pi r_2}{s}(W) + \cosh\frac{m\pi r_2}{s}(V)\right]$$

$$= K_2\left[\sinh\frac{m\pi r_2}{s}(W) + \frac{\cosh^2\frac{m\pi r_2}{s}(1-W)}{\sinh\frac{m\pi r_2}{s}}\right]$$

$$= \frac{K_2\left[\sinh^2\frac{m\pi r_2}{s}(W) + \cosh^2\frac{m\pi r_2}{s} - (W)\cosh^2\frac{m\pi r_2}{s}\right]}{\sinh\frac{m\pi r_2}{s}}$$

$$= \frac{K_2\left[(W)(-1) + \cosh^2\frac{m\pi r_2}{s}\right]}{\sinh\frac{m\pi r_2}{s}}$$

$$= \frac{K_2\left[-\cosh^2\frac{m\pi r_2}{s} + \frac{K_3}{K_2}\sinh^2\frac{m\pi r_2}{s} + \cosh^2\frac{m\pi r_2}{s}\right]}{\sinh\frac{m\pi r_2}{s}}$$

$$= K_3\left[\sinh\frac{m\pi r_2}{s}\right]$$

The only remaining boundary condition to be satisfied is (2.6e): $\phi_1(x,z_0) = f(x)$ where f(x) is given by (2.6f). It is not possible to check this boundary condition by merely substituting $z = z_0$ in (2.107a) in the usual manner, as it is as difficult to tell whether the resulting series satisfies the boundary condition as it is to tell whether the original series represents the solution. Fortunately, we can make reference to some applicable Fourier series theory. The so-called Dirichlet conditions, stated below, guarantee that the upper boundary condition is satisfied:

> "If f(x) is a bounded periodic function which in any one period has at most a finite number of maxima and minima and a finite number of points of discontinuity, then the Fourier series of f(x) converges to f(x) at all points where f(x) is continuous and converges to the average value of the right- and left-hand limits of f(x) at each point where f(x) is discontinuous" (Wylie, 1960).

It is possible to show directly that the upper boundary condition is satisfied for the two end points of the boundary for the case of a single uniform slope from x = 0 to x = s. In this case k = 0, $c_{k+1} = c_1 = c$ and we have from (2.107a):

$$(2.117)\quad \phi_1(x,z_0) = \frac{A_0}{2} + \sum_{m=1}^{\infty} A_m \cos\frac{m\pi x}{s}\left[\cosh\frac{m\pi z_0}{s}(U) + \sinh\frac{m\pi z_0}{s}(Y)\right]$$

or using expressions (2.107d, e and n):

$$\phi_1(x,z_0) = \frac{1}{s}\left[z_0 s + \frac{cs^2}{2}\right] + \sum_{m=1}^{\infty}\left[\frac{2s}{Q\pi^2 m^2}(c\cos m\pi - c)\cos\frac{m\pi x}{s}\right][Q]$$

$$= z_0 + \frac{cs}{2} + \frac{2cs}{\pi^2}\sum_{m=1}^{\infty}(\cos m\pi - 1)\cos\frac{m\pi x}{2}\cdot\frac{1}{m^2}$$

$$= z_0 + \frac{cs}{2} - \frac{4cs}{\pi^2}\sum_{m=1,3,5\ldots.}^{\infty}\frac{1}{m^2}\cos\frac{m\pi x}{s}$$

For x = s we have

$$\phi_1(s,z_0) = z_0 + \frac{cs}{2} + \frac{4cs}{\pi^2}\sum_{m=1,3,5\ldots.}^{\infty}\frac{1}{m^2}$$

But it can be shown (Olmsted, 1959) that:

$$(2.118)\quad \sum_{m=1,3,5,\ldots}^{\infty} \frac{1}{m^2} = \frac{\pi^2}{8}$$

Therefore:

$$(2.119)\quad \phi_1(s,z_o) = z_o + \frac{cs}{2} + \frac{4cs}{\pi^2} \cdot \frac{\pi^2}{8} = z_o + cs$$

Similarly:

$$(2.120)\quad \phi_1(0,z_o) = z_o + \frac{cs}{2} - \frac{4cs}{\pi^2} \cdot \frac{\pi^2}{8} = z_o$$

REDUCTION OF GENERAL SOLUTION TO SIMPLER CASES

The three-layer case with generalized topographic configuration is not the most general problem which can be treated analytically. For example, it would be possible to develop a solution for the n-layer case. It is felt, however, that the three-layer case represents the logical limit to which analytical solutions need be taken. The introduction of more boundary conditions would only result in an excessive amount of laborious mathematics and would lead to solutions which are so cumbersome that evaluation at enough points to define a flow pattern might prove prohibitive, even with the help of a digital computer. Numerical methods, described in Chapter 3, offer a far more suitable method of tackling these more complicated problems.

Of more practical interest is the reduction of the solution developed in the preceding section for the three-layer case to that of simpler cases. In this section, solutions for the two-layer case with generalized topography and the homogeneous case with three different topographic configurations are presented.

Two-Layer Case with Generalized Water Table

If we let $K_3 = K_2$ (Figure 4a) in (2.107f), the expression for W becomes:

$$(2.107f)\quad W = \cosh^2 \frac{m\pi r_2}{s} - \frac{K_3}{K_2} \sinh^2 \frac{m\pi r_2}{s} = 1$$

V then becomes, from (2.107g):

$$V = \frac{1 - W}{\tanh \frac{m\pi r_2}{s}} = 0$$

The expressions for T and R remain unchanged but, upon inserting W = 1 and V = 0 in (2.107k and m), U and Y become:

$$(2.107k)\quad U = (W)(T) + \cosh \frac{m\pi r_1}{s} \cdot \sinh \frac{m\pi r_1}{s} (V) \left(1 - \frac{K_2}{K_1}\right) = T$$

$$(2.107m)\quad Y = (W)(R) + (V)\left(1 + \frac{K_2}{K_1} - T\right) = R$$

Therefore:

$$(2.107n)\quad Q = \cosh \frac{m\pi z_o}{s} (U) + \sinh \frac{m\pi z_o}{s} (Y) = \cosh \frac{m\pi z_o}{s} (T) + \sinh \frac{m\pi z_o}{s} (R)$$

The solution (2.107) therefore reduces to:

$$(2.121a)\quad \phi_1(x,z) = \frac{A_0}{2} + \sum_{m=1}^{\infty} A_m \cos\frac{m\pi x}{s}\left[\cosh\frac{m\pi z}{s}\,(T) + \sinh\frac{m\pi z}{s}\,(R)\right]$$

$$(2.121b)\quad \phi_2(x,z) = \frac{A_0}{2} + \sum_{m=1}^{\infty} A_m \cos\frac{m\pi x}{s}\left[\cosh\frac{m\pi z}{s}\right]$$

$$(2.121c)\quad \phi_3(x,z) = \frac{A_0}{2} + \sum_{m=1}^{\infty} A_m \cos\frac{m\pi x}{s}\left[\cosh\frac{m\pi z}{s}\right]$$

As is to be expected, $\phi_2(x,z) = \phi_3(x,z)$ and the definition of r_2 is rendered meaningless. If we let $r_1 = r$ the solution to the two-layer problem with generalized topography (Figure 5d) is:

$$(2.122a)\quad \phi_1(x,z) = \frac{A_0}{2} + \sum_{m=1}^{\infty} A_m \cos\frac{m\pi x}{s}\left[\cosh\frac{m\pi z}{s}\,(T) + \sinh\frac{m\pi z}{s}\,(R)\right]$$

$$(2.122b)\quad \varphi_2(x,z) = \frac{A_0}{2} + \sum_{m=1}^{\infty} A_m \cos\frac{m\pi x}{s}\cosh\frac{m\pi z}{s}$$

where:

$$(2.122c)\quad \frac{A_0}{2} = \frac{1}{s}\left[z_0 s + \frac{c_{k+1}}{2}s^2 + \sum_{\ell=1}^{k}(c_{\ell+1} - c_\ell)\left(\frac{x_\ell^2}{2} - x_\ell s\right)\right]$$

$$(2.122d)\quad A_m = \frac{2}{sQ}\left\{\left(\frac{s}{m\pi}\right)^2\left[c_{k+1}\cos m\pi - c_1 + \sum_{\ell=1}^{k}(c_\ell - C_{\ell+1})\cos\frac{m\pi x_\ell}{s}\right]\right\}$$

$$(2.122e)\quad T = \cosh^2\frac{m\pi r}{s} - \frac{K_2}{K_1}\sinh^2\frac{m\pi r}{s}$$

$$(2.122f)\quad R = \frac{1 - T}{\tanh\dfrac{m\pi r}{s}}$$

$$(2.122g)\quad Q = \cosh\frac{m\pi z_0}{s}\,(T) + \sinh\frac{m\pi z_0}{s}\,(R)$$

Homogeneous Case

To reduce the two-layer solution (2.122) to the homogeneous case with generalized topography (Figure 5c) let

$K_2 = K_1$. Then $T = 1$, $R = 0$, $Q = \cosh\dfrac{m\pi z_0}{s}$ and

$$(2.123a)\quad \phi(x,z) = \frac{A_0}{2} + \sum_{m=1}^{\infty} A_m \cos\frac{m\pi x}{s}\cosh\frac{m\pi z}{s}$$

where:

$$(2.123b)\quad \frac{A_0}{2} = \frac{1}{s}\left[z_0 s + \frac{c_{k+1}}{2}s^2 + \sum_{\ell=1}^{k}(c_{\ell+1} - c_\ell)\left(\frac{x_\ell^2}{2} - x_\ell s\right)\right]$$

$$(2.123c)\quad A_m = \frac{2}{s\cosh\dfrac{m\pi z_0}{s}}\left\{\left(\frac{s}{m\pi}\right)^2\left[c_{k+1}\cos m\pi - c_1 + \sum_{\ell=1}^{k}(c_\ell - c_{\ell+1})\cos\frac{m\pi x_\ell}{s}\right]\right\}$$

As an example, consider the topographic configuration shown in Figure 5b representing a flat

valley with steep flanks leading up to a shallow regional slope. In the notation of the generalized topography (Figure 4), k = 2 so that (2.123b and c) yield:

$$(2.124)\quad \frac{A_0}{2} = \frac{1}{s}\left[z_0 s + \frac{c_3}{2}s^2 + (c_2 - c_1)\left(\frac{x_1}{2}^2 - x_1 s\right) + (c_3 - c_2)\left(\frac{x_2}{2}^2 - x_2 s\right)\right]$$

$$(2.125)\quad A_m = \frac{2}{s \cosh \frac{m\pi z_0}{s}}\left\{\left(\frac{s}{m\pi}\right)^2\left[c_3 \cos m\pi - c_1 + (c_1 - c_2)\cos\frac{m\pi x_1}{s} + (c_2 - c_3)\cos\frac{m\pi x_2}{s}\right]\right\}$$

The simplest topographic configuration is a uniform valley slope as shown in Figure 5a. In this case $k = 0$, $c_1 = c_{k+1} = c$ and

$$(2.126)\quad \frac{A_0}{2} = \frac{1}{s}\left[z_0 s + \frac{cs^2}{2}\right]$$

$$(2.127)\quad A_m = \frac{2}{s \cosh \frac{m\pi z_0}{s}}\left\{\left(\frac{s}{m\pi}\right)^2\left[c \cos m\pi - c\right]\right\}$$

Therefore:

$$(2.128)\quad \psi(x,z) = \frac{1}{s}\left[z_0 s + \frac{cs^2}{2}\right] + \sum_{m=1}^{\infty}\left[\frac{2}{s}\frac{1}{\cosh\frac{m\pi z_0}{s}}\right]\left[\left(\frac{s}{m\pi}\right)^2(c\cos m\pi - c)\right]\cos\frac{m\pi x}{s}\cosh\frac{m\pi z}{s}$$

$$= z_0 + \frac{cs}{2} - \frac{4gcs}{\pi^2}\sum_{m=1,3,5\ldots}^{\infty}\frac{\cos\frac{m\pi x}{s}\cosh\frac{m\pi z}{s}}{m^2\cosh\frac{m\pi z_0}{s}}$$

This is the solution presented by Tóth (1962).

The five solutions which have been developed in this and the preceding section are summarized in Figure 5 (a through e) beginning with the simplest (Tóth) solution and proceeding to the general three-layer solution.

DIGITAL COMPUTATION

Equation (2.107 a through n) representing the analytical solution to the two-dimensional, three-layer problem with generalized water-table configuration has been programmed, in Fortran IV language, for solution on a digital computer. The required input data are the values of the parameters which describe the geometry and properties of the model. The output is in the form of tables of values of the potential at a specified number of points in the field. In addition, a subroutine has been written, for use on an off-line plotter, which contours the resulting values of ϕ and produces a plotted equipotential net. The complete program printout, a list of variables, an explanation of the required input data and its necessary format, and a list of recommended values for certain computing parameters can be found in Appendix A.

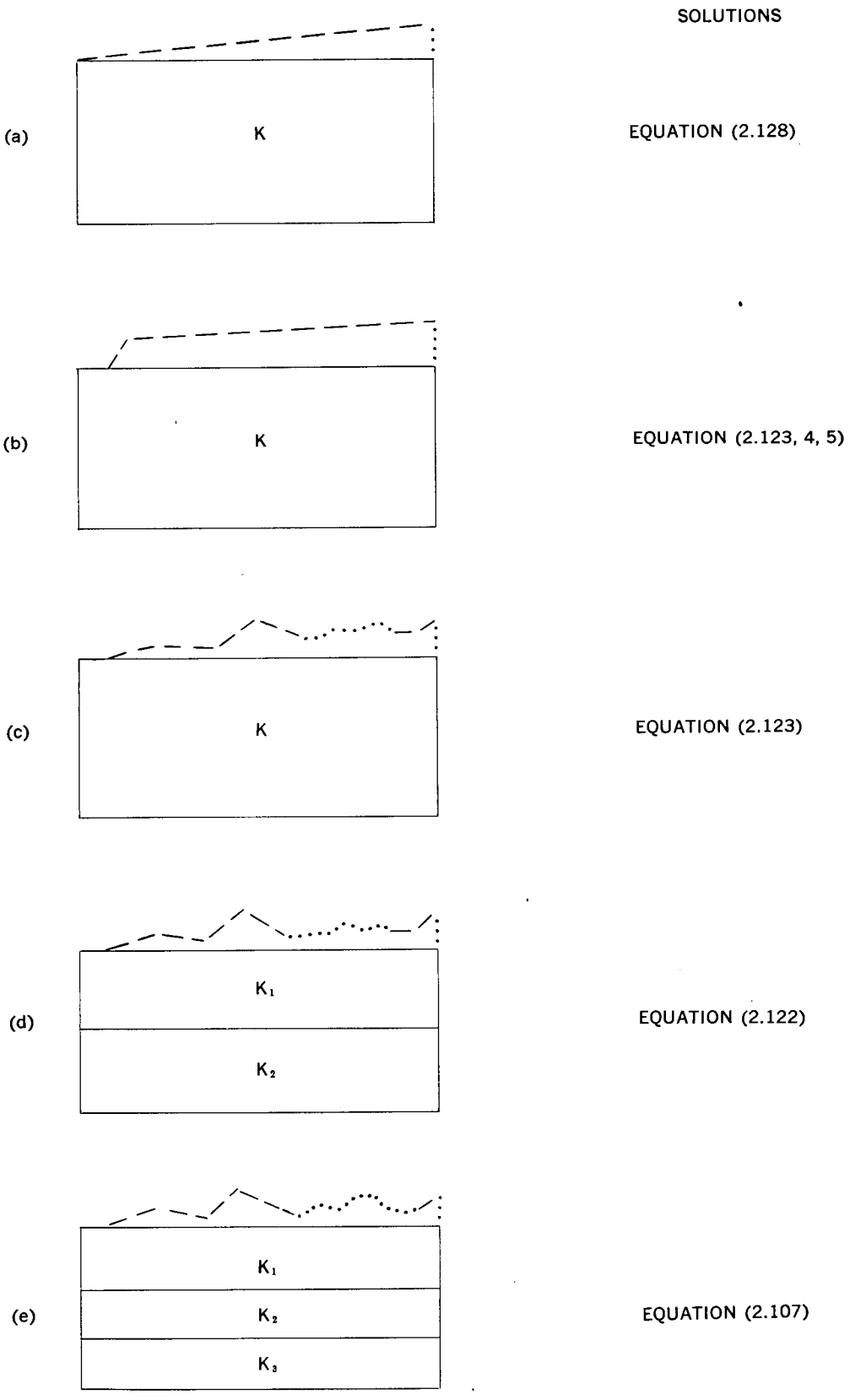

Figure 5. Analytical solutions

This program can, of course, be used for all simpler cases (for example, the homogeneous case) by an appropriate valuation of the parameters.

SELECTED RESULTS FOR COMPARISON WITH THE PREVIOUS ANALYTICAL SOLUTIONS OF TÓTH

Figure 6a shows the potential distribution for a basin with s = 20,000 ft, z_0 = 10,000 ft (i.e., a depth/s ratio of 0.5) and a water table with a constant regional slope of 0.02. The analytical program (Appendix I) was used to calculate the value of the potential at about 5,000 points arranged in an equally-spaced 101 X 51 grid. Referring to Figure 4, the homogeneous basin is simulated by putting $K_1 = K_2 = K_3$ and assigning arbitrary values (which must lie between 0 and z_0) to r_1 and r_2. Similarly, the simple slope is obtained by setting k = 0 and c_1 = 0.02. The result is identical to Figure 3 of Tóth (1962).

Figure 6b is a recomputation of Figure 2g of Tóth (1963b). The water-table configuration is a sine curve imposed on a regional slope of 0.02. The amplitude of the sine curve is 200 ft; the wave length is 5,000 ft. Tóth's solution was programmed and used to obtain this potential pattern.

Figure 6c shows the result when the sine curve is approximated by a series of straight-line segments and the analytical program (Appendix A) is used to calculate the potentials. Even with the rather gross approximation of the sine curve used in Figure 6c, the results are nearly identical with those of Figure 6b. An even closer match could be obtained by considering a more complex configuration of generalized water table, using more straight-line segments to represent the sine curve. It is felt that Figure 6c demonstrates the ability of the generalized water table to approximate, to a very high degree of accuracy, the potential pattern arising from any water table configuration.

APPLICATIONS OF CONFORMAL MAPPING

One of the most displeasing assumptions of the analytical method is that of the rectangular approximation, whereby the polygonal shape of the field (Figure 3) is represented by a rectangle. It is logical to investigate the possibility of avoiding this approximation by the use of conformal mapping.

Conformal mapping is an applied technique of the theory of complex variables by which a region, in which a function is defined which satisfies Laplace's equation, may be transformed into a simpler region where an analytical solution is available. The conformal transformation which is ostensibly applicable to the problem of two-dimensional regional groundwater flow is the so-called Schwarz-Christoffel transformation which maps the upper half plane of the complex, plane onto the interior of a polygon in the image plane. Our problem is just the reverse; we wish to transform the interior of the polygon onto the upper half plane, obtain an analytical solution for the potential function ϕ in this region and then transform the answers back again.

We will present the conclusion to this investigation first. The Schwarz-Christoffel transformation which, in theory, is capable of performing the transformation we wish, cannot be applied in practice to an irregular polygon with more than three finite vertices. By way of explanation, the following brief outline of the theory (after Wylie, 1960) is presented.

The mapping function is given by:

$$(2.129)\quad W = K \int [(z - x_1)^{(\alpha_1/\pi)-1} \cdot (z - x_2)^{(\alpha_2/\pi)-1} \cdots \cdots (z - x_n)^{(\alpha_n/\pi)-1}]dz + c$$

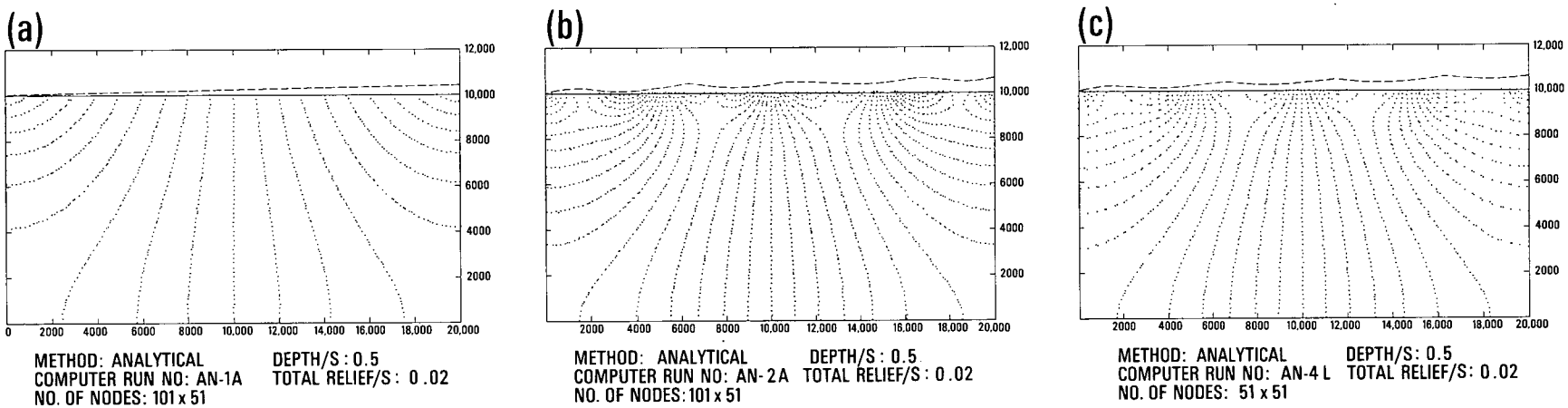

Figure 6. Comparison of general analytical solution with Tóth's solutions

where:

W = image in the W-plane of any point z in the upper half plane of the z-plane.

$x_1, x_2 \ldots\ldots x_n$ = points on the x-axis (real axis) in the x-plane such that the image of the point x_1 under the transformation is the point W_1 in the W-plane. Similarly, $x_2 \rightarrow W_2, \ldots\ldots x_n \rightarrow W_n$ and $W_1, W_2, \ldots\ldots W_n$ form a polygon in the image plane.

$\alpha_1, \alpha_2 \ldots\ldots \alpha_n$ = interior angles of the polygon at the vertices $W_1, W_2, \ldots\ldots W_n$ in the W-plane.

K,C = arbitrary constants.

One can think of (2.129) as the result of two transformation:

$$t = \int [\,''\,]\, dz \tag{2.130}$$

$$W = Kt + C \tag{2.131}$$

The first transforms the x-axis into some polygon; the second translates, rotates and dilates it. If the polygon determined by (2.130) is similar to the given polygon, the constants K and C in (2.131) can be determined to make the two polygons coincide.

To guarantee the similarity of the two polygons, the corresponding angles must be equal and the corresponding sides must be proportional. For polygons of n sides, (n-3) conditions, apart from the equality of corresponding angles, are necessary for similarity. Hence in mapping a polygon of n sides onto a half plane, three of the image points $x_1, x_2, \ldots\ldots x_n$ can be assigned arbitrarily and the remaining n-3 are determined by the n-3 conditions of similarity.

One can see that for n=3 (triangle) all three points x_1, x_2, x_3 can be arbitrarily chosen, and they can be chosen in such a way that the integration in (2.129) is a simple one, in terms of elementary functions. For an n-sided polygon, the resulting integration is usually impossible to carry out; the only exceptions are the so-called degenerate polygons where one or more of the vertices lie at infinity. Since our polygon involves only finite vertices, the Schwarz-Christoffel transformation is inapplicable.

For a complete account of the theory of conformal mapping, the reader is referred to Churchill (1960); an excellent account of the Schwarz-Christoffel transformation is given by Walker (1933); Kober (1957) has prepared a "Dictionary of Conformal Representations" which includes the Schwarz-Christoffel transformation. Harr (1962), Polubarinova-Kochina (1962), Luthin (1957), and Muskat (1946) all contain examples of the application of conformal mapping to hydrogeological problems.

CHAPTER 3

Numerical Solutions

MATHEMATICAL MODEL FOR NUMERICAL METHOD

The partial differential equations which mathematically describe the two-dimensional steady-state regional flow of groundwater have been shown in Chapter 1 to be Laplace's equation:

$$(3.1)\quad \frac{\delta^2\phi}{\delta x^2} + \frac{\delta^2\phi}{\delta z^2} = 0 \quad \text{or} \quad \phi_{xx} + \phi_{zz} = 0$$

for the case of homogeneous permeability; and Richards' equation:

$$(3.2)\quad \frac{\delta}{\delta x}\left[K(x,z)\,\frac{\delta\phi}{\delta x}\right] + \frac{\delta}{\delta z}\left[K(x,z)\,\frac{\delta\phi}{\delta z}\right] = 0$$

$$\text{or}\quad [K(x,z)\ \phi_x]_x + [K(x,z)\phi_z]_z = 0$$

for the non-homogeneous case; where:

$\phi(x,z)$ = hydraulic head = hydraulic potential expressed as the head of water above same datum plane

$K(x,z)$ = permeability

and x and z are the horizontal and vertical coordinate directions. These equations define the flow in a vertical two-dimensional field bounded by the water table on top, a real impermeable boundary on the bottom, and vertical imaginary impermeable boundaries on either side. The following boundary conditions applied to either Laplace's or Richards' equation define the representative boundary value problem (Figure 7a).

$$(3.3)\quad \frac{\delta\phi}{\delta z}(x,0) = 0 \qquad \text{or} \quad \varphi_z(x,0) = 0$$

$$\frac{\delta\phi}{\delta x}(0,z) = 0 \qquad \text{or} \quad \phi_x(0,z) = 0$$

$$\frac{\delta\phi}{\delta x}(s,z) = 0 \qquad \text{or} \quad \phi_x(s,z) = 0$$

$\phi = f(x)$ along the water table.

Analytical solutions to this problem have been given in Chapter 2. They suffer from three severe limitations: the restriction to two dimensions; the rectangular approximation; and the restriction to homogeneous or layered cases.

These limitations are all removed by the use of numerical methods. The field within which the solutions are valid is the complete cross-section (of Figure 7a for example). Both Richards' equation and Laplace's equation are treated in a similar manner and there is no limitation on the geometry of the permeability contrasts. In addition, permeabilities which vary continuously with depth or distance, and anisotropic conditions are easily handled. Three-dimensional problems are also amenable to numerical treatment and such problems are discussed in a separate section following the two-dimensional development.

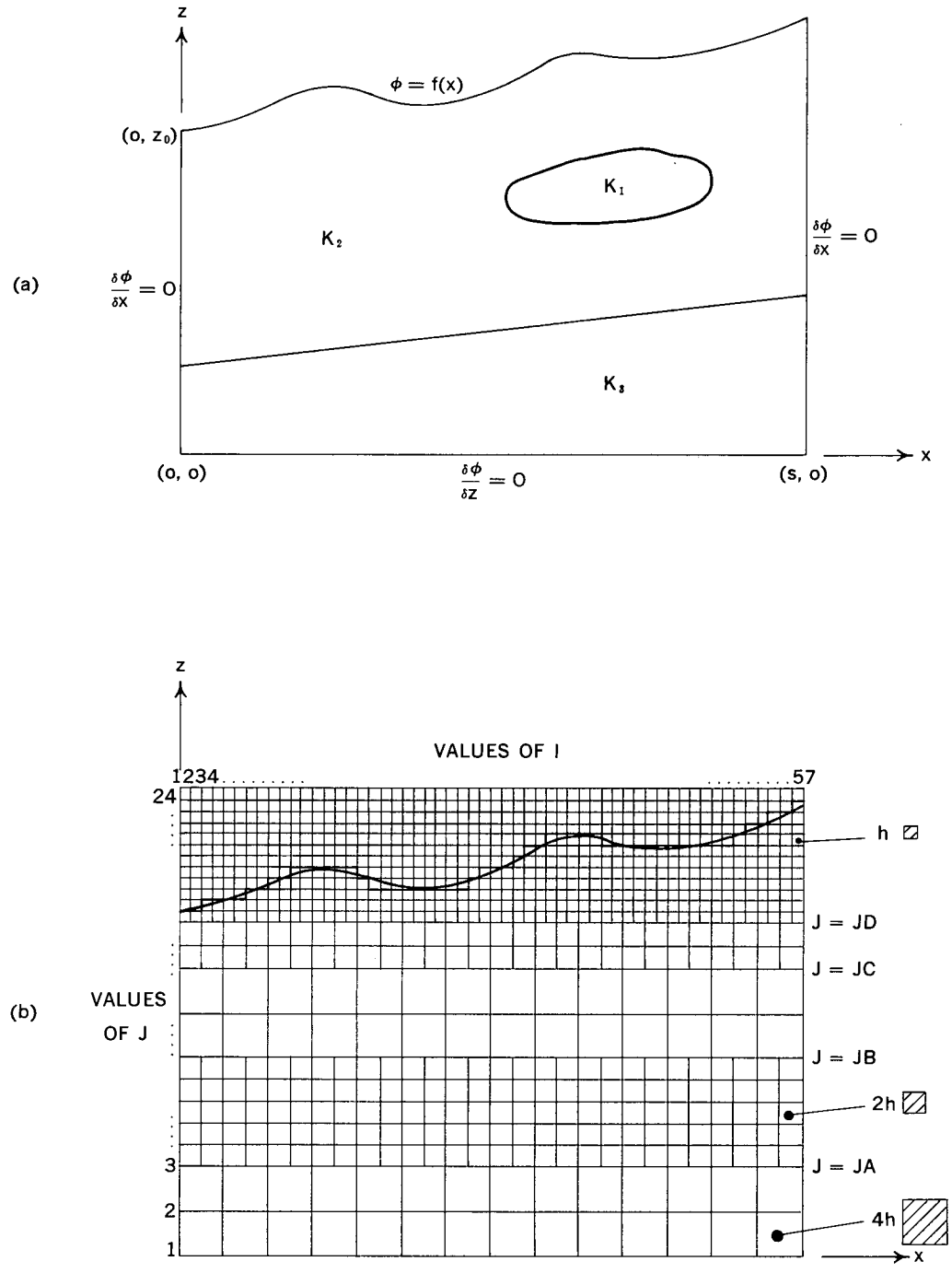

Figure 7. Mathematical model for numerical method

In any numerical technique for solving a partial differential equation, the continuum of points (x,z) making up the field and its boundaries are replaced by a finite set of points (x_p, z_p) arranged in a grid over the region. The partial differential equation (3.1) or (3.2) which determines ϕ (x,z) over the field is then replaced by a finite system of simultaneous linear equations, one equation for each meshpoint. This process is known as discretization and the resulting equations are finite-difference equations. If a mesh containing n nodes is used, the value of ϕ at each of these n points is determined by the solution of the system of n simultaneous linear finite-difference equations. The resulting value ϕ (x_p, z_p) for the meshpoint (x_p, z_p) is considered as a representative value of ϕ (x,z) for a small two-dimensional region of nearby points (x,z) of the field.

The discretization of a partial differential equation boundary value problem and its ultimate solution on a digital computer involves the following series of operations and decisions:

1. A suitable mesh must be chosen.
2. Finite-difference equations must be developed for the interior points of the mesh.
3. Finite-difference equations which suitably represent the boundary conditions must be developed for points on the boundary.
4. Finite-difference equations must be developed for the exceptional points of the mesh, such as along boundaries between different mesh spacings.
5. A method of solution of the resulting system of equations must be chosen.
6. The results of (1.) to (5.) must be programmed for solution on a digital computer.

Each of these aspects of the problem will be discussed in the following sections.

Since the development of the finite difference equations differs slightly between Laplace's and Richards' equation, the homogeneous and non-homogeneous cases will be treated separately.

TWO-DIMENSIONAL HOMOGENEOUS CASE

Mesh

A regular, square, graded mesh, as shown in Figure 7b has been chosen for the solution of both homogeneous and non-homogeneous problems. The term "regular" means that in any given coordinate direction the mesh spacing is constant within each subdivision of the graded net. Forsythe and Wasow (1960) have noted two considerations which favour the regular spacing of nodes in digital computing. First, for irregular nets the determination of the appropriate finite-difference equations to replace the partial differential equation requires an amount of computation which may be prohibitive. Second, for maximum speed, automatic computers demand simplicity of structure in a problem and regular networks are much simpler than irregular ones. Of the available regular meshes (square, rectangular, triangular, hexagonal, etc.) the square net and the rectangular net are the most suitable for the present problem. The availability of the finite-difference mathematics and error analyses for square nets is an added advantage to the non-professional mathematician.

A "graded" net is one in which several degrees of refinement of mesh spacing are used. In the present problem the field is subdivided into five horizontal strips with three different mesh spacings (h, 2h and 4h) as shown in Figure 7b. These are two reasons for using this graded net:

1. The water-table configuration must be approximated by a series of straight-line segments joining various mesh points; a large number of nodes in this region allows a more accurate approximation. On the other hand, the construction of equipotential contours in the lower region does not require this much refinement and a sparser network can be used.
2. A refined mesh is needed to reveal the solution in more detail in interesting regions within the overall field. Such regions are most likely to occur in the upper zone near the surface or as horizontal aquifers or aquicludes at depth; hence the inclusion of the horizontal zones of intermediate mesh spacing (2h).

The method of identifying nodal points can be described with reference to Figure 7b. Each vertical line in the mesh is designated by the notation I = 1, I = 2,. . . . . , I = N; each horizontal line is denoted by J = 1, J = 2,. . . . . , J = L (N = 57, L = 24 in the diagram); the intersection of the Ith vertical line with the Jth horizontal line represents the location of the node (I,J). In the graded mesh many of the vertical lines do not extend across the full field and along such lines, nodal points exist only where the line is defined. For example, there are no nodes at the intersections of the line I = 3 with the horizontal lines J = 1,2,9 or 10. The total number of nodes is thus considerably less than N x L.

The boundaries between regions of different mesh spacing occur along the horizontal nodal lines J = JA, J = JB, J = JC, and J = JD (JA = 3, JB = 8, JC = 10, JD = 12 in the example). These four values are input parameters in the programmed solution and can be varied to suit the needs of each individual problem. In fact, certain of the zones may be omitted, if desired, to create a simpler mesh. In all, seven different networks can be defined by the appropriate designation of the parameters JA, JB, JC and JD. They are denoted by MESH = 1, MESH = 2, ... , MESH = 7 and are shown schematically on Figure 8. MESH = 7 is the general network previously shown in Figure 7b. It should be noted that the refinement across a given interface is always half the larger mesh spacing. This is a necessary condition in the development of the finite-difference equations for interfacial nodes.

While the use of a graded mesh from the point of view expressed above is desirable, in practice a severe limitation on its use was found to exist. This limitation lies in the difficulty of defining the optimum relaxation factor. The nature of this parameter and the difficulties associated with it when working with a graded mesh are discussed later in this chapter under the heading "Solution of finite-difference equations" and in Appendix B where the computer program for the numerical method is presented. Of the six numerical computer programs written, only one incorporates the seven graded meshes. A regular square or rectangular mesh has been used throughout the rest of the study. In the interests of completeness and generality, however, the following sections include discussions of the graded as well as uniform meshes.

Finite-Difference Equations for Interior Nodes

An interior node is one which occurs within one of the graded subdivisions of the field; it does not lie on an external boundary nor on an interfacial boundary between different mesh sizes. Such a node has four neighbouring nodes equidistant from it.

To find the finite-difference equation for an interior node in the homogeneous case, we must replace the second order partial derivatives of Laplace's equation:

$$(3.1)\quad \phi_{xx} + \phi_{zz} = 0$$

by differences. Let us consider the first term of this equation first. recall that the definition of the partial derivative with respect to x of a function of two variables $\phi(x,z)$ is:

$$(3.4)\quad \frac{\delta\phi}{\delta x} = \lim_{h \to 0} \frac{\phi(x + h,z) - \phi(x,z)}{h}$$

On a digital computer it is impossible to take the limit as h→0 but it is possible to approximate the limit by assigning to h some arbitrarily small value; in fact, we have already done so by designing a nodal network with a mesh spacing of h.

For any value of z, say z_0, we can now expand $\phi(x,z_0)$ in a two-term Taylor's series expansion about the point (x_0, z_0) as follows:

$$(3.5)\quad \phi(x,z_0) = \phi(x_0,z_0) + (x - x_0)\,\phi_x(x_0,z_0) + \frac{(x - x_0)^2}{2}\,\phi_{xx}(\xi,z_0)$$

where: $x \leqslant \xi \leqslant x_0$ and $\frac{(x - x_0)^2}{2}\,\phi_{xx}(\xi,z_0)$ is the Lagrangian form of the remainder (Sokolnikoff and Redheffer, 1958). If we let $x = x_0 + h$ (this is known as a forward difference, see Figure 9a), equation (3.5) becomes:

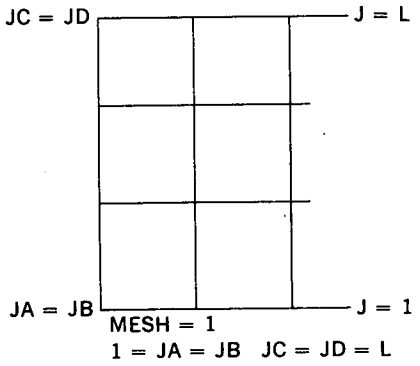

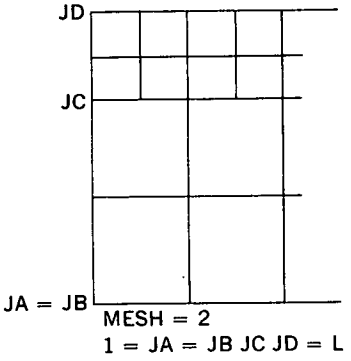

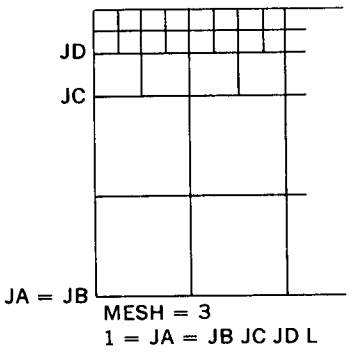

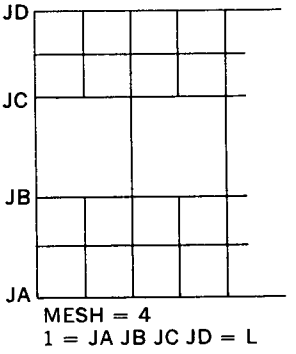

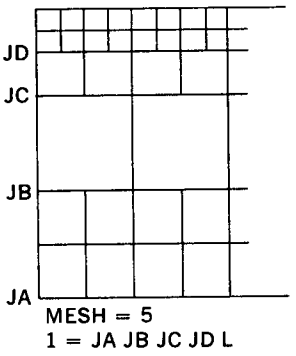

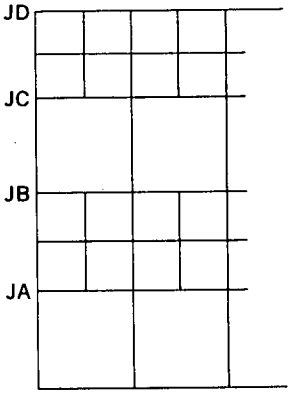

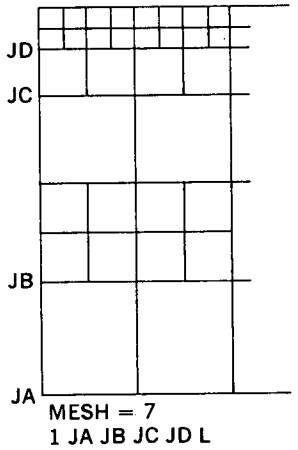

NOTE:

1. ALL LAYERS OF A GIVEN MESH SPACING MUST BE AT LEAST 2 NODAL SPACINGS HIGH
   E.G. MESH = 5 : JB − JA ⩾ 2
   JC − JB ⩾ 2
2. THE WATER-TABLE CONFIGURATION MUST BE APPROXIMATED BY NODES ENTIRELY WITHIN THE UPPERMOST SUBDIVISION (I.E. SMALLEST MESH SPACING)

Figure 8. Computing meshes

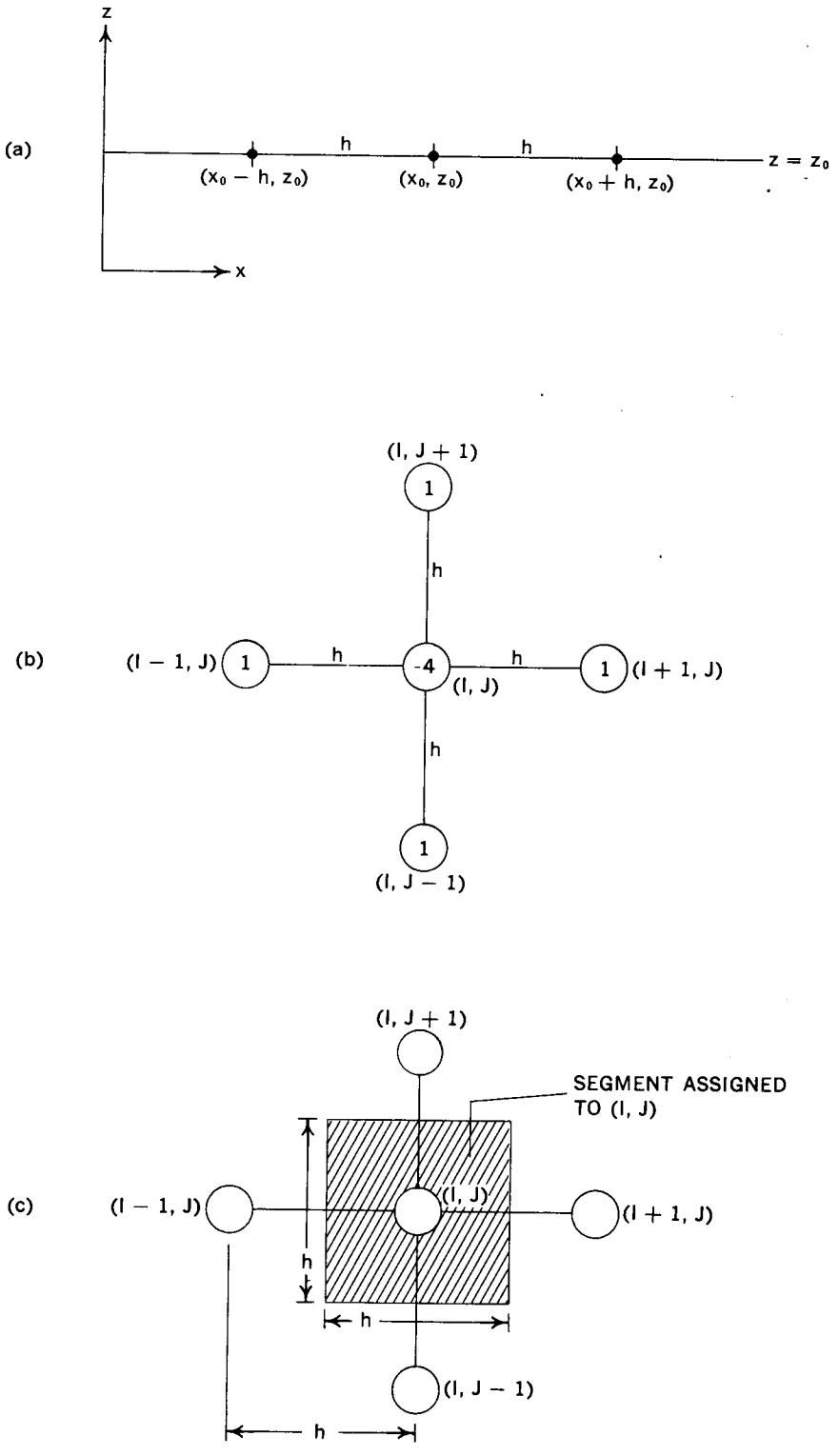

Figure 9. Development of finite-difference equations for two-dimensional homogeneous case

To obtain the approximation for ϕ_{XX} we write the difference equation for ϕ_{XX} in terms of ϕ_X using the forward difference expression (3.8) as follows:

$$(3.6)\quad \phi(x_0 + h,z_0) = \phi(x_0,z_0) + h\phi_X(x_0,z_0) + \frac{h^2}{2}\,\phi_{XX}(\xi,z_0)$$

and

$$(3.7)\quad \phi_X(x_0,z_0) = \frac{\phi(x_0 + h,z_0) - \phi(x_0,z_0)}{h} - \frac{h}{2}\,\phi_{XX}(\xi,z_0)$$

If we approximate ϕ_X by:

$$(3.8)\quad \phi_X(x_0,z_0) = \frac{\phi(x_0 + h,z_0) - \phi(x_0,z_0)}{h}$$

the truncation error will be:

$$(3.9)\quad E_T = -\frac{h}{2}\,\phi_{XX}(\xi,z_0)$$

where: $x_0 \leqslant \xi \leqslant x_0 + h$

We can obtain a similar expression to (3.8) by substituting the backward difference $x=x_0 - h$ into (3.5). This yields:

$$(3.10)\quad \phi_X(x_0,z_0) = \frac{\phi(x_0,z_0) - \phi(x_0 - h,z_0)}{h}$$

with a truncation error

$$(3.11)\quad E_T = -\frac{h}{2}\,\phi_{XX}(\xi,z_0)\ ;\ x_0 - h \leqslant \xi \leqslant x_0$$

$$(3.12)\quad \phi_{XX}(x_0,z_0) = \frac{\phi_X(x_0 + h,z_0) - \phi_X(x_0,z_0)}{h}$$

and substitute the backward difference expression (3.10) for ϕ_X in (3.12).

Therefore:

$$(3.13)\quad \phi_{XX}(x_0,z_0) = \frac{\phi(x_0 + h,z_0) - 2\phi(x_0,z_0) + \phi(x_0 - h,z_0)}{h^2}$$

It can be shown (McCracken and Dorn, 1964) that the error due to truncation is:

$$(3.14)\quad E_T = -\frac{h^2}{12}\,\phi_{XXXX}(\xi,z_0)\ ;\ x_0 - h \leqslant \xi \leqslant x_0 + h$$

In a similar manner, we can develop a difference expression for ϕ_{ZZ}, the second term of Laplace's equation:

$$(3.15)\quad \phi_{ZZ}(x_0,z_0) = \frac{\phi(x_0,z_0 + k) - 2\phi(x_0,z_0) + \phi(x_0,z_0 - k)}{k^2}$$

For a square net, h = k, so that

$$(3.16)\quad \phi_{ZZ}(x_0,z_0) = \frac{\phi(x_0,z_0 + h) - 2\phi(x_0,z_0) + \phi(x_0,z_0 - h)}{h^2}$$

and Laplace's equation:

(3.1) $\phi_{xx} + \phi_{zz} = 0$

becomes:

(3.17) $$\frac{1}{h^2}\left[\phi(x_0 + h,z_0) + \phi(x_0 - h,z_0) + \phi(x_0,z_0 + h) + \phi(x_0,z_0 - h) - 4\phi(x_0,z_0)\right] = 0$$

and

(3.18) $$\phi(x_0,z_0) = \frac{1}{4}\left[\phi(x_0 + h,z_0) + \phi(x_0 - h,z_0) + \phi(x_0,z_0 + h) + \phi(x_0,z_0 - h)\right]$$

for each point (x_0, z_0). If we let (x_0, z_0) be the nodal point (I,J), we have:

(3.19) $$\phi(I,J) = \frac{1}{4}\left[\phi(I + 1,J) + \phi(I - 1,J) + \phi(I,J + 1) + \phi(I,J - 1)\right]$$

For any node (I,J), we can represent (3.19) schematically as shown in Figure 9b. Such a diagram, which depicts the pattern of points involved in a difference operator together with the appropriate numerical coefficients, is called a stencil.

When MESH = 1 (figure 8), equation (3.09) holds for each interior node in the field. For the refined meshes, (3.19) becomes:

(3.20) $$\phi(I,J) = \frac{1}{4}\left[\phi(I + 2,J) + \phi(I - 2,J) + \phi(I,J + 1) + \phi(I,J - 1)\right]$$

for interior points in the zone of intermediate mesh spacing, and

(3.21) $$\phi(I,J) = \frac{1}{4}\left[\phi(I + 4,J) + \phi(I - 4,J) + \phi(I,J + 1) + \phi(I,J - 1)\right]$$

for interior points in the zone of largest mesh spacing.

Equation (3.19) is known as the standard 5-point Laplace difference equation. It is also possible to arrive at a different 5-point approximation using the square of nodes surrounding the node in question. There are also 9-point approximations, 20-point approximations and many others (Forsythe and Wasow, 1960). These more complicated formulae offer higher accuracy but do not offer any other advantages and often have serious disadvantages.

Schenk (1963) has used a less rigorous method of arriving at a finite-difference representation of Laplace's equation in his book on computer methods in heat flow. An analogous groundwater derivation would be as follows. Consider Figure 9c which represents the node (I,J) and its neighbouring nodes. Groundwater is considered to flow between the node (I−1, J) and (I,J) along a channel that is h units long, h units wide, and one unit deep perpendicular to the paper. Darcy's law states that

(3.22) $$Q = KA\frac{\delta\phi}{\delta x}$$

so that the flow into the node along this channel is

(3.23) $$Q = \frac{Kh[\phi(I - 1,J) - \phi(I,J)]}{h}$$

Considering the flow into the node from all four neighbouring nodes we have

(3.24) $$Q = K\left\{[\phi(I - 1,J) - \phi(I,J)] + [\phi(I + 1,J) - \phi(I,J)] + [\phi(I,J + 1) - \phi(I,J)] + [\phi(I,J - 1) - \phi(I,J)]\right\}$$

but Q = 0 for steady-state conditions and we arrive once again at

$$(3.19)\quad \phi(I,J) = \frac{1}{4}[\phi(I+1,J) + \phi(I-1,J) + \phi(I,J-1) + \phi(I,J+1)]$$

A more thorough treatment of the error analysis touched on by equations (3.9), (3.11) and (3.14) can be found in Forsythe and Wasow (1960) or McCracken and Dorn (1964).

We have defined suitable finite-difference approximations (3.19), (3.20), (3.21) for Laplace's equation for each interior node in a square, graded mesh. Similar expressions can be developed for a rectangular mesh by omitting the h = k simplification.

Finite-Difference Equations for Nodes on the Boundary

The finite-difference expressions for nodes on an external boundary must satisfy both Laplace's equation and the boundary conditions at that point. We will consider first the basal impermeable boundary (J = 1). Along this line each node (I, J) has only three neighbouring nodes. For MESH = 1, (Figure 8) they are (I − 1, J), (I + 1, J) and (I, J + 1). In order to satisfy the boundary condition of no flow across the impermeable boundary we imagine an image node (I, J − 1) such that $\phi(I,J-1) = \phi(I,J+1)$. The finite-difference equation then becomes:

$$(3.25)\quad \phi(I,J) = \frac{1}{4}[\phi(I-1,J) + \phi(I+1,J) + \phi(I,J+1) + \phi(I,J-1)]$$

or

$$(3.26)\quad \phi(I,J) = \frac{1}{4}[\phi(I-1,J) + \phi(I+1,J) + 2\phi(I,J+1)]$$

The same result can be obtained using Schenk's analysis with a horizontal flow channel of h/2 units and a vertical channel of h units.

For a node on the left impermeable boundary:

$$(3.27)\quad \phi(I,J) = \frac{1}{4}[\phi(I,J+1) + \phi(I,J-1) + 2\phi(I+1,J)]$$

and for the left corner node:

$$(3.28)\quad \phi(I,J) = \frac{1}{2}[\phi(I,J+1) + \phi(I+1,J)]$$

Similar expressions hold for the right vertical boundary.

If MESH = 1, the I, J coordinates of the neighbouring nodes may differ from the above equations and will vary with the mesh spacing. The stencils for equations (3.26), (3.27) and (3.28) as well as all other boundary configurations are included in Figure 12.

The fourth boundary of the region is the water table. Its configuration is approximated by a series of straight-line segments joining the nodes nearest to the actual position of the water surface (Figure 10a). As shown in Chapter 1, the value of ϕ on the water-table and therefore at these representative nodes is just the elevation of the water table above some basal datum plane. The nodal point location of the water table and the values of ϕ at these nodes are the input parameters in the digital computer solution using the numerical method. All nodes above the water table are given the value 0 and are excluded from the iterative procedure used to solve the array of finite-difference equations.

The possible presence of a steep water table as shown in Figure 10b necessitates the development of another finite-difference expression. The standard 5-point formula (3.19) is not applicable since the point (I-1, J) lies above the water table and $\phi(I-1, J)$ has been arbitrarily set equal to zero. For this situation, the Mikeladze formula for the improvement of boundary values is used (Panov, 1963). The resulting expression is:

(a)

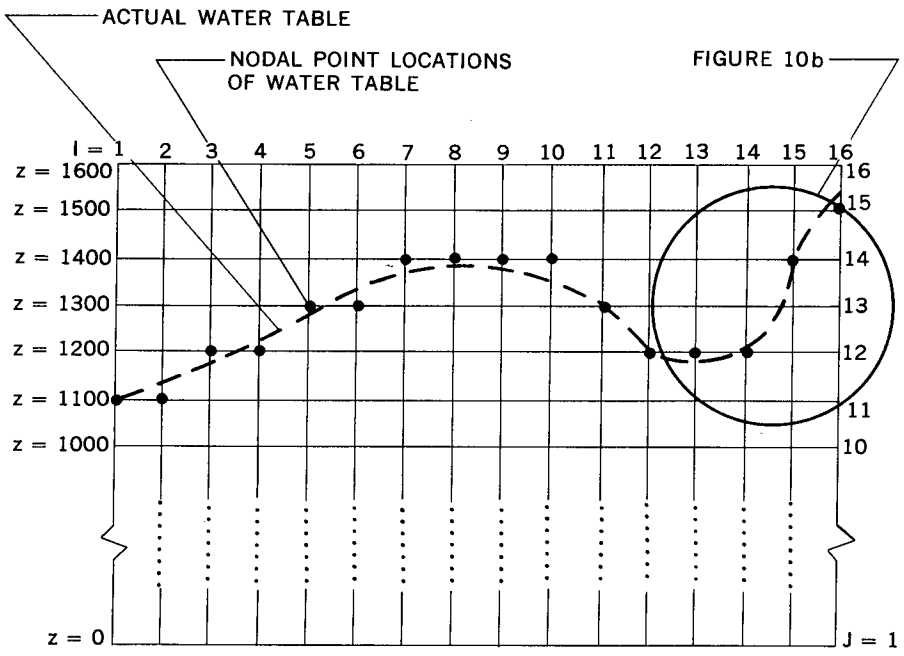

I	WATER TABLE	
	J	ϕ
1	11	1100.0
2	11	1125.0
3	12	1180.0
4	12	1225.0
5	13	1300.0
6	13	1340.0
7	14	1380.0
8	14	1385.0
ETC.	ETC.	ETC.

(b)

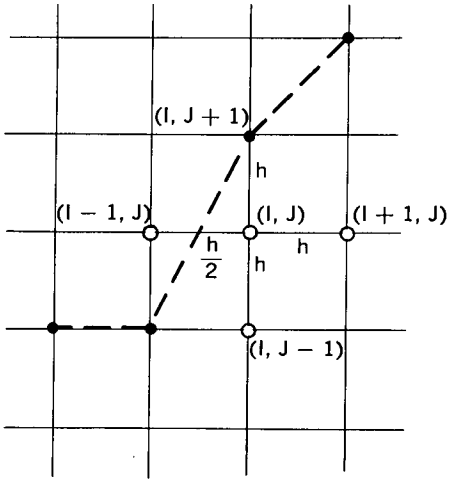

Figure 10. Nodal point representation of water table

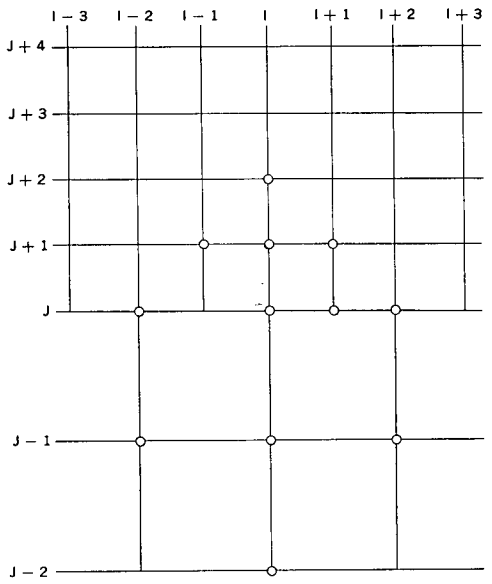

Figure 11. Graded mesh

$$(3.29)\quad \phi(I,J) = \frac{1}{18}\left\{8\phi(I - \tfrac{1}{2}, J) + 4\phi(I + 1,J) + 3[\phi(I,J + 1) + \phi(I,J - 1)]\right\}$$

where by symmetry:

$$(3.30)\quad \phi(I - \tfrac{1}{2}, J) = \frac{1}{2}[\phi(I,J + 1) + \phi(I - 1, J - 1)]$$

Similar expressions can be developed for steeper water tables (for example, one which traverses three vertical squares to one horizontal), as well as for negative slopes. The various possibilities are included in Figure 12 and the stencils in Figure 13.

Finite-Difference Equations for Nodes on Interfacial Boundaries in a Refined Mesh

Figure 11 shows a typical boundary between two sizes of mesh spacing. The standard 5-point formula can be used for points such as (I, J−1) which are entirely within the large mesh or for points entirely within the small mesh such as (I,J + 1). For the node (I,J) we have:

$$(3.31)\quad \phi(I,J) = \frac{1}{4}[\phi(I - 2,J) + \phi(I + 2,J) + \phi(I,J + 2) + \phi(I,J - 1)]$$

There are several possible formulae for the node (I + 1, J) (Forsythe and Wasow, 1960). The simplest is to obtain ϕ(I + 1, J) as an average of its two nearest horizontal neighbours.

Nodes which are on both an external boundary and an interfacial boundary have separate finite-difference expressions but offer no new concepts. Special formulae are also necessary when the water-table configuration is represented by a node on the first horizontal line above a mesh interface (for example: the line J + 1 in figure 11). In all, 40 different finite-difference expressions are needed to treat all the nodal cases which occur in the most general mesh. Their occurrence is shown in Figure 12 for MESH = 7, and the corresponding stencils are detailed in Figure 13.

Solution of Finite-Difference Equations

The previous sections have shown how Laplace's equation (3.1) and its attendant boundary conditions (3.3) can be discretized into a system of n simultaneous linear algebraic equations, one for each node of an n-node mesh. There are also n unknowns, namely, the values of ϕ at each of the n nodes. The method of solution of such a system of equations varies with n;

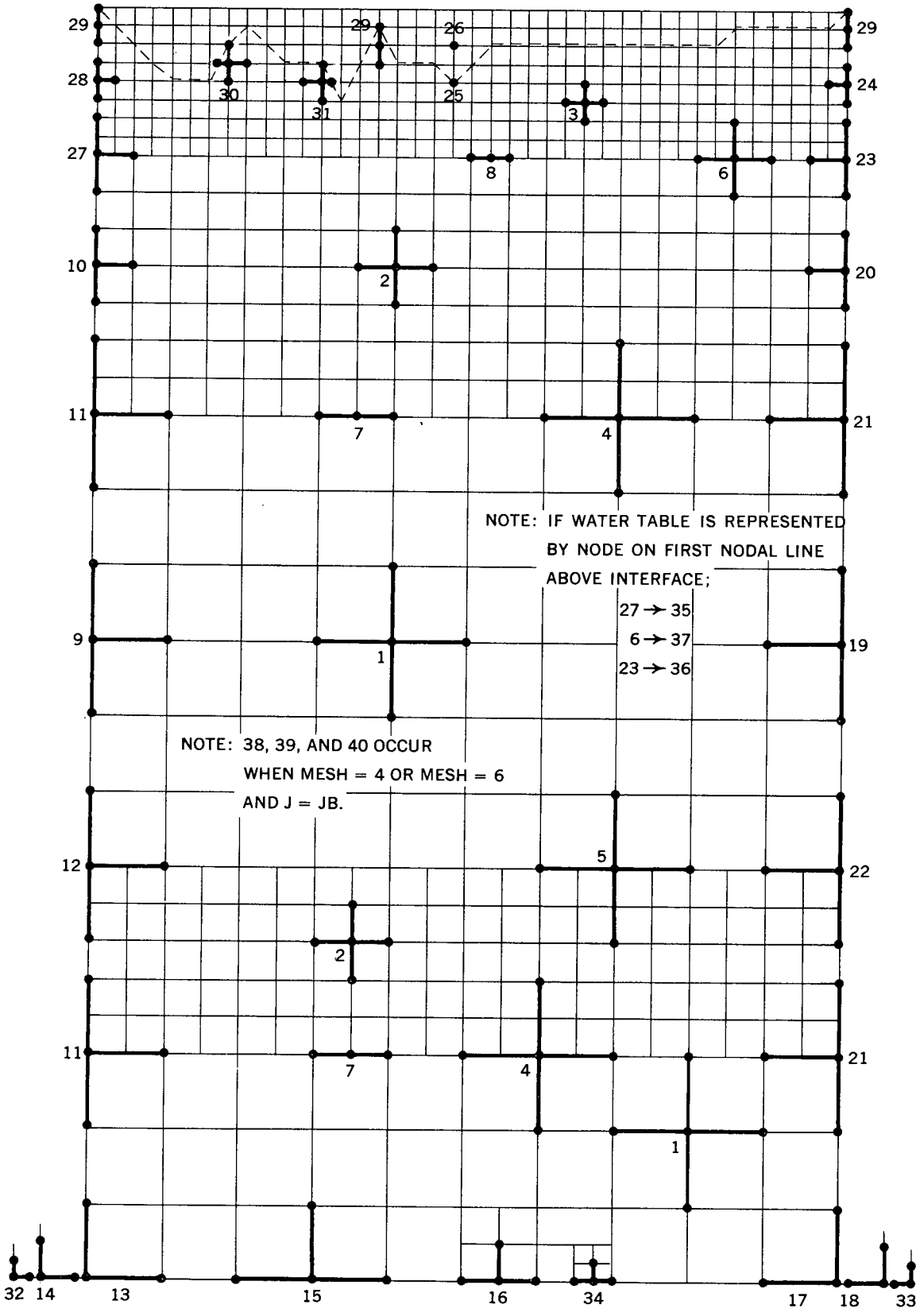

Figure 12. Location of finite-difference stencils

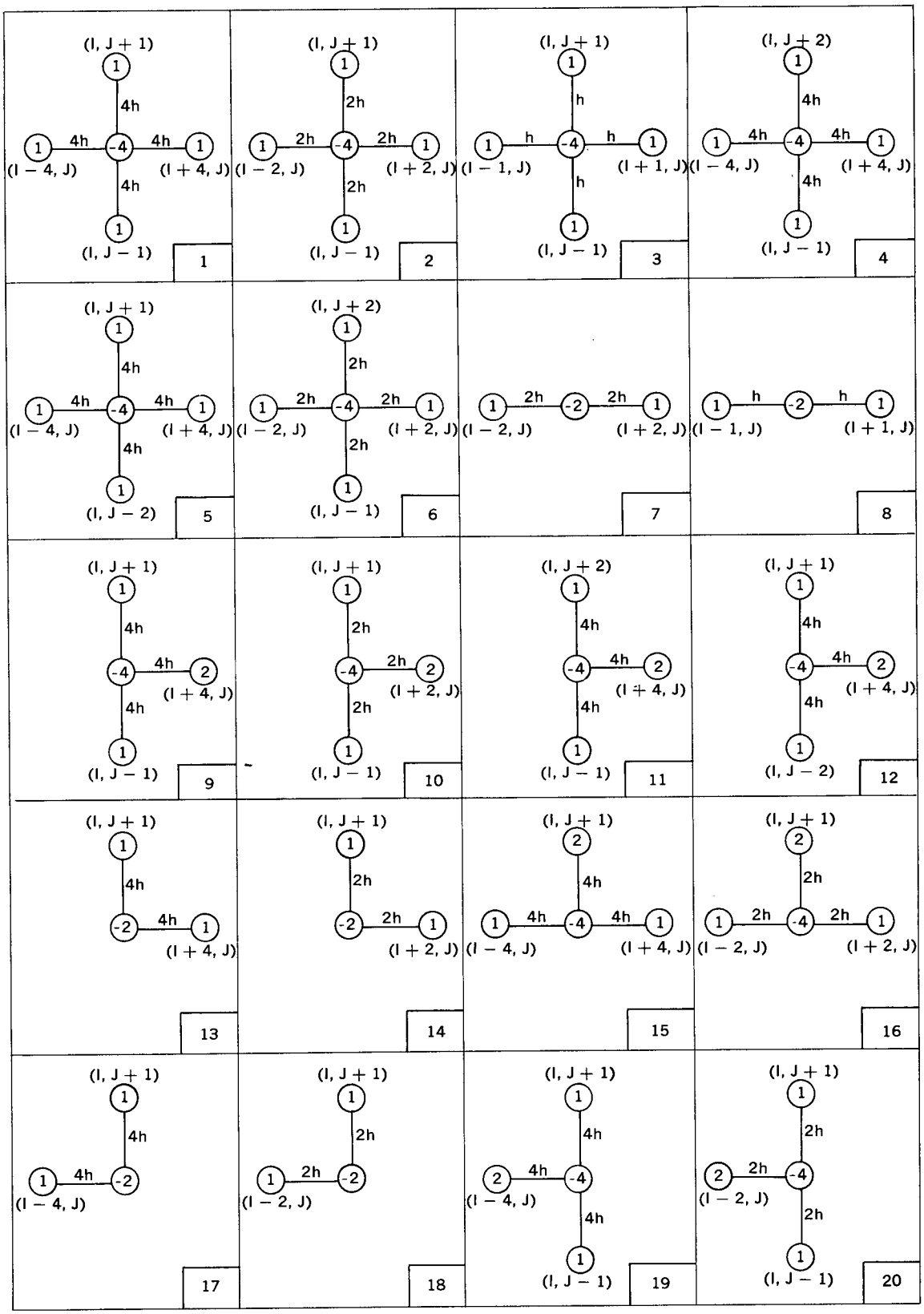

Figure 13. Finite-difference stencils

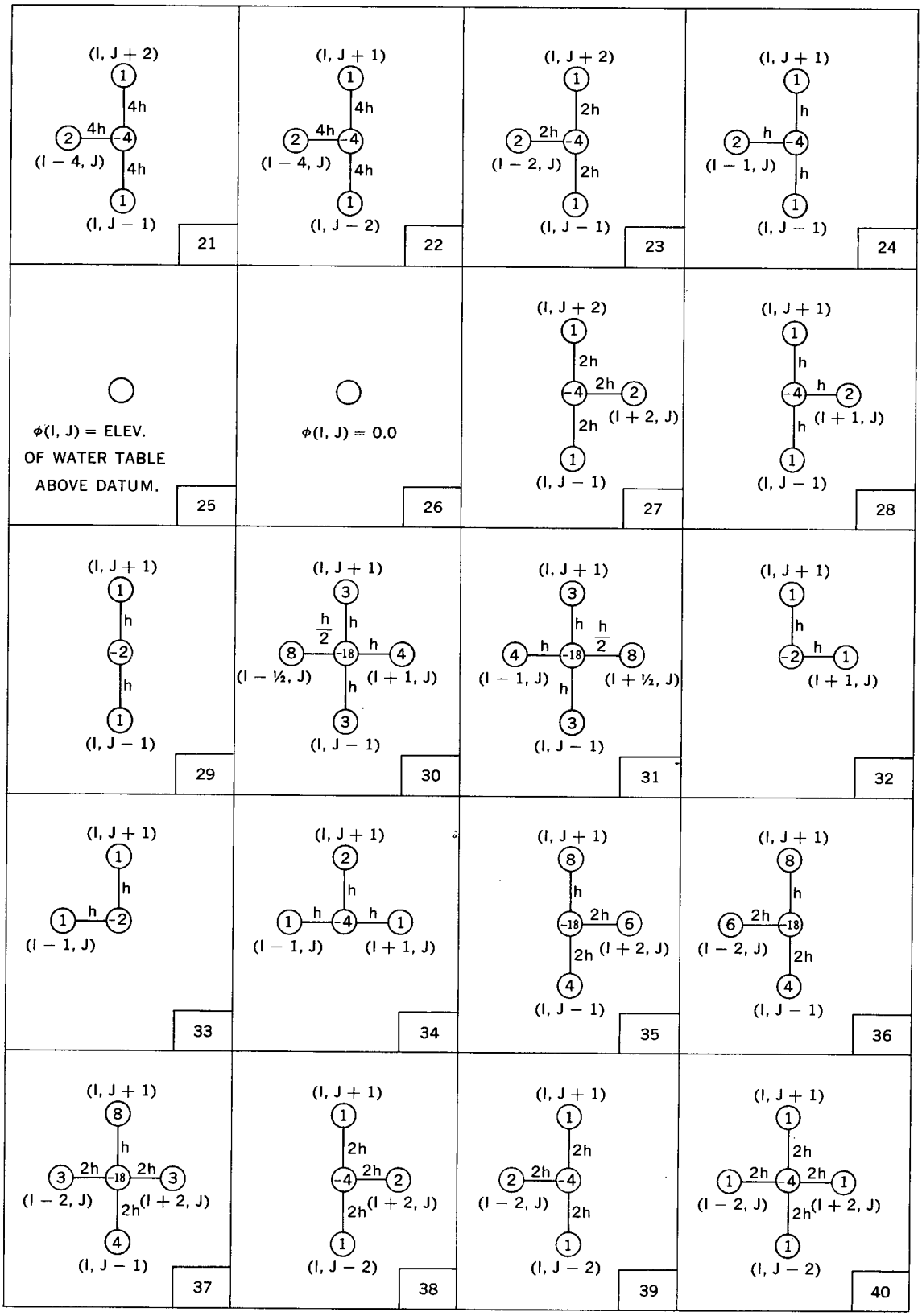

Figure 13(continued). Finite-difference stencils

Cramer's rule or Gauss elimination is used for small n (say 3 or 4), hand relaxation when n is larger but tractable, and iterative solutions using a digital computer for very large n. For the problem of regional groundwater flow, large intricate meshes are necessary and the value of n is generally of the order 2,000 to 12,000. In this case, the only possible method is an iterative solution.

The simplest iterative procedure is the Gauss-Seidel method which can best be described following the treatment in McCracken and Dorn (1964). Consider as an example, n = 3 (i.e. 3 equations in 3 unknowns):

(3.32a) $a_{11}x_1 + a_{12}x_2 + a_{13}x_3 = b_1$

(3.32b) $a_{21}x_1 + a_{22}x_2 + a_{23}x_3 = b_2$

(3.32c) $a_{31}x_1 + a_{32}x_2 + a_{33}x_3 = b_3$

If a_{11}, a_{22}, and a_{33} are all non-zero, we can rearrange (3.32) to read:

(3.33a) $x_1 = \frac{1}{a_{11}} (b_1 - a_{12}x_2 - a_{13}x_3)$

(3.33b) $x_2 = \frac{1}{a_{22}} (b_2 - a_{21}x_1 - a_{23}x_3)$

(3.33c) $x_3 = \frac{1}{a_{33}} (b_3 - a_{31}x_1 - a_{32}x_2)$

Take any first approximation to the solution and call it $x_1^{(0)}$, $x_2^{(0)}$, $x_3^{(0)}$. This approximation can then be used in (3.33a) to solve for a new approximation as follows:

(3.34a) $x_1^{(1)} = \frac{1}{a_{11}} (b_1 - a_{12}x_2^{(0)} - a_{13}x_3^{(0)})$

Then using (3.33b) and the value $x_1^{(1)}$ from (3.34a), we can calculate:

(3.34b) $x_2^{(1)} = \frac{1}{a_{22}} (b_2 - a_{21}x_1^{(1)} - a_{23}x_3^{(0)})$

Similarly:

(3.34c) $x_3^{(1)} = \frac{1}{a_{33}} (b_3 - a_{31}x_1^{(1)} - a_{32}x_2^{(1)})$

We have now completed the first iteration. The resulting values of $x_1^{(1)}$, $x_2^{(1)}$, $x_3^{(1)}$ are then used in the same way to obtain the results of the second iteration $x_1^{(2)}$, $x_2^{(2)}$, $x_3^{(2)}$. The process is continued until the results of two successive iterations differ by an amount that falls within a specified tolerance. The convergence of the iterative scheme is guaranteed in the case of a system of n equations if two conditions are satisfied. In the nomenclature of (3.32) these sufficient conditions are:

(3.35) $|a_{ii}| \geqslant |a_{11}| + \cdots + |a_{i,i-1}| + |a_{i,i+1}| + \cdots + |a_{in}|$

for all i; and for at least one i:

(3.36) $|a_{ii}| > |a_{11}| + \cdots + |a_{i,i-1}| + |a_{i,i+1}| + \cdots + |a_{in}|$

Now let us examine a few of the finite-difference equations of our discretized boundary value problem. Figure 14 lists the appropriate equations for nine points about the origin, together with the (I, J) coordinates of these points and the number of the source finite-difference equations as developed in the preceding sections.

It is immediately evident that the system of n equations is sparse (i.e. most of the coefficients are zero) and it can be seen by inspection that the conditions (3.35) and (3.36) are satisfied.

The case of n equations in n unknowns can be expressed in matrix form as

(3.37) $A\phi = B$

or

(3.38) $a_{ij}\phi_j = b_i$

where

$A = a_{ij}$ = matrix representation of the coefficients of ϕ (I, J).

$B = b_i$ = matrix representation of the elements of the right-hand side of the n finite-difference equations (Figure 14). For those points where one of the terms in the finite-difference expression is an input value along the water table, the right-hand side will be non-zero.

Another way of stating the sufficient conditions (3.35) and (3.36) is that the iterative procedure will converge if the spectral norm $\bar{\mu}$ of the matrix C = I-A is less than one. A is defined above and I is the identity matrix. The spectral norm is always less than one for Laplace's equation (Young, 1954; Fayers and Sheldon, 1962), if a uniform mesh is used.

A marked improvement in computing time can be accomplished by introducing a relaxation parameter, ω, in the Gauss-Seidel method. This is done by overcorrecting the values of ϕ (I,J) obtained from (3.19) through (3.30) as follows:

(3.39) $$\phi(I,J)^{(k)}_{corr} = \omega\phi(I,J)^{(k)} + (1 - \omega)\,\phi(I,J)^{(k-1)}_{corr}$$

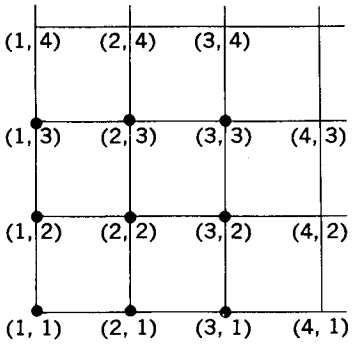

(I, J) COORDINATES OF POINTS	SOURCE FINITE-DIFFERENCE EQUATION	NINE REPRESENTATIVE FINITE-DIFFERENCE EQUATIONS FROM THE SYSTEM OF n EQUATIONS
(1, 1)	3.28	$2\phi(1,1) - \phi(2,1) \ldots\ldots - \phi(1,2) = 0$
(2, 1)	3.26	$-\phi(1,1) + 4\phi(2,1) - \phi(3,1) \ldots\ldots - 2\phi(2,2) = 0$
(3, 1)	3.26	$\ldots\ldots - \phi(2,1) + 4\phi(3,1) - \phi(4,1) - 2\phi(3,2) = 0$
(1, 2)	3.27	$-\phi(1,1) \ldots\ldots + 4\phi(1,2) - 2\phi(2,2) - \phi(1,3) = 0$
(2, 2)	3.19	$\ldots\ldots - \phi(2,1) \ldots\ldots - \phi(1,2) - 4\phi(2,2) - \phi(3,2) - \phi(2,3) = 0$
(3, 2)	3.19	$\ldots\ldots - \phi(3,1) \ldots\ldots - \phi(2,2) - 4\phi(3,2) - \phi(4,2) - \phi(3,3) = 0$
(1, 3)	3.27	$\ldots\ldots - \phi(1,2) + 4\phi(1,3) - 2\phi(2,3) - \phi(1,4) = 0$
(2, 3)	3.19	$\ldots\ldots - \phi(2,2) - \phi(1,3) + 4\phi(2,3) - \phi(3,3) - \phi(2,4) = 0$
(3, 3)	3.19	$\ldots\ldots - \phi(3,2) - \phi(2,3) + 4\phi(3,3) - \phi(4,3) - \phi(3,4) = 0$

Figure 14. Representative finite-difference equations

where:

$\phi(I,J)^{(k)}_{corr}$ = corrected value of $\phi(I,J)$ for k^{th} iteration

$\phi(I,J)^{(k)}$ = value of $\phi(I,J)$ obtained from (3.19) through (3.30) for k^{th} iteration

$\phi(I,J)^{(k-1)}_{corr}$ = corrected value of $\phi(I,J)$ for previous iteration

ω = relaxation factor

When $\omega = 1$, (3.39) reduces to the Gauss-Seidel method. This method when applied to elliptic difference equations is called the Liebmann method or the method of successive displacements. For $1<\omega<2$ the procedure is known as the extrapolated Liebmann method or the successive over-relaxation method. The optimum value of ω is given by (Young, 1954):

$$(3.40) \quad \omega_{opt} = 1 + \left[\frac{\bar{\mu}}{1 + (1 - \bar{\mu}^2)^{\frac{1}{2}}}\right]^2$$

where:

$\bar{\mu}$ = spectral norm of C (see discussion following (3.38)). Fayers and Sheldon (1962) note that "it is difficult to make reliable estimates for μ. μ is known exactly for Laplace's equation in a rectangle but is not known for regions of general shape and properties". McCracken and Dorn (1964) have shown the relation between the number of iterations and ω for a particular problem involving Laplace's equation in a square region with Dirichlet boundary conditions. This figure and a corresponding one for the problem under consideration are included in Appendix B. Young (1954) has shown that, using the optimum ω, reductions in computer time of up to 100 times over the standard Liebmann method are possible for large meshes.

Unfortunately, the extrapolated Liebmann method, using the relaxation factor ω, does not always converge. Certain necessary conditions on the matrix A (3.37) have been established by Young (1954) and reported in Forsythe and Wasow (1960). An advanced knowledge of matrix theory would be necessary to grasp the full meaning of these conditions. They are stated here in their simplest form and without further explanation; the interested reader is referred to the paper and text quoted above.

1. Matrix A must be definite.
2. Matrix A must have property (A). A square matrix A of order N is said to have property (A) if there exists a permutation matrix B such that BAB^T is diagonally block tridiagonal. B^T is the transpose of B.

When a regular square of rectangular mesh is used in the numerical mathematical model representing regional groundwater flow the resulting matrix satisfies the above conditions and the extrapolated Liebmann method always converges. The use of a graded mesh, however, and its attendant finite-difference expressions causes changes in the properties of the matrix such that the above two conditions are not always satisfied. Under these circumstances, the definition of the optimum ω, or indeed the question of whether an optimum ω exists at all, becomes a difficult if not impossible task for the non-professional mathematician. The practical aspects of this problem are discussed further in Appendix B.

The extrapolated Liebmann method, described above, is an example of an "explicit" iterative method. That is, at the kth iteration, we arrive at a value of ϕ (I,J) which can be determined by itself without the necessity of simultaneously determining a group of other values of ϕ for other (I, J). "In contrast are implicit formulas, by which a group of components of ϕ (I, J) are defined simultaneously in such an interrelated manner that it is necessary to solve a linear subsystem for the whole subset of components at once before a single one can be determined," (Forsythe and Wasow, 1960). An implicit procedure which has been successful in many cases and which can result in savings in computer time of up to 25 times over the extrapolated Liebmann method is the alternating direction implicit method of

Peaceman and Rachford (1955). Fayers and Sheldon (1962) state: "For Laplace's equation in a rectangular region it has been demonstrated that the method will converge significantly faster than the successive overrelaxation procedure. Unfortunately, a mathematical analysis of the rate of convergence of the method does not exist for general problems ....." Young also warns in Todd (1962): "In spite of the apparent advantages of the Peaceman-Rachford method, there are several reasons why one might hesitate to use it for some problems in preference to successive overrelaxation. The latter method is undoubtedly simpler. Also the basic formulas for the Peaceman-Rachford method are considerably more complicated ..... The Peaceman-Rachford method may well be better for sufficiently small h but it is not clear whether, for a given case, it will be better for the particular value of h being used. Moreover, although the theory underlying the successive overrelaxation method has been extended to include a wide class of partial differential equations, including Laplace's and to include nonrectangular regions, the theory for the Peaceman-Rachford method is limited to problems involving a very restricted class of partial differential equations and the rectangle."

For these reasons and because computer times were not found to be excessive, the extrapolated Liebmann method of successive overrelaxation has been used in the present study. The use of alternating direction implicit scheme should not, however, be ruled out for hydrogeological studies. In particular, the adaptation of the Peaceman-Rachford method to three dimensions by Douglas and Rachford (1956) may prove useful.

TWO-DIMENSIONAL NON-HOMOGENEOUS CASE

The regular square and rectangular mesh configurations used in the homogeneous case are equally suitable for the non-homogeneous case.

The fundamental difference between the two cases is the necessity of solving Richards' equation:

$$(3.2)\quad [K(x,z)\phi_x]_x + [K(x,z)\phi_z]_z = 0$$

when the permeability becomes a function of position as opposed to the simpler Laplace equation (3.1) which holds when the permeability is homogeneous. Richards' equation (3.2) belongs to a class of equations known as "quasi-plane-harmonic" (Southwell, 1946). Discretization of boundary value problems involving quasi-plane-harmonic partial differential equations can be carried out using the usual finite-difference approximations to the first and second order partial derivatives occurring in the equations. As shown in the development of the finite-difference expressions for Laplace's equation in the homogeneous case, we can approximate ϕ_x at the point (x_0, z_0) by:

$$(3.8)\quad \phi_x(x_0,z_0) = \frac{\phi(x_0 + h,z_0) - \phi(x_0,z_0)}{h}$$

or by:

$$(3.10)\quad \phi_x(x_0,z_0) = \frac{\phi(x_0,z_0) - \phi(x_0 - h,z_0)}{h}$$

Adding (3.8) and (3.10) yields:

$$(3.41)\quad 2\phi_x(x_0,z_0) = \frac{\phi(x_0 + h,z_0) - \phi(x_0 - h,z_0)}{h}$$

Therefore:

$$(3.42)\quad \phi_x(x_0,z_0) = \frac{\phi(x_0 + h,z_0) - \phi(x_0 - h,z_0)}{2h}$$

We have now defined a third finite-difference approximation to $\phi_x(x_0,z_0)$.

Similarly:

$$(3.43)\quad \phi_z(x_0,z_0) = \frac{\phi(x_0,z_0 + h) - \phi(x_0,z_0 - h)}{2h}$$

In the simplified notation of Figure 15a, we let (x_0, z_0) be the node A and let B, C, D and E represent the surrounding nodes. We then have:

$$(3.44)\quad (\phi_z)_A = \frac{\phi_B - \phi_D}{2h}$$

$$(3.45)\quad (\phi_x)_A = \frac{\phi_E - \phi_C}{2h}$$

It is not necessary, however, that h always represent the nodal spacing and ϕ_x and ϕ_z always be approximated at a node. The finite-difference expressions are equally valid if we let h become half the mesh spacing h/2 and use (3.42) and (3.43) to approximate the derivatives of ϕ at the mid-points between the nodes. Referring to Figure 15b we then have:

$$(3.46)\quad (\phi_z)_I = \frac{\phi_B - \phi_A}{h}$$

$$(3.47)\quad (\phi_z)_{III} = \frac{\phi_A - \phi_D}{h}$$

$$(3.48)\quad (\phi_x)_{IV} = \frac{\phi_E - \phi_A}{h}$$

$$(3.49)\quad (\phi_x)_{II} = \frac{\phi_A - \phi_C}{h}$$

Returning to Richards' equation (3.2) we now approximate the first term at the point A by:

$$(3.50)\quad ([K(x,z)\phi_x]_x)_A = \frac{(K\phi_x)_{II} - (K\phi_x)_{IV}}{h}$$

then using (3.48) and (3.49) we obtain:

$$(3.51)\quad ([K(x,z)\phi_x]_x)_A = \frac{K_{II}(\phi_A - \phi_C) - K_{IV}(\phi_E - \phi_A)}{h^2}$$

Similarly the second term of Richards' equation becomes, using (3.48) and (3.49):

$$(3.52)\quad ([K(x,z)\phi_z]_z)_A = \frac{K_{III}(\phi_A - \phi_D) - K_I(\phi_B - \phi_A)}{h^2}$$

Adding (3.51) and (3.52) and equating to zero as in (3.2) yields for the finite-difference approximation at the point A:

$$(3.53)\quad K_I(\phi_B - \phi_A) - K_{III}(\phi_A - \phi_D) + K_{IV}(\phi_E - \phi_A) - K_{II}(\phi_A - \phi_C) = 0$$

or

$$(3.54)\quad \phi_A = \frac{K_I\phi_B + K_{II}\phi_C + K_{III}\phi_D + K_{IV}\phi_E}{K_I + K_{II} + K_{III} + K_{IV}}$$

Reverting to our (I, J) coordinate system, let us consider an interior node (I, J) and its four nearest neighbours. In the general non-homogeneous, anisotropic case we allow a different horizontal and vertical permeability to be associated with each nodal point. If we arbitrarily select the notation shown

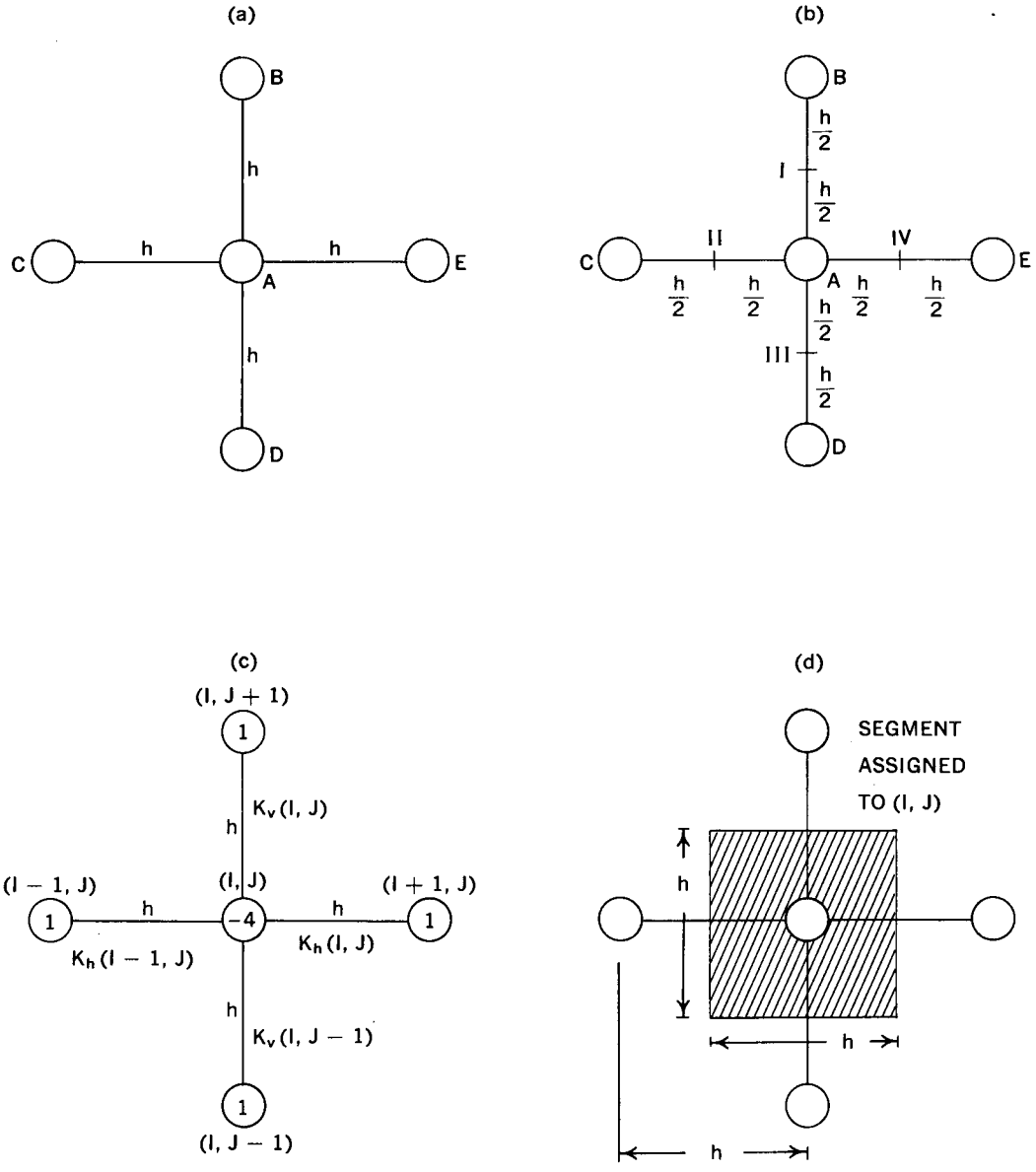

Figure 15. Development of finite-difference equations for two-dimensional, non-homogeneous case

in Figure 15c with $K_V(I, J)$ referring to the permeability between the nodes (I, J) and (I, J + 1) and $K_H(I, J)$ referring to that between (I, J) and (I + 1,J), equation (3.54) becomes:

$$(3.55)\quad \phi(I,J) = \frac{[K_H(I,J)\cdot\phi(I+1,J) + K_V(I,J)\,\phi(I,J+1) + K_H(I-1,J)\cdot\phi(I-1,J) + K_V(I,J-1)\,\phi(I,J-1)]}{[K_H(I,J) + K_V(I,J) + K_H(I-1,J) + K_V(I,J-1)]}$$

Once again the non-rigorous Darcy's Law approach can be used to gain an intuitive understanding of the physical meaning of the finite-difference equation. In Figure 15d, the inflow into the node (I, J) from the node (I–1, J) is:

$$(3.56)\quad Q = \frac{K_H(I-1,J)\cdot h\cdot[\phi(I-1,J) - \phi(I,J)]}{h}$$

Upon considering the components of flow into (I, J) along the flow channels from the other three neighbouring nodes and summing to zero (steady-state conditions), we are led once again to (3.55).

Equation (3.55) is the finite-difference expression for an interior node in the general non-homogeneous, anisotropic problem. For the non-homogeneous but isotropic problem where:

$$(3.57)\quad K_H(I,J) = K_V(I,J) = K(I,J)$$

(3.55) becomes:

$$(3.58)\quad \phi(I,J) = \frac{\{K(I,J)[\phi(I+1,J) + \phi(I,J+1)] + K(I-1,J)\phi(I-1,J) + K(I,J-1)\phi(I,J-1)\}}{2K(I,J) + K(I-1,J) + K(I,J-1)}$$

If we wish to study layered structures in which the permeability remains constant across an entire horizontal line of nodes, then K varies only with depth and (3.55) becomes:

$$(3.59)\quad \phi(I,J) = \frac{\{K(J)[\phi(I+1,J) + \phi(I-1,J) + \phi(I,J+1)] + K(J-1)\phi(I,J-1)\}}{3K(J) + K(J-1)}$$

Comparison of equation (3.55) and its corresponding stencil (Figure 15c) with equation (3.19) and its stencil (3 in Figure 13) will reveal a close relationship between the finite-difference equations of the homogeneous and non-homogeneous cases. In fact, all 40 homogeneous finite-difference equations can be adapted to suit the non-homogeneous and/or anisotropic cases with the aid of the stencils of Figure 13 and the permeability notation shown in Figure 15c. As an example, consider equation (3.27) (stencil 28 of Figure 13) for the isotropic non-layered case. The new finite-difference expression is:

$$(3.60)\quad \phi(I,J) = \frac{K(I,J)[\phi(I,J+1) + 2\phi(I+1,J)] + K(I,J-1)\phi(I,J-1)}{3K(I,J) + K(I,J-1)}$$

A more complicated example would be the adaptation of (3.29) (stencil 30 of Figure 13) to the case of a layered media. The new equation is:

$$(3.61)\quad \phi(I,J) = \frac{\{K(J)[3\phi(I,J+1) + 4\phi(I+1,J) + 8\phi(I-\tfrac{1}{2},J)] + K(J-1)\cdot 3\phi(I,J-1)\}}{15K(J) + 3K(J-1)}$$

For those cases such as equation (3.31) (stencil 6 of Figure 13), it is necessary to average K(J) and K(J + 1) to obtain the permeability to be applied between the nodes (I, J) and (I, J + 2).

THREE-DIMENSIONAL CASE

The mathematical model for the three-dimensional case is a nodal array (Figure 16a) with a mesh spacing of h in the x and y directions and a mesh spacing of k in the z direction. In plan (i.e., looking down from above at any x-y plane) the model may approximate any arbitrary areal extent of a groundwater basin (Figure 16b). As in the two-dimensional case, the model is bounded on all sides by vertical impermeable boundaries and at the base by a horizontal impermeable boundary. The values of the potential (expressed as the head of water above the basal datum) along the water table are inserted in the appropriate nodes to approximate the position of the water-table surface. The computer program is limited to cases where, the water table does not jump more than one vertical node in each horizontal mesh spacing. The origin is at the front lower left of the model, and as shown, it may be outside the actual physical extent of the groundwater model. The manner in which such nodes are removed from the iterative procedure is covered in the data deck instructions for Numerical Program 6 in Appendix B. This computer program is written for the three-dimensional case which is non-homogeneous but isotropic, with respect to permeability. We will use the Darcy Law approach to calculate the finite-difference expression for an interior node in the array for the non-homogeneous isotropic case. The permeability K (I, K, J) associated with any node (I, K, J) is assumed to apply along the three positive axes extending from (I, K, J) to its neighbouring nodes. Referring to Figure 16c, consider the steady-state flow into the node (I, K, J,) from its six neighbouring nodes. We have:

$$(3.62)\quad K(I-1,K,J)\frac{[\phi(I-1,K,J)-\phi(I,K,J)]}{h}hk + K(I,K-1,J)\frac{[\phi(I,K-1,J)-\phi(I,K,J)]}{h}hk$$
$$+ K(I,K,J-1)\frac{[\phi(I,K,J-1)-\phi(I,K,J)]}{k}h^2 + K(I,J,K)\frac{[\phi(I,K+1,J)-\phi(I,K,J)]}{h}hk$$
$$+ K(I,K,J)\frac{[\phi(I+1,K,J)-\phi(I,K,J)]}{h}hk + K(I,K,J)\frac{[\phi(I,K,J+1)-\phi(I,K,J)]}{k}h^2 = 0$$

Multiplying through by 1/k and letting $h/k = a$ we have, after collecting terms:

$$(3.63)\quad \phi(I,K,J) = \frac{\{K(I,K,J)[\phi(I+1,K,J) + \phi(I,K+1,J) + a^2\phi(I,K,J+1)] + K(I-1,K,J)\phi(I-1,K,J) + K(I,K-1,J)\phi(I,K-1,J) + K(I,K,J-1)\phi(I,K,J-1)a^2\}}{\{[2+a^2]K(I,K,J) + K(I-1,K,J) + K(I,K-1,J) + a^2K(I,K,J-1)\}}$$

The same expression may be developed using the standard finite-difference approximations used in the previous section.

Similar equations may be derived by either method for nodes on an external boundary.

A uniform mesh is used in the three-dimensional model so there are no finite-difference expressions for nodes on a mesh boundary.

The extrapolated Liebmann method using the relaxation factor ω is employed in the computer program (Numerical Program 6, Appendix B) for the three-dimensional case.

DIGITAL COMPUTATION

Six computer programs have been written using the numerical method to solve the boundary value problem representing regional groundwater flow. The computing meshes and finite-difference equations used in the programs have been developed in the preceding sections; the extrapolated Liebmann method has been used throughout. The complete FORTRAN IV printout of each program,

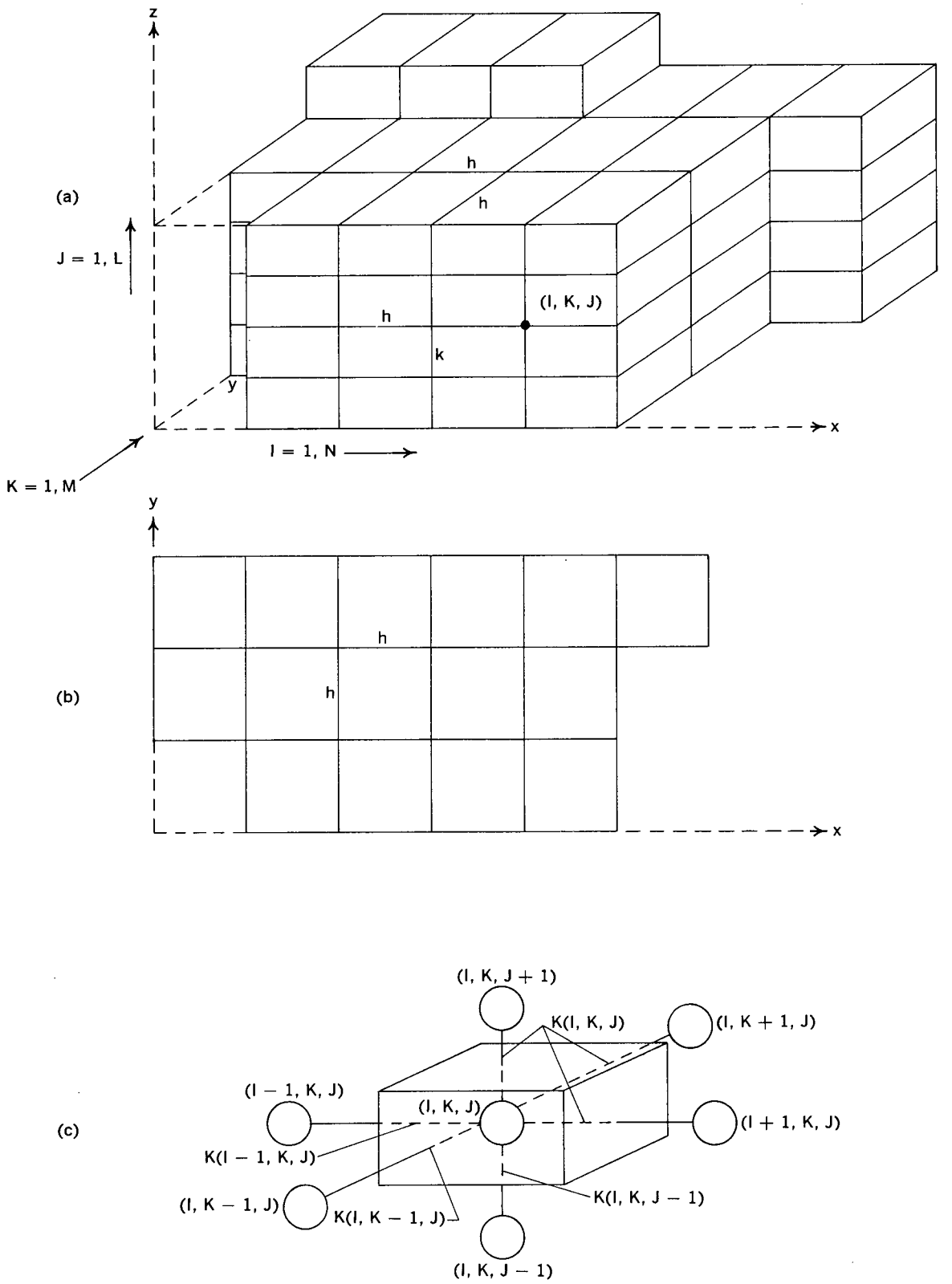

Figure 16. Mathematical model for three-dimensional case

together with a listing of the FORTRAN variable names, the necessary input data, the input deck format, recommended values for certain parameters and a discussion of the factors affecting solution speed are included in Appendix B.

The output from these programs is a printout of the value of ψ expressed as the head of water above the basal datum plane, at each node point in the mesh. Special subroutines, for use on an automatic x-y plotter, which enable contoured plots of the potential field to be constructed, can be incorporated in the program if a plotter is available. These subroutines are included in the programs in Appendix B. Having once obtained the plotted results, the flow pattern can easily be constructed by drawing flow lines orthogonal to the plotted equipotential lines. Numerous examples of the resulting flow nets are included in Chapters 4, 5 and 6.

CHAPTER 4

Comparison of Analytical and Numerical Methods

INDEPENDENCE OF METHODS

Analytical solutions to the mathematical model representing regional groundwater flow have been presented in Chapter 2 and numerical solutions in Chapter 3. It is important to note that the two methods are entirely independent. While both approaches employ mathematical solutions, they represent two different branches of mathematics. In the analytical solutions, the theory of partial differential equations and Fourier series is used; in the numerical method, recourse is made to the field of numerical analysis. One can therefore consider the two approaches as two different modelling methods as independent from one another as, say, a sand model is from an electric analog.

Having clarified this point, we can proceed to compare the solutions obtained by the two methods so that each can be used as a check on the other.

MATCHED SOLUTIONS

We are limited, of course, in our comparison of solutions, to cases which can be solved by both methods. Due to the limitations of the analytical method, we are restricted to homogeneous or layered media. In addition, the analytical solutions are obtained using the rectangular approximation while the numerical solutions can be obtained in a region more representative of the true groundwater basin.

Figure 17 shows four sets of matched solutions. Only the potential nets are shown. Flow lines could be constructed orthogonal to the equipotential lines but for the sake of clarity they have been omitted. (Several of the flow nets in Chapter 5 show both flow lines and equipotential lines.)

Figure 17a is an analytical solution, using the rectangular approximation, for a homogeneous medium with a water-table configuration represented by a sine curve superimposed on a constant regional slope of 0.02. This is one of the cases treated by Tóth (1963). Figure 17b is the identical problem solved by the numerical method. For the sake of comparison the rectangular approximation has been maintained. Qualitatively the results are identical; quantitatively there are some very slight differences. At point A, the equipotential lines are closer together in the numerical solution than in the analytical; at point B in Figure 17b, the equipotential has a configuration somewhat different from the corresponding equipotential in Figure 17a.

The reason for these minor deviations lies in the nature of the convergence inherent in each method. In the analytical solution, the result is in the form of an infinite series which, when programmed for the computer, must be represented by a finite number of terms. A small truncation error is thus introduced. In the numerical method, the iterative procedure converges to a solution. It, too, must be truncated when an acceptable tolerance has been reached. Therefore, a slight error due to incomplete convergence is always introduced.

Considering the total independence of the two approaches, and despite the very minor variations, the author considers Figure 17 (a and b) to represent an excellent check on the methods.

Figure 17c is a numerical solution to the same problem as Figure 17 (a and b) but without the rectangular approximation. The values of the potential along the water table, rather than being placed along a single horizontal line are inserted at the node nearest the actual position of the water table. In Figure 17c, a small nodal array (51 x 27) was used and the "nearest node" was always located on one of two horizontal nodal lines. In this problem, the rectangular approximation is improved only to the

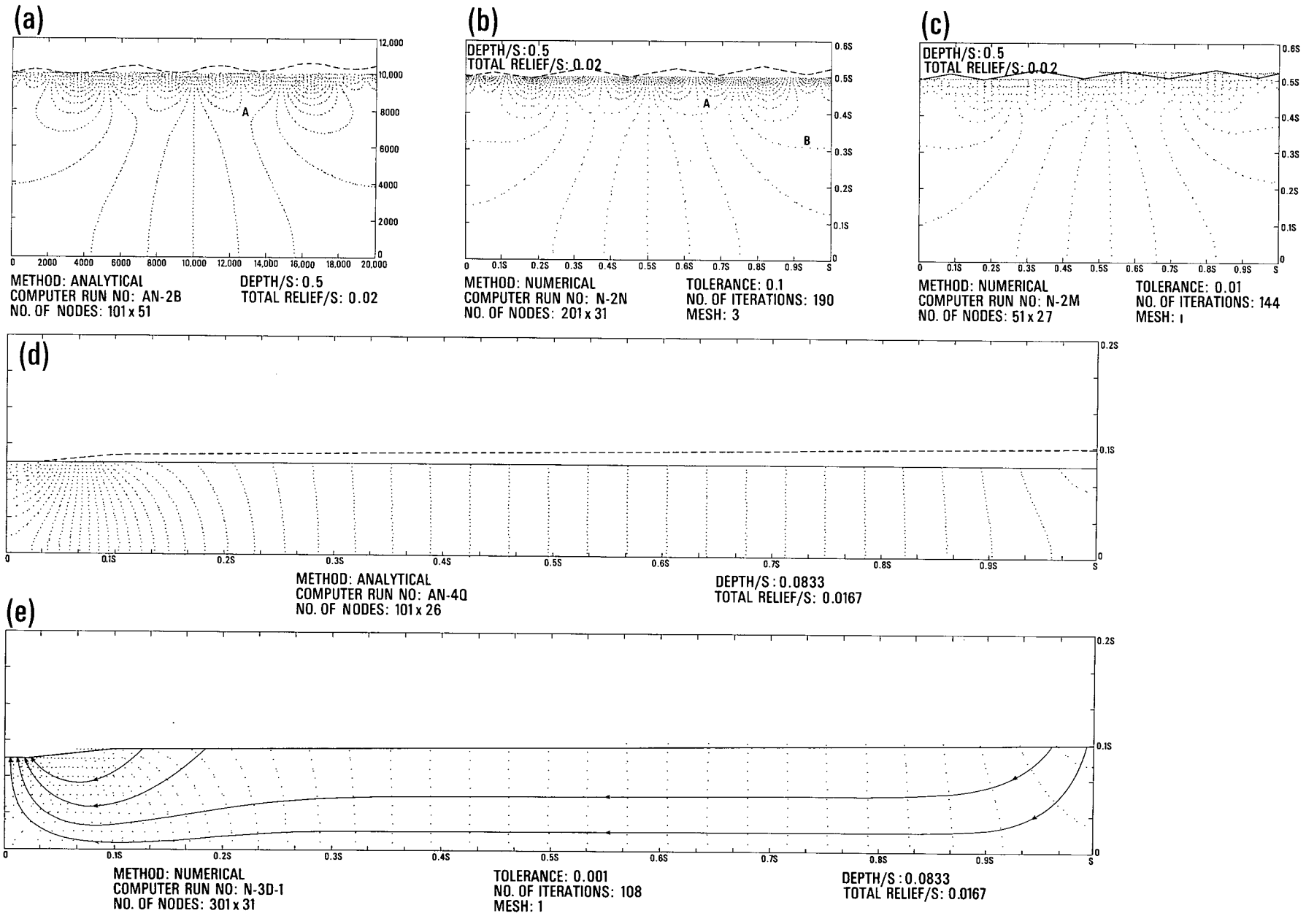

Figure 17. Comparison of analytical and numerical solutions

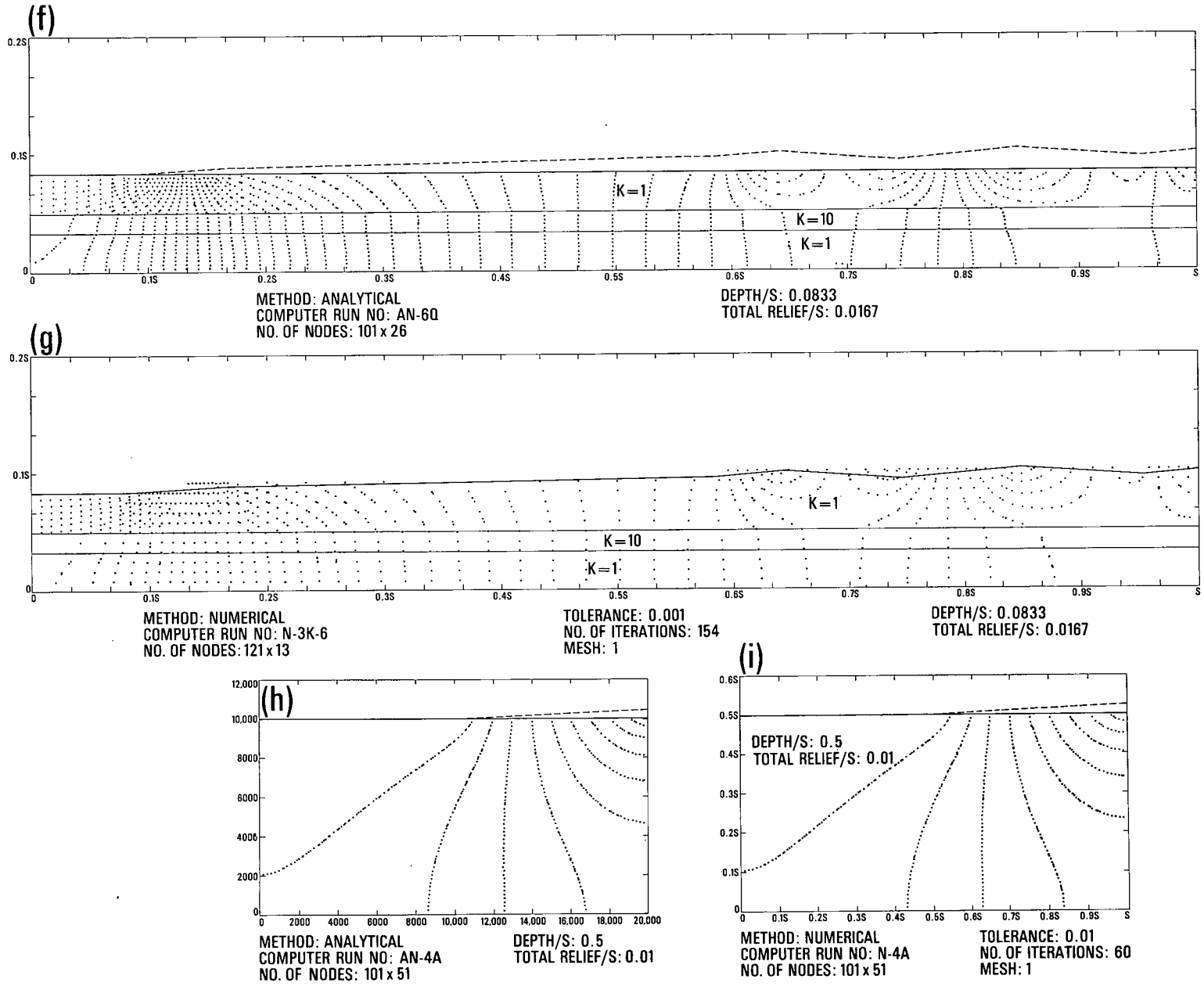

Figure 17(continued). Comparison of analytical and numerical solutions

degree that a single step is introduced. The use of a larger nodal array would allow the water table to be represented in a stepwise fashion involving several steps instead of just one.

The quantitative effect of this slight improvement in the representation of the groundwater basin can be seen in Figure 17c. The central equipotential which meets the basal boundary at 0.5s in Figure 17b is shifted upstream in 17c. The configuration of the equipotentials in the upper right-hand corner is also somewhat affected.

Figure 17 (d and e) represents an analytical and numerical solution in a region more representative of a real groundwater basin. The lateral extent of the basin is 12 times its depth. The water-table configuration is that of a flat alluvial valley at the left, a steep valley flank, and a gentle constant regional slope. The total relief over the area is 0.0167 times the lateral extent of the basin (1,000 ft in 60,000). The media is homogeneous. In Figure 17d (the analytical solution), the rectangular approximation is used. In Figure 17e (the numerical solution), the water table is represented in stepwise fashion. Once again the results are qualitatively identical but the closer approximation to the true basin inherent in the numerical method results in slight quantitative differences in the upstream half of the basin.

Figure 17 (f and g) shows a non-homogeneous example, involving three layers with the relatively more permeable layer in the middle. The water-table configuration might result from a composite topography consisting of a major valley, a gentle constant slope, and hummocky terrain in the upstream portion of the basin.

All the previous examples involve rather complex water-table configurations. Figure 17 (h and i) shows the perfect match obtained for a homogeneous case with a simple water table.

Many other anlytical-numerical matched solutions were obtained but the four presented in this section should be sufficient to indicate the compatibility of the results. The fact that the answers obtained by the two independent methods are, in effect, identical is taken as proof that the results of each method are correct.

RANGE OF VALIDITY OF THE RECTANGULAR APPROXIMATION

The matched solutions of Figure 17 show the deviations from the true answer which result from the use of the rectangular approximation. A natural question arises: "What is the range of validity of the rectangular approximation? ", or more succinctly: "Is there a limiting value of the regional water-table slope above which the analytical method of solution is not valid? ".

The answer is somewhat nebulous and can best be summed up as follows: qualitatively, the rectangular approximation is valid for large regional slopes of 5-10 degrees; quantitatively, it becomes invalid at very small regional slopes of the order of 1-2 degrees.

The qualitative aspects of a regional groundwater flow system consist of the relative distribution of recharge and discharge areas and the depth, extent, and order of the component sub-basins within the large regional basin. The quantitative results are the numerical values, at any point in the flow system, of the hydraulic potential, the groundwater velocity, and the quantity of groundwater flow.

As shown by the comparisons of Figure 17, the qualitative aspects of the flow patterns are unchanged by the use of the rectangular approximation. This has been shown to be true for regional slopes of up to 5 per cent and would apparently hold for any realistic regional water-table slope.

Quantitatively, the approximation becomes worse as the slope becomes greater and as the depth of the groundwater basin becomes less. Figure 18 (a through g) shows the effect.

Figure 18a gives the potential pattern for a cross-section through a basin 20,000 feet long and 1,000 feet deep with a uniform regional water-table slope of 0.02. The solution is analytical, employing the rectangular approximation. Figure 18b is the numerical solution showing the potential values in the true region. Figure 18c shows the result for a slope of 0.05. In Figure 18, b and c are shown with dimensionless values along the coordinates. If one considers s = 20,000 feet as in Figure 18a, then the

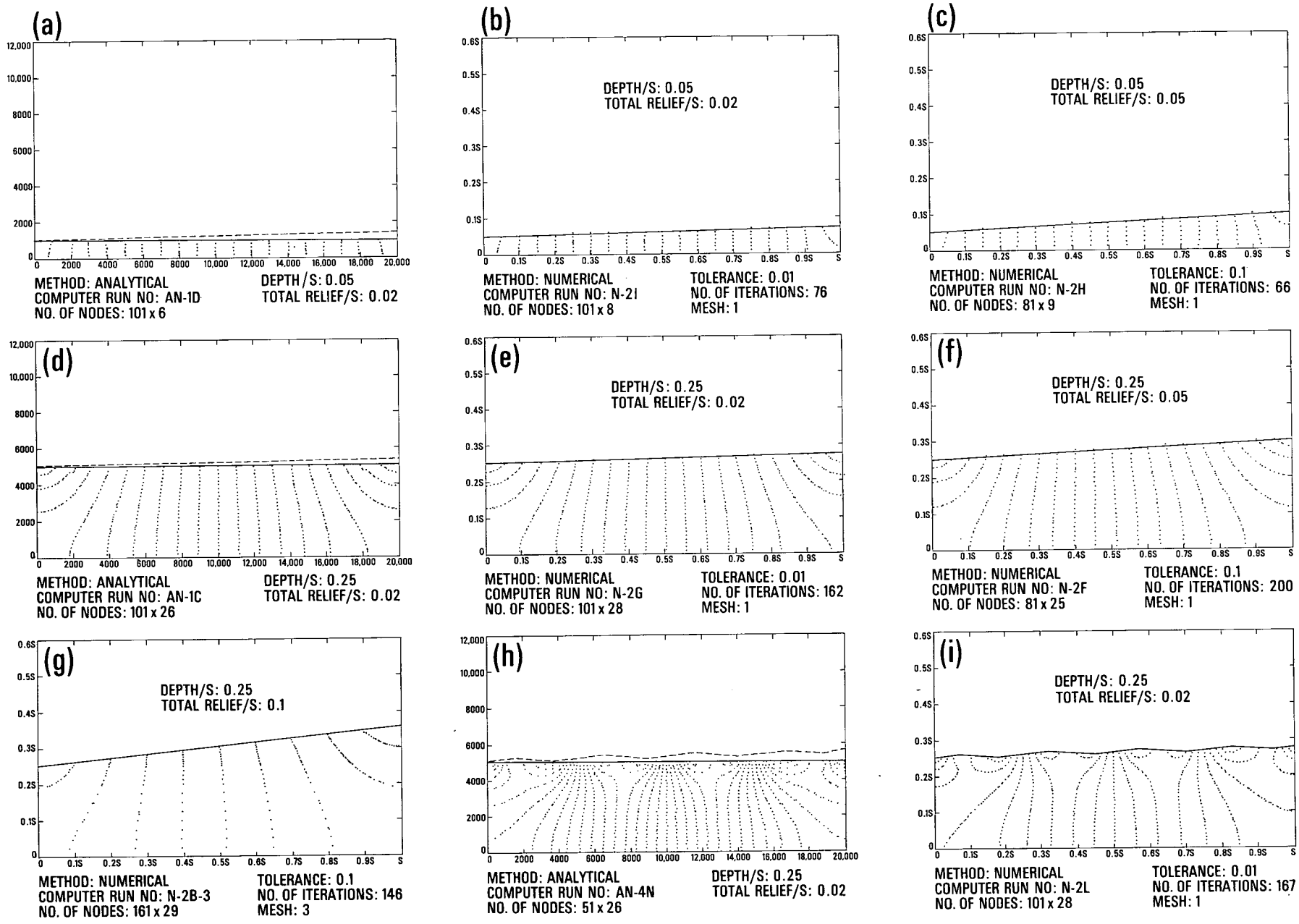

Figure 18. Quantitative validity of the rectangular approximation

contour interval in Figure 18 (a and b) is 20 feet and in 18c is 50 feet.

Figure 18 (d and e) shows the case of a 2 per cent regional water table slope as the upper boundary of a deeper groundwater basin. Figure 18f is for a 5 per cent slope and Figure 18g, a 10 per cent slope. The contour interval in Figure 18 (d, e and f) is one twentieth of the total head; in Figure 18g it is one tenth of the total head.

These seven diagrams show that, while the nature of the potential pattern is unchanged, the actual quantitative value of the potential at any point in the section, especially in the upstream half, may be overestimated by the use of the rectangular approximation, even for very small regional water-table slopes. For example, the uppermost equipotential contour in Figure 18a lies to the left of the lower right-hand corner of the region while it is to the right of the corner in Figure 18b. The correct value of the potential at this point, as found by the numerical method (Figure 18b), is less than that found using the analytical method and the rectangular approximation (Figure 18a).

Figure 18 (h and i) offers a comparison for a hummocky water-table configuration. The contour interval in Figure 18i is twice that in Figure 18h.

ADVANTAGES OF NUMERICAL METHOD

The superiority of the numerical method of solution has been made clear in the previous chapters of this report. It is the purpose of this section to review the objections to the analytical method and to list in one place the advantages of the numerical method.

Analytical solutions suffer from three severe limitations:

1. The field must be approximated by a rectangle, thus limiting the quantitative validity of the results to small regional water-table slopes.
2. Richard's equation is not amenable to analytical solution. The only non-homogeneous case which can be solved analytically is the case of n horizontal layers. If $n > 3$, the solutions become mathematically inconvenient.
3. It is impossible to represent realistic three-dimensional, water-table configurations by a suitable boundary condition. Analytical methods are thus limited to two dimenstions.

The advantages of the numerical method can be summed up as follows:

1. The three restrictions listed above are all removed:
   (a) The true shape of the field may be represented to a very close approximation. There is no limit on the regional water-table slope.
   (b) Richards' equation and Laplace's equation are handled in an identical fashion. The numerical method is thus capable of treating the general non-homogeneous anisotropic case.
   (c) It is possible to construct three-dimensional models representing groundwater basins.
2. The numerical solution is general. Only one mathematical derivation is necessary in order to design a computer program which can handle any water-table configuration and any geologic configuration. (The six numerical computer programs listed in Appendix B all contain the identical mathematical steps. The difference lies in the complexity of the problem each program can handle, the corresponding method of punched card input and the resultant limiting size of the problems.) The analytical method, on the other hand, requires a separate mathematical derivation for each change in the model. In addition, the mathematics involved in the numerical method is far simpler than that used in the analytical method.
3. For simple cases, the computer time is approximately the same for either method. As the complexity of the problem increases, however, the computer times involved in the analytical solutions increase, whereas those for the numerical programs remain more nearly constant.

4. Remson, Appel and Webster (1965) have noted that "a great advantage of the finite-difference digital computer approach is that it is compatible with machine-oriented methods of data storage and retrieval". They further state their belief that "machine-oriented storage will eventually be used for most types of groundwater data. It is likely that groundwater investigators will have libraries of programs capable of achieving certain types of solutions. It will be necessary only to take the data deck or tape for a given aquifer and the suitable program to a nearby computer to achieve a solution".

For the reasons listed above and particularly in view of the scientific advantages in Section 1 (a), (b), and (c), the numerical method outlined in Chapter 3 is considered to be the fulfillment of the first objective of this study, namely to develop a suitable mathematical model and method of solution for the case of a non-homogeneous anisotropic groundwater basin with any water-table configuration.

The numerical method has therefore been used to carry out the second objective which is the investigation of the qualitative effects of the water-table configuration and geologic configuration on regional groundwater flow. The results of this investigation are recorded in Chapters 5 and 6.

The next two chapters are restricted to two-dimensional vertical sections through the basin. The use of three-dimensional models is discussed in Chapter 7.

CHAPTER 5

Qualitative Results; The Effect of Water-Table Configuration and Geology on Regional Groundwater Flow

FACTORS AFFECTING THE POTENTIAL FIELD

Any potential field defining any flow system, whether it be groundwater, heat, electricity, or otherwise, results from the interrelation of three governing factors:

1. The shape of the region in which the potential field is defined.
2. The existing boundary conditions.
3. The nature of the inhomogeneities in the properties which control the flow within the region.

For the specific potential field representing regional groundwater flow, we have defined the shape of the region in our two-dimensional numerical mathematical model. The region is roughly rectangular with vertical sides, a horizontal base and an irregular upper boundary (the water table). There are two ways in which we can control the shape of the region; by changes in the water-table configuration, which result in minor changes in the shape of the region; or by changing the "depth/lateral extent" ratio. By changing this ratio, we can examine all cases from that of a deep basin of limited lateral extent, to the more usual case of a shallow groundwater basin of large lateral extent.

The boundary conditions which exist on the external boundaries of the region are also explicitly defined by the mathematical model. The only boundary condition which we can tamper with is that of the water table and it is not the nature of the boundary condition that we can change but merely its numerical value and the position at which it is applied. This is done by the delineation of the water-table configuration.

The property of the medium which affects the nature of the potential field within the region is, of course, the permeability. We must therefore investigate the effect of inhomogeneity and anisotropy of permeability on the groundwater flow patterns. In this study we have concentrated our attack on an investigation of the effects of inhomogeneity; in particular the effect of various geometric configurations of permeability ratios and the effect of changing the numerical values of the ratios themselves. A short section on anisotropy, with several examples, is presented to show the applicability of the method.

We can summarize the factors affecting the potential field as follows:

1. The depth/lateral extent ratio.
2. The water-table configuration.
3. The geologic configuration controlling the permeability contrasts.

The effect of these factors is investigated in the remaining sections of this chapter.

POTENTIAL DIAGRAMS

The results of this chapter are presented in the form of potential field diagrams, representing solutions to the various cases considered. Seventy-four diagrams are shown (Figures 19 through 25). The majority of the diagrams show the equipotential net only. A few diagrams (Figure 19 a and h for

example) include the flow pattern itself in the form of streamlines. (These are not quantitative flow nets but serve only to indicate the direction of flow.) It is felt that the interested reader can construct the streamlines either on paper or in his mind, for those cases in which they are not included.

The diagrams are dimensionless, having a lateral length of "s". The horizontal and vertical coordinate axes are divided into segments 0.1s, 0.2s, etc. (In the computer programs it is necessary to specify numerical values for the dimensions of the region; in Figure 19a, s = 60,000 feet. The resulting flow net will apply to any region with the same depth/lateral extent ratio.)

Three different depth/lateral extent ratios were used, resulting in three different sizes of diagram (e.g., Figure 19 d, e and f). The least depth/lateral extent ratio was used most because it was considered to be the most representative of a real groundwater basin.

The diagrams are true scale; there is no vertical exaggeration.

The water-table configuration is shown by a heavy line at the top of the contoured region. Those plotted points which appear above the water table are due to the approximation of the slope of the water table in stepwise fashion.

The permeability contrasts are denoted within the field. The permeabilities may also be considered as dimensionless as it is the permeability ratio which controls the nature of the potential field. For example, in Figure 20a, the same potential net would result from permeabilities of 10 and 100 as exists for 1 and 10. The quantity of flow through the basin would of course be different.

All the solutions presented in this chapter were obtained using the numerical method.

The computing parameters together with the "depth/s" and "total relief/s" ratios are labelled beneath each diagram. The depth is measured at the lowest topographic point. The total relief is the difference in elevation of the water table between its highest and lowest points. For example, in Figure 19a the depth = 0.0833s, total relief = 0.0167s and depth + total relief = 0.1s which is where the water table meets the right-hand boundary.

The computer run number also gives a certain amount of information. Referring once again to Figure 19a, the number N-3G-1 tells us that the numerical (N) method was used, employing Numerical Program 3 and topographic configuration G. The 1 is the actual run number and is of no significance to the reader. All diagrams which have a G in their computer run number have the same topography. Other topographies are represented by the letters D, E, F, H, K etc.

In some diagrams, the closeness of the contour interval results in a hodgepodge of dots in one particular portion of the plot, usually near the major valley sink at the left of the diagram. The author is assuming that the interested reader can properly appraise each situation without the help of interpretive lines. For example, at the left end of the K = 1 layer in Figure 20a, the vertical rows of points are actually the result of closely-spaced near-horizontal equipotential lines. The flow is upward and the valley is a discharge area as one would expect.

GENERAL EFFECT OF WATER-TABLE CONFIGURATION

The investigation of the effect of the water-table configuration on regional groundwater flow patterns was begun by Tóth (1962, 1963b, c). He considered two cases: a constant gentle regional slope such as one would expect to find in the flat prairie, and a water table with the configuration of a sine curve as one might expect in hummocky terrain. With the increased versatility of the methods introduced in this report, we can now investigate water-table configurations of a more irregular nature, and ones more representative of actual field conditions.

Figure 19 (a through j) presents 10 flow patterns representative of 10 different water-table configurations bounding a homogeneous basin. The following table describes the water-table configurations shown in the diagrams.

It is recognized that these water-table configurations do not represent all possible cases but it is felt that they constitute a broad enough spectrum with which to obtain generalized conclusions.

Figure	Water-Table Configuration	Description
19a	G	Gentle, constant, regional slope.
19b	F	Broad flat valley, with gentle, constant regional slope extending from valley edge to topographic high.
19c	T	Flat valley, with water table from valley edge to topographic high represented by a parabola, approximated by five straight line segments of decreasing slope. The fifth segment is horizontal.
19d	E	Narrow flat valley with steep valley flank and constant regional slope extending from valley edge to topographic high. (Configuration D which appears in Figure 20 is similar to E but one half of the total relief is taken up in the steep valley flank in D, only one quarter in E.)
19e	N	As E, but with depth/lateral extent ratio of 0.125 (1:8) instead of 0.08333 (1:12).
19f	R	As E, but with depth/lateral extent ratio of 0.25 (1:4).
19h	H	Broad flat valley, with water table from valley edge to topographic high consisting of a series of highs and lows superimposed on a regional slope.
19g	K	A composite of E and H with a broad valley, a steep valley flank, a gentle regional slope in the downstream half of the basin and a hummocky configuration in the upstream half.
19i	P	As H, but with depth/lateral extent ratio of 0.125.
19j	S	Depth/lateral extent ratio of 0.25. Water table consists of a broad flat valley and several segments of varying slope.

As stated earlier, we are avoiding the controversy as to whether the water table always mirrors the topography. It is undoubtedly true, however, that in many cases the water-table configuration and the topographic configuration will be the same.

The directions of the stream lines are shown in Figure 19 (a and h). Figure 19a is a recalculation of one of Tóth's earlier results. The recharge area is the upstream half of the basin, the discharge area the downstream half of the basin and the so-called "mid-line" is at the centre point. The position of the mid line at the mid point occurs only for this constant slope case. It is therefore better defined as a "hinge line" (or hinge point in two dimensions) which hinges the recharge area and the discharge area. In this simple case, there is only one recharge area and one discharge area. In Figure 19h, it can be seen that the result of a hummocky water-table configuration is a series of recharge and discharge areas with many hinge lines.

The diagrams speak for themselves and little discussion is necessary. The interested reader should examine each potential plot for its quantitative and qualitative ramifications. Quantitatively, one can note the gradient at various points in the region and the intensity of recharge or discharge at various points along the water table. Chapter 6 contains a detailed discussion of quantitative interpretations. Qualitative points of interest are the distribution of recharge and discharge areas, and the depth and lateral extent of the component sub-basins of the major groundwater basin. These latter two points are of sufficient importance to warrant separate sections of this chapter for discussion.

The following is a summary of the conclusions inherent in a perusal of Figures 19a through 19j:

1. In a recharge area, the equipotential lines meet the water table obliquely with the acute angle on the upslope side. In a discharge area, the acute angle is on the downslope side. At the hinge point, the equipotential meets the water table at right angles.

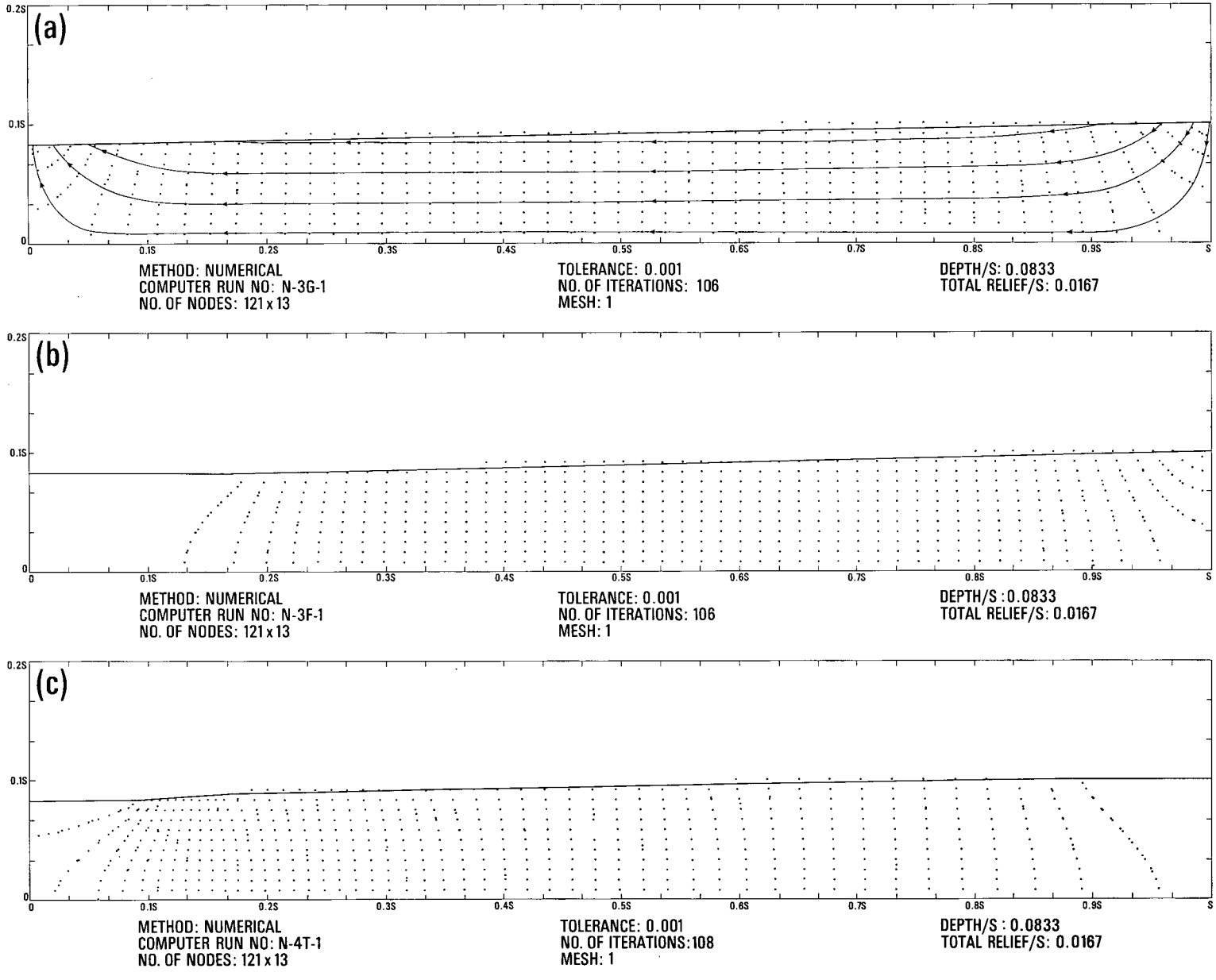

Figure 19. Effect of water-table configuration

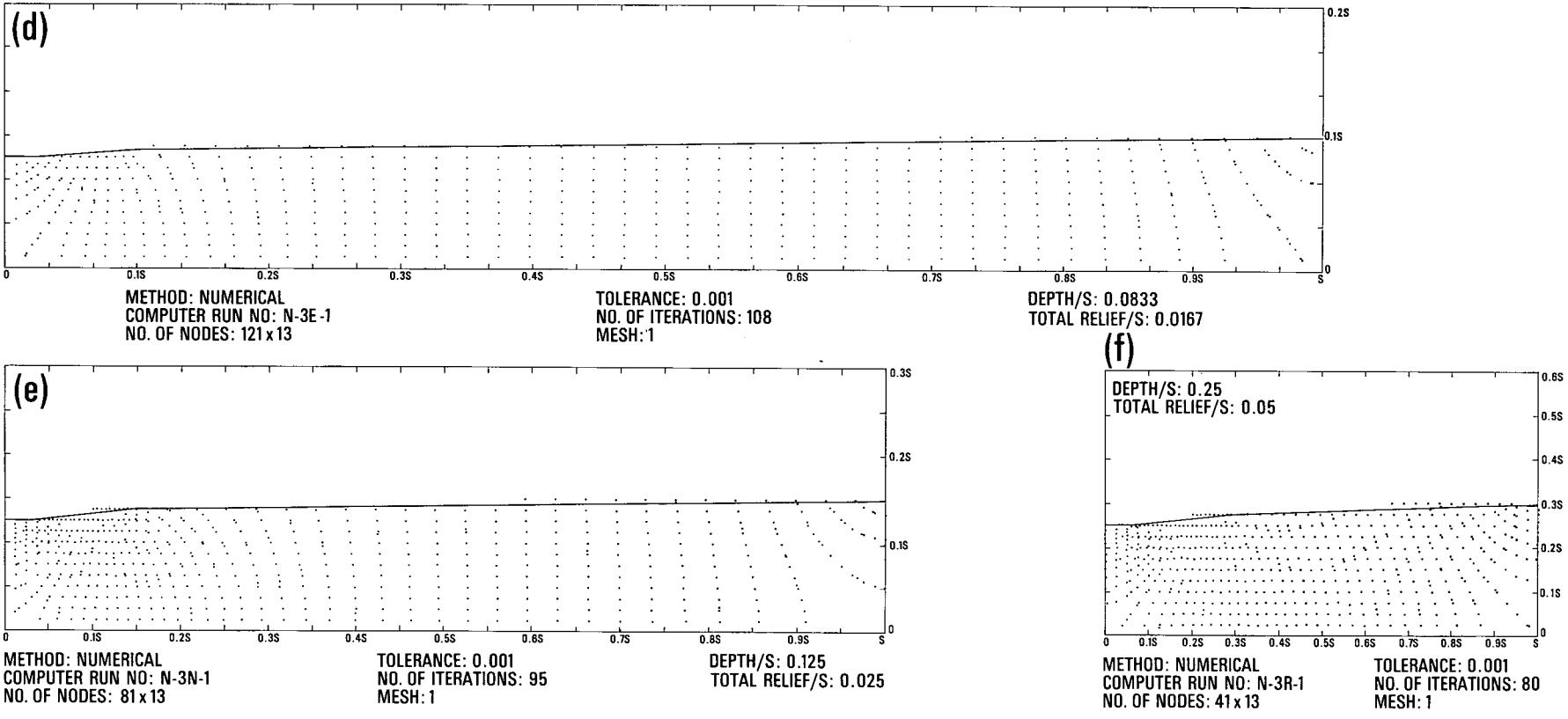

Figure 19(continued). Effect of water-table configuration

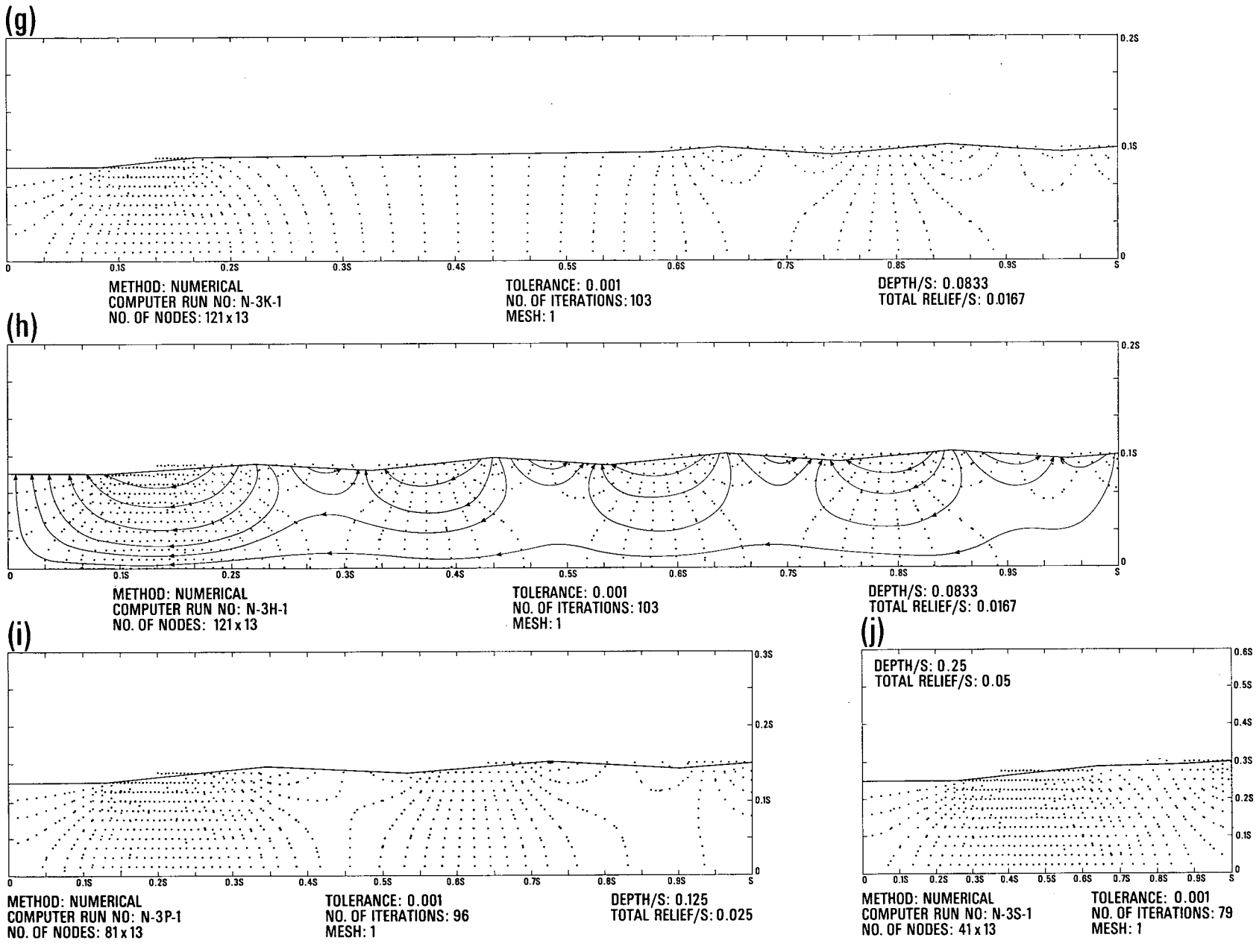

Figure 19(continued). Effect of water-table configuration

2. The existence of a high in the water-table configuration, whether it be a major regional high or a minor reversal in slope, results in recharge at that point and for some distance on either side. The existence of a low results in discharge at that point and for some distance on either side. (This conclusion holds only for two-dimensional sections taken parallel to the direction of dip of the water-table slope. In Chapter 7, consideration is given to the adaptation of this principle to three dimensions.)

3. If the spacing between equipotential contours is x feet, then an equipotential line must meet the water table at every point along its length which represents an increase in elevation of x feet. Steep water-table slopes therefore result in many equipotential lines and high gradients near the water table (and indeed to some depth). Shallow slopes are conducive to low gradients and near-horizontal flow. Flat slopes represent equipotential lines themselves and result in very low upward (valley bottom) or downward (hilltop) gradients.

4. A gentle constant regional water-table slope over a homogeneous medium (Figure 19a) results in flow which is essentially horizontal. Recharge is concentrated at the upstream end of the recharge area, discharge at the downstream end of the discharge area.

5. The existence of a broad flat valley (Figure 19b) means that while the hinge line is still at about 0.5s it is now closer to the downstream end of the constant regional slope.

6. A parabolic water table (Figure 19c) results in recharge which is more evenly distributed down the slope.

7. The existence of a major valley (Figure 19d, e and f) concentrates the discharge in the valley. The hinge line occurs midway up the steep valley flank. Two zones of concentration of recharge occur one at the upstream end of the recharge area and the other in the recharge portion of the steep valley flank and extending just above the break in slope. This quantitative ramification may be exaggerated in Figure 19d in that the parabolic water table of Figure 19c is a more likely configuration than that of Figure 19d.

8. The existence of a hummocky water-table configuration (Figure 19h) results in numerous sub-basins within the major groundwater basin. Water which enters the flow system in a given recharge area may be discharged in the nearest topographic low (first-order basin), or may be transmitted to a distant minor topographic low (second-order basin) or to the regional discharge area in the major valley bottom (third-order basin).

9. Larger depth/lateral extent ratios (Figure 19i) result in a larger proportion of the recharge entering the higher-order flow system (i.e., the individual hummocks exert smaller influence on the total flow pattern).

GENERAL EFFECT OF GEOLOGY

In this section, 26 potential patterns are presented (Figure 20, a through z) in order to show the effect of a wide range of geologic configurations on regional groundwater flow patterns. In order to isolate the effect of the geology from that of the topography, only two water-table configurations have been used. Figure 20 (a through q) uses water-table configuration D (a major valley at the left of a constant regional slope); Figure 20 (r through z) uses water-table configuration H (hummocky topography). For each of these water-table configurations, a wide range of permeability contrasts are investigated including two-layer cases, three-layer cases, partial aquifers, and sloping aquifers and "aquicludes". Most of the diagrams consist only of the equipotential patern, but a, 1, q and t show the streamlines. In this section, the diagrams are discussed individually or in small groups in order to isolate the various features they show. Generalizations regarding the effect of the geologic configuration are included in the following two sections under the heading "Factors controlling the distribution of recharge and discharge areas" and "Factors controlling the depth and lateral extent of groundwater basins".

Figures 17e and 20 (a and b)

Figure 17e presents the potential pattern resulting from water-table configuration D and a homogeneous medium. Figure 20 (a and b) shows the effect of the introduction of a basal aquifer with a permeability 10 times that of the overlying layer. The result is essentially horizontal flow through the aquifer. It is recharged through the low permeability layer above. A vertical component to the flow is thus introduced in the upper layer, one which did not exist in the homogeneous case. One should note the downstream increase in the gradient in the aquifer. The increase in gradient makes it possible for the aquifer to accept an increasing number of flowlines from the upper layer. The discharge is concentrated in the valley bottom; the entire constant regional slope is a recharge area.

The thickness of the basal aquifer has little effect on the nature of the flow pattern as shown by a comparison of a and 20b of Figure 20. The quantity of water flowing through the system represented by Figure 20b would of course be much less than that flowing through the system represented by Figure 20a.

Figure 20 (b, c, d and e).

This group of potential patterns shows the effect of increasing the permeability of the basal aquifer. As the permeability ratio increases, the following changes can be noted:

1. The vertical upward or downward flow through the overlying low-permeability layer becomes more pronounced. For example, in the upstream recharge areas at the right-hand side of the diagrams, the flow becomes more vertical, the vertical flow exists over a larger area and the vertical gradient increases.
2. The horizontal gradient in the aquifer decreases but the quantity of flow (which can be calculated using Darcy's Law) increases.
3. The hinge line moves upslope, creating larger discharge areas. This is a result of the increased quantity of water flowing through the basal aquifer which must escape as the influence of the left-hand vertical impermeable boundary is felt. The magnitude of the effect may not be entirely realistic as it is possible that, for permeability ratios of 1000:1 (Figure 20e), the "major valley" at the left of the diagram would not create an imaginary impermeable boundary. Horizontal flow through the aquifer might proceed to the left until a more pronounced topographic influence was encountered.

Figure 20 (f, g and h).

A comparison of f, g and h of Figure 20 with Figure 17e, and with each other, shows that the flow pattern resulting from a two-layer case when the upper layer has the largest permeability is almost identical to that of the homogeneous case. The quantity of flow is, of course, considerably different in each of the four cases. The fact that a geologic configuration exists which results in a potential pattern identical to that of the homogeneous case points out the fallacy of using piezometric data to obtain quantities of regional flow. In a common method, the potential pattern is delineated by piezometric information, and if it looks homogeneous, the permeability is measured near the surface and assumed to hold at depth. These diagrams, particularly 20h, show that a grossly erroneous figure could be obtained. It is clear that good permeability data are necessary before quantitative estimates of regional flow can be obtained.

Figure 20 (i, j and k)

These diagrams show three three-layer cases; no new concepts are introduced but the effect on the potential pattern of various permeability contrasts in three-layer configuration.

Figure 20 (l, m and n)

The effect of lenticular bodies of high permeability and the particular importance of their position in the basin are shown in Figure 20 (l, m and n.)

The presence of a partial basal aquifer in the upstream half of the basin (Figure 20 l) results in a discharge area which occurs in the middle of the constant regional slope. The occurrence of such a discharge area under strictly topographic control would, of course, be impossible. The majority of the flow which has entered the system in the upper half-basin is discharged at this point. What was originally a single basin in the homogeneous case has become two basins under the influence of the partial aquifer.

When the partial, basal aquifer occurs in the downstream half of the basin (Figure 20m), the central discharge area does not exist and indeed recharge in the region over the aquifer is concentrated. The zone of most intensive recharge is thus shifted from the upstream portion of the basin in the homogeneous case to the downstream portion when the partial aquifer exists.

Figure 20n shows the aquifer in a lens-like position. In this case there is recharge over the upstream end of the lens and discharge over the downstream end. There is horizontal flow through the lens and in a "shadow zone" beneath it.

The effects shown in Figure 20 (l, m and n) for a permeability ratio of 10:1 would be more pronounced were a higher permeability contrast used.

Figure 20 (o, p and q)

Figure 20 (o and p) shows the effect of a sloping aquifer on the flow pattern. In Figure 20o, there is concentrated recharge (quantitatively) where the K = 10 layer outcrops. The point where the upper boundary of the K = 10 layer meets the water table is a major hinge line with a large discharge area below it. Recharge again takes over just above the break in slope and discharge occurs once again in the major valley.

In Figure 20p, a completely different situation results. Here, recharge occurs through the K = 1 layer in the upper three quarters of the basin and flow through the aquifer is up and out of the system, creating a discharge area at the outcrop.

Figure 20q shows the reverse situation to that of 20o and the result is a rather unexpected discharge area at the outcrop of the low-permeability layer. The general nature of the pattern reflects the desire of the water to take the shortest route across the low-permeability layer between the two K = 10 aquifers.

Figure 20 (r, s and t).

These diagrams show three two-layer cases where the water-table configuration is hummocky. Once again, Figure 20r, with the high permeability layer at the surface, shows little difference from the homogeneous case (Figure 19h). The effect of a basal aquifer (Figure 20, s and t) is to provide a highway for the flow which passes under the low-permeability surface layer and restricts the depth of the small first-order basins so that their entire flow is contained in the low-permeability surface layer.

Figure 20 (u, v, w, x, y and z).

Figure 20 (u and v) shows two three-layer cases. Diagrams w and x show the effect of increasing the permeability in a lenticular aquifer beneath hummocky terrain. Note the shadow zone beneath the aquifer. Diagrams y and z show the effect of increasing the permeability in a sloping aquifer.

FACTORS CONTROLLING DISTRIBUTION OF RECHARGE AND DISCHARGE AREAS

The water-table configuration and the geologic configuration have been identified throughout this report as the broad governing factors which control regional groundwater flow. Both these properties of the basin can exist in a infinite variety; it is the challenge of this section to extract from this infinite variety a set of governing principles deduced from the type situations for which potential patterns have been developed in this study. Sixteen potential plots (Figure 21, a through p) are presented.

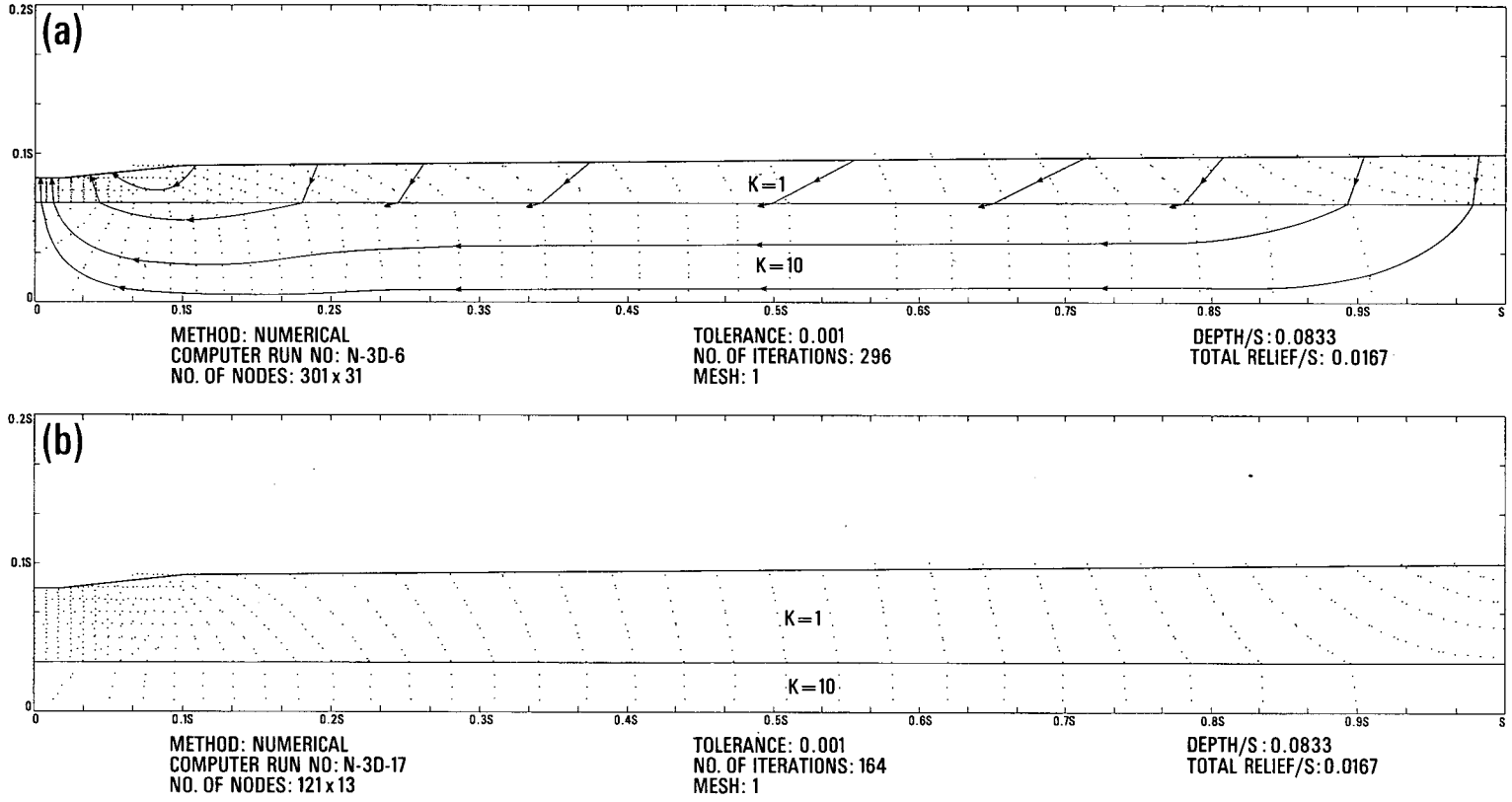

Figure 20. Effect of geology

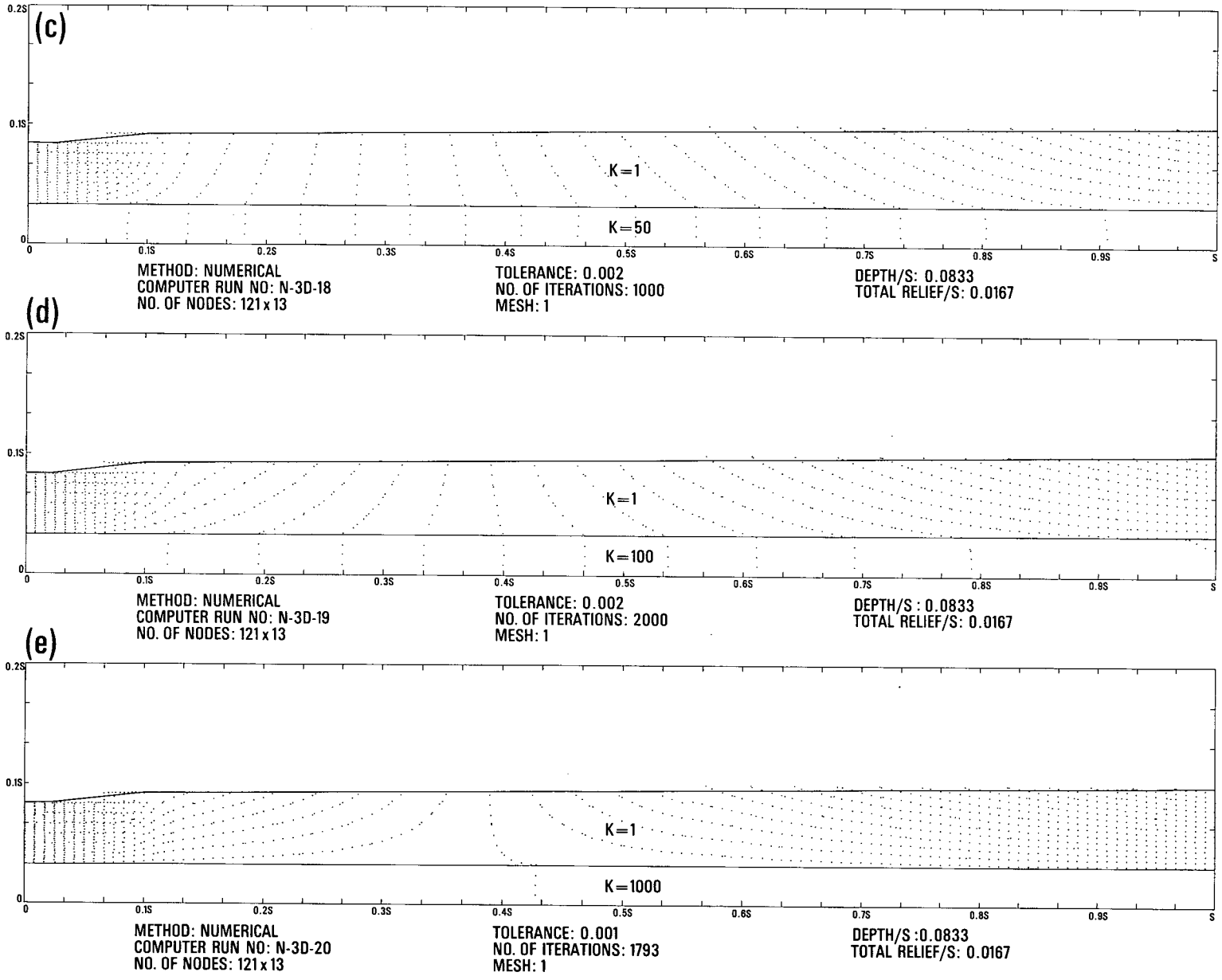

Figure 20(continued). Effect of geology

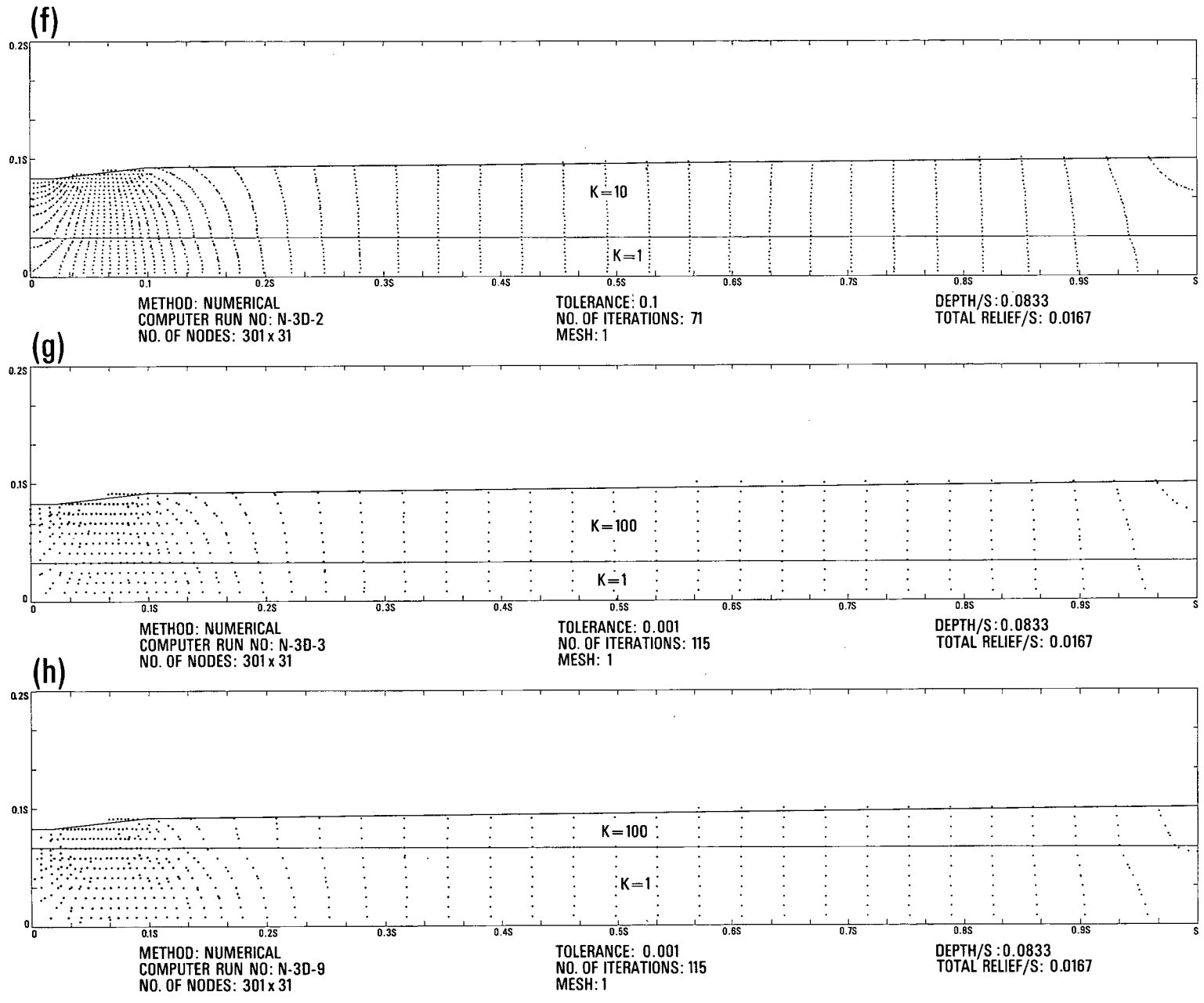

Figure 20(continued). Effect of geology

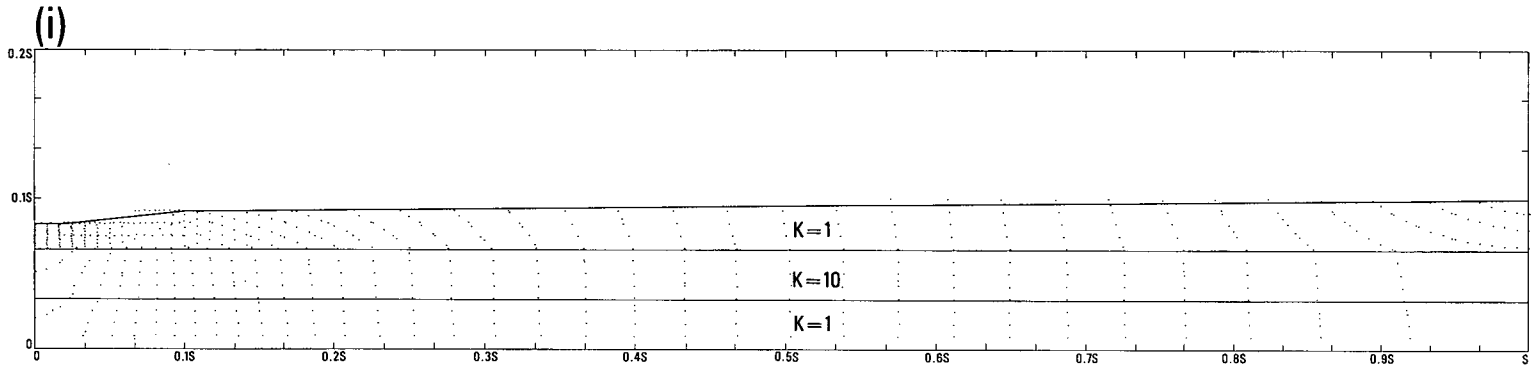

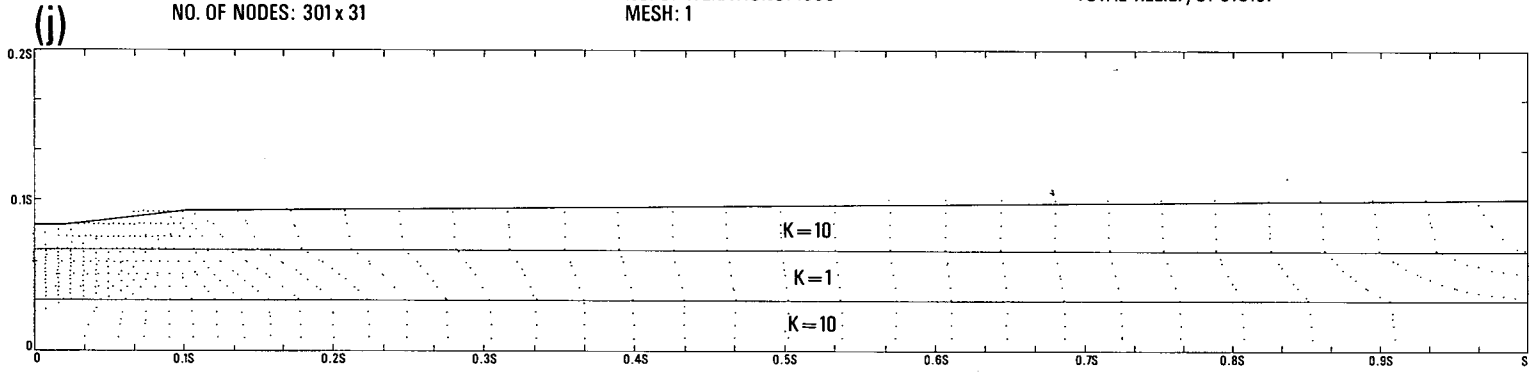

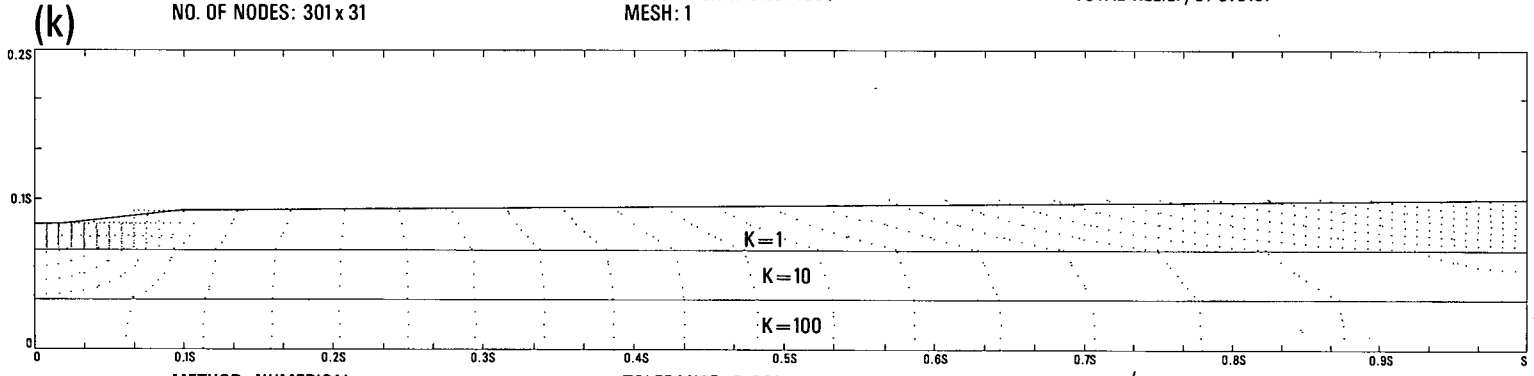

Figure 20(continued). Effect of geology

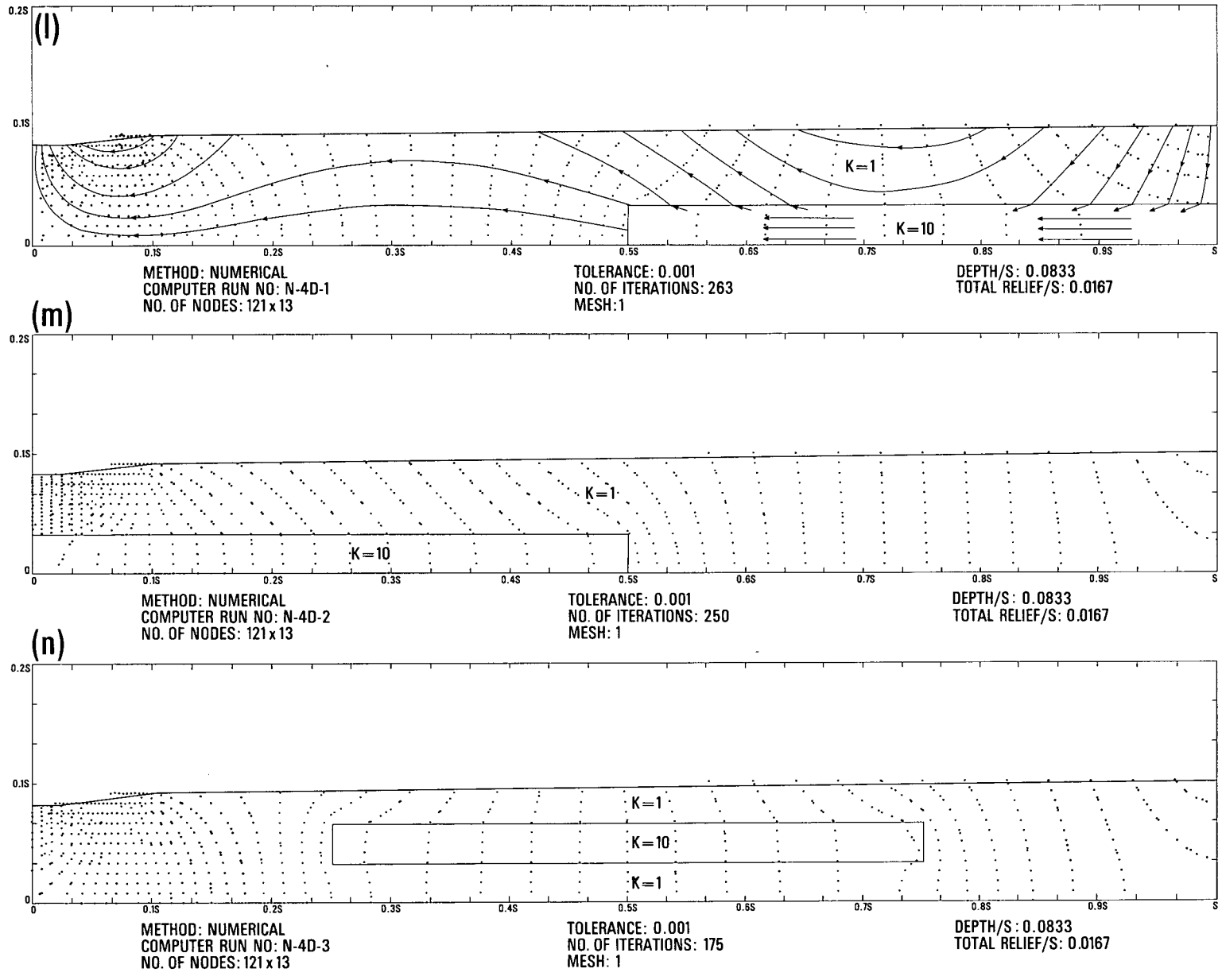

Figure 20(continued). Effect of geology

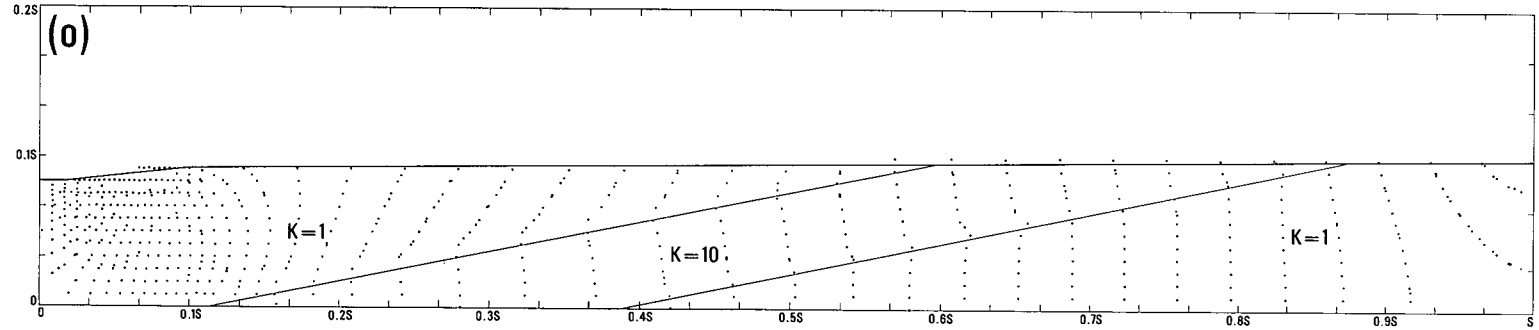

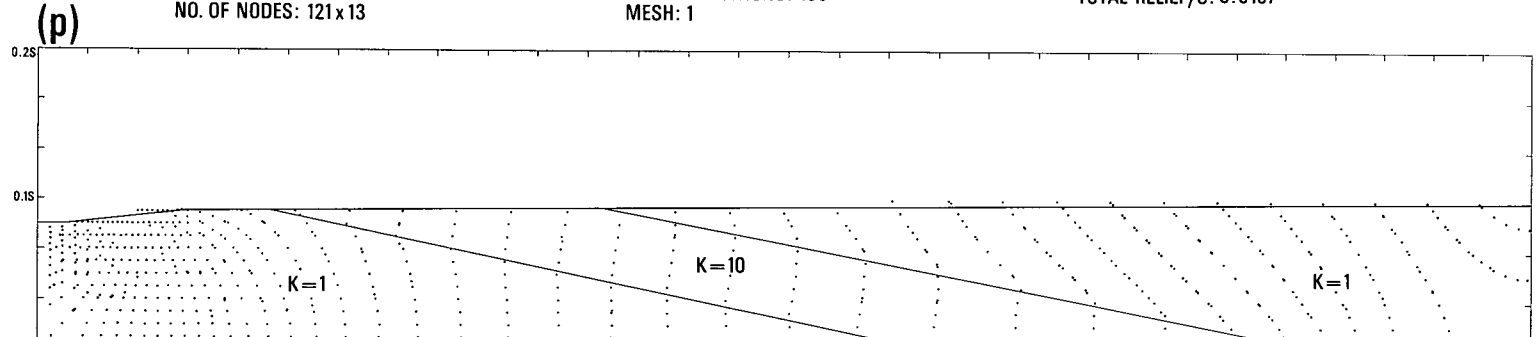

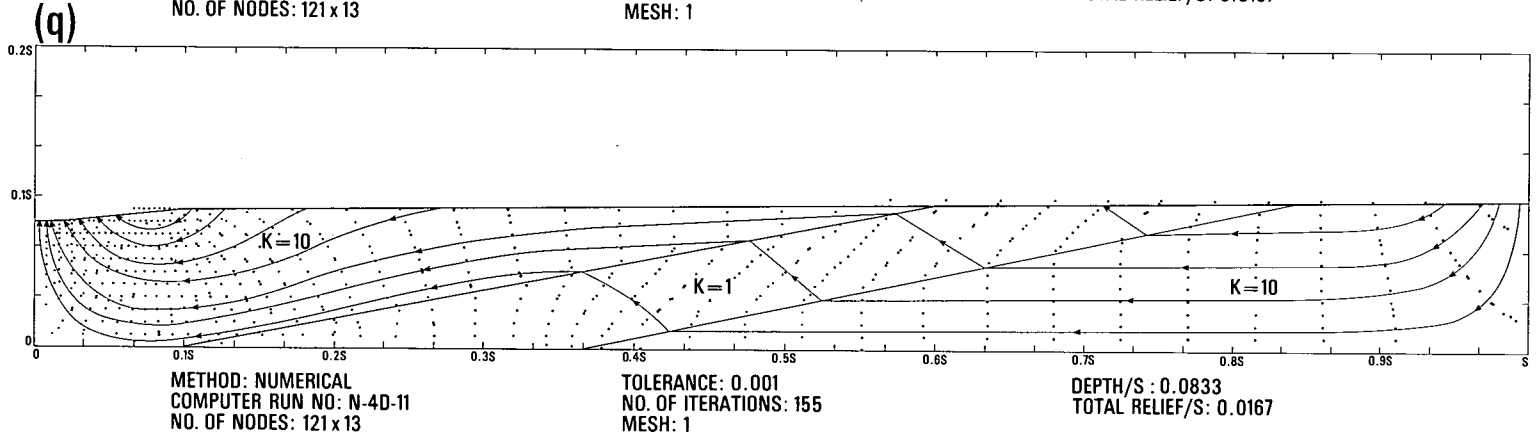

Figure 20(continued). Effect of geology

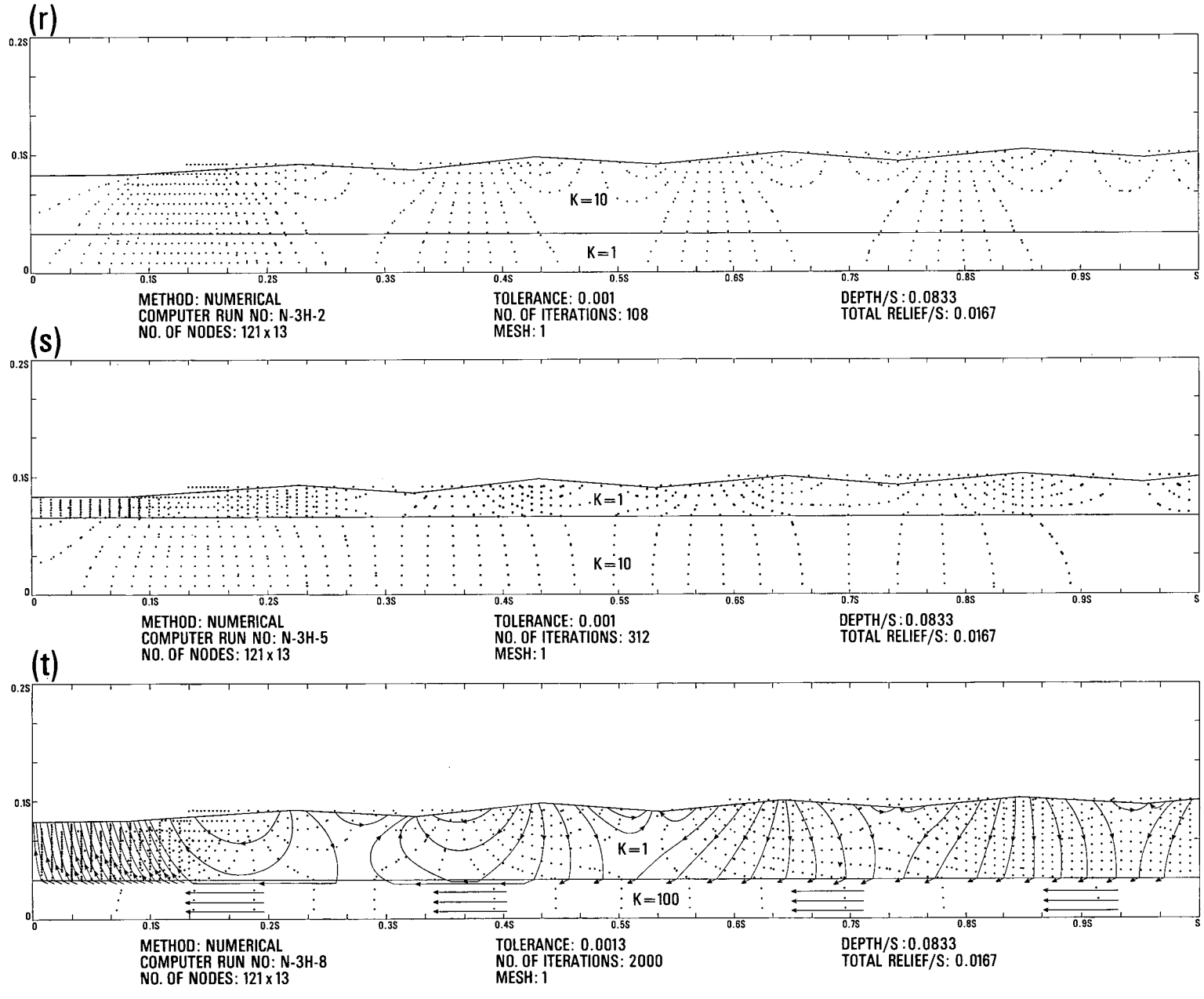

Figure 20(continued). Effect of geology

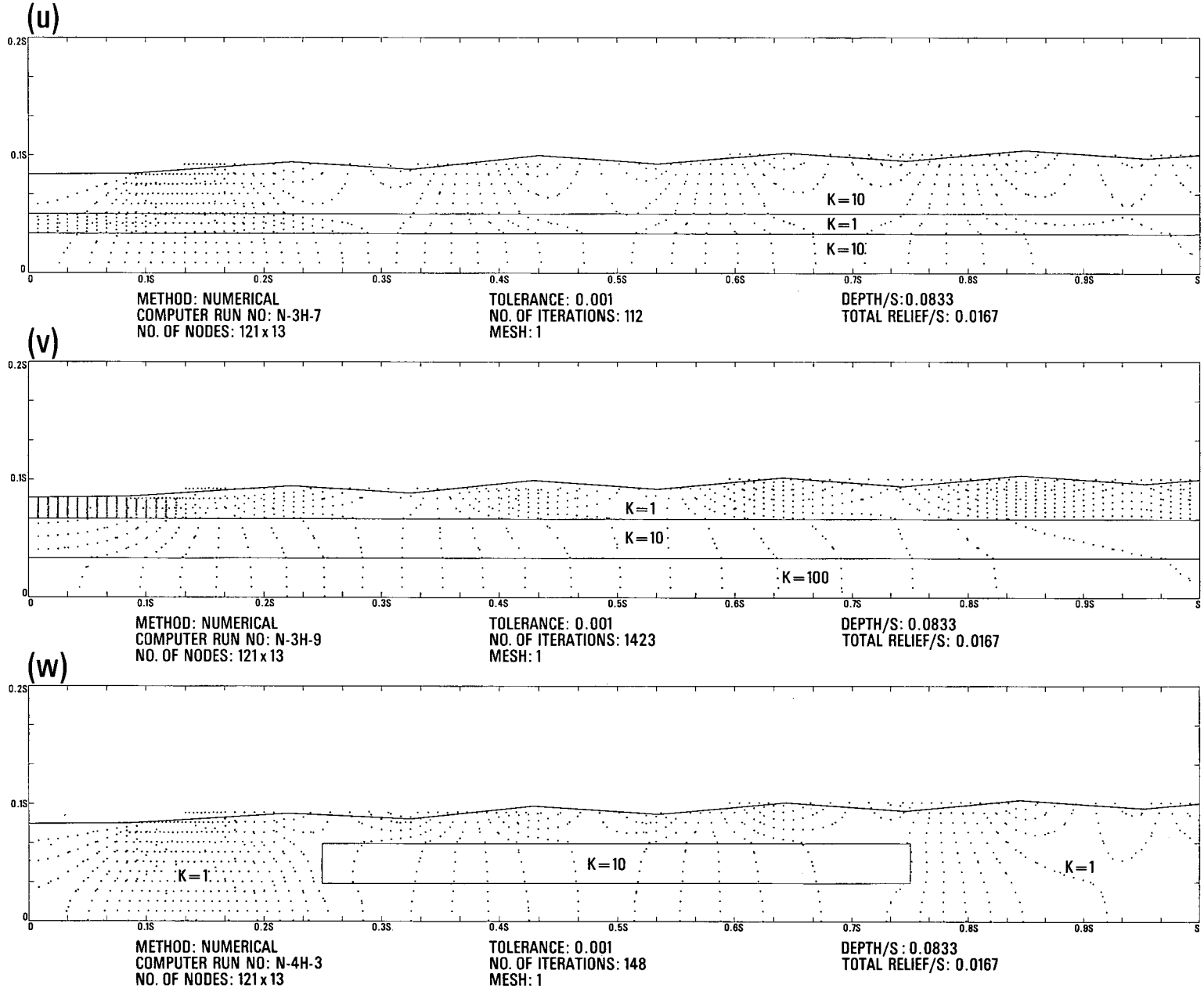

Figure 20(continued). Effect of geology

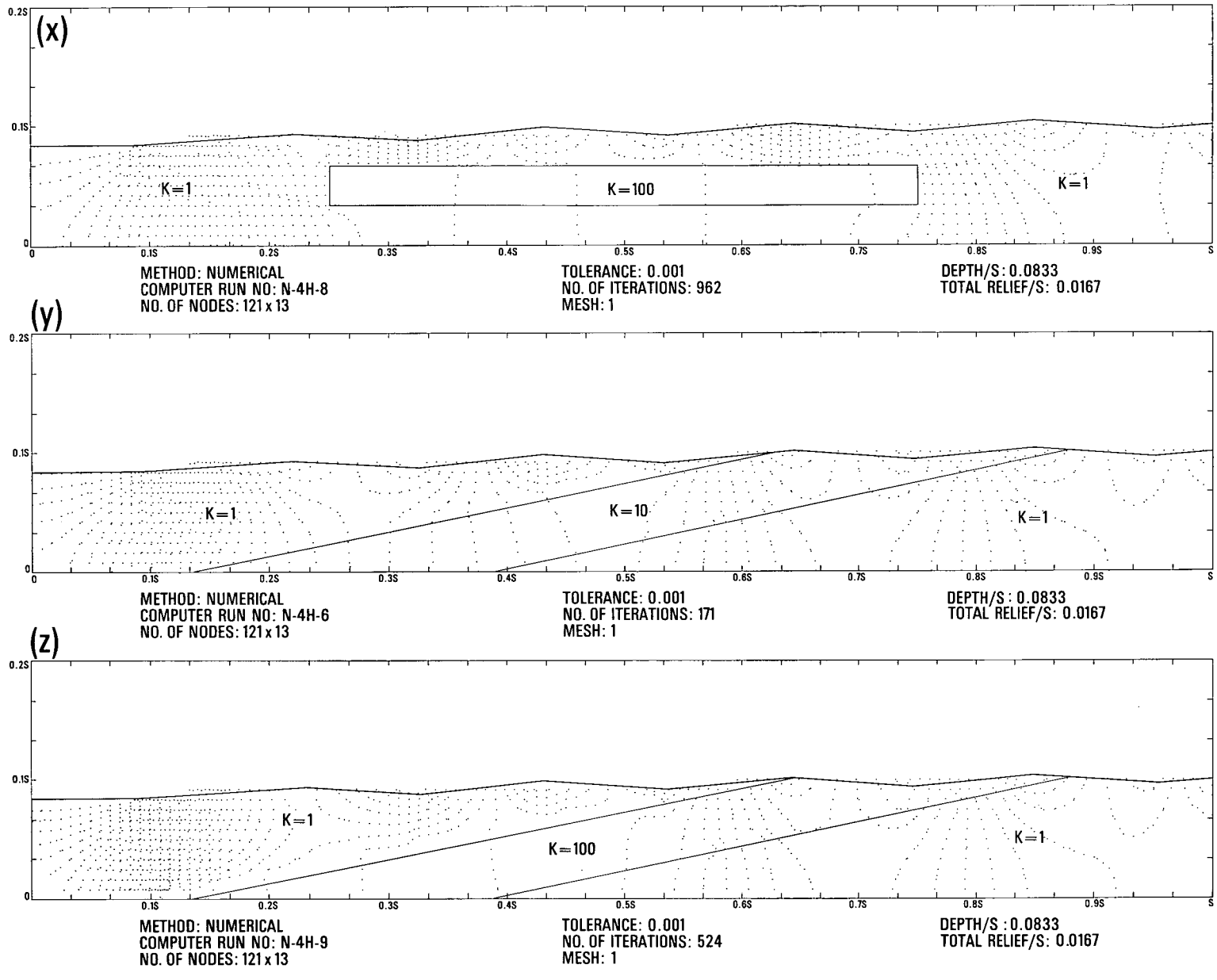

Figure 20(continued). Effect of geology

Position of the Hinge-Line in a Simple System

A simple flow system is one with a single recharge area and a single discharge area. The boundary between the two is the hinge line.

The position of the hinge line can be affected by both water-table configuration and geologic configuration. Figure 21 (a, b, and c) shows the effect exerted on the hinge line by the water-table configuration in a simple two-layer system. In Figure 21a, the case of a constant regional slope, the hinge line occurs at the midpoint of the basin. The introduction of a broad flat valley with no steep valley flank (Figure 21b) produces little change but the presence of a deeply incised valley (Figure 21c) causes the hinge line to shift over to the valley flank. The discharge is thus concentrated in the valley and along the lower portion of the valley flank. The percentage of the surface area of the drainage basin which can be considered as a discharge area is 50 per cent in diagrams a and b, Figure 21, but less than 10 per cent in diagram c. In a three-dimensional basin it could be even less.

The effect of the permeability of the basal aquifer on the hinge line has already been shown in b, c, d, and e of Figure 20. Reference to these diagrams will show that the hinge line moves upslope as the permeability ratio increases. Large permeability ratios are thus conducive to large discharge areas in a simple system where a subsurface "highway" exists.

Causes of Discharge

At least 7 distinguishable type configurations of topography and geology which lead to groundwater discharge can be ascertained.

1. The existence of a major topographic low of sufficient magnitude to create an imaginary vertical impermeable boundary which extends the full depth of the basin will cause concentrated groundwater discharge into the valley. In Figure 21d, two such discharge areas are apparent, one at either end of the basin. A third valley, having less relief, exists at the centre of the diagram between two local highs. This valley also forms a discharge area but the discharge is restricted to flow which has entered the flow system in one of the two portions of the recharge area shown. Any water which enters the K = 10 basal layer is transmitted beneath the valley to one of the two major discharge areas. In other words, the imaginary impermeable boundary beneath the central valley exists only in the upper layer.

2. Minor topographic lows will also cause discharge areas. These first-order systems may be sufficient to capture the flow from the entire depth of the basin (Tóth, 1963b, c) in the homogeneous case or may be restricted to the upper layers as in Figure 21 (e and f).

3. A break in slope, even though both slopes are positive, may be sufficient to cause small quantities of groundwater discharge just below the steep components of slope. This phenomenon is illustrated in Figure 21g. The major discharge area for the basin is located at C; isolated points of discharge occur at A and B.

4. Discharge areas which are entirely the result of geologic control occur at the surface above the pinchout of a high-permeability layer. The extent of the discharge area and the intensity of discharge depends on (a) the position of the partial aquifer within the basin and (b) the permeability contrast between the aquifer and the surrounding medium.

   The various possibilities are shown in Figure 21 (h, i, j, k, l and m). The least effect is caused by partial aquifers near the surface (Figure 21j), and the greatest effect by high-permeability partial aquifers (Figure 21m) and those located in the upstream portion of the basin (Figure 21h). Figure 21k portrays the effect of an alluvial fill of high permeability. It exerts little influence on the flow pattern.

5. The intensity of discharge and the size of the discharge area can be increased by the presence of a downstream sloping aquifer of high permeability (Figure 21n). The outcrop of the aquifer is a recharge area.

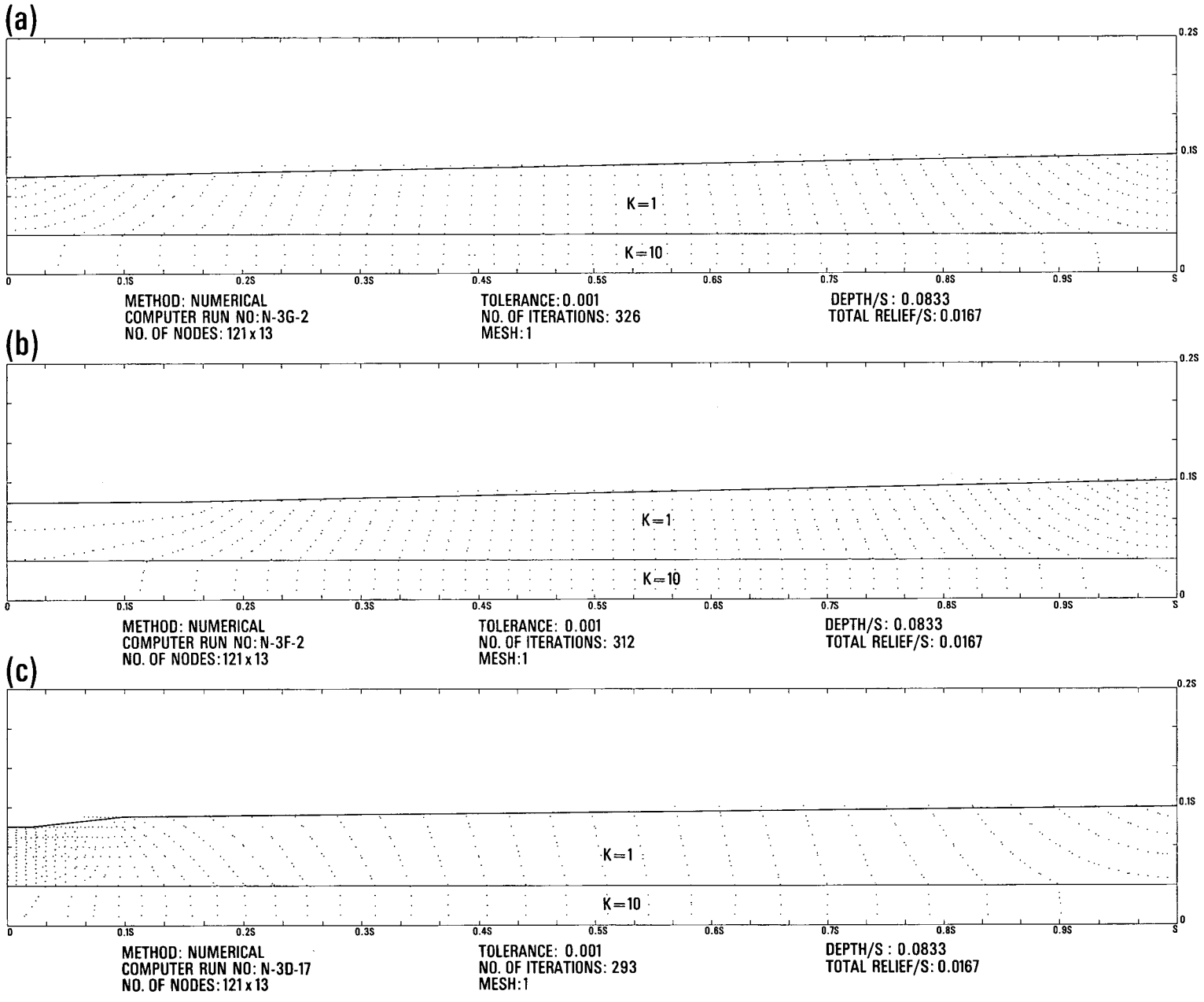

Figure 21. Distribution of recharge and discharge areas

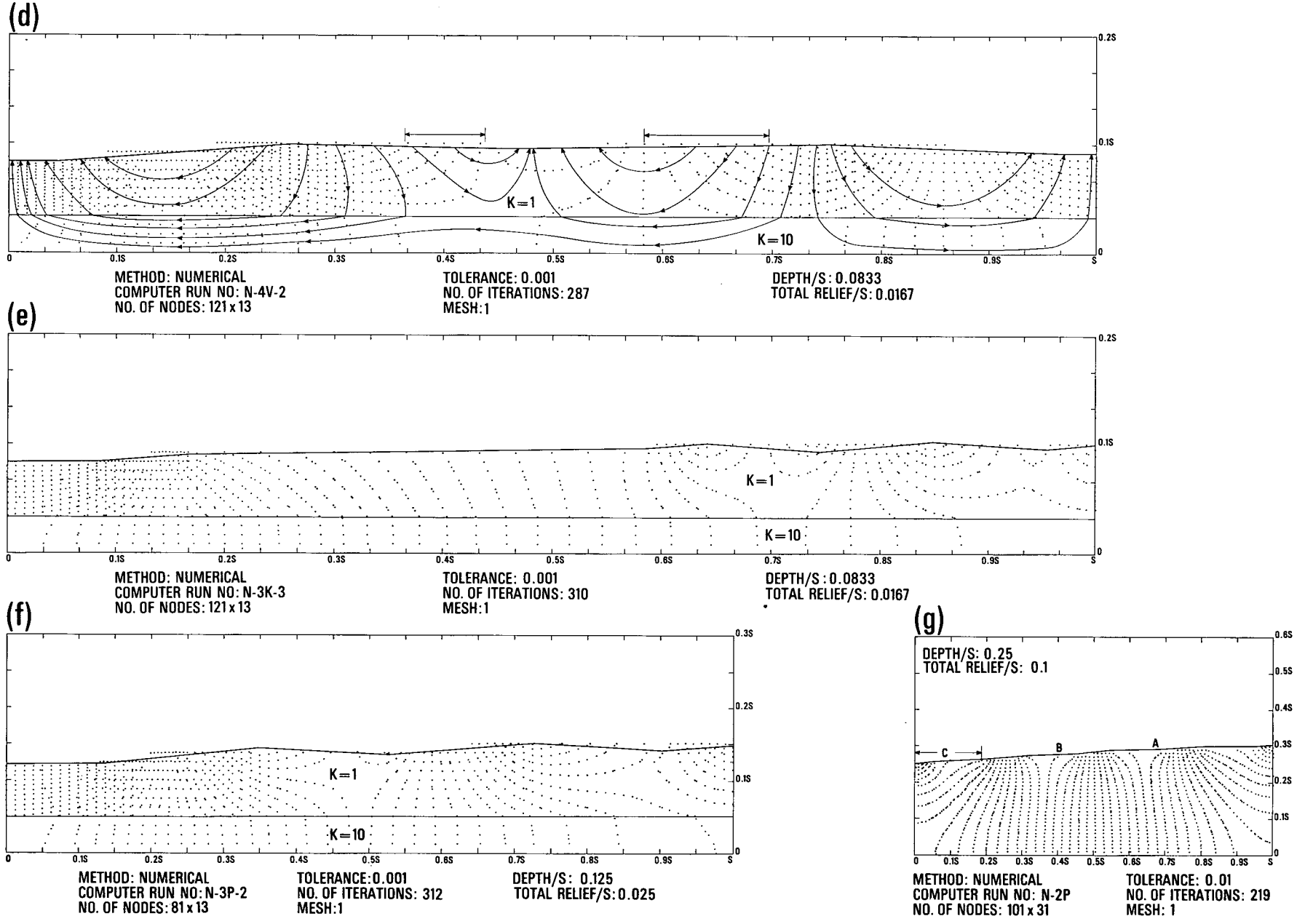

Figure 21(continued). Distribution of recharge and discharge areas

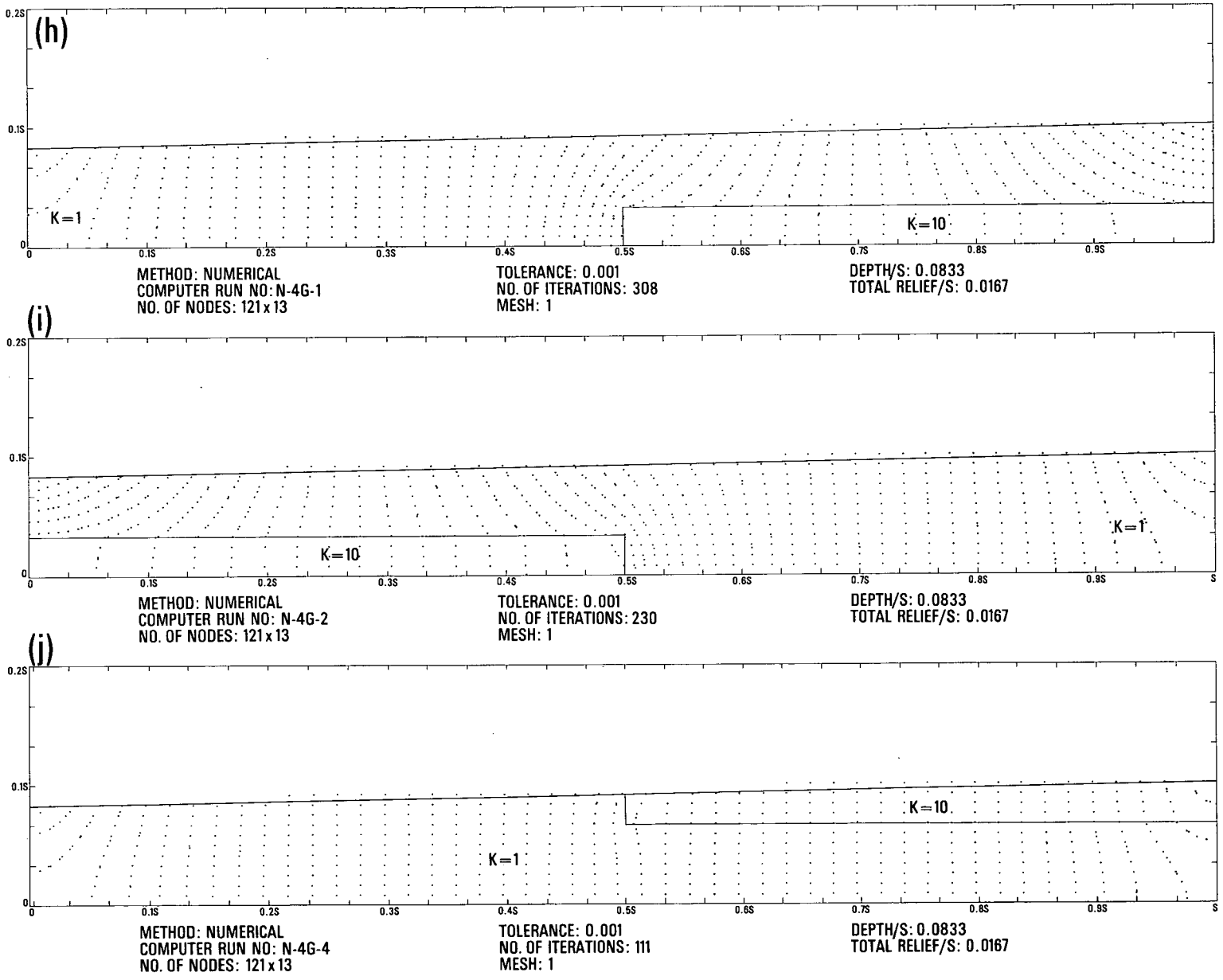

Figure 21(continued). Distribution of recharge and discharge areas

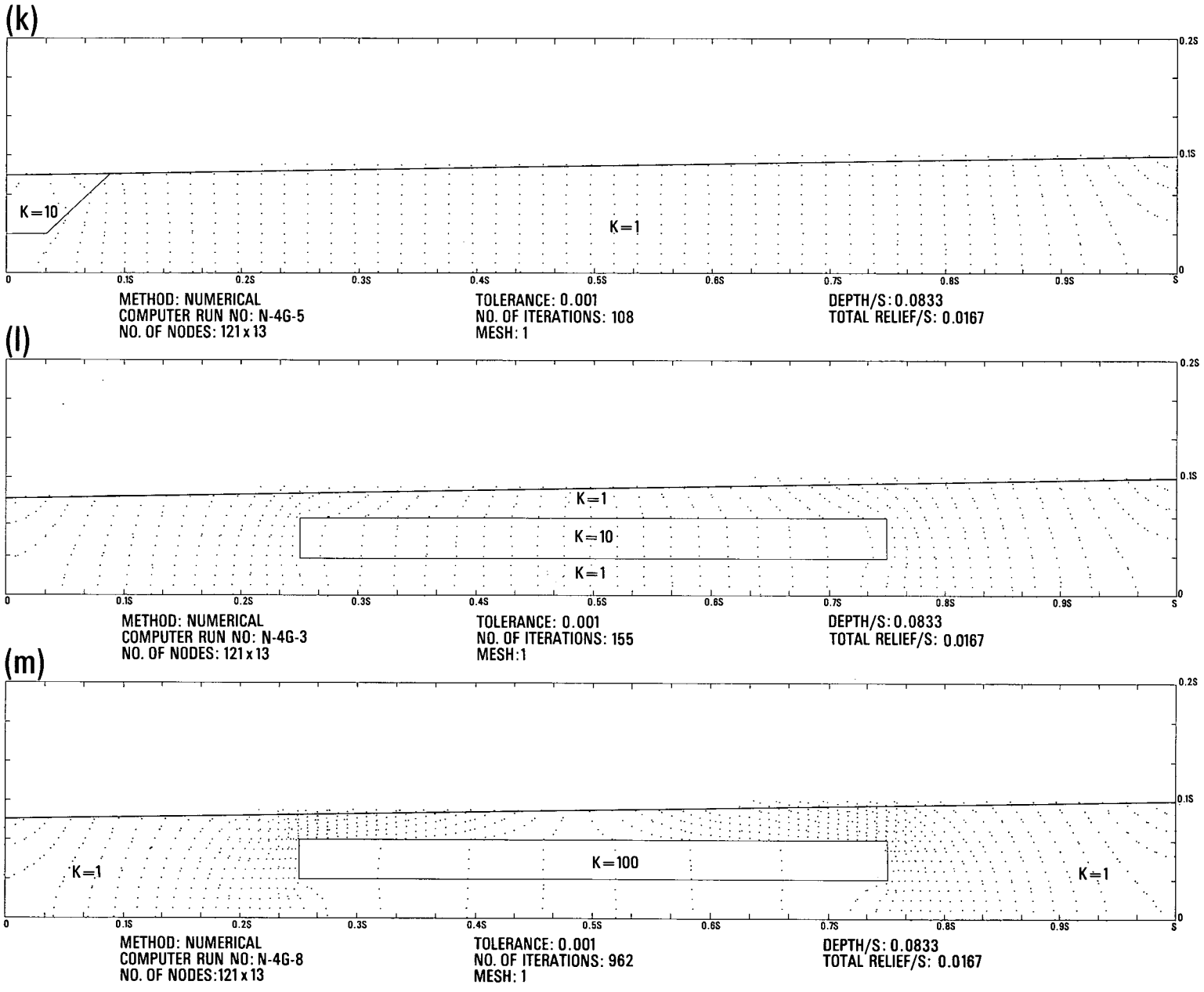

Figure 21(continued). Distribution of recharge and discharge areas

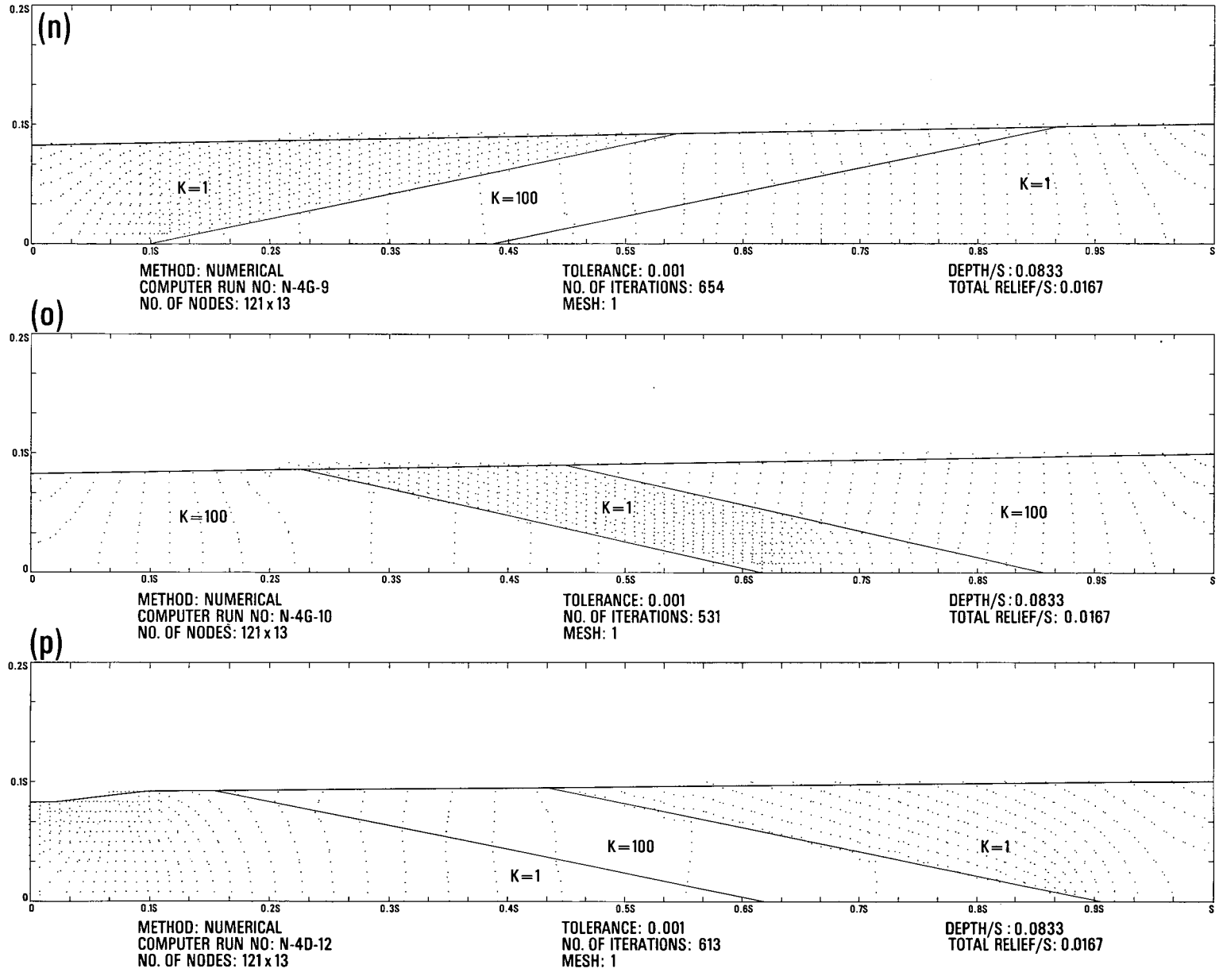

Figure 21(continued). Distribution of recharge and discharge areas

6. If the aquifer slopes upstream, its outcrop will become a discharge area as shown in Figure 21p.

7. The existence of an upstream-sloping, low-permeability layer will result in groundwater discharge just upstream from the outcrop area (Figure 21o). The intensity of discharge and the size of the discharge area will depend on the thickness and orientation of the low-permeability layer and on the permeability contrast. An example of a downstream-sloping, low-permeability layer is shown in Figure 20g.

FACTORS CONTROLLING DEPTH AND LATERAL EXTENT OF GROUNDWATER BASINS

The best introduction to this section consists of a re-examination of many of the diagrams in Figure 21, this time considering the changes which have been wrought in the size of groundwater basins by the changes in geologic or water-table configuration. For example, in Figure 21 (h through o), topographic configuration G is used. One can recall that, for the homogeneous case (Figure 19a), simple, uniform, near-horizontal flow system resulted. The introduction of the geological inhomogeneities in Figure 21 create sub-basins within the major basin. The concept of a total basin yield is thus negated and one must consider each component basin separately. It is logical, therefore, to examine the factors which control the depth and lateral extent of these sub-basins. To this end, 12 potential patterns. Figure 22 (a through l) are presented in this section. Since it is the hummocky water-table configurations which are most conducive to the establishment of small first-and second-order flow systems, configurations H and K are used in Figure 22.

We must first draw the readers attention to an earlier diagram, Figure 19h, which shows a homogeneous basin with water-table configuration H. Here we find that the majority of flow takes place near the surface in small first order basins but that a certain amount of flow circumvents these near surface systems to enter higher order flow systems. At least one flow path traverses the entire basin. Tóth (1963b, c) has shown that the influence of the hummocks increases as: (a) the amplitude of the hummocks increases and (b) the depth/lateral extent ratio decreases. The groundwater basin may even be broken up into a series of small first-order sub-basins with no flow traversing the entire basin.

The effect of introducing an aquifer into the system is to create a highway for groundwater flow such that the percentage flow traversing the entire basin increases. The percentage of total flow which enters the basin-wide flow system depends on three parameters:

1. The permeability ratio between the aquifer and the low permeability layers.

2. The depth/lateral extent ratio of the basin.

3. The percentage of the total depth taken up by the high-permeability layer.

The effect of these factors is shown in Figure 22(a, b, c and d). Diagrams a, b, and c show the influence of the high-permeability highway. In Figure 22d, the low-permeability ratio, small depth/lateral extent ratio, and narrow thickness of the aquifer combine to reduce the effectiveness of the aquifer. In this case, the major groundwater basin has been transformed into a series of first order basins with no basin-wide groundwater flow.

In Figure 22, e and f show the effect of partial layers; g, h, i and j show four different geologic configurations beneath water-table configuration K. In each case, at least two orders of groundwater basin are evident.

In Figure 22, the effect of sloping stratigraphy is examined in k and l. An interesting pair of streamlines to consider is shown in Figure 22k; here, the difference of a few feet in the point of recharge will make the difference between the water entering a minor first-order system or the major regional system.

The practical significance of the discussions presented in this and preceding sections of this chapter is discussed more fully in Chapter 8.

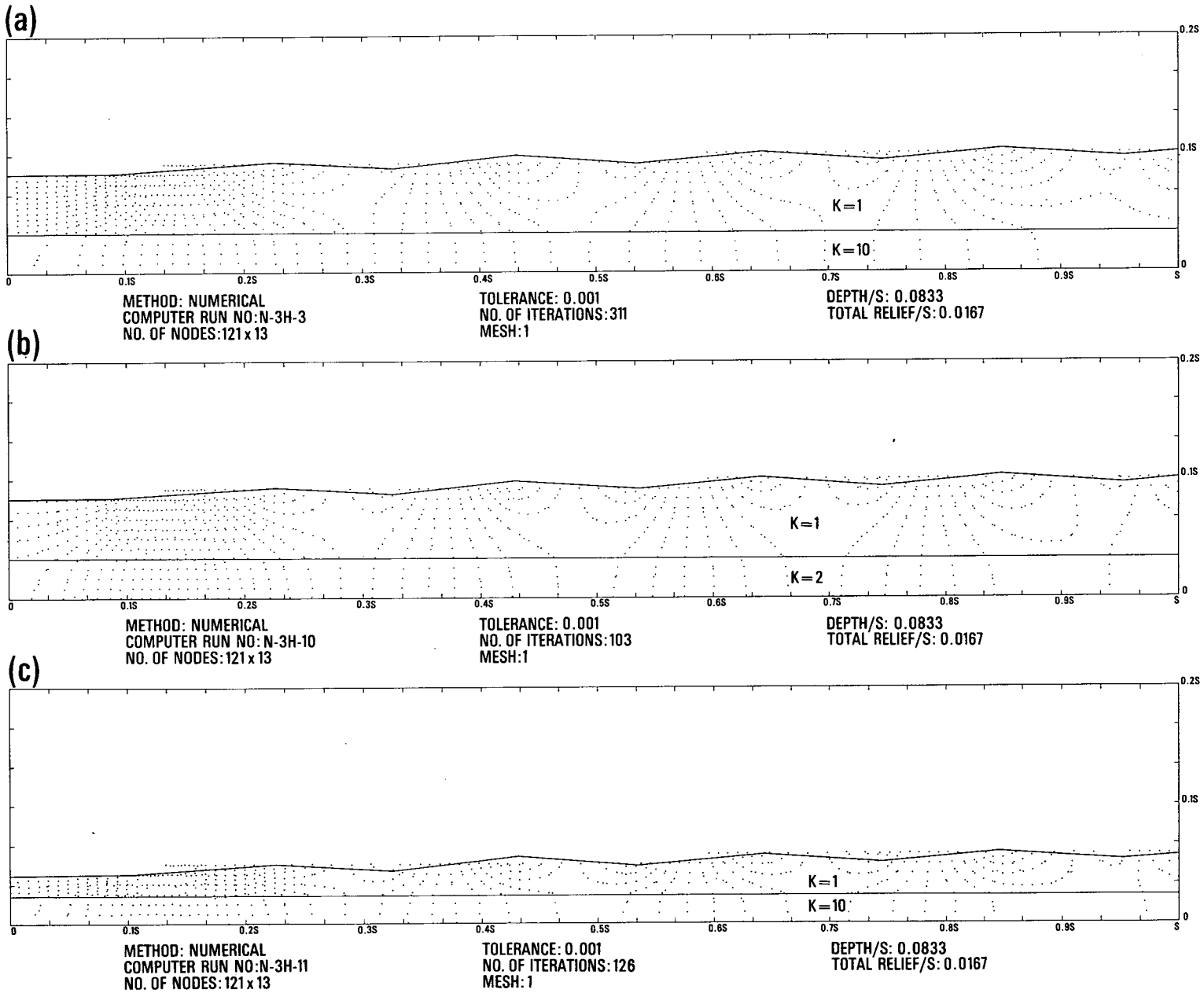

Figure 22. Lateral extent of groundwater basins

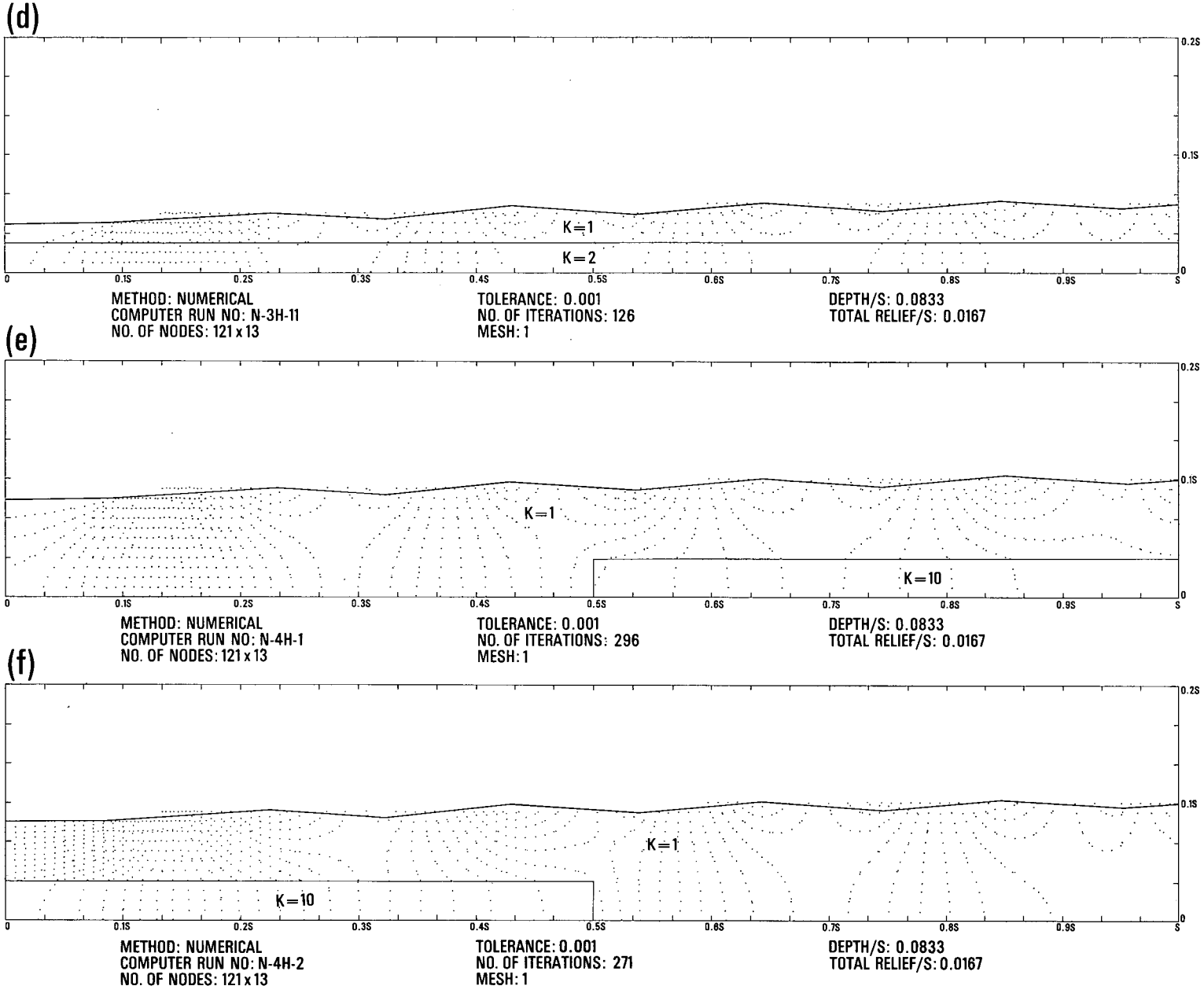

Figure 22(continued). Lateral extent of groundwater basins

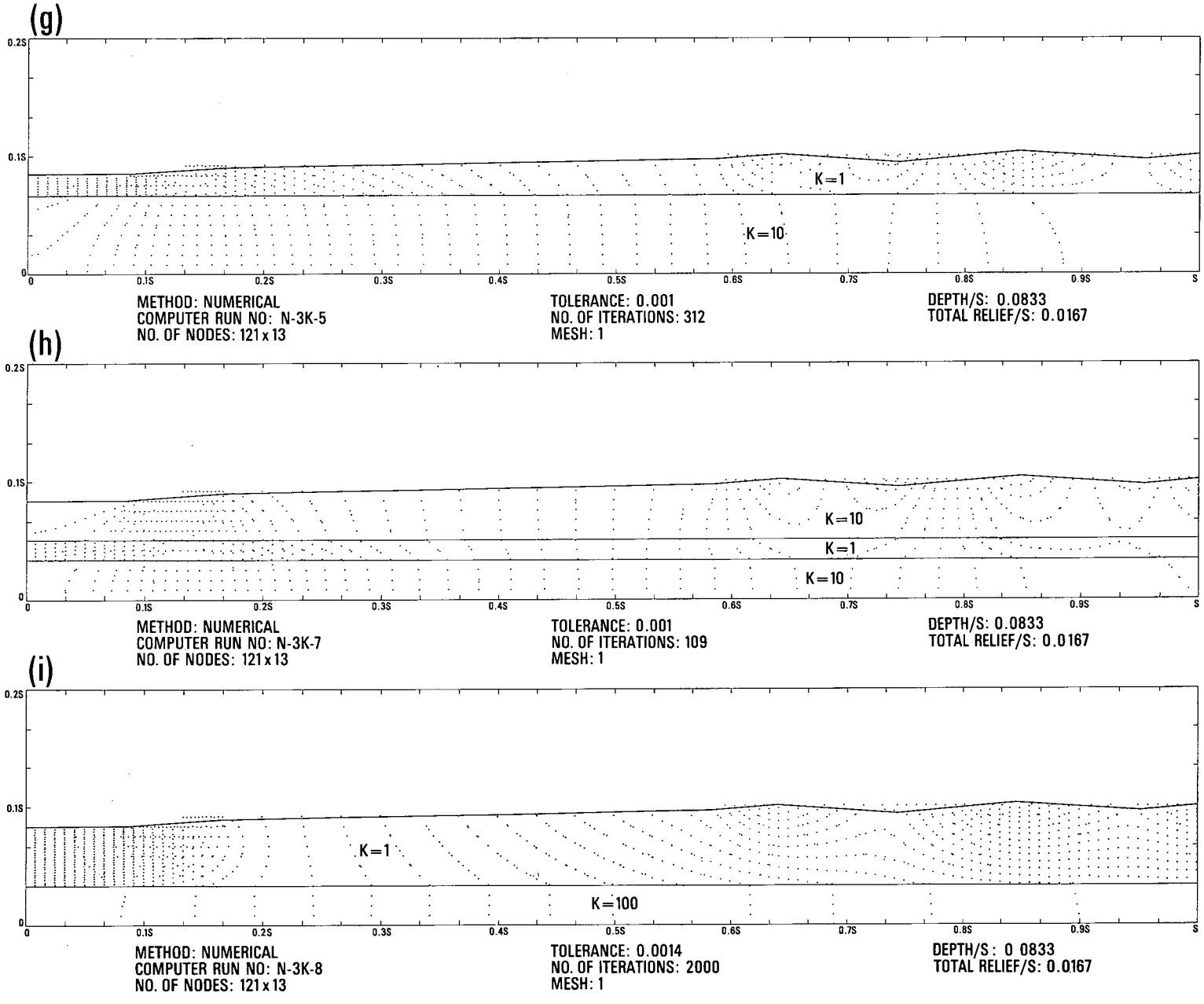

Figure 22(continued). Lateral extent of groundwater basins

(j)

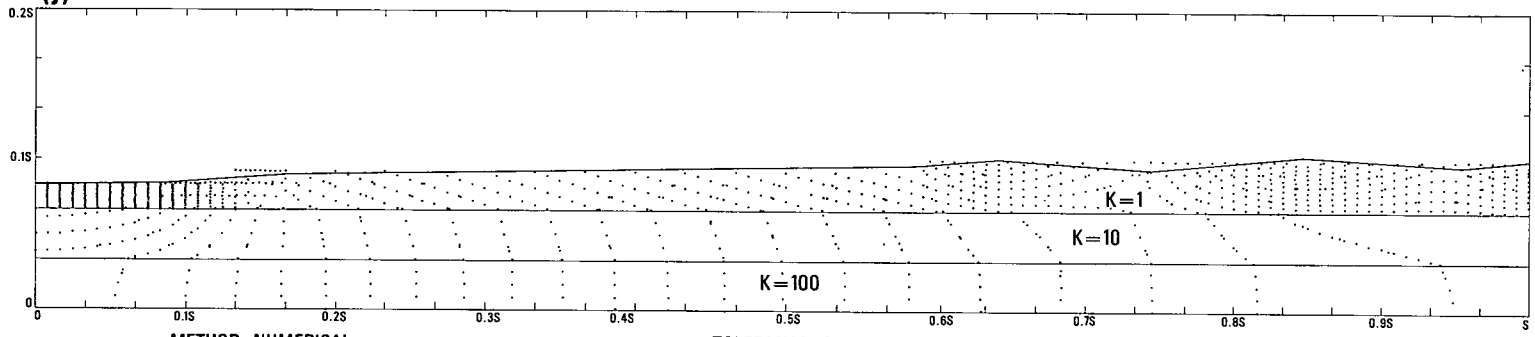

METHOD: NUMERICAL
COMPUTER RUN NO: N-3K-9
NO. OF NODES: 121 x 13

TOLERANCE: 0.001
NO. OF ITERATIONS: 1409
MESH: 1

DEPTH/S: 0.0833
TOTAL RELIEF/S: 0.0167

(k)

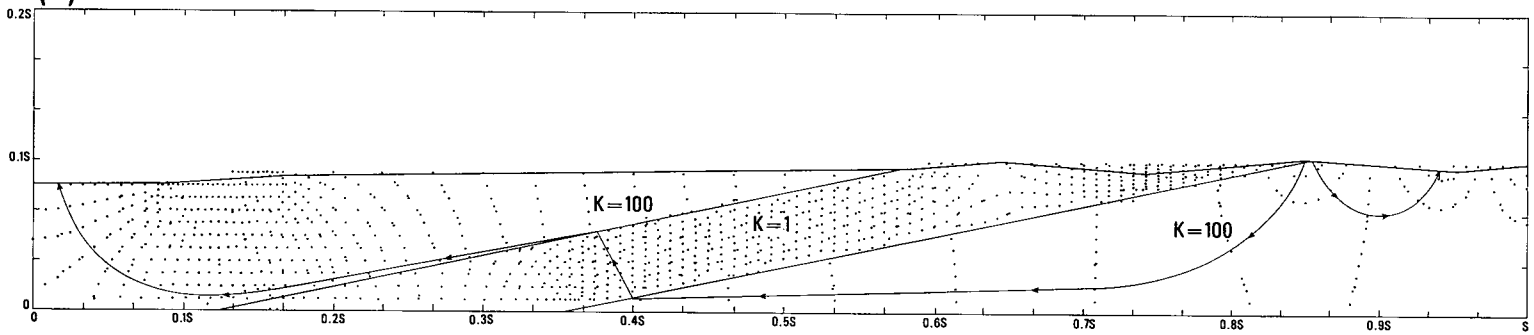

METHOD: NUMERICAL
COMPUTER RUN NO: N-4K-11
NO. OF NODES: 121 x 13

TOLERANCE: 0.001
NO. OF ITERATIONS: 623
MESH: 1

DEPTH/S: 0.0833
TOTAL RELIEF/S: 0.167

(l)

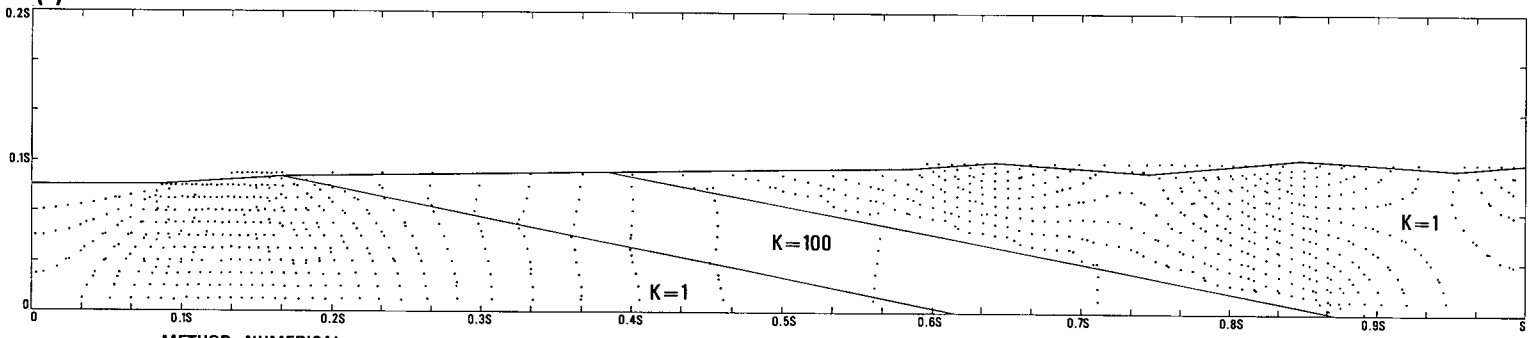

METHOD: NUMERICAL
COMPUTER RUN NO: N-4K-12
NO. OF NODES: 121 x 13

TOLERANCE: 0.001
NO. OF ITERATIONS: 612
MESH: 1

DEPTH/S: 0.0833
TOTAL RELIEF/S: 0.0167

THE EFFECTIVE DEPTH TO A BASAL IMPERMEABLE BOUNDARY

One of the basic assumptions of this study requires the presence of a horizontal impermeable boundary at some depth. Another assumption suggests that there is no such thing as a completely impermeable formation. The resolution of this seeming paradox lies in the fact that there are certain geologic configurations which create the same effect on the potential pattern as would an impermeable boundary.

Figure 23a shows a two-layer case with a simple water-table configuration. The equipotential lines cross the K = 10 layer vertically and meet the assumed impermeable boundary perpendicularly as they must. In Figure 23b another low-permeability layer has been added beneath the aquifer. The effect on the flow pattern is negligible. The equipotential lines still cross the aquifer vertically and meet its lower boundary perpendicularly. They proceed without refraction (except at the extremities of the flow net) vertically over most of the K = 1 layer to the assumed impermeable boundary at the base of the model. In effect, the lower boundary of the K = 10 layer has acted as a horizontal "impermeable boundary". Figure 23c shows the same phenomenon for a model with a more complex water-table configuration.

The conclusion, which is an important one from the point of view of designing models to represent actual groundwater basins, can be stated as follows: the effective depth to a basal-impermeable boundary can be taken as the depth to the lower boundary of the lowermost high-permeability layer in the system; equipotential lines below this boundary can be assumed to remain vertical. This statement will be quantitatively more exact as the permeability contrasts increase.

THE VALIDITY OF THE ASSUMPTION OF VERTICAL IMPERMEABLE BOUNDARIES

All of the hypothetical groundwater basins modelled in this study are assumed to be bounded on either side by imaginary vertical impermeable boundaries. The presence of such boundaries beneath major topographic divides and even beneath small hummocks in the water table is well documented and is not in doubt. Whether these boundaries are indeed vertical is a question which bears investigation.

The controlling factor is the symmetry of the water-table configuration on either side of the divide. In Figure 24, the water-table slope to the right of the valley is kept constant in all three diagrams. The slope to the left of the valley is equal to the right-hand slope in Figure 24a, half the right-hand slope in Figure 24b, and twice the right-hand slope in Figure 24c. The latter two diagrams represent extreme cases of assymmetry which would not often exist in the field.

It can be seen that the imaginary impermeable boundary will be exactly vertical only if the water-table configuration is symmetric on either side of the valley. The deviation from the vertical in Figure 24(b and c), however, is not large, and comparison of the potential nets in the right-hand portion of the three diagrams shows that the effect on the flow pattern is small and is restricted to the vicinity of the valley. Considering the extremeness of the cases considered, it is concluded that, in general, the assumption of vertical impermeable boundaries is valid, and that the effect of assymmetry across water-table divides is small.

ANISOTROPIC FORMATIONS

Thus far, the study of the effect of geology on regional flow patterns has been restricted to cases involving large-scale inhomogeneities in permeability. All the geological formations have been assumed to be isotropic with respect to permeability.

When anisotropy exists, the problem of analysing regional groundwater flow becomes more complex. The numerical method is well suited to the analysis of such problems, and Figure 25 shows three simple cases to illustrate the method.

In Figure 25, a and b show the effect of anisotropy on the regional groundwater flow pattern in a

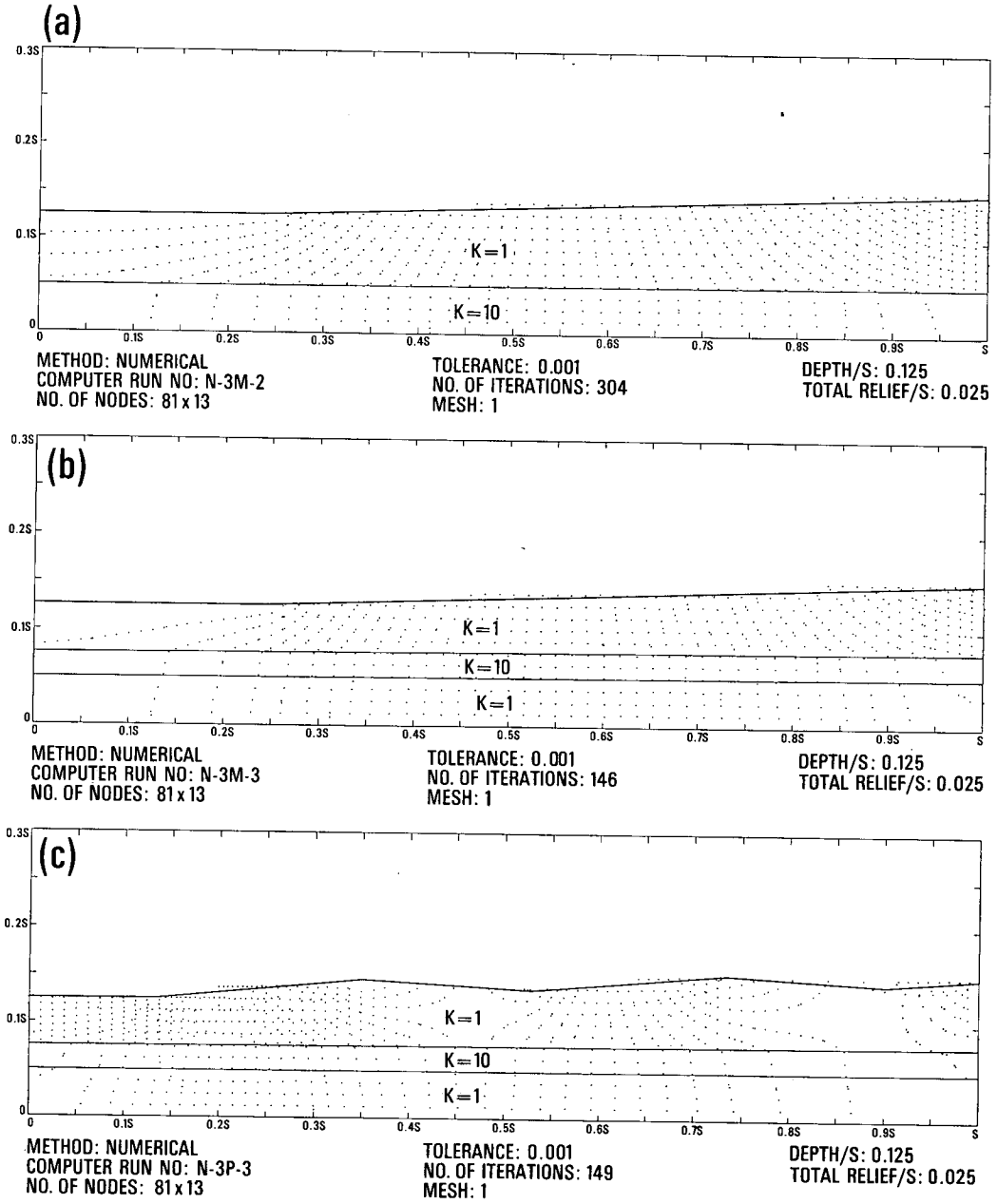

Figure 23. Effective depth to a basal impermeable boundary

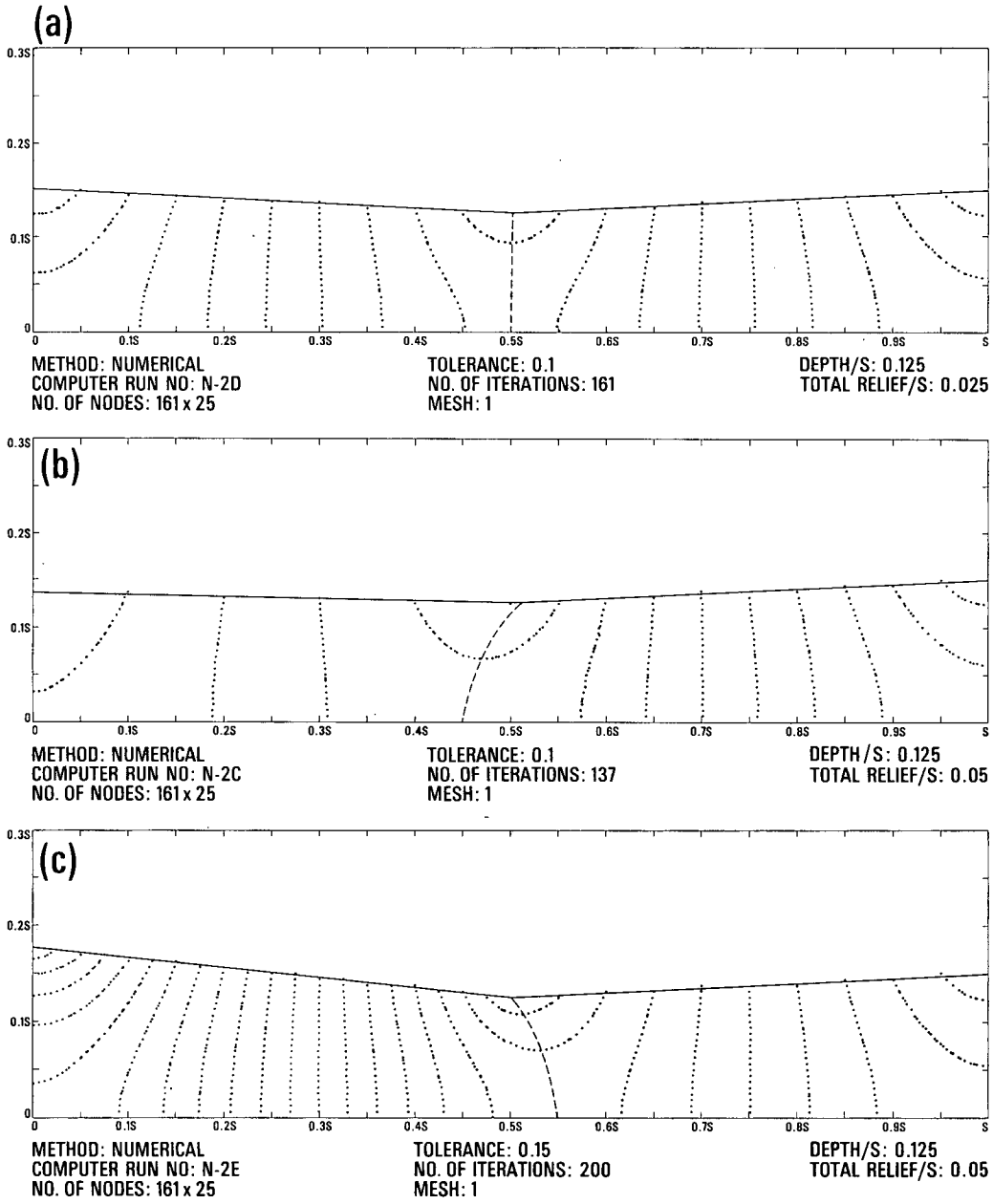

Figure 24. Validity of the assumption of vertical impermeable boundaries

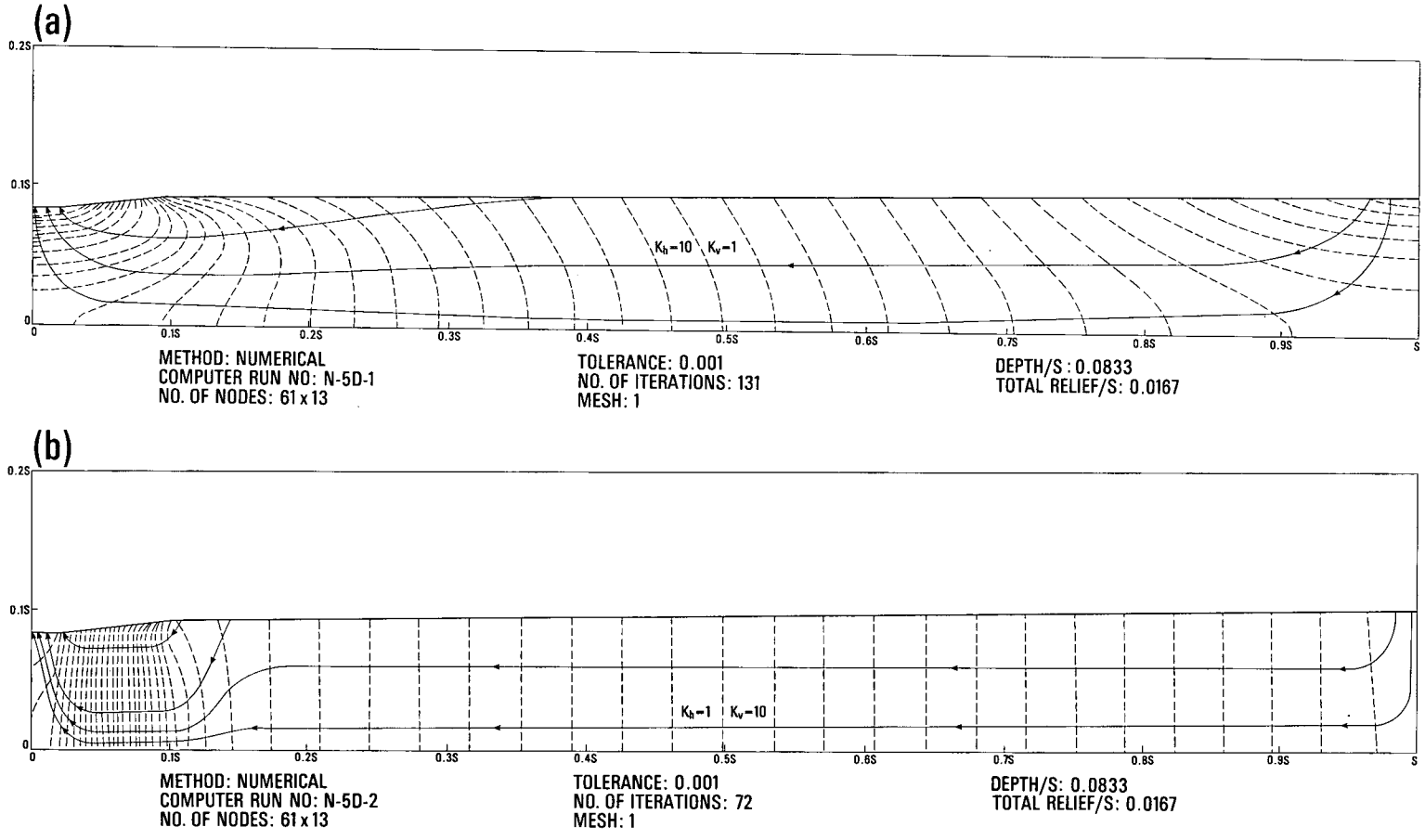

Figure 25. An anisotropic case

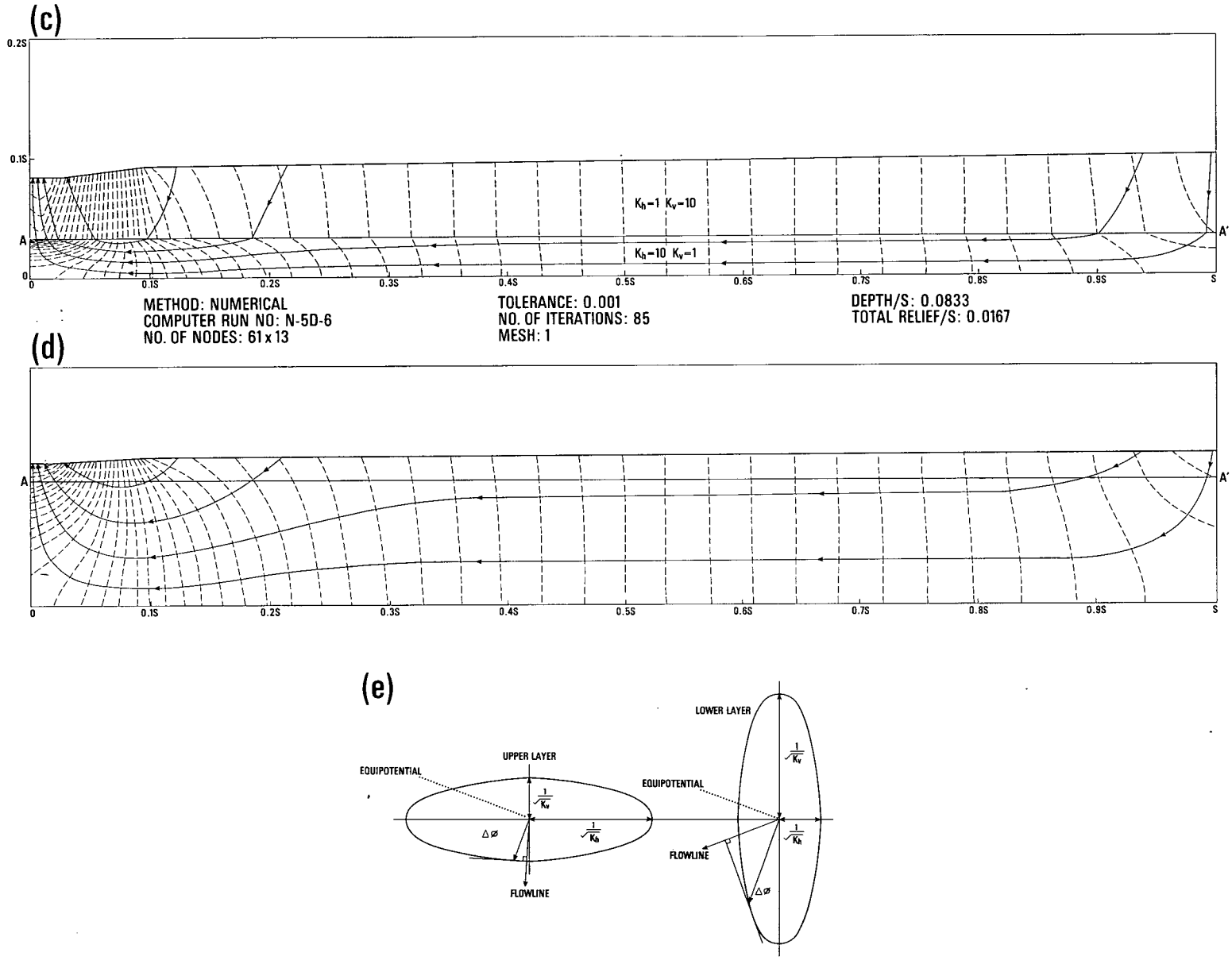

Figure 25(continued). An anisotropic case

homogeneous medium bounded by the same simple water-table slope of Figure 19d. In Figure 25a, the horizontal permeability is 10 times the vertical, and for illustrative purposes, this situation is reversed in Figure 25b. The effect of these permeability configurations is best realized by comparing the flowlines of these figures with those of Figure 19d for the isotropic case. Figure 25c is a two-layer case that combines the anisotropy conditions a and b of Figure 25 in one system. This could be representative of a vertically-fractured formation overlying a horizontally-stratified layer.

Considerable care must be exercised in the construction of flowlines in anisotropic media since the flowlines will not in general intersect the equipotentials at right angles. Two methods are available. The first (Maasland, 1957) utilizes the transformed section whereby an equivalent homogeneous isotropic system is obtained by suitably expanding or shrinking the coordinates of each point in the anisotropic medium. The transformation is:

$$x' = (K_o/K_h)^{1/2} x$$

$$y' = (K_o/K_v)^{1/2} y$$

where x and y are the original coordinates, x' and y' the transformed coordinates, K_h and K_v the horizontal and vertical permeabilities, and K_o is an arbitrary constant having the dimensions of K_h and K_v.

Figure 25d shows the transformed section for the two-layer case of Figure 25c. In the upper layer, we choose $K_o = 1$; then $x' = x$, $y' = y/\sqrt{10}$, and the vertical dimension is reduced by a factor of $\sqrt{10}$. In the lower layer, we choose $K_o = 10$; then $x' = x$, $y' = \sqrt{10}\, y$, and the vertical dimension is expanded by a factor of $\sqrt{10}$. The position of the interlayer boundary AA′ is shown on both diagrams.

Once the equipotentials have been transferred from the real (Figure 25c) to the transformed (Figure 25d) section, a homogeneous isotropic flownet can be drawn in the transformed section and the flowlines transferred back to the true case. Several random flowlines are shown to illustrate the direction of flow.

The method of the transformed section indicates that the effect of varying the anisotropic ratio in a homogeneous medium is identical to that of varying the depth lateral extent ratio. The diagrams presented by Tóth (1963b), which were designed to show the effect of the depth lateral extent ratio in a homogeneous basin bounded by a hummocky water table, could therefore also be interpreted in terms of the effects of anisotropy.

A second method has recently been described (Liakopoulos, 1965), whereby the direction of flow at any point in an anisotropic medium can be determined with the aid of the permeability ellipse and without the necessity of a transformed section. Figure 25e shows the permeability ellipses for both upper and lower layers of Figure 25c. The direction of flow at any point can be obtained graphically as follows:

1. Draw a vector in the direction of the hydraulic gradient (i.e., perpendicular to the equipotential at the point in question).
2. Draw a tangent to the ellipse at the point where the vector cuts the ellipse.
3. The direction of flow is perpendicular to the tangent line.

In the constructions shown on the two ellipses in Figure 25e, the direction of the hydraulic gradient is the same in each case. The resulting direction of flow, however, is radically different and is dependent on the prevailing direction of anisotropy.

It should be noted that all the cases treated in Figure 25 have axes of anisotropy that coincide with the coordinate directions. The more general case of a skewed anisotropy requires a more complicated mathematical approach utilizing the concept of permeability in tensor form. Numerical solutions employing the finite element method (Zienkiewicz, 1966) appear to be well suited to this problem.

CHAPTER 6

Quantitative Results; Natural Basin Yield

QUANTITATIVE FLOW NETS

The diagrams in the preceding chapter were limited to potential nets and qualitative flow nets in which the streamlines indicated the direction of flow but did not have quantitative significance. It is possible, of course, to construct quantitative flow nets from the potential patterns representing regional groundwater flow. Figure 26 shows a quantitative flow net for the case of a partial basal aquifer with a water-table configuration consisting of major topographic valleys at both left and right and a lesser topographic low in the centre of the diagram between two regional highs. The flow lines are drawn orthogonal to the equipotential lines and in such a way that curvilinear squares are formed throughout the K = 1 region. Due to the refraction of the flow lines at the permeability interface, curvilinear rectangles ten times as long as they are wide will result in the K = 10 layer. The flow net shown in Figure 26 was constructed graphically. Harr (1962) provides a good reference for the graphical construction of quantitative flow nets.

Once having defined the flow net, one can calculate the discharge in each flow channel by Darcy's Law:

$$(6.1) \quad Q = K \cdot \frac{\Delta\phi}{\Delta s} \cdot \Delta m\text{-}w$$

where Q = discharge through a segment of the flow net.

K = permeability.

$\Delta\phi$ = drop in hydraulic head between equipotential surfaces.

Δs = length of flow path in the segment of the flow net.

Δm = width of the segment of the flow net perpendicular to direction of flow.

w = thickness of the flow system perpendicular to the plane of the diagram.

For the square portion of the net, $\Delta s = \Delta m$, and considering a unit thickness of the system ($w = 1$) we are left with

$$(6.2) \quad Q = K \cdot \Delta\phi$$

The discharge in each flow channel remains constant throughout its length and the discharge in all flow channels is equal. One can therefore determine the total discharge through the groundwater basin by summing the quantities of flow in the individual channels.

Although Figure 26 and the above discussion are in terms of a two-dimensional flow system, the same approach can be used in a three-dimensional basin.

Referring once again to Figure 26, one can see that the existing water-table configuration and geologic conditions give rise to three separate groundwater basins (separated by a dashed line in the diagram and denoted by A, B, and C). It is interesting to note that basin A has a small arm extending up to the right flank of the central valley, a situation that could not have been anticipated by other means than that of a theoretical model.

Using (6.2), one can easily calculate the quantity of flow in each basin. For $s = 60{,}000$ ft, $\Delta\phi = 20$ ft, and recalling that the K = 1 and K = 10 values were relative, we will arbitrarily assign to the upper layer a permeability of 5 gpd/ft^2. This gives rise to a flow channel discharge of 100 gpd (per foot of

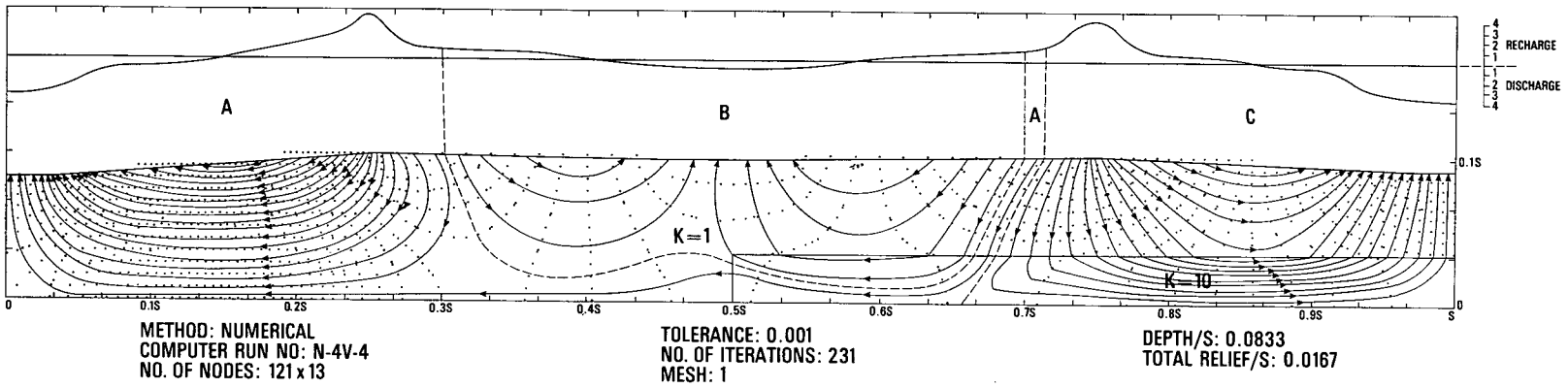

Figure 26. Quantitative flow net

thickness of the flow system perpendicular to the diagram). By simply counting the flow channels in the three basins, we arrive at the following discharges:

Q_A = 1950 gpd
$Q_{B'}$ = 800 gpd
Q_C = 1450 gpd

NATURAL BASIN YIELD

The quantity of flow through an undeveloped basin under natural conditions is hereby defined as the "natural basin yield". The quantities calculated in the preceding section represent the natural basin yields of the three component basins of Figure 26.

Under the assumption of a steady-state water table, the value of the natural basin yield will represent a constant discharge which does not change with time. It is important to recall that our definition of a "steady-state" water table (Chapter 1) does not deny the existence of water table fluctuations. It does state that their effect on the flow patterns will be small, if:

(a) the zone of fluctuation of the water table is only a small percentage of the total saturated depth of the groundwater basin; and

(b) The relative configuration of the water table remains the same throughout the cycle of fluctuations.

If these two conditions are satisfied, the small uniform fluctuations in the water table will not result in any significant change in the nature of the flow pattern, or therefore in the quantity of flow through the basin. The natural basin yield is therefore a near-constant quantity which represents a unique property of the basin; it will not fluctuate significantly with time and is relatively independent of rainfall conditions.

The effect of small-scale cycles of rainfall resulting in wet and dry periods through the year will serve to cause the fluctuations in the water table which we have pointed out can often be approximated by a steady-state average. The effect of an increase in the total annual precipitation would be a more permanent raising of the water table which, while it would increase the groundwater storage of the basin, would not significantly affect the natural basin yield. The natural basin yield can be considered as a measure of the quantity of water which a given basin can accept, and is therefore a measure of the groundwater recharge to the basin. The ultimate effect of a long-term increase in annual precipitation would therefore be that a greater proportion of the increased rainfall would become surface runoff.

In defence of requirement (a), it can be noted that in the semi-arid Canadian prairies, the usual annual fluctuations in the water table are of the order of 5 feet and are always less than 10; the maximum difference in elevation of the water table between an extended period of wet years and dry is of the order of 20 feet and the depths of groundwater basins are 300-2000 feet. Under these conditions, if requirement (b) is not violated, the concept of natural basin yield is valid.

If either of the conditions (a) or (b) is violated, then the methods of this chapter must be adapted. It may be necessary to calculate the natural basin yield on a monthly basis, for example, using twelve different water table configurations representing the fluctuating position of the water table throughout the year. For example, Meyboom (1966) has shown that, in the vicinity of a willow ring in hummocky moraine, the water table undergoes transient fluctuations such that the enclosed temporary slough is a recharge area at certain times of the year and a discharge area at others. He has prepared a water balance for the slough which required consideration of 29 separate time intervals throughout the year. A mathematical model analysis of such a flow system would presumably require a similar number of steady-state runs. In such cases, a transient mathematical model would probably be more efficient.

The natural basin yield is a consequence of the existing potential field which in turn is controlled by the water table configuration and the geometry and value of the permeability contrasts created by the geologic configuration.

THE ESTIMATION OF BASIN SAFE YIELD

The safe yield of a groundwater basin is the amount of water which can be withdrawn from it annually without producing an undesired result (Todd, 1959). The undesired result may be depletion of the resource, impairment of the quality of the water, or the creation of an economic or legal problem. Considering the safe yield from a strictly quantitative point of view, it is logical to inquire as to the relation between the safe yield and the natural yield of a basin.

They are not the same thing because the natural basin yield refers to a virgin basin which has not undergone groundwater development. The introduction of a major well field will change the conditions governing the existing flow pattern by creating a cone of depression in the water table in the case of an "unconfined aquifer" or lessening the potential at depth as would be the case in the development of a "confined aquifer". The effect of this artificial discharge from the basin will be to create a new flow pattern from which a new basin yield can be derived for that stage of development. Further development will result in further changes which usually tend to increase the groundwater yield. There is some optimum development for the basin which maximizes the safe yield.

When the initial groundwater development of a virgin basin is contemplated, calculation of the natural basin yield as determined from the results of a mathematical model analysis will provide a conservative estimate of the basin groundwater yield which could be tapped in the initial development. When the effects of this initial development on the previously existing flow pattern have been determined, a new model can be constructed which includes the effects of the well field. This model can then be used to estimate the expected basin yield from further groundwater development.

Used in this stepwise fashion, the mathematical model can be useful in estimating the order of magnitude of the basin safe yield.

This is an important concept which has ramifications in the basin-wide development of groundwater resources. For example, consider the three component basins of Figure 26. While all three have an approximately equal surface area, basins A and C have a natural basin yield nearly twice that of B (Q_A = 1,850 gpd, Q_B = 800 gpd, Q_C = 1,450 gpd). Because basin C also has a permeable basal aquifer, it would seem to be the optimum location for groundwater development.

This method may have only limited application to basins which are already heavily developed such as those around the large metropolitan centres of the United States and Canada, but it can be very useful in planning the development of the many virgin basins which abound in the Canadian prairies and northland.

THE EFFECT OF THE GROUNDWATER FLOW PATTERN ON THE COMPONENTS OF THE HYDROLOGIC CYCLE

Above the flow net in Figure 26 is a recharge-discharge profile showing the quantitative distribution of recharge and discharge across the basin. The cross-hatched areas above the centre line represent recharge; below the line is discharge. Different hatchings are used for each of the three basins. The areas above and below the line must be equal for each basin. The units are arbitrary.

This form of plot was introduced by Davis (1963) in a criticism of Tóth's first paper (1962). Davis held that the concentrations of discharge and recharge required by Tóth's flow patterns were impossible. Tóth (1963) countered in a reply that, while the distribution of recharge and discharge required by his theory may seem unconventional, it is probably correct. The results of the present study confirm Tóth's opinion. The construction of quantitative flow nets for any of the seventy-one potential plots included in Chapter 5 will reveal concentrations of discharge and recharge at various points on the surface of the basin. In Figure 26, basins A and C have zones of concentrated discharge in the valley and zones of concentrated recharge near their upstream ends. The zones of concentration are separated by zones in which the quantity of both recharge and discharge is low. In basin B the quantity of recharge and discharge is more evenly spaced.

Klute, Scott and Whisler (1965) have noted similar concentrations in their analysis of steady-state flow in a saturated inclined-soil slab. Further field studies are needed to confirm the existence of such zones of concentration in nature.

This recharge-discharge regime will have an important effect on the other components of the hydrologic cycle. For example, evapotranspiration will be concentrated in discharge areas where the water table is kept high by the upward rising groundwater. If all the discharge in basin B were discharged by evapotranspiration over the entire discharge area (s = 60,000 ft, $\Delta\phi$ =20 ft, Q_B = 800 gpd/ft thickness ⊥ plane of the diagram), the rate of evapotranspiration would be 0.11 inch/day.

Similarly the average annual groundwater component of surface runoff could be calculated using the mathematical model. The effects of bank storage, a major factor in the fluctuation of the baseflow with time, however, cannot be taken into account, so the method is not practicable without further adaptation.

If a stream were flowing parallel to the plane of the paper in Figure 26, say down the left-hand flank in basin A, one would expect the groundwater component of the stream to increase downstream. In theory there should be no groundwater component to the stream while it traverses the recharge area; indeed the stream may be influent at this point. Several methods for separating the groundwater component from a stream hydrograph are available (Meyboom, 1961; Kunkle, 1962; Linsley, Kohler and Paulhus, 1949).

While the rainfall falling on a basin can be assumed to be areally uniform, taking no note of whether it is falling on a recharge area or a discharge area, its behaviour upon reaching the ground will be influenced by the existing groundwater flow pattern. In recharge area, a downward potential gradient exists which would tend to take a larger percentage of the moisture surplus into the ground than in a discharge area. Water which infiltrates to the water table in a recharge area will enter the dynamic groundwater flow system and be transmitted to a distant point of discharge. Water which infiltrates to the water table in a discharge area can only be transmitted back to the surface again by an agent of discharge, such as evapotranspiration, when conditions permit.

In summary, it can be stated that the nature of the groundwater flow pattern will have an important effect on the quantity and areal concentration of the other components of the hydrologic cycle, in particular the evapotranspiration and surface runoff. The use of the mathematical model to derive theoretical quantitative flow nets can be an important tool in the calculation of a basin-wide water balance.

CHAPTER 7

Three-Dimensional Models

SAMPLE SOLUTION

Figure 27 is a map showing the assumed water-table configuration for an area in the vicinity of the towns of Readlyn and Ormiston in southwestern Saskatchewan, Canada. The region is bounded on the west and south by a major drainage divide and on the north and east by a major topographic high. The area forms a sub-basin of the Old Wives Lake internal drainage basin.

The geologic configuration has been represented by a two-layer case, the upper layer representing the relatively impermeable glacial till and underlying deposits of silt and clay of the Tertiary Ravenscrag Formation, and the lower layer the highly permeable sands of the Cretaceous Eastend Formation. A permeability ratio of 50:1, based on the few known measurements in the vicinity, has been used. The Eastend Formation is underlain by several hundred feet of relatively impermeable shale of the Cretaceous Bearpaw Formation, so the base of the Eastend sands was considered to be the effective impermeable boundary.

Initial runs in which the permeabilities in each layer were assumed to be isotropic failed to give results consistent with field observation. A solution which did provide good agreement was obtained using a horizontal: vertical anisotropy factor of 20:1 in both layers. The resulting permeability configuration is therefore:

$K_{uh} = 1.0$	(upper layer, horizontal)
$K_{uv} = 0.05$	(upper layer, vertical)
$K_{lh} = 50.0$	(lower layer, horizontal)
$K_{lv} = 2.5$	(lower layer, vertical)

The potential values were obtained at each node in a 25 x 25 x 10 mesh using Numerical Program 6 (Appendix B). This program is not designed to accept anisotropic problems, but the desired anisotropy can be simulated by expanding the vertical dimensions of the model in the same manner as in the graphical construction of flow patterns (see Harr, 1962). The output for the problem is a printout of the potential at each node in the three-dimensional mesh, and a series of vertical two-dimensional sections through the model. Six of these sections are shown in Figure 28; their locations are indicated in Figure 27. The sections are plotted with an exaggerated vertical scale of 20:1.

In general, flow lines and equipotential lines will not meet at right angles in anisotropic cases (Liakopoulos, 1965) or cases where the results are represented on diagrams with an exaggerated vertical scale (van Everdingen, 1963). Caution must therefore be exercised in the delineation of flow patterns using potential nets obtained from the solution of mathematical models. In Figure 28, for example, the vertical exaggeration would have to be reduced to 4.47 to 1 ($\sqrt{K_h/K_v} = 4.47$) before flow lines could be constructed orthogonal to the equipotential lines.

It is interesting to note that the concepts developed in the two-dimensional studies are upheld in the sections taken through the three-dimensional model. A few observations of interest are:

1. There are several groundwater basins within the system.
2. The size of the discharge area is controlled to a large degree by the valley slope. Large flat valleys (left centre BB′, right centre EE′) have large discharge areas; shallow slopes (left AA′) create medium-sized discharge areas; and steep valley flanks (left DD′, left EE′) produce small discharge areas.

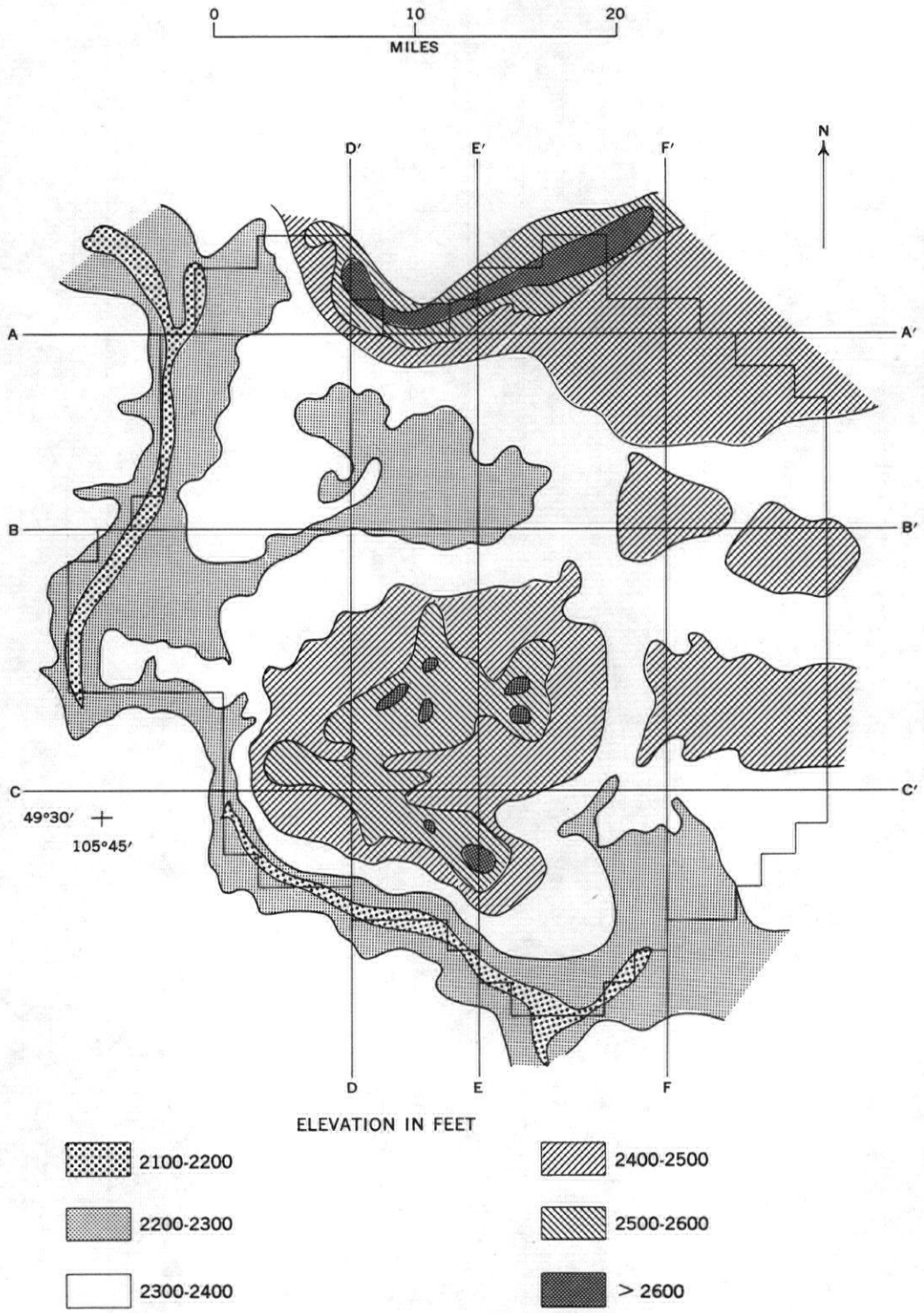

Figure 27. Water-table topography for three-dimensional model

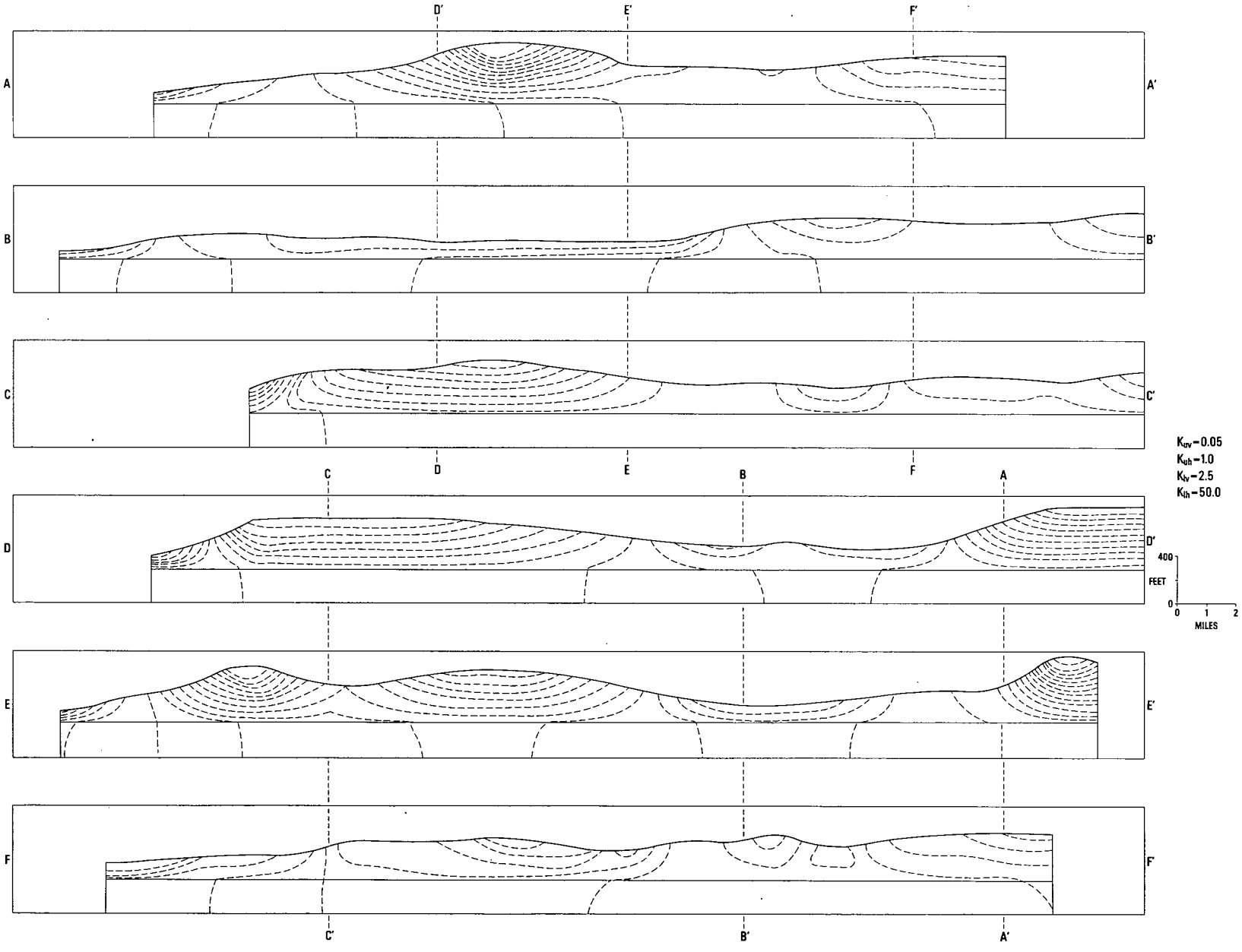

Figure 28. Potential diagrams for three-dimensional case

3. In the left centre of cross-section EE′, there is a topographic low which acts as a recharge area rather than a discharge area. This could not exist in a strictly two-dimensional model or in a two-dimensional section taken parallel to the direction of slope of the water table. It does exist in this arbitrarily-oriented section through the three-dimensional potential field because the valley itself has a gradient perpendicular to the paper and the section is cutting the valley near its upstream end, where it acts as part of the surrounding recharge area, rather than in its downstream portion where it becomes a discharge area.

From the three-dimensional model, one can produce a map showing the distribution of recharge and discharge areas, as well as cross-sections which show the depth, lateral extent, and order of the component groundwater basins.

LIMITATIONS AT THE PRESENT TIME (1966)

In theory it is possible to represent any groundwater basin by a three-dimensional mathematical model. The previous section illustrates the type of solution which can be obtained. The completely general application of the methods and programs presented in this report is restricted by a computer limitation. This limitation involves the available core storage in the computer which in turn limits the number of nodes which can be used to represent the groundwater basin. The author found that with an IBM 7094 computer with a storage capacity of 32,000, models were limited to 7,500 nodes. This means a maximum model size of 25 x 25 x 12.

It is clear that this number of nodes is not sufficient to represent complicated water table topographies or geological configurations for large basins. It is sufficient, however, to produce meaningful results for small basins with simple water table configurations and geology.

It is possible to increase the effective core storage by use of intermediate storage on magnetic tape or auxiliary disc storage. It is not practical to use tapes when iterative numerical procedures are employed, but three dimensional programs can be written, using disc storage to overcome the above limitation.

There is a further encouraging aspect to this problem and that is the rate at which core storage is being increased as bigger and better computers come onto the market. Computers with 200,000 memory are now available. Forsythe and Wasow (1960) have summarized the situation as follows: "Problems with three-space dimensions cannot possibly be solved in great detail now, and probably will not be solvable in great detail with the machines of the foreseeable future. They are currently possible in moderate detail if there is no time dependence and are now very easy in sketchy detail even if they depend on time. The machines of the 1960's should permit time-dependent problems in three dimensions to be attacked in moderate detail".

In summary, we conclude that, at the present time (1966), the use of three-dimensional mathematical models should be limited to small, simple basins that can be adequately represented by 7,500 nodes. The best way to handle large, complex basins is with a series of two-dimensional models representing vertical sections taken parallel to the direction of dip of the water-table slope. An example of such a section through an actual groundwater basin is given in Chapter 8.

CHAPTER 8

Integration of Theoretical Approach with Field Methods

PRACTICAL SIGNIFICANCE OF THEORETICAL RESULTS

An understanding of the regional groundwater flow regime is a prerequisite to basin-wide development of groundwater resources. The qualitative and quantitative ramifications of the existing flow pattern must be taken into account in order to determine the optimum location and design of any proposed project in the development. To emphasize the practical significance of the type of results which can be obtained with the mathematical model approach, a few pertinent examples follow:

1. In order to calculate the basin safe yield, the depth and lateral extent of the basin must be known. This is not as simple a task as it may first appear and the theoretical results are invaluable in delineating the size and order of the component basins.
2. The natural basin yield obtained from a quantitative analysis of the theoretical flow pattern will provide a conservative estimate of the probable basin safe yield.
3. The geometry of the flow pattern will pinpoint zones of concentration of flow and may suggest optimum locations for well fields.
4. The chemical quality of the groundwater will be inferior in a discharge area, due to the progressive solution of salts over the flow route and the effectiveness of the evapotranspirative process in the concentration of salts in near-surface discharging groundwater. If the flow routes are long enough to establish a Chebotarev sequence (Chebotarev, 1955), the chemical nature of the groundwater will change from recharge to discharge area.
5. The location of recharge and discharge areas is also important if artificial recharge is proposed. Obviously recharge rates will be greater and the process more effective if the project is located in a natural zone of concentrated recharge.
6. As pointed out in Chapter 6, the nature of the groundwater flow pattern may exert considerable influence on the surface water hydrology.

It is felt that the use of the mathematical-model approach may be valuable at two different stages of a groundwater investigation, first as a reconnaissance tool preceding the field investigation, and second as an interpretive tool following the field investigation.

AS A RECONNAISSANCE TOOL

The investigation of a groundwater basin, whether it be for research purposes or for expected or increased groundwater development, must include a well-designed and economic field program. The theoretical approach can be used at the planning stage to optimize the field program.

At this stage of the investigation, the model would consist of an estimated water-table configuration, probably based on the assumption that the water table mirrors the topography, and a geologic configuration based on any available information. To prepare such a model, reference need only be made to topographic maps and geologic maps and sections. Any other available information, such as soils maps, water-level records, or results of previous hydrological investigations, should be incorporated. The resulting flow pattern can then be used to determine the optimum locations for piezometer installations, pump tests, and the collection of water samples for chemical analysis. It can

also act as a guide in the mapping of recharge and discharge areas, the location of springs, and the expected occurrence of phreatophytic vegetation.

The field program should also be designed to check the assumptions of the method and to improve on the basic data used in the reconnaissance model. This would involve actual measurement of the water table configuration, determination of the permeability contrasts by pump test or Hvorslev piezometer test, delineation of the geometry of the permeabilities by drilling or geophysical means, and an investigation to determine whether the assumption of a steady-state water table is valid (i.e., the fluctuations in water-table elevation with time must be small in comparison with the total saturated depth of the basin, and the relative highs and lows in the water-table configuration must be maintained throughout the year).

AS AN INTERPRETIVE TOOL

Following the field program, a second mathematical model can be prepared, utilizing the information obtained in the field investigation. The results of this model can be used to calculate the natural basin yield. They may also be useful in the design of the component projects in a basin-wide groundwater development.

If this interpretive model is not compatible with field observation, then it can be assumed that some major factor has been misinterpreted or overlooked. For example, the permeability configuration at depth may be more complex than that assumed in the model, or the formations may possess a higher or lower factor of anisotropy than that considered. The mathematical model can then be used on a trial-and-error basis in an attempt to pinpoint the unsuspected situations which have eluded the investigator in the field.

GRAVELBOURG AQUIFER

An example of the application of the two-dimensional, mathematical-model approach to a field situation is provided by the Gravelbourg aquifer. This is a shallow sand and gravel aquifer which occurs within the glacial deposits near Gravelbourg, Saskatchewan, Canada. The hydrogeology of the aquifer has been studied in detail by the author (Freeze, 1964). Figure 29a shows the potential net and interpretive flow directions deduced from the extensive field investigation.

Figure 29b shows the flow pattern obtained from a reconnaissance two-dimensional mathematical model based on the known water-table configuration, known geometry of geological formations (see Legend), and assumed values of the permeability contrasts. The permeability of the aquifer was known from the results of a pump test (K = 130 gal. per day per ft^2), whereas the other values had to be estimated from measurements by other workers in similar formations nearby (Meyboom and van Everdingen, personal communication). All four values were then reduced to the simple dimensionless ratio 100:10:1:0.5. All formations were assumed to be isotropic. The resulting potential net is a peculiar one showing almost entirely vertical equipotentials. All flow is near-horizontal and each topographic divide acts as a vertical impermeable boundary. The results of the model clearly do not correspond with the more complex potential pattern found in the field.

Consequently, a series of interpretive models was designed using the same water-table and geological configurations but varying the permeability (which in this case was the property most open to question). A straight increase in the permeability ratios failed to resolve the question but the introduction of a 100:1 horizontal: vertical anisotropy together with increased permeability ratios produced a potential pattern (Figure 29c) which, while not identical to the field results, was very similar.

In an attempt to determine the upper limit of possible permeability values, the model in Figure 29d was run. The true values of the average formation-wide permeabilities must lie between those of c and d, Figure 29d. This trial-and-error approach points out how the mathematical-model method can be used to determine basin-wide permeability values. It is possible that such values have more validity in the study of basin-wide resources than do permeability values determined by in-situ point determinations such as pump test or piezometer tests.

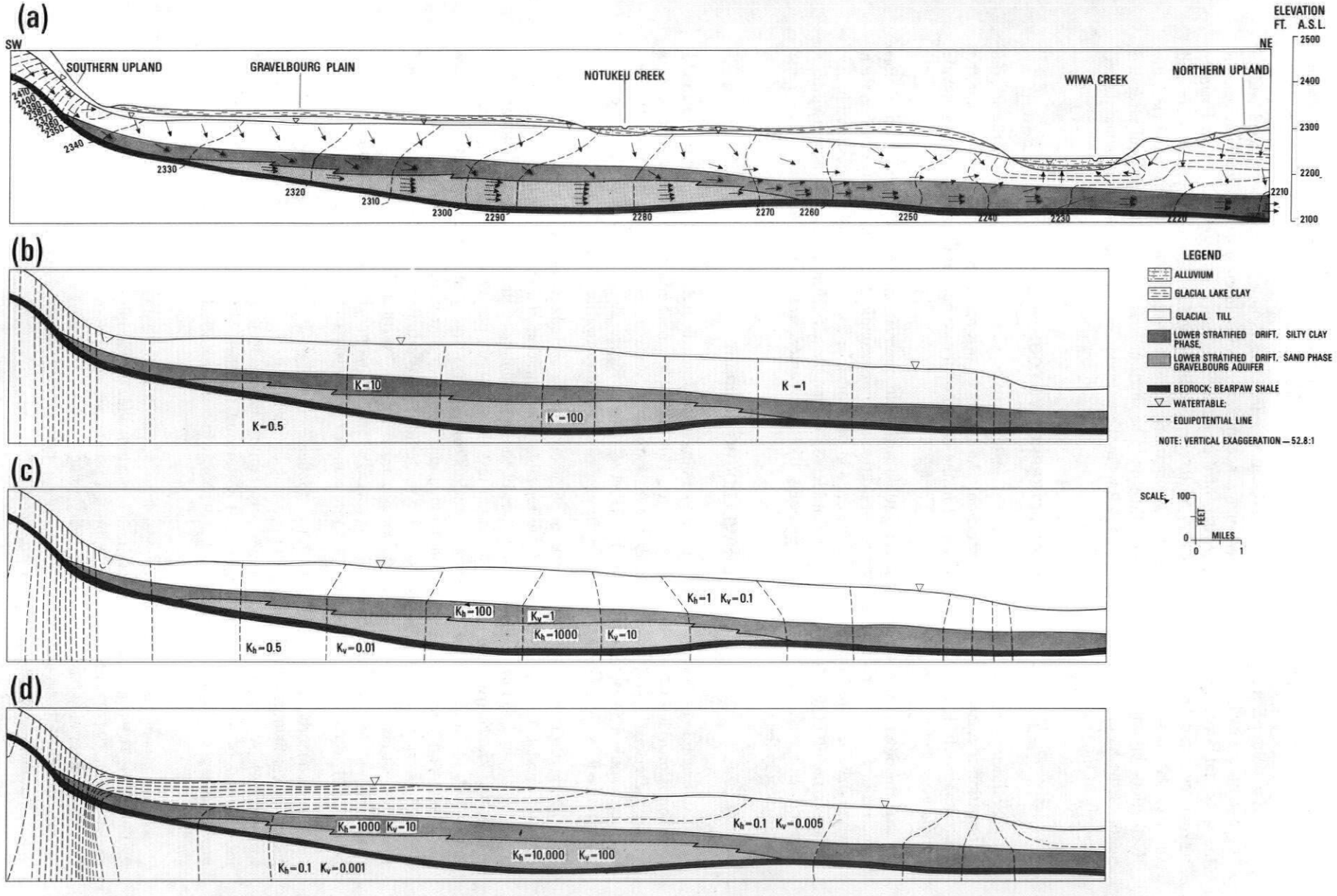

Figure 29. Gravelbourg aquifer

Further changes in the model which might produce an even closer fit to the observed data (Figure 29a) are:

1. A smaller factor of anisotropy.
2. Anisotropy only in the "lower stratified drift", or possibly even a vertical anisotropy in the glacial till.
3. Inclusion of the glacial lake clay (low permeability) in the model. It was excluded in the models shown because it was assumed to lie above the water table.

Used as an interpretive tool, the results of the theoretical flow patterns suggest:

1. A large factor of anisotropy, which was not discovered in the field studies, probably exists in the Gravelbourg aquifer.
2. The flow through the silty clay does not extend under Wiwa Creek as suggested by the field investigation. Several models, were extended further to the northeast as far as Old Wives Lake, the major discharge area in the vicinity of the Gravelbourg aquifer. The results of these models thus included the effects of the northern upland (Figure 29a). In all cases, an imaginary, vertical impermeable boundary was created beneath Wiwa Creek. Wiwa Creek valley apparently acts as the major discharge area for the Gravelbourg aquifer. (It should be noted that less anisotropy and a larger permeability ratio might result in underflow beneath Wiwa Creek. This is an example of a question which has been raised by the use of the mathematical model but which should be solved in the field. In this case a piezometer nest around Wiwa Creek valley would resolve the question.)

SUGGESTIONS FOR FUTURE WORK

1. With the present mathematical model:
   (a) A study of the effect of anisotropy of permeability on regional groundwater flow patterns.
2. Adaptation of the mathematical model:
   (a) To treat transient water-table conditions.
   (b) To include the effect of well fields as a source of discharge or recharge.
   (c) To include the unsaturated zone above the water table in such a way that the position of the water table can be calculated from a boundary condition involving the rainfall pattern.
3. Improvements in the computer technology:
   (a) An investigation into the possible uses of intermediate storage with the computer so that large three-dimensional problems can be run.
   (b) An investigation of implicit iterative procedures.
   (c) An investigation of the properties of the relaxation factor ω so that the optimum value of ω may be found for each problem and divergent iterative cases can be avoided.
4. In the field:
   (a) A correlation between flow patterns obtained by field investigation, and interpretive theoretical models. (This is presently being done by the author in the Old Wives Lake drainage basin in southern Saskatchewan, Canada.)
   (b) An investigation of the field occurrence of anisotropic formations with the aim of delineating the usual and maximum factors of anisotropy present in various geological formations.
   (c) An examination of streamflow records to determine the quantitative effect of existing groundwater flow patterns on surface water hydrology.

CHAPTER 9

Conclusions

1. It is possible to develop a mathematical model such that theoretical solutions can be obtained for the problem of regional groundwater flow in a three-dimensional, non-homogeneous, anisotropic groundwater basin. The potential function is the hydraulic head. The applicable partial differential equations are Laplace's equation for the homogeneous case and Richards' equation for the non-homogeneous case. The field is bounded by a horizontal impermeable boundary at the base, imaginary vertical impermeable boundaries on all sides and a steady-state water table on top. The solutions are in the form of potential nets from which flow patterns can be constructed.

2. Two independent methods of solution are available:

   (a) The formal analytical theory of the solution of partial differential equations using Fourier series.

   (b) The finite-difference approach of numerical analysis. The analytical method is restricted to two-dimensional, homogeneous or layered cases and must be solved using the rectangular approximation. The numerical method removes these restrictions and in addition is mathematically simpler and well suited to computer-oriented methods of data storage and retrieval.

3. Computer programs have been written for both methods and matched solutions obtained.

4. The Schwarz-Christoffel transformation cannot be applied in practice to remove the assumption of the rectangular approximation from the analytical solution. The rectangular approximation is qualitatively valid for large water-table slopes but becomes quantitatively invalid at small regional slopes.

5. The following three factors affect the qualitative nature of the flow pattern:

   (a) The depth/lateral extent ratio of the basin.

   (b) The configuration of the water table.

   (c) The geological configuration and the values of the resulting permeability contrasts.

   The flow patterns for seventy-one hypothetical cases are shown in Chapter 5 to illustrate the control these factors exert on the size of the component sub-basins of the major groundwater basin, and the distribution of recharge and discharge areas.

6. For any groundwater basin with a given water-table configuration and geologic configuration, the quantity of flow through the basin is a unique property which is defined to be the "natural basin yield". It can be used to estimate the basin safe yield.

7. The amount of recharge and discharge varies across a basin. The zones of concentration can best be delineated using a recharge-discharge profile. The configuration of the groundwater flow pattern exerts a quantitative influence on the other components of the hydrologic cycle. In particular, it will serve to concentrate evapotranspiration and the groundwater component of surface runoff in certain areas of the basin.

8. The three-dimensional program is at present (1966) limited to small basins. Larger, more complex basins are best treated by representive two-dimensional models. The improvement of high-speed digital computers will remove this limitation in the near future.

9. The mathematical model approach using numerical solutions and the digital computer can be

used in practice both as a reconnaissance tool preceding field investigation and as an interpretive tool following the field program.

10. The results of mathematical model analyses on two actual groundwater basins in the Canadian prairies have emphasized the importance of horizontal-vertical anisotropy of permeability on regional groundwater flow patterns.

References

Byerly, W.E. 1959. Fourier's Series; Dover Publications, 287 pp.

Carslaw, H.S., and J.C. Jaeger. 1959. Conduction of heat in solids; Clarendon Press, 510 pp.

Chebotarev, I.I. 1955. Metamorphism of natural waters in the crust of weathering; Geochimica et Cosmochimia Acta, vol. 8, pp. 22-49 (Part I), pp. 137-171 (Part II), pp. 198-213 (Part III).

Churchill, R.V. 1960. Complex variables and applications; McGraw-Hill, 279 pp.

Davis, S.N. 1963. Discussion of a Paper by J. Tóth. A theory of groundwater motion in small drainage basins in Central Alberta, Canada; J.G.R., vol. 68, No. 8, pp. 2352-2353.

Douglas, J. Jr., and H.H. Rachford, Jr. 1956. On the numerical solution of heat conduction problems in two and three space variables; Trans. Am. Math. Soc., vol. 82, pp. 421-439.

Van Everdingen, R.O. 1963. Groundwater flow-diagrams in sections with exaggerated vertical scale; G.S.C. Paper 63-27, 21 pages.

Fayers, F.J., and J.W. Sheldon. 1962. The use of a high speed digital computer in the study of the hydrodynamics of geologic basins. J.G.R., vol. 67, No. 6, pp. 2421-2431.

Forsythe, G.E., and W.R. Wasow. 1960. Finite-difference methods for partial differential equations; John Wiley and Sons, 443 pp.

Freeze, R.A. 1964. Hydrogeology and groundwater resources of the Gravelbourg aquifer, Saskatchewan, Canada; M.Sc. Thesis, Univ. of California at Berkeley; Scientific Series No. 6 (in press), Inland Waters Branch.

Freeze, R.A. 1966. Theoretical analysis of regional groundwater flow; Ph.D. Thesis, Univ. of California, Berkeley.

Freeze, R.A., and P.A. Witherspoon. 1966. Theoretical analysis of regional groundwater flow. I. Analytical and numerical solutions to the mathematical model; Water Resources Res., vol. 2, No. 4.

Freeze, R.A., and P.A. Witherspoon. 1967. Theoretical analysis of regional groundwater flow. II. Effect of water-table configuration and sub-surface permeability variation; Water Resources Res., vol. 3, No. 2.

Freeze, R.A., and P.A. Witherspoon. 1968. Theoretical analysis of regional groundwater flow. III. Quantitative interpretations; Water Resources Res., vol. 4, No. 3.

Harr, M.E. 1962. Groundwater and seepage; McGraw-Hill, 315 pp.

Hubbert, M.K. 1940. Theory of groundwater motion; Jour. of Geol., vol. 48, No. 8, Pt. I., pp. 785-944.

Kellogg, O.D. 1953. Foundations of potential theory; Dover Publications, 384 pp.

Kirkham, Don. 1958. Seepage of steady rainfall through soils into drains; Trans. A.G.U., vol. 39, No. 5, pp. 892-908.

Kirkham, Don., and R.E. Gaskell. 1951. Falling water table in tile and ditch drainage; Soil. Sc. Soc. of Am., vol. 15, pp. 37-42.

Klute, A., E.J. Scott and F.D. Whisler. 1965. Steady state water flow in a saturated inclined soil slab; Wat. Resources Res., vol. 1, No. 2, pp. 287-294.

Kober, H. 1957. Dictionary of conformal representations; Dover Publications, 208 pp.

Kunkle, G.R. 1962. The baseflow-duration curve, a technique for the study of groundwater discharge from a drainage basin; J.G.R., vol. 67, No. 4, pp. 1543-1554.

Liakopoulos, A.C. 1965. Variation of the permeability tensor ellipsoid in homogeneous, anisotropic soils, Wat. Resources Res., vol. 1, No. 1.

Linsley, R.K. Jr., M. Kohler and J.L. Paulhus. 1949. Applied hydrology; McGraw-Hill, 689 pp.

Luthin, J.N., editor. 1957. Drainage of agricultural lands; Am. Soc. of Agronomy, 620 pp.

Luthin, J.N., and P.R. Day. 1955. Lateral flow above a sloping water table, Soil Sc. Soc. Amer., Proc., vol. 19, pp. 406-410.

Luthin, J.N., and R.E. Gaskell. 1950. Numerical solutions for tile drainage of layered soils; Trans. A.G.U., vol. 31, pp. 595-602.

Maasland, M. 1957. Soil anisotropy and land drainage, in: drainage of agricultural lands, J.N. Luthin, ed., Am. Soc. of Agronomy, 216-285.

McCracken, D.D., and W.S. Dorn. 1964. Numerical methods and Fortran programming; John Wiley and Sons, 457 pp.

Meyboom, P. 1961. Estimating groundwater recharge from stream hydrographs; J.G.R., vol. 66, No. 4, pp. 1203-1214.

Meyboom, P. 1966. Unsteady groundwater flow near a willow ring in hummocky moraine; Jour. Hydrology, vol. 4, pp. 38-62.

Meyboom, P., and R.O. van Everdingen. 1964. Personal communication.

Moon, P., and D.E. Spencer. 1961. Field theory for engineers; D. Van Nostrand Co. Inc., 530 pp.

Muskat, M. 1946. Flow of homogeneous fluids, J.W. Edwards Inc., 763 pp.

Olmsted, J.M.H. 1956. Real variables; Appleton-Century-Crafts Inc. 621 pp.

Panov, D.J. 1963. Formulas for the numerical solution of partial differential equations by the method of differences; Frederick Ungar Publishing Co. 133 pp.

Peaceman, D.W., and H.H. Rachford, Jr. 1955. The numerical solution of parabolic and elliptical difference equations; Jour. Soc. Industrial and Applied Math., vol. 3, No. 11, pp. 28-41.

Polubarinova-Kochina, P.Ya. 1962. Theory of groundwater movement; Princeton Univ., Press, 613 pp.

Ralston, A., and H.S. Wilf. 1960. Mathematical methods for digital computing; John Wiley and Sons, 293 pp.

Remson, I., C.A. Appel and R.A. Webster. 1965. Groundwater models solved by a digital computer; Jour. Hydraulics Division, Proc. A.S.C.E., vol. 91, No. HY3, pp. 133-147.

Richards, L.A. 1931. Capillary conduction of liquids through porous mediums; Physics, 1, 318-333.

Salvadori, M.G., and M.L. Baron. 1961. Numerical methods in engineering; Prentice-Hall, 302 pp.

Scheidegger, A.E. 1960. The physics of flow through porous media; MacMillan, 313 pp.

Scheidegger, A.E. 1963. Theoretical aspects of quantitative groundwater flow studies; NRC (Canada), Ass. Comm. on Geodesy and Geophysics, Subcomm. on Hydrology, Proc. of Hydrology Symposium No. 3, pp. 107-116.

Schenk, H. Jr. 1963. Fortran methods in heat flow; Ronald Press Co., 289 pp.

Shaw, F.S., and R.V. Southwell. 1941. Relaxation methods applied to engineering problems, VII, Problems relating to the percolation of fluids through porous materials; Proc. Roy. Soc., Ser. A, vol. 178, pp. 1-17.

Sneddon, Ian. 1957. Elements of partial differential equations; McGraw-Hill, 327 pp.

Sokolnikoff, I.S., and R.M. Redheffer. 1958. Mathematics of physics and modern engineering, McGraw-Hill, 812 pp.

Southwell, R.V. 1946. Relaxation methods in theoretical physics, Oxford Univ. Press, London, 248 pp.

Stallman, R.W. 1956. Use of numerical methods for analyzing data on groundwater levels; Symposia Darcy, Ass. Int. d'Hydrologie Scientifique, Publ. 41, pp. 227-231.

Thom, A., and C.J. Appelt. 1961. Field computations in engineering and physics; D. Van Nostrand Co., Ltd., 165 pp.

Todd, D.K. 1959. Groundwater hydrology; John Wiley and Sons, 336 pp.

Todd, J., editor. 1962. Survey of numerical analysis; McGraw-Hill, 589 pp.

Tóth, J. 1962. A theory of groundwater motion in small drainage basins in Central Alberta, Canada; J.G.R., vol. 67, No. 11, pp. 4375-4387.

Tóth, J. 1963a. Reply to S.N. Davis re Tóth (1962); J.G.R., vol. 68, No. 8, pp. 2354-2356.

Tóth, J. 1963b. A theoretical analysis of groundwater flow in small drainage basins; J.G.R., vol. 68, No. 16, pp. 4795-4812.

Tóth, J. 1963c. A theoretical analysis of groundwater flow in small drainage basins; NRC (Canada), Ass. Comm. on Geodesy and Geophysics, Subcomm. on Hydrology, Proc. of Hydrology Symposium, No. 3, pp. 75-96.

Tyson, H.N. Jr., and E.M. Weber. 1964. Computer simulation of groundwater basins; Jour. Hydraulics Division, Proc. A.S.C.E. vol. 90, No. HY4, pp. 59-77.

Walker, M. 1964. The Schwarz-Christoffel transformation and its applications – a simple exposition; Dover Publications, 116 pp.

Walton, W.C. 1962. Selected analytical methods for well and aquifer evaluation; Ill. St. Water Survey, Bull. 49, 81 pp.

Wesseling, J. 1964. A comparison of the steady state drain spacing formulas of Hooghoudt and Kirkham in connection with design practice; Jour. of Hydrology, vol. II, No. 1, pp. 25-33.

Wylie, C.R. Jr. 1960. Advanced engineering mathematics, McGraw-Hill, 696 pp.

Young, David. 1954. Iterative methods for solving partial differential equations of the elliptic type; Trans. Am. Math. Soc., vol. 76, pp. 92-111.

APPENDIX A

Computer Program for Analytical Solution

This appendix contains:

1. A complete printout of Analytical Program 6, the programmed solution of equation (2.107) representing the analytical solution for the two-dimensional, three-layer problem with generalized water-table configuration. The programming language is FORTRAN IV.
2. A list of the program variables, related to the algebraic parameters they represent. Reference to equation (2.107) and Figure 4 is recommended.
3. A table of instructions for the assembling of an input data deck, listing the required input and the necessary format.
4. A table of recommended values for cartain of the computing parameters.
5. The results of an analysis of the parameters W, V, T, R, U, Y, and RATIO. The expressions representing these variables must be reduced to their simplest form at each step in the solution. The degree of reduction is dependent on the x and z value of the point at which it is being calculated and also varies with the term of the infinite series (the value of m). A failure to take this analysis into account when preparing the program results in overflows within the computer. Only the results of the analysis are presented; the developments are simple and are left to the reader. The only purpose of including such an analysis here is to enable the reader to follow the steps in the program if he wishes.

The programs were run at the University of California Computer Centre at Berkeley on a Direct Couple System consisting of an IBM 7040 and an IBM 7094. Plotting was carried out by a Calcomp 565 x-y plotter.

Computer times varied between 2 and 10 minutes depending on the complexity of the problem.

The plotting subroutine is adapted from J6 BC XYP4; writeups of this program are available from the Library, University of California Computer Center, Berkeley.

List of Program Variables

Basic Parameters

Program		Model
S		s
ZZERO		Z_0
EX(LA)	LA = 1, K	X_ℓ
C(LA)	LA = 1, K+1	C_ℓ
M		m
K		k
PI		π
RONE		r_1
RTWO		r_2
PERM1		K_1
PERM2		K_2
PERM3		K_3
X(I)	I = 1,N	x
Z(J)	J = 1,L	z
PHI(I,J)		ϕ
DELX		Δx } grid spacing
DELZ		Δz } grid spacing
DELPHI		$\Delta\varphi$ – for contours
PHIMIN		φ – minimum
PHIMAX		$\bar{\varphi}$ – maximum
XONE = X(1)		value of x at origin
ZONE = Z(1)		value of z at origin

SWITCH = SLIMIT = value of y at which e^{-y} becomes negligible in comparison with e^{y}. (The two terms are identical but were given different names to differentiate their roles – see "Analysis of Parameters".)

IPLOT = 1, equipotential plot will be plotted in 8″ x 5″ field (to fully fill field, must use
s = 20,000 ft
z_0 = 12,000 ft)

= 2 equipotential plot will be plotted in 16″ x 5″ field (to fully fill field must use
s = 40,000 ft
z_0 = 12,000 ft)

= 3 equipotential plot will be plotted in 24″ x 5″ field (to fully fill field must use
s = 60,000 ft
z_0 = 12,000 ft)

Defined in Program

$$\text{SUMA} = \sum_{\ell=1}^{k} (c_{\ell+1} - c_\ell)\left(\frac{x_\ell^2}{2} - x_\ell s\right)$$

$$\text{CONST} = \frac{1}{s}[z_0 s + \text{SUMA} + \frac{c_{k+1}}{2} \cdot s^2] = \frac{A_0}{2}$$

$$\text{SUMB} = \sum_{\ell=1}^{k} (c_\ell - c_{\ell+1}) \cos \frac{m\pi x_\ell}{s}$$

$$\text{COEFF(M)} = \frac{2}{s}\left(\frac{s}{m\pi}\right)^2 [c_{k+1} \cos m\pi - c_1 + \text{SUMB}]$$

$$\text{RAT1} = K_2/K_1$$

$$\text{RAT2} = K_3/K_2$$

$$\text{ONE} = \frac{m\pi x}{s}$$

$$\text{TWO} = \frac{m\pi z}{s}$$

$$\text{THREE (M)} = \frac{m\pi z_0}{s}$$

$$\text{FOUR(M)} = \frac{m\pi r_1}{s}$$

$$\text{FIVE(M)} = \frac{m\pi r_2}{s}$$

$$\text{SIX} = \text{THREE(M)} - \text{TWO}$$

$$\text{SEVEN} = \text{THREE(M)} + \text{TWO}$$

$$\left.\begin{aligned} W(M) &= W \\ V(M) &= V \\ T(M) &= T \\ R(M) &= R \\ U(M) &= U \\ Y(M) &= Y \\ UY(M) &= U + Y \end{aligned}\right\} \quad M = 1, \text{KUTOFF}$$

RATIO:

In ϕ_1 zone; $$\text{RATIO} = \frac{\left[\cosh \frac{m\pi z}{s}(U) + \sinh \frac{m\pi z}{s}(Y)\right]}{\left[\cosh \frac{m\pi z_0}{s}(U) + \sinh \frac{m\pi z_0}{s}(Y)\right]}$$

In ϕ_2 zone; $$\text{RATIO} = \frac{\left[\cosh \frac{m\pi z}{s}(W) + \sinh \frac{m\pi z}{s}(V)\right]}{\left[\cosh \frac{m\pi z_0}{s}(U) + \sinh \frac{m\pi z_0}{s}(Y)\right]}$$

In ϕ_3 zone; $$\text{RATIO} = \frac{\left[\cosh \frac{m\pi z}{s}\right]}{\left[\cosh \frac{m\pi z_0}{s}(U) + \sinh \frac{m\pi z_0}{s}(Y)\right]}$$

$$\text{FACT} = \cos \frac{m\pi x}{s} \cdot \text{RATIO}$$

$$\text{TERM} = \text{COEFF} \cdot \text{FACT}$$

$$\text{SUM} = \text{sum of TERMs}$$

$$\text{PHI (I,J)} = \text{CONST} + \text{SUM}$$

Data Deck — Analytical Program 6

Group	Card	Format	Data
A	1	2A6	any desired title.
B	1	7I10	N,L,K, KUTOFF, IPLOT
C	1	4F18.8	PI,S,ZZERO,DELX
	2	"	DELZ,DELPHI,PHIMIN,PHIMAX
	3	"	ZONE,XONE,RONE,RTWO
	4	"	PERM1,PERM2,PERM3,SWITCH
	5	"	SLIMIT
D	1	4F18.8	EX(LA), LA=1,K; 4 values per card.
	2	"	
	⋮		
E	1	4F18.8	C(LA), LA=1,K+1; 4 values per card
	2	"	
	⋮		

Recommended Values

KUTOFF = 50

PI = 3.14159

DELPHI = $\frac{1}{10}$ to $\frac{1}{20}$ of (PHIMAX − PHIMIN)

ZONE = 0.0

XONE = 0.0

SWITCH = 20.0

SLIMIT = 20.0

Note: r_1 and r_2 must not equal z_0 or zero.

Analysis of Parameters

Case 1

FOUR(M) > SWITCH

FIVE(M) > SWITCH

$$W(M) = [\cosh^2 (FIVE)] \left[1 - \frac{K_3}{K_2}\right] + \frac{K_3}{K_2}$$

$$V(M) = 1 - W(M)$$

$$T(M) = [\cosh^2 (FOUR)] \left[1 - \frac{K_2}{K_1}\right] + \frac{K_2}{K_1}$$

$$R(M) = 1 - T(M)$$

$$U(M) = T(M) + W(M) \frac{K_2}{K_1} - \frac{K_2}{K_1}$$

$$Y(M) = 1 - U(M)$$

RATIO: ϕ_1, ϕ_2 or ϕ_3 ZONE:

(i) SIX > SWITCH: RATIO = 0.0

(ii) SIX < SWITCH: RATIO = e^{-SIX}

Case 2

FOUR(M) > SWITCH

FIVE(M) < SWITCH

$$W(M) = [\cosh^2 (FIVE)] \left[1 - \frac{K_3}{K_2}\right] + \frac{K_3}{K_2}$$

$$V(M) = \frac{1 - W(M)}{\tanh (FIVE)}$$

$$T(M) = [\cosh^2 (FOUR)] \left[1 - \frac{K_2}{K_1}\right] + \frac{K_2}{K_1}$$

$$R(M) = 1 - T(M)$$

$$U(M) = W(M)\ T(M) + \frac{\left[T(M) - \frac{K_2}{K_1} - W(M) \cdot T(M) + W(M) \frac{K_2}{K_1}\right]}{\tanh (FIVE)}$$

$$Y(M) = W(M) + \frac{[1 - W(M)]}{\tanh (FIVE)} - U(M)$$

RATIO: ϕ_1 zone

(i) SIX > SWITCH: RATIO = 0.0

(ii) SIX < SWITCH: RATIO = e^{-SIX}

RATIO: ϕ_2 zone

(a) TWO > SWITCH

(i) SIX > SWITCH: RATIO = 0.0

(ii) SIX < SWITCH: RATIO = e^{-SIX}

(b) TWO < SWITCH

(i) SEVEN > SLIMIT

1. SIX > SWITCH: RATIO = 0.0

2. SIX < SWITCH: RATIO = e^{-SIX}

(ii) SEVEN < SLIMIT:

$$RATIO = \frac{1}{U+Y}\left[W\left(e^{-SIX} + e^{-SEVEN}\right) + V\left(e^{-SIX} - e^{-SEVEN}\right)\right]$$

RATIO: ϕ_3 zone

(a) SIX > SWITCH: RATIO = 0.0

(b) SIX < SWITCH

(i) SEVEN > SLIMIT

1. SIX > SLIMIT: RATIO = 0.0

2. SIX < SLIMIT: RATIO = $\frac{1}{U+Y} e^{-SIX}$

(ii) SEVEN < SLIMIT

$$RATIO = \frac{1}{U+Y}\left(e^{-SIX} + e^{-SEVEN}\right)$$

Case 3

FOUR(M) < SWITCH

FIVE(M) < SWITCH

W(M)
V(M)
T(M)
R(M)
U(M)
Y(M)

} as defined in (2.107)

RATIO: ϕ_1 zone

(a) THREE < SWITCH

$$\text{RATIO} = \frac{\cosh \text{ TWO (U)} + \sinh \text{ TWO (Y)}}{\cosh \text{ THREE (U)} + \sinh \text{ THREE (Y)}}$$

(b) THREE > SWITCH

(i) SEVEN > SLIMIT

1. SIX > SLIMIT: RATIO = 0.0
2. SIX < SLIMIT: RATIO = $e^{-\text{SIX}}$

(ii) SEVEN < SLIMIT

$$\text{RATIO} = \frac{1}{\text{U+Y}}\left[(\text{U})\left(e^{-\text{SIX}} + e^{-\text{SEVEN}}\right) + (\text{Y})\left(e^{-\text{SIX}} - e^{-\text{SEVEN}}\right)\right]$$

RATIO: ϕ_2 zone

(a) THREE < SWITCH

$$\text{RATIO} = \frac{\cosh \text{ TWO (W)} + \sinh \text{ TWO (V)}}{\cosh \text{ THREE (U)} + \sinh \text{ THREE (Y)}}$$

(b) THREE > SWITCH

(i) SEVEN > SLIMIT

1. SIX > SLIMIT: RATIO = 0.0
2. SIX < SLIMIT: RATIO = $\frac{\text{W+V}}{\text{U+Y}} \cdot e^{-\text{SIX}}$

(ii) SEVEN < SLIMIT

$$\text{RATIO} = \frac{1}{\text{U+Y}}\left[(\text{W})\left(e^{-\text{SIX}} + e^{-\text{SEVEN}}\right) + (\text{V})\left(e^{-\text{SIX}} - e^{-\text{SEVEN}}\right)\right]$$

RATIO: ϕ_3 zone

(a) THREE < SWITCH

$$\text{RATIO} = \frac{\cosh \text{ TWO}}{\cosh \text{ THREE (U)} + \sinh \text{ THREE (Y)}}$$

(b) THREE > SWITCH

(i) SEVEN < SLIMIT

$$\text{RATIO} = \frac{1}{U+Y}\left(e^{-\text{SIX}} + e^{-\text{SEVEN}}\right)$$

(ii) SEVEN > SLIMIT

1. SIX > SLIMIT: RATIO = 0.0
2. SIX < SLIMIT: $\text{RATIO} = \frac{1}{U+Y}\, e^{-\text{SIX}}$

```
C ANALYTICAL PROGRAM 6
      DIMENSION X(101),Z(61),PHI(101,61),EX(10 ),C(101),W(100),V(100),
     1T(100),R(100),U(100),Y(100),UY(100),COEFF(100),THREE(100),
     2FOUR(100),FIVE(100),EMPI(100)
      COMMON PHI,N,L,PHIMIN,PHIMAX,DELPHI,XONE,ZONE,DELX,DELZ,IPLOT
  542 READ 540,TITLE1,TITLE2
  540 FORMAT (2A6)
      IF (TITLE1) 541,1000,541
  541 READ 1, N,L,K,KUTOFF,IPLOT
    1 FORMAT (7I10)
      READ 2,PI,S,ZZERO,DELX,DELZ,DELPHI,PHIMIN,PHIMAX,ZONE,XONE,RONE,
     1RTWO,PERM1,PERM2,PERM3,SWITCH,SLIMIT
    2 FORMAT (4F18.8)
      READ 2,(EX(LA),LA=1,K)
      KK=K+1
      READ 2,(C(LA),LA=1,KK)
      IF (K-0) 23,23,21
   23 SUMA=0.0
      GO TO 25
   21 DO 22 LA=1,K
      TERMA=(C(LA+1)-C(LA))*(EX(LA)**2/2.0-EX(LA)*S)
      IF (LA-1) 15,15,20
   15 SUMA=TERMA
      GO TO 22
   20 SUMA=SUMA+TERMA
   22 CONTINUE
   25 CONST=(ZZERO*S+C(KK)*S**2/2.0+SUMA)/S
      RAT1=PERM2/PERM1
      RAT2=PERM3/PERM2
      DO 100 M=1,KUTOFF
      CM=FLOAT(M)
      EMPI(M)=CM*PI
      IF (K-0) 161,161,160
  161 SUMB=0.0
      GO TO 101
  160 DO 180 LA=1,K
      CONE=EMPI(M)*EX(LA)/S
      TERMB=(C(LA)-C(LA+1))*COS(CONE)
      IF (LA-1) 165,165,170
  165 SUMB=TERMB
      GO TO 180
  170 SUMB=SUMB+TERMB
  180 CONTINUE
  101 COEFF(M)=(S/EMPI(M))**2*(C(KK)*COS(EMPI(M))-C(1)+SUMB)*2.0/S
      THREE(M)=EMPI(M)*ZZERO/S
      FOUR(M)=EMPI(M)*RONE/S
      FIVE(M)=EMPI(M)*RTWO/S
      IF (FOUR(M)-SWITCH) 203,203,205
  205 IF (FIVE(M)-SWITCH) 202,202,100
  202 EXP5=EXP(FIVE(M))
      COSH5=(EXP5+1.0/EXP5)/2.0
      SINH5=(EXP5-1.0/EXP5)/2.0
      TANH5=SINH5/COSH5
      W(M)=COSH5**2*(1.0-RAT2)+RAT2
      V(M)=(1.0-W(M))/TANH5
      UY(M)=W(M)+V(M)
      GO TO 100
  203 EXP5=EXP(FIVE(M))
      COSH5=(EXP5+1.0/EXP5)/2.0
```

```
      SINH5=(EXP5-1.0/EXP5)/2.0
      TANH5=SINH5/COSH5
      EXP4=EXP(FOUR(M))
      COSH4=(EXP4+1.0/EXP4)/2.0
      SINH4=(EXP4-1.0/EXP4)/2.0
      TANH4=SINH4/COSH4
      W(M)=COSH5**2*(1.0-RAT2)+RAT2
      V(M)=(1.0-W(M))/TANH5
      T(M)=COSH4**2*(1.0-RAT1)+RAT1
      R(M)=(1.0-T(M))/TANH4
      U(M)=W(M)*T(M)+COSH4*SINH4*V(M)*(1.0-RAT1)
      Y(M)=W(M)*R(M)+V(M)*(1.0+RAT1-T(M))
      UY(M)=U(M)+Y(M)
  100 CONTINUE
      DO 26 I=1,N
      IF (I-1) 13,13,14
   13 X(1)=XONE
      GO TO 16
   14 X(I)=X(I-1)+DELX
   16 DO 26 J=1,L
      IF(J-1) 6,6,8
    6 Z(1)=ZONE
      GO TO 11
    8 Z(J)=Z(J-1)+DELZ
   11 DO 24 M=1,KUTOFF
      ONE=EMPI(M)*X(I)/S
      TWO=EMPI(M)*Z(J)/S
      SIX=THREE(M)-TWO
      SEVEN=THREE(M)+TWO
      IF (FOUR(M)-SWITCH) 303,303,305
  305 IF (FIVE(M)-SWITCH) 302,302,306
  302 IF (Z(J)-RTWO) 633,633,308
  308 IF (Z(J)-RONE) 310,310,306
  310 IF (TWO-SWITCH) 311,311,306
  311 IF (SEVEN-SLIMIT) 405,405,306
  303 IF (Z(J)-RTWO)  318,318,314
  314 IF (Z(J)-RONE) 315,315,312
  312 IF (THREE(M)-SWITCH) 404,404,313
  313 IF (SEVEN-SLIMIT) 403,403,306
  315 IF (THREE(M)-SWITCH) 406,406,316
  316 IF (SEVEN-SLIMIT) 405,405,317
  317 IF (SIX-SLIMIT) 407,407,401
  306 IF (SIX-SWITCH) 402,402,401
  318 IF (TWO-SWITCH) 320,320,319
  319 IF (SIX-SLIMIT) 408,408,401
  320 IF (THREE(M)-SWITCH) 411,411,321
  633 IF (SIX-SWITCH) 321,321,401
  321 IF (SEVEN-SLIMIT) 409,409,322
  322 IF (SIX-SLIMIT) 408,408,401
  401 RATIO=0.0
      GO TO 400
  402 RATIO=1.0/EXP(SIX)
      GO TO 400
  403 EXP6=EXP(SIX)
      EXPN6=1.0/EXP6
      EXP7=EXP(SEVEN)
      EXPN7=1.0/EXP7
      RATIO=(U(M)*(EXPN6+EXPN7)+Y(M)*(EXPN6-EXPN7))/UY(M)
      GO TO 400
  404 EXP2=EXP(TWO)
```

```
      EXPN2=1.0/EXP2
      EXP3=EXP(THREE(M))
      EXPN3=1.0/EXP3
      COSH2=(EXP2+EXPN2)/2.0
      SINH2=(EXP2-EXPN2)/2.0
      COSH3=(EXP3+EXPN3)/2.0
      SINH3=(EXP3-EXPN3)/2.0
      RATIO=(U(M)*COSH2+Y(M)*SINH2)/(U(M)*COSH3+Y(M)*SINH3)
      GO TO 400
  405 EXP6=EXP(SIX)
      EXPN6=1.0/EXP6
      EXP7=EXP(SEVEN)
      EXPN7=1.0/EXP7
      RATIO=(W(M)*(EXPN6+EXPN7)+V(M)*(EXPN6-EXPN7))/UY(M)
      GO TO 400
  406 EXP2=EXP(TWO)
      EXPN2=1.0/EXP2
      EXP3=EXP(THREE(M))
      EXPN3=1.0/EXP3
      COSH2=(EXP2+EXPN2)/2.0
      SINH2=(EXP2-EXPN2)/2.0
      COSH3=(EXP3+EXPN3)/2.0
      SINH3=(EXP3-EXPN3)/2.0
      RATIO=(W(M)*COSH2+V(M)*SINH2)/(U(M)*COSH3+Y(M)*SINH3)
      GO TO 400
  407 RATIO=(W(M)+V(M))/(EXP(SIX)*UY(M))
      GO TO 400
  408 RATIO=1.0/(UY(M)*EXP(SIX))
      GO TO 400
  409 EXP6=EXP(SIX)
      EXPN6=1.0/EXP6
      EXP7=EXP(SEVEN)
      EXPN7=1.0/EXP7
      RATIO=(EXPN6+EXPN7)/UY(M)
      GO TO 400
  411 EXP2=EXP(TWO)
      EXPN2=1.0/EXP2
      EXP3=EXP(THREE(M))
      EXPN3=1.0/EXP3
      COSH2=(EXP2+EXPN2)/2.0
      COSH3=(EXP3+EXPN3)/2.0
      SINH3=(EXP3-EXPN3)/2.0
      RATIO=COSH2/(U(M)*COSH3+Y(M)*SINH3)
  400 IF (RATIO-0.0001) 26,1400,1400
 1400 FACT=RATIO*COS(ONE)
      TERM=COEFF(M)*FACT
      IF (M-1) 801,801,810
  801 SUM=TERM
      GO TO 24
  810 SUM=SUM+TERM
   24 CONTINUE
   26 PHI(I,J)=CONST+SUM
      PRINT 30,TITLE1,TITLE2
   30 FORMAT (1H1,22H      NUMERICAL PROBLEM 2A6//12X,4HX(I)//)
      PRINT 60,(X(I),I=1,N)
      PRINT 50
   50 FORMAT (1H1,12X,4HZ(J)//)
      PRINT 60,(Z(J),J=1,L)
   60 FORMAT (10F12.4)
```

```
      PRINT 70
   70 FORMAT (1H1,10X,8HPHI(I,J)//)
      DO 80 I=1,N
      PRINT 72,I
   72 FORMAT (1H0,12X,2HI=,I3//)
   80 PRINT 82,(PHI(I,J),J=1,L)
   82 FORMAT (10F12.4)
      CALL CONTOR
      CALL CCNEXT
      GO TO 542
 1000 CALL CCEND
      STOP
      END
C
C
C
      SUBROUTINE CONTOR
      DIMENSION PHI(101,61),T(4,3),XX(2),ZZ(2),XXX(2),ZZZ(2)
      COMMON PHI,N,L,PHIMIN,PHIMAX,DELPHI,XONE,ZONE,DELX,DELZ,IPLOT
      COMMON /CCPOOL/ XMIN,XMAX,YMIN,YMAX,CCXMIN,CCXMAX,CCYMIN,CCYMAX
      IF (IPLOT-2) 40,41,42
   40 XMIN=-1875.0
      XMAX=23125.0
      YMIN=-4250.0
      YMAX=12250.0
      CCXMIN=100.0
      CCXMAX=1100.0
      CCYMIN=250.0
      CCYMAX=910.0
      CALL CCBGN
      CALL CCGRID (6HNOLBLS)
      XMIN=0.0
      XMAX=20000.0
      YMIN=0.0
      YMAX=12000.0
      CCXMIN=175.0
      CCXMAX=975.0
      CCYMIN=420.0
      CCYMAX=900.0
      CALL CCBGN
      CALL CCGRID (1,10,6HNOLBLS,1,6)
      WRITE (98,20)
   20 FORMAT (116H0        0.1S          .2S        0.3S          0.4S
     1  0.5S        0.6S          0.7S          .8S          0.9S          S)
      CALL CCALTR (175.0,405.0,0,1)
      CALL CCALTR ( 980.0,420.0,0,1,1H0)
      CALL CCALTR (980.0,500.0,0,1,4H0.1S)
      CALL CCALTR (980.0,580.0,0,1,4H0.2S)
      CALL CCALTR (980.0,660.0,0,1,4H0.3S)
      CALL CCALTR (980.0,740.0,0,1,4H0.4S)
      CALL CCALTR (980.0,820.0,0,1,4H0.5S)
      CALL CCALTR (980.0,900.0,0,1,4H0.6S)
      GO TO 43
   41 XMIN=-1875.0
      XMAX=43125.0
      YMIN=-4250.0
      YMAX=12250.0
      CCXMIN=100.0
      CCXMAX=2100.0
      CCYMIN=250.0
```

```
      CCYMAX=910.0
      CALL CCBGN
      CALL CCGRID (6HNOLBLS)
      XMIN=0.0
      XMAX=40000.0
      YMIN=0.0
      YMAX=12000.0
      CCXMIN=175.0
      CCXMAX=1775.0
      CCYMIN=420.0
      CCYMAX=900.0
      CALL CCBGN
      CALL CCGRID (1,20,6HNOLBLS,1,6)
      WRITE (98,21)
   21 FORMAT (117H0                          .1S                          0.2S
     1              0.3S                          .4S                          0.5S)
      CALL CCALTR (175.0,405.0,0,1)
      WRITE (98,23)
   23 FORMAT (113H                       0.6S                          0.7S
     1           0.8S                          .9S                               S)
      CALL CCALTR (989.0,405.0,0,1)
      CALL CCALTR (1780.0,420.0,0,1,1H0)
      CALL CCALTR (1780.0,580.0,0,1,4H0.1S)
      CALL CCALTR (1780.0,740.0,0,1,4H0.2S)
      CALL CCALTR (1780.0,900.0,0,1,4H0.3S)
      GO TO 43
   42 XMIN=-1875.0
      XMAX=63125.0
      YMIN=-4250.0
      YMAX=12250.0
      CCXMIN=100.0
      CCXMAX=3100.0
      CCYMIN=250.0
      CCYMAX=910.0
      CALL CCBGN
      CALL CCGRID (6HNOLBLS)
      XMIN=0.0
      XMAX=60000.0
      YMIN=0.0
      YMAX=12000.0
      CCXMIN=175.0
      CCXMAX=2575.0
      CCYMIN=420.0
      CCYMAX=900.0
      CALL CCBGN
      CALL CCGRID (1,30,6HNOLBLS,1,6)
      WRITE (98,22)
   22 FORMAT (115H0                                        0.1S
     1              .2S                                        0.3S           )
      CALL CCALTR (175.0,405.0,0,1)
      WRITE (98,24)
   24 FORMAT (114H                       0.4S
     1 0.5S                                    .6S                          )
      CALL CCALTR (980.0,405.0,0,1)
      WRITE (98,25)
   25 FORMAT (114H         0.7S                                        0.8S
     1                          0.9S                                     S)
      CALL CCALTR (1778.0,405.0,0,1)
      CALL CCALTR (2580.0,420.0,0,1,1H0)
```

```
      CALL CCALTR (2580.0,660.0,0,1,4H0.1S)
      CALL CCALTR (2580.0,900.0,0,1,4H0.2S)
   43 LL=L-1
      NN=N-1
      DO 1 J=1,LL
      DO 2 I=1,NN
      PHILOW=AMIN1 (PHI(I,J),PHI(I+1,J),PHI(I+1,J+1),PHI(I,J+1))
      PHIHI=AMAX1 (PHI(I,J),PHI(I+1,J),PHI(I+1,J+1),PHI(I,J+1))
      IF (PHIHI-PHILOW) 2,2,51
   51 IF (PHILOW-PHIMAX) 53,53,2
   53 IF (PHIHI-PHIMIN) 2,5,5
    5 IF (PHILOW-PHIMIN) 54,54,55
   54 AA=PHIMIN
      GO TO 3
   55 AA= FLOAT(IFIX((PHILOW-PHIMIN)/DELPHI)+1)*DELPHI+PHIMIN
    3 IFLAG=0
      T(1,1)=PHI(I,J)
      T(2,1)=PHI(I+1,J)
      T(3,1)=PHI(I+1,J+1)
      T(4,1)=PHI(I,J+1)
      T(1,2)=XONE+FLOAT(I-1)*DELX
      T(2,2)=T(1,2)+DELX
      T(3,2)=T(2,2)
      T(4,2)=T(1,2)
      T(1,3)=ZONE+FLOAT(J-1)*DELZ
      T(2,3)=T(1,3)
      T(3,3)=T(1,3)+DELZ
      T(4,3)=T(3,3)
    4 K=0
    6 IF(T(1,1)-T(2,1)) 7,11,7
    7 F=(AA-T(1,1))/(T(2,1)-T(1,1))
      IF (F-1.0) 71,71,11
   71 IF(F) 11,11,8
    8 IDIOT=1+IFLAG
      XX(IDIOT)=(1.0-F)*T(1,2)+F*T(2,2)
      ZZ(IDIOT)=(1.0-F)*T(1,3)+F*T(2,3)
      F=XX(IDIOT)/25.0
      G=FLOAT(IFIX(F))
      H=F-G
      IF(H-0.50) 75,75,76
   75 XXX(IDIOT)=G*25.0
      GO TO 80
   76 XXX(IDIOT)=FLOAT(IFIX(XX(IDIOT)/25.0)+1)*25.0
   80 FF=ZZ(IDIOT)/25.0
       GG=FLOAT(IFIX(FF))
      HH=FF-GG
      IF(HH-0.50) 82,82,83
   82 ZZZ(IDIOT)=GG*25.0
      GO TO 85
   83 ZZZ(IDIOT)=FLOAT(IFIX(ZZ(IDIOT)/25.0)+1)*25.0
   85 IF(IFLAG) 10,10,9
    9 CALL CCPLOT(XXX,ZZZ,2,6HNOJOIN,1,1)
      XXX(1)=XXX(2)
      ZZZ(1)=ZZZ(2)
      GO TO 11
   10 IFLAG=1
   11 K=K+1
      IF(K-4) 13,12,12
   13 TT1=T(1,1)
      TT2=T(1,2)
```

```
      TT3=T(1,3)
      DO 131 NA=1,3
      DO 131 NB=1,3
  131 T(NB,NA)=T(NB+1,NA)
      T(4,1)=TT1
      T(4,2)=TT2
      T(4,3)=TT3
      GO TO 6
   12 AA=AA+DELPHI
   14 IF(AA-PHIHI) 15,15,2
   15 IF (AA-PHIMAX) 3,3,2
    2 CONTINUE
    1 CONTINUE
      RETURN
      END
```

APPENDIX B

Computer Programs for Numerical Solutions

Table 1 lists the six numerical programs and the salient features of each. A more complete presentation in the form of (1) complete program printouts for each program, (2) list of variables, (3) tables of data deck instructions, and (4) table of recommended values for certain of the computing parameters is given after the following discussion of the computer aspects of this study.

The major limitation in the use of the numerical method is the availability of core storage in the computer. This creates an upper limit to the number of nodes which can be used for a given problem. For Numerical Programs 1, 2 and 3 (Table 1) the maximum number of nodes which can be accommodated on an IBM 7094 is approximately 12,000. A net with N = 301, L = 41 was used for many of the problems, a 201 x 61 mesh for others. The program printouts are dimensioned for the 301 x 41 case. In Numerical Programs 4 and 5, the necessity of dimensioning the permeability values associated with each node reduces the possible number of nodes to 6,000 and 3,000 respectively. The three-dimensional case, Numerical Program 6, is designed for 7,500 nodes.

The computing time required to obtain a solution to a given problem depends on (1) the number of nodes in the mesh, (2) the value of the relaxation parameter ω, (3) the desired tolerance, and (4) the size of the discrepancy between the initial inserted values and the final results.

The effect of the first factor is self evident. More nodes lead to a larger number of iterations and hence longer computing times.

As mentioned in Chapter 3, the choice of the optimum value of ω on mathematical grounds can be a difficult task. McCracken and Dorn (1964) give some indication of the range of values which should be considered by way of a graph showing the relation between the number of iterations and ω

Table 1

Program	Content	Main Program	Sub-routines	Max. No. of Nodes	Contouring Subroute
Numerical Program 1	Two dim., homogeneous, square mesh	1	1	301x41	CONONE
Numerical Program 2	Two dim., homogeneous, 7 meshes (Figure 8)	1	18	301x41	CONTWO
Numerical Program 3	Two dim., layered, isotropic, square mesh	1	2	301x41	CONTHR
Numerical Program 4	Two dim., non-homogeneous, isotropic, square mesh	1	2	151x41	CONFOR
Numerical Program 5	Two dim., non-homogeneous, anisotropic, rectangular mesh	1	2	101x31	CONFIV
Numerical Program 6	Three dim., non-homogeneous, isotropic, 3D rectangular mesh.	1	4	25x25x12	CONSIX CONSJX CONSKX

for a particular problem involving Laplace's equation in a square region with Dirichlet boundary conditions (Figure 30a). A similar graph (Figure 30b) for a simple two-layer problem using Numerical Program 3 indicates the optimum value of ω to be 1.85. This value was used for most runs with Numerical Programs, 1, 3, 4, 5 and 6.

For Numerical Program 2, the introduction of the refined mesh and the corresponding three-term finite-difference expressions caused changes in the properties of the matrix (representing the n simultaneous linear equations) which affected the optimum value of ω. For $\omega = 1.85$, the iterative procedure diverged in many cases and did not lead to a solution, $\omega = 1.2$ was found satisfactory in several cases but an insufficient number of runs were made to determine the optimum ω. In fact the optimum ω may be different for each problem. To avoid the divergent results, the ordinary Liebmann method ($\omega = 1.0$) was used for most runs using Numerical Program 2. Due to the resultant lengthy computing times, this program, and therefore the refined meshes, were used very little in the study. Further work must be carried out to delineate the factors which affect the overrelaxation factor before the extrapolated Liebmann method can be applied systematically to cases involving refined meshes. A short discussion of the cause of the divergent results is included in Chapter 3 under "Solution of finite-difference equations".

The computer programs are written so that the iterative procedure continues until the difference between the computed values of ϕ(I,J) from one iteration to the next is less than some desired tolerance for all nodes in the mesh. Experience has shown that a tolerance of 0.1 or 0.01 often gives satisfactory results, but not always; 0.001 always represents satisfactory convergence and does not involve a significant increase in the number of iterations; 0.0001 lengthens the computing time significantly with little improvement in results. It has been noted that the greater the permeability difference within the model, the smaller the tolerance must be. The conclusions stated above apply to permeability ratios of up to 1:1,000.

An important warning must be issued here. Incomplete convergence due to the specification of too large a tolerance can lead to an equipotential plot which may appear correct but is in fact wrong. Figure 31 shows the effect of decreasing the tolerance on the results of a specific problem. Only Figure 31c is correct; the specification for any lower tolerance would result in the same potential configuration.

Perhaps the most influential factor in controlling computing time is the insertion into the mesh of the initial values of ϕ from which the iterative method proceeds toward the final result. If a reasonably accurate guess of the final result can be made, a very few iterations will produce an answer, whereas the insertion of a poor set of initial values may lead to the use of a prohibitive amount of computer time. A method of inserting initial values in vertical bands (and in layers within each band in Programs, 3, 4 and 5) was found to lead to reasonably rapid convergence without the necessity of punching an unreasonable number of data cards. The method is documented in the data deck instructions for each of the programs.

The work reported in this study was done at the University of California Computer Center at Berkeley. The Center operates a Direct Couple System (DCS) consisting of an IBM 7040 and an IBM 7094. In this configuration, the 7040 handles all input/output, while the 7094 compiles, assembles and executes programs. An off-line Calcomp 565 plotter in connection with an IBM 1401 was used to obtain the equipotential plots.

Computer times for the majority of two-dimensional cases reported in Chapters 5 and 6 were between 2 and 3 minutes. Problems involving high permeability ratios ran somewhat longer. Three-dimensional problems required 30-60 minutes computer time.

The contouring method in the eight plot subroutines in Table 1 is the same. The only differences in the program lie in their correspondence with the main program through DIMENSION and COMMON statements and in their generality. CONONE through CONFOR are restricted to three sizes of plot; CONFIV and the sections through the 3D model can handle any size of plot acceptable to the plotter. The plotting subrouting is adapted from J6 BC XYP4; writeups of this program are available from the Library, University of California Computing Center, Berkeley.

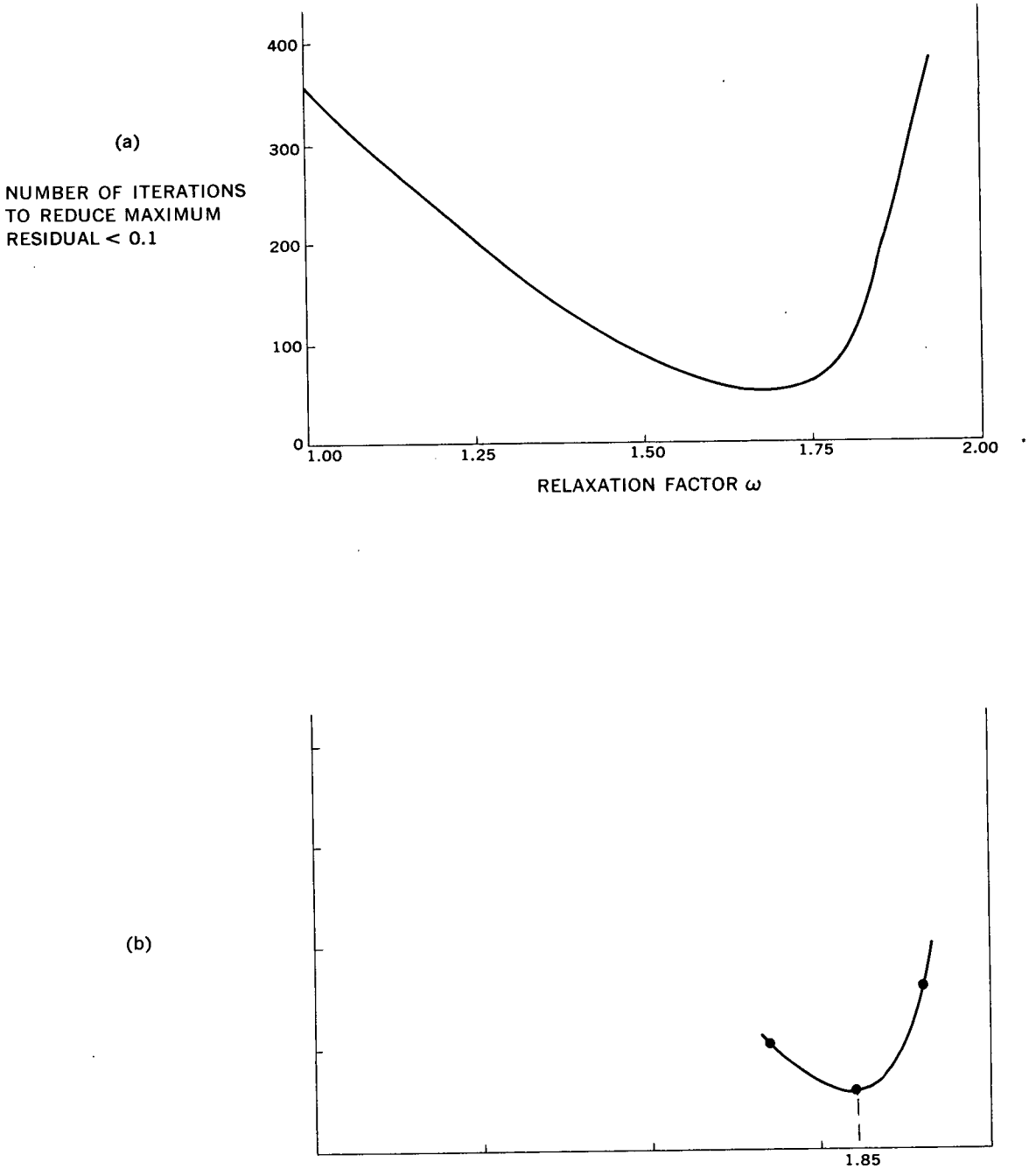

Figure 30. Number of iterations required for convergence as a function of the relaxation factor ω

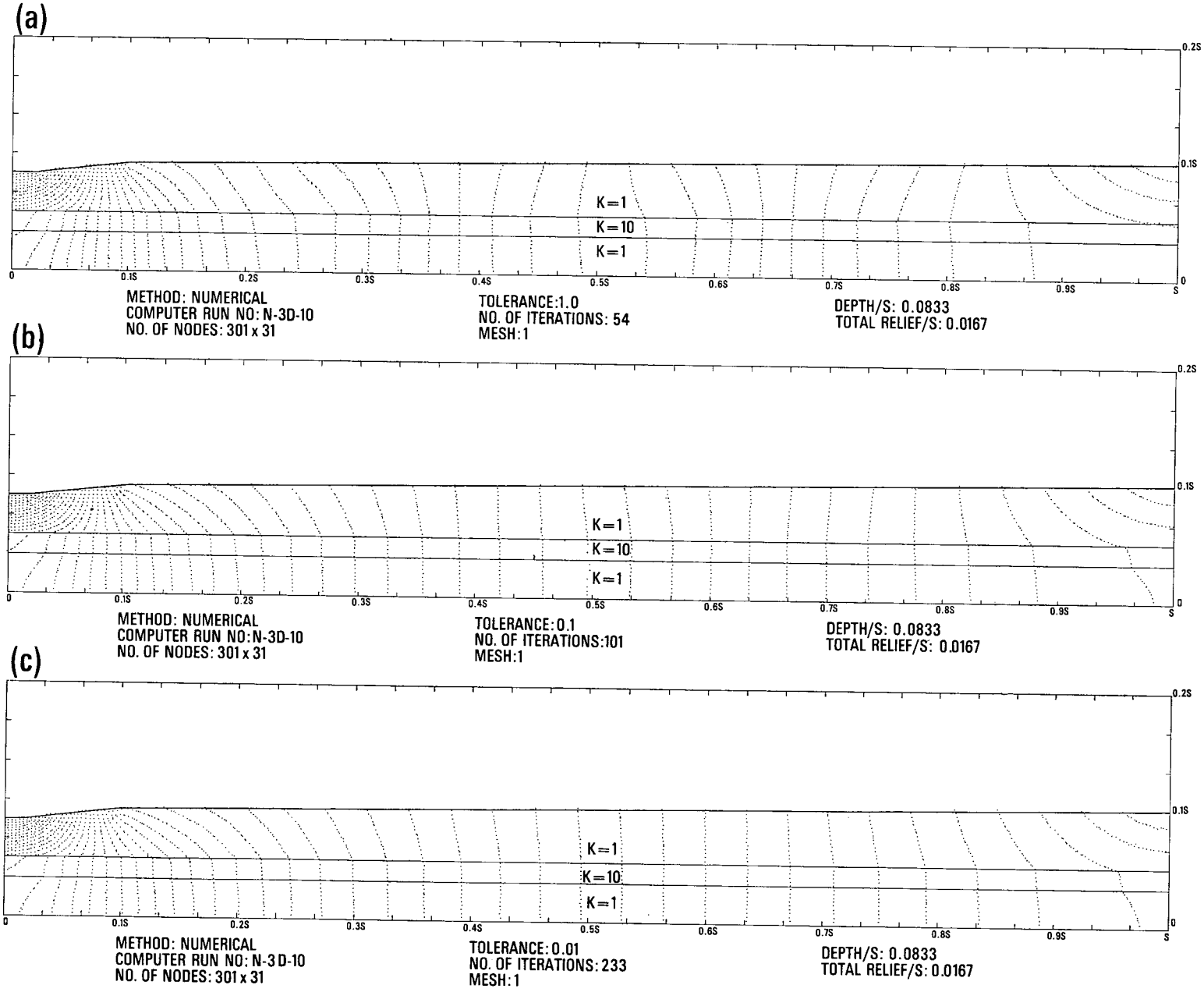

Figure 31. The effect of the tolerance on the convergence of the solution

List of Program Variables for Two-Dimensional Programs
(Numerical Programs 1 Through 5)

Parameter	Definition	Program				
		1	2	3	4	5
N	Number of x nodes	x	x	x	x	x
L	Number of z nodes	x	x	x	x	x
X(I)	x values of N nodes	x	x	x	x	x
Z(J)	z values of L nodes	x	x	x	x	x
DELX	Δx (= Δz in 1,2,3,4)	x	x	x	x	x
DELZ	Δz					x
ALPHA	DELX / DELZ					x
ALFA	$(ALPHA)^2$					x
XONE	X(1) = value of x at origin	x	x	x	x	x
ZONE	Z(1) = value of z at origin	x	x	x	x	x
MESH			x			
JA	Mesh configuration, see Figure 8		x			
JB			x			
JC			x			
JD			x			
S	s	x	x	x	x	x
ZZERO	z_0	x	x	x	x	x
PHI(I,J)	ϕ	x	x	x	x	x
DELPHI	$\Delta\phi$ – for contours	x	x	x	x	x
PHIMIM	Minimum value of ϕ	x	x	x	x	x
PHIMAX	Maximum value of ϕ	x	x	x	x	x
OMEGA	relaxation factor ω	x	x	x	x	x
TOL	tolerance (i.e. tolerable residue)	x	x	x	x	x
KART	maximum number of iterations	x	x	x	x	x
KAR	number of iteration	x	x	x	x	x
RES	residue after KAR^{th} iteration	x	x	x	x	x
JJ(I)	value of J at each value of I for which boundary values of PHIN(I) apply	x	x	x	x	x
PHIN(I)	boundary values of ψ along water-table	x	x	x	x	x
JRITE(I)	JJ(I) – JJ(I+1)	x	x	x	x	x
JLEFT(I)	JJ(I) – JJ(I–1)	x	x	x	x	x
MM	no. of vertical fields used in inserting GUEST(M) initial values	x	x	x	x	x
MMM	MM + 1	x	x	x	x	x
NP(M)	values of I, bounding vertical fields. Note: NP (1) = 1, NP(MMM) = N	x	x	x	x	x
GUEST(M)	initial values inserted in the MM vertical strips, converted to GUESS(I)	x	x	x	x	x
GUESS(I)	initial values for each column of nodes, from GUEST(M)	x	x	x	x	x

Parameter	Definition	Program				
		1	2	3	4	5
INPUT	= 0: 1 layer per vertical strip = 1: 2 layers per vertical strip			x	x	x
JI	value of J above which initial values given by GUESS(I), below which initial values given by GUESQ(I); used only when INPUT = 1			x	x	x
GUESR(M)	initial values inserted in the MM vertical strips above J = JI, converted to GUESQ(I)			x	x	x
GUESQ(I)	initial values for each column of nodes; from GUESR(M)			x	x	x
PERM(J)	permeability of J^{th} layer of nodes			x		
MP	number of horizontal strips used in inserting PERK(M)			x	x	x
LP(M)	values of J, bounding horizontal strips Note: LP(1) = 1, LP(MMP) = L			x	x	x
MMP	MP + 1			x	x	x
PERK(M)	values of permeability inserted in the MP strips, then converted to PERM(J)			x	x	
IMPERM	= 0: 1 zone per horizontal strip = 1: MA(J) zones per layer of nodes				x	x
MA(J)	MA zones in the J^{th} layer of nodes				x	x
MC(M)	values of I which bound the MA zones. Note: MC(1) = 1, MC(MA(J)) = N. There must be L sets of values of MC(M), one for each layer of nodes				x	x
PERM(I,J)	permeability of node (I,J)				x	
PERMH(I,J)	horizontal permeability of (I,J)					x
PERMV(I,J)	vertical permeability of (I,J)					x
PERKH(M) PERKV(M)	identical to PERK(M) but for anisotropic case					x x
IPLOT	= 1 = 2 = 3 } see Apendix I	x	x	x	x	
SX	= X(N)					x
SZ	= Z(L)					x
SXPL	Horizontal width of plot equals (SXPL – 1.75) inches					x
SZPL	Vertical height of plot equals (SZPL – 4.20) inches					x

Data Deck — Numerical Problem 1

Group	Card	Format	Data
A	1	2A6	any desired title
B	1	14I5	N, L, MM, IPLOT, KART
C	1	7F10.2	DELX, DELPHI, PHIMIN, PHIMAX, TOL, XONE, ZONE
	2	"	OMEGA, S, ZZERO
D	1	7F10.2	PHIN(I), I = 1,N; 7 values / card
	2	⋮	⋮
	3	⋮	⋮
	⋮		
E	1	24I3	JJ(I), I = 1,N; 24 values / card
	2	⋮	⋮
	3	⋮	⋮
	⋮		
F	1	14I5	NP(M), M = 1,MMM; 14 values / card
	2	7F10.2	GUEST(M), M = 1,MM; 7 values / card

Data Deck — Numerical Problem 2

Identical to Numerical Problem 1 except:

B	1	14I5	N, L, MM, MESH, JA, JB, JC, JD, IPLOT, KART

Note: 1. All layers of a given mesh spacing must be at least 2 nodal spacings high.

2. The water-table configuration must be approximated by nodes entirely within the uppermost subdivision.

Data Deck — Numerical Problem 3

Group	Card	Format	Data
A	1	2A6	any desired title
B	1	14I5	N, L, MM, MP, IPLOT, INPUT, JI, KART
C	1	7F10.2	DELX, DELPHI, PHIMIN, PHIMAX, TOL, XONE, ZONE
	2	"	OMEGA, S, ZZERO
D	1	7F10.2	PHIN(I), I = I,N; 7 values / card
	2	⋮	⋮
	3	⋮	⋮
	⋮		
E	1	24I3	JJ(I), I − 1,N; 24 values / card
	2	⋮	⋮
	3	⋮	⋮
	⋮		
F	1	14I5	NP(M), M = 1,MMM; 14 values / card
	2	7F10.2	GUEST(M), M = 1,MM; 7 values / card
	if INPUT = 1, add:		
	3	7F10.2	GUESR(M), M = 1,MM; 7 values / card
G	1	14I5	LP(M), M = 1,MMP; 14 values / card
	2	7F10.2	PERK(M), M = 1,MP; 7 values / card

Data Deck – Numerical Problem 4

Group	Card	Format	Data
A	1	2A6	any desired title
B	1	14I5	N, L, MM, MP, IPLOT, INPUT, JI, INPERM, KART
C	1	7F10.2	DELX, DELPHI, PHIMIN, PHIMAX, TOL, XONE, ZONE
	2	"	OMEGA, S, ZZERO
D	1	7F10.2	PHIN(I), I = 1,N; 7 values / card
	2	⋮	⋮
	3	⋮	⋮
	⋮		
E	1	24I3	JJ(I), I = 1,N; 24 values / card
	2	⋮	⋮
	3	⋮	⋮
	⋮		
F	1	14I5	NP(M), M = 1,MMM; 14 values / card
	2	7F10.2	GUEST(M), M = 1,MM; 7 values / card
	if INPUT = 1, add:		
	3	7F10.2	GUESR(M), M = 1,MM; 7 values / card
G	**if INPERM = 0, use:**		
	1	14I5	LP(M), M = 1,MMP; 14 values / card
	2	7F10.2	PERK(M), M = 1,MP; 7 values / card
	if IMPERM = 1, use:		
	1	14I5	MA(J), J = 1,L; 14 values / card
	(a) 2	14I5	MC(M), M = 1,MA(1)+1; 14 values / card
	(a) 3	7F10.2	PERK(M), M = 1,MA(1); 7 values / card
	(b) 4	14I5	} same as (a) but for J = 2
	(b) 5	7F10.2	
			etc. up to J = L

Data Deck – Numerical Problem 5

Identical to Numerical Problem 4 except:

Group	Card	Format	Data
B	1	14I5	N, L, MM, MP, INPUT, JI, INPERM, KART
C	1	7F10.2	DELX, DELZ, DELPHI, PHIMIN, PHIMAX, TOL, XONE
	2	"	ZONE, OMEGA, S, ZZERO, SXPL, SZPL, SX
	3	"	SZ
G	**if IMPERM = 0, Use:**		
	1	14I5	LP(M), M = 1,MMP; 14 values / card
	2	7F10.2	PERKH(M), M = 1,MP; 7 values / card
	3	"	PERKV(M), M = 1,MP; 7 values / card
	if INPERM = 1, Use:		
	1	14I5	MA(J), J = 1,L; 14 values / card
	(a) 2	14I5	MC(M), M = 1,MA(1) + 1; 14 values / card
	(a) 3	7F10.2	PERKH(M), M = 1,MA(1); 7 values / card
	(a) 4	7F10.2	PERKV(M), M = 1,MA(1); 7 values / card
	(b) 5	14I5	
	(b) 6	7F10.2	Same as (a) but for J = 2
	(b) 7	7F10.2	
			Etc. up to J = L

List of Program Variables for Numerical Program 6

1. The following parameters are identical with those of the two-dimensional programs:

N	ALPHA	KAR
L	ALFA	KART
X(I)	PHIMIN	SX
Z(J)	PHIMAX	SZ
DELX	OMEGA	
DELZ	TOL	
DELPHI	RES	

2. The following parameters are identical with those of the two-dimensional programs, except for an increase in dimension:

   PHI (I, K, J)
   JJ (I, K)
   PHIN (I,K)
   PERM (I,K,J)

3. All other parameters listed for two-dimensional problems are not used or are replaced in the three-dimensional program.

4. The following new parameters are introduced:

M	Number of y nodes
Y(K)	y values of M nodes
SY	Y(M)
SXPL	Horizontal width of plot equals (SXPL − 1.0) inches
SYPL	Horizontal width of plot equals (SYPL − 1.0) inches
SZPL	Vertical height of plot equals (SZPL − 1.0) inches
MAY	= 0, initial values are inserted by planes in y–z direction = 1, initial values are inserted by planes in x–z direction
GUESI(I)	initial values for each plane of nodes in y–z direction; used only when MAY = 0
GUESK(K)	initial values for each plane of nodes in x–z direction; used only when MAY = 1
IPLOT(I)	=0, plot =1, no plot for each value of I, i.e., for each y–z section through the 3D model.
KPLOT(K) JPLOT(J)	same as IPLOT(I) but for other two coordinate directions
IPERM(J)	= 1 − single permeability for entire J^{th} layer of nodes = 2 − each row of nodes in J^{th} layer given its own permeability. Rows taken in y-direction = 3 − as 2 but rows taken in x-direction = 4 − each y-direction row may be broken up into MA(I) segments and MA(I) permeabilities entered. = 5 − each x-direction row may be broken up into NA(K) segments and NA(K) permeabilities entered.

PERL1	the single permeability for IPERM(J) = 1
PERL2(I)	the row permeabilities for IPERM(J) = 2
PERL3(K)	the row permeabilities for IPERM(J) = 3
MA(I)	no. of segments in each y-direction row for IPERM(J) = 4
MB(MK)	values of K bounding each segment. Note: MB(1) = 1, MB(MA(I)+1) = M
PERL4(ME)	permeabilities entered in segments for IPERM(J) = 4
NA(K)	no. of segments in each x-direction row for IPERM(J) = 5
NB(NK)	values of I bounding each segment. Note: NB(1) = 1, NB(NA(K) + 1) = N
PERL5(NE)	permeabilities entered in segments for IPERM(J) = 5

Data Deck – Numerical Problem 6

Group	Card	Format	Data
A	1	2A6	any title desired
B	1	14I5	N, M, L, MAY, KART
C	1	7F10.2	DELX, DELZ, TOL, OMEGA, SX, SY, SZ
	2	"	ALPHA, PHIMIN, PHIMAX, SXPL, SYPL, SZPL, DELPHI
D	1	7F10.2	PHIN(I,K), I = 1,N; K = 1,M, 7 values / card
	2	⋮	i.e. K = 1; I = 1,N
	3	⋮	K = 2; I = 1,N
	⋮	⋮	etc.
E	1	24I3	KPLOT(K), K = 1,M; 24 values / card
	2	"	IPLOT(I), I = 1,N; 24 values / card
	3	"	JPLOT(J), J = 1,L; 24 values / card
F	1	24I3	JJ(I,K) I = 1,N; K = 1,M; 24 values / card
	2	⋮	i.e. K = 1; I = 1,N
	3	⋮	K = 2; I = 1,N
	⋮	⋮	etc.
G	1	24I3	IPERM(J), J = 1,L; 24 values / card
H		**if MAY = 0, use:**	
	1	7F10.2	GUESI(I), I = 1,N; 7 values / card
	2	⋮	⋮
	⋮		
		if MAY = 1, use:	
	1	7F10.2	GUESK(K), K = 1,M; 7 values / card
	2	⋮	⋮
	⋮		
I		**if IPERM(J) = 1, use:**	
	1	7F10.2	PERL1
		if IPERM(J) = 2, use:	
	1	7F10.2	PERL2(I), I = 1,N; 7 values / card
	2	⋮	⋮
	⋮		

			if IPERM(J) = 3, use:	
		1	7F10.2	PERL3(K), K = 1,M; 7 values / card
		2	:	:
		:		
			if IPERM(J) = 4, use:	
(a)		1	14I5	MA(I), I = 1,N; 14 values / card
		2	:	:
(b)	(A)	1	14I5	MB(MK), MK = 1,MA(1)+1; 14 values / card
		2	7F10.2	PERL4(ME), ME = 1,MA(1); 7 values / card
	(B)	3	14I5	same as (A) but for I = 2
		4	7F10.2	etc. up to I = N
		:	:	
			if IPERM(J) = 5, use:	
(a)		1	14I5	NA(K), K = 1,M; 14 values / card
		2	:	:
(b)	(A)	1	14I5	NB(NK), NK = 1,NA(1)+1; 14 values / card
		2	7F10.2	PERL5(NE), NE = 1,NA(1); 7 values / card
	(B)	3	14I5	same as (A) but for K = 2
		4	7F10.2	etc. up to K = M

REPEAT GROUP I FOR EACH VALUE OF J

Note: For those columns of nodes in an (I,K) position which are outside the physical extent of the model (Figure 16) use the following values:

JJ (I, K) = 1
PHIN(I,K) = 0.0

These nodes will then be ignored in the iterative procedure and the vertical impermeable boundaries will be simulated in the correct position.

Recommended Values of Certain Computing Parameters

XONE = 0.0

ZONE = 0.0

DELPHI = 1/10 to 1/20 of (PHIMAX – PHIMIN)

TOL = 0.001 (or less if permeability ratio exceeds 1:1000)

KART = 3000

OMEGA = 1.85 for Numerical Programs 1, 3, 4, 5, 6
= 1.00 for Numerical Program 2 (Pending further investigation)

PHI(I,J) must always be > 0.0

```
C NUMERICAL PROGRAM 1
      COMMON X(301),Z(41),PHI(301,41),PHIN(301),JJ(301),GUESS(301),
     1NP(10),GUEST(10),JRITE(301),JLEFT(301),N,L,MM,IPLOT,DELX,DELPHI,
     2PHIMIN,PHIMAX,TOL,XONE,ZONE,OMEGA,S,ZZERO,RES
 1001 READ 13,TITLE1,TITLE2
      IF (TITLE1) 1000,90,100
 1000 READ 10, N,L,MM,IPLOT,KART
      READ 11, DELX,DELPHI,PHIMIN,PHIMAX,TOL,XONE,ZONE,OMEGA,S,ZZERO
      READ 11, (PHIN(I),I=1,N)
      READ 12, (JJ(I),I=1,N)
      MMM=MM+1
      READ 10, (NP(M),M=1,MMM)
      READ 11,(GUEST(M),M=1,MM)
   10 FORMAT (14I5)
   11 FORMAT (7F10.2)
   12 FORMAT (24I3)
   13 FORMAT (2A6)
      DO 305 M=1,MM
      NPR=NP(M)
      NPQ=NP(M+1)
      DO 306 I=NPR,NPQ
  306 GUESS(I)=GUEST(M)
  305 CONTINUE
C
      ZZERA=FLOAT(JJ(1)-1)*DELX
      SA=FLOAT(N-1)*DELX
      IF (ZZERA-ZZERO) 38,140,38
  140 IF (SA-S) 38,130,38
   38 PRINT 39
   39 FORMAT (1H1,18H     CHECK GEOMETRY)
      GO TO 1001
  130 DO 60 I=1,N
      IF (I-1) 62,62,64
   62 X(1)=XONE
      GO TO 60
   64 X(I)=X(I-1)+DELX
   60 CONTINUE
      DO 70 J=1,L
      IF (J-1) 72,72,74
   72 Z(1)=ZONE
      GO TO 70
   74 Z(J)=Z(J-1)+DELX
   70 CONTINUE
C
      DO 1050 I=1,N
      JRITE(I)=JJ(I)-JJ(I+1)
      JLEFT(I)=JJ(I)-JJ(I-1)
      DO 1050 J=1,L
      IF (J-JJ(I)) 1051,1049,1048
 1048 PHI(I,J)=0.0
      GO TO 1050
 1049 PHI(I,J)=PHIN(I)
      GO TO 1050
 1051 PHI(I,J)=GUESS(I)
 1050 CONTINUE
C
      DO 105 KAR=1,KART
      RES=0.0
      DO 701 K=1,L
```

```
      J=L+1-K
      DO 701 I=1,N
      IF (I-1) 41,41,42
   41 IF (J-1) 32,32,43
   43 IF(J-JJ(I)) 44,25,26
   44 IF (JRITE(I)-1) 28,28,180
   42 IF (I-N) 46,47,47
   46 IF (J-1) 34,34,48
   48 IF (J-JJ(I)) 49,25,26
   49 IF (JLEFT(I)-1) 50,50,181
   50 IF (JRITE(I)-1) 3,3,182
   47 IF (J-1) 33,33,51
   51 IF (J-JJ(I)) 52,25,26
   52 IF (JLEFT(I)-1) 24,24,183
  180 IF (J-JJ(I+1)) 28,28,29
  183 IF (J-JJ(I-1)) 24,24,29
  182 IF (J-JJ(I+1)) 3,3,193
  181 IF (JRITE(I)-1) 185,185,186
  185 IF (J-JJ(I-1)) 3,3,192
  186 IF (JJ(I-1)-JJ(I+1)) 188,187,190
  187 IF (J-JJ(I-1)) 3,3,29
  188 IF (J-JJ(I-1)) 3,3,189
  189 IF (J-JJ(I+1)) 192,192,29
  190 IF (J-JJ(I+1)) 3,3,191
  191 IF (J-JJ(I-1)) 193,193,29
  193 JJA=JJ(I)-JJ(I+1)
      JJB=JJ(I)-J
      DELTA=DELX*FLOAT(JJB/JJA)
      PHIT=PHIN(I)-FLOAT(JJB/JJA)*(PHIN(I)-PHIN(I+1))
      GO TO 31
  192 JJC=JJ(I)-JJ(I-1)
      JJD=JJ(I)-J
      DELTA=DELX*FLOAT(JJD/JJC)
      PHIT=PHIN(I)-FLOAT(JJD/JJC)*(PHIN(I)-PHIN(I-1))
      GO TO 30
    3 DDF=(PHI(I+1,J)+PHI(I-1,J)+PHI(I,J+1)+PHI(I,J-1))/4.0
      GO TO 702
   24 DDF=(PHI(I,J+1)+PHI(I,J-1)+2.0*PHI(I-1,J))/4.0
      GO TO 702
   25 DDF=PHIN(I)
      GO TO 702
   26 DDF=0.0
      GO TO 702
   28 DDF=(PHI(I,J+1)+PHI(I,J-1)+2.0*PHI(I+1,J))/4.0
      GO TO 702
   29 DDF=(PHI(I,J+1)+PHI(I,J-1))/2.0
      GO TO 702
   30 DDF=(DELX*(DELX*PHIT+DELTA*PHI(I+1,J)))/(DELX+DELTA)**2+(DELTA*
     1(PHI(I,J+1)+PHI(I,J-1)))/(2.0*(DELX+DELTA))
      GO TO 702
   31 DDF=(DELX*(DELX*PHIT+DELTA*PHI(I-1,J)))/(DELX+DELTA)**2+(DELTA*
     1(PHI(I,J+1)+PHI(I,J-1)))/(2.0*(DELX+DELTA))
      GO TO 702
   32 DDF=(PHI(I,J+1)+PHI(I+1,J))/2.0
      GO TO 702
   33 DDF=(PHI(I,J+1)+PHI(I-1,J))/2.0
      GO TO 702
   34 DDF=(PHI(I+1,J)+PHI(I-1,J)+2.0*PHI(I,J+1))/4.0
  702 GAF=ABS(DDF-PHI(I,J))
      IF (GAF-RES) 701,701,703
```

```
  703 RES=GAF
  701 PHI(I,J)=OMEGA*DDF+(1.0-OMEGA)*PHI(I,J)
      IF (RES-TOL) 120,105,105
  105 CONTINUE
C
  120 PRINT 200,KAR,RES
  200 FORMAT (1H1,I10,F10.5)
C
      PRINT 300,TITLE1,TITLE2
  300 FORMAT (1H1,24H1      NUMERICAL PROBLEM 2A6//12X,4HX(I)//)
      PRINT 600, (X(I),I=1,N)
      PRINT 500
  500 FORMAT (1H1,12X,4HZ(J)//)
      PRINT 600,(Z(J),J=1,L)
  600 FORMAT (10F12.4)
      PRINT 700
  700 FORMAT (1H1,10X,8HPHI(I,J)//)
      DO 800 I=1,N
      PRINT 720,I
  720 FORMAT (1H0,12X,2HI=,I3//)
  800 PRINT 820, (PHI(I,J),J=1,L)
  820 FORMAT (10F12.4)
      CALL CONONE
      CALL CCNEXT
      GO TO 1001
   90 CALL CCEND
      STOP
      END
C
C
C
      SUBROUTINE CONONE
      COMMON X(301),Z(41),PHI(301,41),PHIN(301),JJ(301),GUESS(301),
     1NP(10),GUEST(10),JRITE(301),JLEFT(301),N,L,MM,IPLOT,DELX,DELPHI,
     2PHIMIN,PHIMAX,TOL,XONE,ZONE,OMEGA,S,ZZERO,RES
      DIMENSION T(4,3),XX(2),ZZ(2)
      COMMON /CCPOOL/ XMIN,XMAX,YMIN,YMAX,CCXMIN,CCXMAX,CCYMIN,CCYMAX
      IF (IPLOT-2) 40,41,42
   40 XMIN=-1875.0
      XMAX=23125.0
      YMIN=-4250.0
      YMAX=12250.0
      CCXMIN=100.0
      CCXMAX=1100.0
      CCYMIN=250.0
      CCYMAX=910.0
      CALL CCBGN
      CALL CCGRID (6HNOLBLS)
      XMIN=0.0
      XMAX=20000.0
      YMIN=-0.001
      YMAX=12000.0
      CCXMIN=175.0
      CCXMAX=975.0
      CCYMIN=420.0
      CCYMAX=900.0
      CALL CCBGN
      CALL CCGRID (1,10,6HNOLBLS,1,6)
      WRITE (98,20)
```

```
20 FORMAT (116H0         0.1S          .2S         0.3S         0.4S
  1  0.5S        0.6S         0.7S          .8S          0.9S          S)
   CALL CCALTR (175.0,405.0,0,1)
   CALL CCALTR ( 980.0,420.0,0,1,1H0)
   CALL CCALTR (980.0,500.0,0,1,4H0.1S)
   CALL CCALTR (980.0,580.0,0,1,4H0.2S)
   CALL CCALTR (980.0,660.0,0,1,4H0.3S)
   CALL CCALTR (980.0,740.0,0,1,4H0.4S)
   CALL CCALTR (980.0,820.0,0,1,4H0.5S)
   CALL CCALTR (980.0,900.0,0,1,4H0.6S)
   GO TO 43
41 XMIN=-1875.0
   XMAX=43125.0
   YMIN=-4250.0
   YMAX=12250.0
   CCXMIN=100.0
   CCXMAX=2100.0
   CCYMIN=250.0
   CCYMAX=910.0
   CALL CCBGN
   CALL CCGRID (6HNOLBLS)
   XMIN=0.0
   XMAX=40000.0
   YMIN=-0.001
   YMAX=12000.0
   CCXMIN=175.0
   CCXMAX=1775.0
   CCYMIN=420.0
   CCYMAX=900.0
   CALL CCBGN
   CALL CCGRID (1,20,6HNOLBLS,1,6)
   WRITE (98,21)
21 FORMAT (117H0                          .1S                          0.2S
  1             0.3S                           .4S                           0.5S)
   CALL CCALTR (175.0,405.0,0,1)
   WRITE (98,23)
23 FORMAT (113H                     0.6S                          0.7S
  1          0.8S                          .9S                               S)
   CALL CCALTR (989.0,405.0,0,1)
   CALL CCALTR (1780.0,420.0,0,1,1H0)
   CALL CCALTR (1780.0,580.0,0,1,4H0.1S)
   CALL CCALTR (1780.0,740.0,0,1,4H0.2S)
   CALL CCALTR (1780.0,900.0,0,1,4H0.3S)
   GO TO 43
42 XMIN=-1875.0
   XMAX=63125.0
   YMIN=-4250.0
   YMAX=12250.0
   CCXMIN=100.0
   CCXMAX=3100.0
   CCYMIN=250.0
   CCYMAX=910.0
   CALL CCBGN
   CALL CCGRID (6HNOLBLS)
   XMIN=0.0
   XMAX=60000.0
   YMIN=-0.001
   YMAX=12000.0
   CCXMIN=175.0
   CCXMAX=2575.0
```

```
      CCYMIN=420.0
      CCYMAX=900.0
      CALL CCBGN
      CALL CCGRID (1,30,6HNOLBLS,1,6)
      WRITE (98,22)
   22 FORMAT (115H0                                        0.1S
     1              .2S                                        0.3S          )
      CALL CCALTR (175.0,405.0,0,1)
      WRITE (98,24)
   24 FORMAT (114H                        0.4S
     1 0.5S                                      .6S                         )
      CALL CCALTR (980.0,405.0,0,1)
      WRITE (98,25)
   25 FORMAT (114H         0.7S                                          0.8S
     1                       0.9S                                            S)
      CALL CCALTR (1778.0,405.0,0,1)
      CALL CCALTR (2580.0,420.0,0,1,1H0)
      CALL CCALTR (2580.0,660.0,0,1,4H0.1S)
      CALL CCALTR (2580.0,900.0,0,1,4H0.2S)
   43 LL=L-1
      NN=N-1
      DO 1 J=1,LL
      DO 2 I=1,NN
      PHILOW=AMIN1(PHI(I,J),PHI(I+1,J),PHI(I+1,J+1),PHI(I,J+1))
      PHIHI =AMAX1(PHI(I,J),PHI(I+1,J),PHI(I+1,J+1),PHI(I,J+1))
      IF (PHIHI-PHILOW) 2,2,51
   51 IF (PHILOW-PHIMAX) 53,53,2
   53 IF (PHIHI-PHIMIN) 2,5,5
    5 IF (PHILOW-PHIMIN) 56,54,55
   56 IF (PHILOW-10.0) 101,101,54
  101 TA=PHI(I,J)
      TB=PHI(I+1,J)
      TC =PHI(I+1,J+1)
      TD=PHI(I,J+1)
      IF (TA-10.0) 102,102,103
  102 IF (TB-10.0) 2,2,105
  105 IF (TC-10.0) 2,2,106
  106 PHILOW=AMIN1(TB,TC)
      GO TO 55
  103 IF (TB-10.0) 107,107,108
  107 IF(TD-10.0) 2,2,109
  109 PHILOW=AMIN1(TA,TD)
      GO TO 55
  108 IF (TC-TD) 110,112,111
  110 IF (TD-10.0) 112,112,113
  113 PHILOW=AMIN1(TA,TB,TD)
      GO TO 55
  111 IF (TC-10.0) 112,112,114
  114 PHILOW=AMIN1(TA,TB,TC)
      GO TO 55
  112 PHILOW=AMIN1(TA,TB)
      GO TO 55
   54 AA=PHIMIN
      GO TO 3
   55 AA= FLOAT(IFIX((PHILOW-PHIMIN)/DELPHI)+1)*DELPHI+PHIMIN
    3 IFLAG=0
      T(1,1)=PHI(I,J)
      T(2,1)=PHI(I+1,J)
      T(3,1)=PHI(I+1,J+1)
```

```
      T(4,1)=PHI(I,J+1)
      T(1,2)=X(I)
      T(2,2)=T(1,2)+DELX
      T(3,2)=T(2,2)
      T(4,2)=T(1,2)
      T(1,3)=Z(J)
      T(2,3)=T(1,3)
      T(3,3)=T(1,3)+DELX
      T(4,3)=T(3,3)
    4 K=0
  613 IF (T(1,1)-10.0) 11,11,600
  600 IF (T(2,1)-10.0) 11,11,6
    6 IF(T(1,1)-T(2,1)) 7,11,7
    7 F=(AA-T(1,1))/(T(2,1)-T(1,1))
      IF (F-1.0) 71,71,11
   71 IF(F) 11,11,8
    8 IDIOT=1+IFLAG
      XX(IDIOT)=(1.0-F)*T(1,2)+F*T(2,2)
      ZZ(IDIOT)=(1.0-F)*T(1,3)+F*T(2,3)
   85 IF(IFLAG) 10,10,9
    9 CALL CCPLOT (XX,ZZ,2,6HNOJOIN,1,1)
      XX(1)=XX(2)
      ZZ(1)=ZZ(2)
      GO TO 11
   10 IFLAG=1
   11 K=K+1
      IF(K-4) 13,12,12
   13 TT1=T(1,1)
      TT2=T(1,2)
      TT3=T(1,3)
      DO 131 NA=1,3
      DO 131 NB=1,3
  131 T(NB,NA)=T(NB+1,NA)
      T(4,1)=TT1
      T(4,2)=TT2
      T(4,3)=TT3
      GO TO 613
   12 AA=AA+DELPHI
   14 IF(AA-PHIHI) 15,15,2
   15 IF (AA-PHIMAX) 3,3,2
    2 CONTINUE
    1 CONTINUE
      RETURN
      END
```

```
C NUMERICAL PROGRAM 2
      COMMON X(301),Z(41),PHI(301,41),PHIN(301),JJ(301),GUESS(301),
     1NP(10),GUEST(10),JRITE(301),JLEFT(301),N,L,MM,MESH,JA,JB,JC,JD,
     2IPLOT,DELX,DELPHI,PHIMIN,PHIMAX,TOL,XONE,ZONE,OMEGA,S,ZZERO,RES,
     3NA,NB,KAR,J
 7000 READ 7001,TITLE1,TITLE2
 7001 FORMAT (2A6)
      IF (TITLE1) 7300,1000,7300
 7300 READ 300,N,L,MM,MESH,JA,JB,JC,JD,IPLOT,KART
      READ 301,DELX,DELPHI,PHIMIN,PHIMAX,TOL,XONE,ZONE,OMEGA,S,ZZERO
      READ 301, (PHIN(I),I=1,N)
      READ 302,(JJ(I),I=1,N)
      MMM=MM+1
      READ 300,(NP(M),M=1,MMM)
      READ 301,(GUEST(M),M=1,MM)
  300 FORMAT (14I5)
  301 FORMAT (7F10.2)
  302 FORMAT (24I3)
      DO 305 M=1,MM
      NPR=NP(M)
      NPQ=NP(M+1)
      DO 306 I=NPR,NPQ
  306 GUESS(I)=GUEST(M)
  305 CONTINUE
C
      DO 330 I=1,N
      IF (I-1) 331,331,332
  331 X(1)=XONE
      GO TO 330
  332 X(I)=X(I-1)+DELX
  330 CONTINUE
C
      DO 340 J=1,L
      IF (J-1) 341,341,362
  341 Z(1)=ZONE
      GO TO 340
  362 IF (JC-L) 363,350,350
  363 IF(JD-L) 342,343,343
  342 IF (J-JA) 344,344,345
  345 IF (J-JB) 346,346,347
  347 IF (J-JC) 344,344,349
  349 IF (J-JD) 346,346,350
  343 IF (J-JA) 346,346,352
  352 IF (J-JB) 350,350,353
  353 IF (J-JC) 346,346,350
  344 Z(J)=Z(J-1)+4.0*DELX
      GO TO 340
  346 Z(J)=Z(J-1)+2.0*DELX
      GO TO 340
  350 Z(J)=Z(J-1)+DELX
  340 CONTINUE
C
      ZI=FLOAT(JJ(1)-JC)*DELX
      ZJ=FLOAT(JJ(1)-JD)*DELX
      ZK=FLOAT(JD-JC)*2.0*DELX
      ZL=FLOAT(JC-JB)*4.0*DELX
      ZM=FLOAT(JB-JA)*2.0*DELX
      ZN=FLOAT(JA-1)*4.0*DELX
      ZO=FLOAT(JC-JB)*2.0*DELX
      ZP=FLOAT(JB-JA)*DELX
```

```
      ZQ=FLOAT(JA-1)*2.0*DELX
      ZR=FLOAT(JJ(1)-JB)*DELX
      IF (JC-L) 370,371,371
  371 ZZERA=ZR
      GO TO 375
  370 IF (JD-L) 372,373,373
  373 ZZERA=ZQ+ZP+ZO+ZI
      GO TO 375
  372 ZZERA=ZJ+ZK+ZL+ZM+ZN
  375 IF (ZZERA-ZZERO) 376,377,376
  377 SA=FLOAT(N-1)*DELX
      IF (SA-S) 376,320,376
  376 PRINT 378
  378 FORMAT (1H1,18H     CHECK GEOMETRY)
      GO TO 7000
C
  320 DO 328 I=1,N
      JRITE(I)=JJ(I)-JJ(I+1)
      JLEFT(I)=JJ(I)-JJ(I-1)
      DO 328 J=1,L
      IF (J-JJ(I)) 325,326,327
  327 PHI(I,J)=0.0
      GO TO 328
  326 PHI(I,J)=PHIN(I)
      GO TO 328
  325 PHI(I,J)=GUESS(I)
  328 CONTINUE
C
      DO 206 KAR=1,KART
      RES=0.0
      GO TO (40,60,80,100,120,140,160),MESH
   40 CALL MESH1
      GO TO 205
   60 CALL MESH2
      GO TO 205
   80 CALL MESH3
      GO TO 205
  100 CALL MESH4
      GO TO 205
  120 CALL MESH5
      GO TO 205
  140 CALL MESH6
      GO TO 205
  160 CALL MESH7
  205 IF (RES-TOL) 400,206,206
  206 CONTINUE
C
  400 PRINT 401,KAR,RES
  401 FORMAT (1H1,I10,F10.5)
C
      PRINT 403,TITLE1,TITLE2
  403 FORMAT (1H1,24H1     NUMERICAL PROBLEM 2A6//12X,4HX(I)//)
      PRINT 404,(X(I),I=1,N)
      PRINT 405
  405 FORMAT (1H1,12X,4HZ(J)//)
      PRINT 404,(Z(J),J=1,L)
  404 FORMAT (10F12.4)
      PRINT 415
  415 FORMAT (1H1,10X,8HPHI(I,J)//)
```

```
      DO 406 I=1,N
      PRINT 407,I
  407 FORMAT (1H0,12X,2HI=,I3//)
  406 PRINT 408, (PHI(I,J),J=1,L)
  408 FORMAT (10F12.4)
  414 CALL CONTWO
      CALL CCNEXT
      GO TO 7000
 1000 CALL CCEND
      STOP
      END
C
C
C
      SUBROUTINE MESH1
      COMMON X(301),Z(41),PHI(301,41),PHIN(301),JJ(301),GUESS(301),
     1NP(10),GUEST(10),JRITE(301),JLEFT(301),N,L,MM,MESH,JA,JB,JC,JD,
     2IPLOT,DELX,DELPHI,PHIMIN,PHIMAX,TOL,XONE,ZONE,OMEGA,S,ZZERO,RES,
     3NA,NB,KAR,J
      DO 701 K=1,L
      J=L+1-K
      DO 701 I=1,N
      IF (I-1) 41,41,42
   41 IF (J-1) 32,32,43
   43 IF(J-JJ(I)) 44,25,26
   44 IF (JRITE(I)-1) 28,28,180
   42 IF (I-N) 46,47,47
   46 IF (J-1) 34,34,48
   48 IF (J-JJ(I)) 49,25,26
   49 IF (JLEFT(I)-1) 50,50,181
   50 IF (JRITE(I)-1) 3,3,182
   47 IF (J-1) 33,33,51
   51 IF (J-JJ(I)) 52,25,26
   52 IF (JLEFT(I)-1) 24,24,183
  180 IF (J-JJ(I+1)) 28,28,29
  183 IF (J-JJ(I-1)) 24,24,29
  182 IF (J-JJ(I+1)) 3,3,193
  181 IF (JRITE(I)-1) 185,185,186
  185 IF (J-JJ(I-1)) 3,3,192
  186 IF (JJ(I-1)-JJ(I+1)) 188,187,190
  187 IF (J-JJ(I-1)) 3,3,29
  188 IF (J-JJ(I-1)) 3,3,189
  189 IF (J-JJ(I+1)) 192,192,29
  190 IF (J-JJ(I+1)) 3,3,191
  191 IF (J-JJ(I-1)) 193,193,29
  193 JJA=JJ(I)-JJ(I+1)
      JJB=JJ(I)-J
      DELTA=DELX*FLOAT(JJB/JJA)
      PHIT=PHIN(I)-FLOAT(JJB/JJA)*(PHIN(I)-PHIN(I+1))
      GO TO 31
  192 JJC=JJ(I)-JJ(I-1)
      JJD=JJ(I)-J
      DELTA=DELX*FLOAT(JJD/JJC)
      PHIT=PHIN(I)-FLOAT(JJD/JJC)*(PHIN(I)-PHIN(I-1))
      GO TO 30
    3 DDF=(PHI(I+1,J)+PHI(I-1,J)+PHI(I,J+1)+PHI(I,J-1))/4.0
      GO TO 702
   24 DDF=(PHI(I,J+1)+PHI(I,J-1)+2.0*PHI(I-1,J))/4.0
      GO TO 702
   25 DDF=PHIN(I)
```

```
      GO TO 702
   26 DDF=0.0
      GO TO 702
   28 DDF=(PHI(I,J+1)+PHI(I,J-1)+2.0*PHI(I+1,J))/4.0
      GO TO 702
   29 DDF=(PHI(I,J+1)+PHI(I,J-1))/2.0
      GO TO 702
   30 DDF=(DELX*(DELX*PHIT+DELTA*PHI(I+1,J)))/(DELX+DELTA)**2+(DELTA*
     1(PHI(I,J+1)+PHI(I,J-1)))/(2.0*(DELX+DELTA))
      GO TO 702
   31 DDF=(DELX*(DELX*PHIT+DELTA*PHI(I-1,J)))/(DELX+DELTA)**2+(DELTA*
     1(PHI(I,J+1)+PHI(I,J-1)))/(2.0*(DELX+DELTA))
      GO TO 702
   32 DDF=(PHI(I,J+1)+PHI(I+1,J))/2.0
      GO TO 702
   33 DDF=(PHI(I,J+1)+PHI(I-1,J))/2.0
      GO TO 702
   34 DDF=(PHI(I+1,J)+PHI(I-1,J)+2.0*PHI(I,J+1))/4.0
  702 GAF=ABS(DDF-PHI(I,J))
      IF (GAF-RES) 701,701,703
  703 RES=GAF
  701 PHI(I,J)=OMEGA*DDF+(1.0-OMEGA)*PHI(I,J)
      RETURN
      END
C
C
C
      SUBROUTINE MESH2
      COMMON X(301),Z(41),PHI(301,41),PHIN(301),JJ(301),GUESS(301),
     1NP(10),GUEST(10),JRITE(301),JLEFT(301),N,L,MM,MESH,JA,JB,JC,JD,
     2IPLOT,DELX,DELPHI,PHIMIN,PHIMAX,TOL,XONE,ZONE,OMEGA,S,ZZERO,RES,
     3NA,NB,KAR,J
      DO 704 K=1,L
      J=L+1-K
      NA=N-1
      IF (J-JC) 61,63,75
   61 CALL AAA
      GO TO 704
   63 CALL BBB
      GO TO 704
   75 CALL CCC
  704 CONTINUE
      RETURN
      END
C
C
C
      SUBROUTINE MESH3
      COMMON X(301),Z(41),PHI(301,41),PHIN(301),JJ(301),GUESS(301),
     1NP(10),GUEST(10),JRITE(301),JLEFT(301),N,L,MM,MESH,JA,JB,JC,JD,
     2IPLOT,DELX,DELPHI,PHIMIN,PHIMAX,TOL,XONE,ZONE,OMEGA,S,ZZERO,RES,
     3NA,NB,KAR,J
      DO 710 K=1,L
      J=L+1-K
      NA=N-1
      NB=N-2
      IF (J-JC) 81,83,82
   82 IF (J-JD) 84,85,96
   81 CALL DDD
```

```
      GO TO 710
   83 CALL EEE
      GO TO 710
   84 CALL FFF
      GO TO 710
   85 CALL GGG
      GO TO 710
   96 CALL CCC
  710 CONTINUE
      RETURN
      END
C
C
C
      SUBROUTINE MESH4
      COMMON X(301),Z(41),PHI(301,41),PHIN(301),JJ(301),GUESS(301),
     1NP(10),GUEST(10),JRITE(301),JLEFT(301),N,L,MM,MESH,JA,JB,JC,JD,
     2IPLOT,DELX,DELPHI,PHIMIN,PHIMAX,TOL,XONE,ZONE,OMEGA,S,ZZERO,RES,
     3NA,NB,KAR,J
      DO 720 K=1,L
      J=L+1-K
      NA=N-1
      IF (J-JB) 101,102,733
  733 IF (J-JC) 734,735,736
  101 CALL HHH
      GO TO 720
  102 CALL PPP
      GO TO 720
  734 CALL AAA
      GO TO 720
  735 CALL BBB
      GO TO 720
  736 CALL CCC
  720 CONTINUE
      RETURN
      END
C
C
C
      SUBROUTINE MESH5
      COMMON X(301),Z(41),PHI(301,41),PHIN(301),JJ(301),GUESS(301),
     1NP(10),GUEST(10),JRITE(301),JLEFT(301),N,L,MM,MESH,JA,JB,JC,JD,
     2IPLOT,DELX,DELPHI,PHIMIN,PHIMAX,TOL,XONE,ZONE,OMEGA,S,ZZERO,RES,
     3NA,NB,KAR,J
      DO 750 K=1,L
      J=L+1-K
      NA=N-1
      NB=N-2
      IF (J-JB) 121,122,752
  752 IF (J-JC) 753,754,755
  755 IF (J-JD) 756,757,778
  121 CALL AAA
      GO TO 750
  122 CALL RRR
      GO TO 750
  753 CALL DDD
      GO TO 750
  754 CALL EEE
      GO TO 750
  756 CALL FFF
```

```
      GO TO 750
  757 CALL GGG
      GO TO 750
  778 CALL CCC
  750 CONTINUE
      RETURN
      END
C
C
C
      SUBROUTINE MESH6
      COMMON X(301),Z(41),PHI(301,41),PHIN(301),JJ(301),GUESS(301),
     1NP(10),GUEST(10),JRITE(301),JLEFT(301),N,L,MM,MESH,JA,JB,JC,JD,
     2IPLOT,DELX,DELPHI,PHIMIN,PHIMAX,TOL,XONE,ZONE,OMEGA,S,ZZERO,RES,
     3NA,NB,KAR,J
      DO 782 K=1,L
      J=L+1-K
      NA=N-1
      IF (J-JA) 783,784,785
  785 IF (J-JB) 786,787,788
  788 IF (J-JC) 789,790,791
  783 CALL AAA
      GO TO 782
  784 CALL BBB
      GO TO 782
  786 CALL HHH
      GO TO 782
  787 CALL PPP
      GO TO 782
  789 CALL AAA
      GO TO 782
  790 CALL BBB
      GO TO 782
  791 CALL CCC
  782 CONTINUE
      RETURN
      END
C
C
C
      SUBROUTINE MESH7
      COMMON X(301),Z(41),PHI(301,41),PHIN(301),JJ(301),GUESS(301),
     1NP(10),GUEST(10),JRITE(301),JLEFT(301),N,L,MM,MESH,JA,JB,JC,JD,
     2IPLOT,DELX,DELPHI,PHIMIN,PHIMAX,TOL,XONE,ZONE,OMEGA,S,ZZERO,RES,
     3NA,NB,KAR,J
      DO 792 K=1,L
      J=L+1-K
      NA=N-1
      NB=N-2
      IF (J-JA) 793,794,795
  795 IF (J-JB) 796,797,798
  798 IF (J-JC) 799,800,801
  801 IF (J-JD) 802,803,804
  793 CALL DDD
      GO TO 792
  794 CALL EEE
      GO TO 792
  796 CALL AAA
      GO TO 792
```

```
  797 CALL RRR
      GO TO 792
  799 CALL DDD
      GO TO 792
  800 CALL EEE
      GO TO 792
  802 CALL FFF
      GO TO 792
  803 CALL GGG
      GO TO 792
  804 CALL CCC
  792 CONTINUE
      RETURN
      END
C
C
C
      SUBROUTINE AAA
      COMMON X(301),Z(41),PHI(301,41),PHIN(301),JJ(301),GUESS(301),
     1NP(10),GUEST(10),JRITE(301),JLEFT(301),N,L,MM,MESH,JA,JB,JC,JD,
     2IPLOT,DELX,DELPHI,PHIMIN,PHIMAX,TOL,XONE,ZONE,OMEGA,S,ZZERO,RES,
     3NA,NB,KAR,J
      IF (KAR-1) 499,499,498
  499 DO 500 I=2,NA,2
  500 PHI(I,J)=0.0
  498 DO 706 I=1,N,2
      IF (J-1) 64,64,65
   64 IF (I-1) 14,14,66
   66 IF (I-N) 16,18,18
   65 IF (I-1) 10,10,67
   67 IF (I-N) 2,20,20
    2 DDF=(PHI(I+2,J)+PHI(I-2,J)+PHI(I,J+1)+PHI(I,J-1))/4.0
      GO TO 702
   10 DDF=(PHI(I,J+1)+PHI(I,J-1)+2.0*PHI(I+2,J))/4.0
      GO TO 702
   14 DDF=(PHI(I,J+1)+PHI(I+2,J))/2.0
      GO TO 702
   16 DDF=(PHI(I+2,J)+PHI(I-2,J)+2.0*PHI(I,J+1))/4.0
      GO TO 702
   18 DDF=(PHI(I-2,J)+PHI(I,J+1))/2.0
      GO TO 702
   20 DDF=(PHI(I,J+1)+PHI(I,J-1)+2.0*PHI(I-2,J))/4.0
  702 GAF=ABS(DDF-PHI(I,J))
      IF (GAF-RES) 701,701,703
  703 RES=GAF
  701 PHI(I,J)=OMEGA*DDF+(1.0-OMEGA)*PHI(I,J)
  706 CONTINUE
      RETURN
      END
C
C
C
      SUBROUTINE BBB
      COMMON X(301),Z(41),PHI(301,41),PHIN(301),JJ(301),GUESS(301),
     1NP(10),GUEST(10),JRITE(301),JLEFT(301),N,L,MM,MESH,JA,JB,JC,JD,
     2IPLOT,DELX,DELPHI,PHIMIN,PHIMAX,TOL,XONE,ZONE,OMEGA,S,ZZERO,RES,
     3NA,NB,KAR,J
      DO 707 I=1,N,2
      IF (JJ(I)-JC) 25,25,68
   68 JCC=JC+1
```

```
      IF (JJ(I)-JCC) 25,69,89
   69 IF (I-1) 35,35,70
   70 IF (I-N) 37,36,36
   89 IF (I-1) 27,27,90
   90 IF (I-N) 6,23,23
    6 DDF=(PHI(I+2,J)+PHI(I-2,J)+PHI(I,J+2)+PHI(I,J-1))/4.0
      GO TO 702
   23 DDF=(PHI(I,J+2)+PHI(I,J-1)+2.0*PHI(I-2,J))/4.0
      GO TO 702
   25 DDF=PHIN(I)
      GO TO 702
   27 DDF=(PHI(I,J+2)+PHI(I,J-1)+2.0*PHI(I+2,J))/4.0
      GO TO 702
   35 DDF=4.0*PHI(I,J+1)/9.0+2.0*PHI(I,J-1)/9.  PHI(I+2,J)/3.0
      GO TO 702
   36 DDF=4.0*PHI(I,J+1)/9.0+2.0*PHI(I,J-1)/9.  PHI(I-2,J)/3.0
      GO TO 702
   37 DDF=4.0*PHI(I,J+1)/9.0+2.0*PHI(I,J-1)/9.  (PHI(I+2,J)+PHI(I-2,J))/
     16.0
  702 GAF=ABS(DDF-PHI(I,J))
      IF (GAF-RES) 701,701,703
  703 RES=GAF
  701 PHI(I,J)=OMEGA*DDF+(1.0-OMEGA)*PHI(I,J)
  707 CONTINUE
      DO 502 I=2,NA,2
  502 PHI(I,J)=(PHI(I+1,J)+PHI(I-1,J))/2.0
      RETURN
      END
C
C
C
      SUBROUTINE CCC
      COMMON X(301),Z(41),PHI(301,41),PHIN(301),JJ(301),GUESS(301),
     1NP(10),GUEST(10),JRITE(301),JLEFT(301),N,L,MM,MESH,JA,JB,JC,JD,
     2IPLOT,DELX,DELPHI,PHIMIN,PHIMAX,TOL,XONE,ZONE,OMEGA,S,ZZERO,RES,
     3NA,NB,KAR,J
      DO 708 I=1,N
      IF (J-JJ(I)) 71,25,26
   71 IF (I-1) 72,72,73
   72 IF (JRITE(I)-1) 28,28,180
   73 IF (I-N) 74,75,75
   75 IF (JLEFT(I)-1) 24,24,183
   74 IF (JLEFT(I)-1) 76,76,181
   76 IF (JRITE(I)-1) 3,3,182
  180 IF (J-JJ(I+1)) 28,28,29
  183 IF (J-JJ(I-1)) 24,24,29
  182 IF (J-JJ(I+1)) 3,3,193
  181 IF (JRITE(I)-1) 185,185,186
  185 IF (J-JJ(I-1)) 3,3,192
  186 IF (JJ(I-1)-JJ(I+1)) 188,187,190
  187 IF (J-JJ(I-1)) 3,3,29
  188 IF (J-JJ(I-1)) 3,3,189
  189 IF (J-JJ(I+1)) 192,192,29
  190 IF (J-JJ(I+1)) 3,3,191
  191 IF (J-JJ(I-1)) 193,193,29
  193 JJA=JJ(I)-JJ(I+1)
      JJB=JJ(I)-J
      DELTA=DELX*FLOAT(JJB/JJA)
      PHIT=PHIN(I)-FLOAT(JJB/JJA)*(PHIN(I)-PHIN(I+1))
```

```
      GO TO 31
  192 JJC=JJ(I)-JJ(I-1)
      JJD=JJ(I)-J
      DELTA=DELX*FLOAT(JJD/JJC)
      PHIT=PHIN(I)-FLOAT(JJD/JJC)*(PHIN(I)-PHIN(I-1))
      GO TO 30
    3 DDF=(PHI(I+1,J)+PHI(I-1,J)+PHI(I,J+1)+PHI(I,J-1))/4.0
      GO TO 702
   24 DDF=(PHI(I,J+1)+PHI(I,J-1)+2.0*PHI(I-1,J))/4.0
      GO TO 702
   25 DDF=PHIN(I)
      GO TO 702
   26 DDF=0.0
      GO TO 702
   28 DDF=(PHI(I,J+1)+PHI(I,J-1)+2.0*PHI(I+1,J))/4.0
      GO TO 702
   29 DDF=(PHI(I,J+1)+PHI(I,J-1))/2.0
      GO TO 702
   30 DDF=(DELX*(DELX*PHIT+DELTA*PHI(I+1,J)))/(DELX+DELTA)**2+(DELTA*
     1(PHI(I,J+1)+PHI(I,J-1)))/(2.0*(DELX+DELTA))
      GO TO 702
   31 DDF=(DELX*(DELX*PHIT+DELTA*PHI(I-1,J)))/(DELX+DELTA)**2+(DELTA*
     1(PHI(I,J+1)+PHI(I,J-1)))/(2.0*(DELX+DELTA))
  702 GAF=ABS(DDF-PHI(I,J))
      IF (GAF-RES) 701,701,703
  703 RES=GAF
  701 PHI(I,J)=OMEGA*DDF+(1.0-OMEGA)*PHI(I,J)
  708 CONTINUE
      RETURN
      END
C
C
C
      SUBROUTINE DDD
      COMMON X(301),Z(41),PHI(301,41),PHIN(301),JJ(301),GUESS(301),
     1NP(10),GUEST(10),JRITE(301),JLEFT(301),N,L,MM,MESH,JA,JB,JC,JD,
     2IPLOT,DELX,DELPHI,PHIMIN,PHIMAX,TOL,XONE,ZONE,OMEGA,S,ZZERO,RES,
     3NA,NB,KAR,J
      IF (KAR-1) 510,510,511
  510 DO 512 I=2,NA,2
  512 PHI(I,J)=0.0
      DO 513 I=3,NB,4
  513 PHI(I,J)=0.0
  511 DO 712 I=1,N,4
      IF (J-1) 87,87,88
   87 IF (I-1) 13,13,89
   89 IF (I-N) 15,17,17
   88 IF (I-1) 9,9,90
   90 IF (I-N) 1,19,19
    1 DDF=(PHI(I+4,J)+PHI(I-4,J)+PHI(I,J+1)+PHI(I,J-1))/4.0
      GO TO 702
    9 DDF=(PHI(I,J+1)+PHI(I,J-1)+2.0*PHI(I+4,J))/4.0
      GO TO 702
   13 DDF=(PHI(I,J+1)+PHI(I+4,J))/2.0
      GO TO 702
   15 DDF=(PHI(I+4,J)+PHI(I-4,J)+2.0*PHI(I,J+1))/4.0
      GO TO 702
   17 DDF=(PHI(I-4,J)+PHI(I,J+1))/2.0
      GO TO 702
   19 DDF=(PHI(I,J+1)+PHI(I,J-1)+2.0*PHI(I-4,J))/4.0
```

```
      GO TO 702
  702 GAF=ABS(DDF-PHI(I,J))
      IF (GAF-RES) 701,701,703
  703 RES=GAF
  701 PHI(I,J)=OMEGA*DDF+(1.0-OMEGA)*PHI(I,J)
  712 CONTINUE
      RETURN
      END
C
C
C
      SUBROUTINE EEE
      COMMON X(301),Z(41),PHI(301,41),PHIN(301),JJ(301),GUESS(301),
     1NP(10),GUEST(10),JRITE(301),JLEFT(301),N,L,MM,MESH,JA,JB,JC,JD,
     2IPLOT,DELX,DELPHI,PHIMIN,PHIMAX,TOL,XONE,ZONE,OMEGA,S,ZZERO,RES,
     3NA,NB,KAR,J
      IF (KAR-1) 514,514,515
  514 DO 516 I=2,NA,2
  516 PHI(I,J)=0.0
  515 DO 715 I=1,N,4
      IF (I-1)  11,11,91
   91 IF (I-N) 4,21,21
    4 DDF=(PHI(I+4,J)+PHI(I-4,J)+PHI(I,J+2)+PHI(I,J-1))/4.0
      GO TO 702
   11 DDF=(PHI(I,J+2)+PHI(I,J-1)+2.0*PHI(I+4,J))/4.0
      GO TO 702
   21 DDF=(PHI(I,J+2)+PHI(I,J-1)+2.0*PHI(I-4,J))/4.0
  702 GAF=ABS(DDF-PHI(I,J))
      IF (GAF-RES) 701,701,703
  703 RES=GAF
  701 PHI(I,J)=OMEGA*DDF+(1.0-OMEGA)*PHI(I,J)
  715 CONTINUE
      DO 517 I=3,NB,4
  517 PHI(I,J)=(PHI(I+2,J)+PHI(I-2,J))/2.0
      RETURN
      END
C
C
C
      SUBROUTINE FFF
      COMMON X(301),Z(41),PHI(301,41),PHIN(301),JJ(301),GUESS(301),
     1NP(10),GUEST(10),JRITE(301),JLEFT(301),N,L,MM,MESH,JA,JB,JC,JD,
     2IPLOT,DELX,DELPHI,PHIMIN,PHIMAX,TOL,XONE,ZONE,OMEGA,S,ZZERO,RES,
     3NA,NB,KAR,J
      IF (KAR-1) 518,518,519
  518 DO 520 I=2,NA,2
  520 PHI(I,J)=0.0
  519 DO 716 I=1,N,2
      IF (I-1) 10,10,92
   92 IF (I-N) 2,20,20
    2 DDF=(PHI(I+2,J)+PHI(I-2,J)+PHI(I,J+1)+PHI(I,J-1))/4.0
      GO TO 702
   10 DDF=(PHI(I,J+1)+PHI(I,J-1)+2.0*PHI(I+2,J))/4.0
      GO TO 702
   20 DDF=(PHI(I,J+1)+PHI(I,J-1)+2.0*PHI(I-2,J))/4.0
      GO TO 702
  702 GAF=ABS(DDF-PHI(I,J))
      IF (GAF-RES) 701,701,703
  703 RES=GAF
```

```
  701 PHI(I,J)=OMEGA*DDF+(1.0-OMEGA)*PHI(I,J)
  716 CONTINUE
      RETURN
      END
C
C
C
      SUBROUTINE GGG
      COMMON X(301),Z(41),PHI(301,41),PHIN(301),JJ(301),GUESS(301),
     1NP(10),GUEST(10),JRITE(301),JLEFT(301),N,L,MM,MESH,JA,JB,JC,JD,
     2IPLOT,DELX,DELPHI,PHIMIN,PHIMAX,TOL,XONE,ZONE,OMEGA,S,ZZERO,RES,
     3NA,NB,KAR,J
      DO 718 I=1,N,2
      IF (JJ(I)-JD) 25,25,93
   93 JDD=JD+1
      IF (JJ(I)-JDD) 25,94,96
   94 IF (I-1) 35,35,95
   95 IF (I-N) 37,36,36
   96 IF (I-1) 27,27,97
   97 IF (I-N) 6,23,23
    6 DDF=(PHI(I+2,J)+PHI(I-2,J)+PHI(I,J+2)+PHI(I,J-1))/4.0
      GO TO 702
   23 DDF=(PHI(I,J+2)+PHI(I,J-1)+2.0*PHI(I-2,J))/4.0
      GO TO 702
   25 DDF=PHIN(I)
      GO TO 702
   27 DDF=(PHI(I,J+2)+PHI(I,J-1)+2.0*PHI(I+2,J))/4.0
      GO TO 702
   35 DDF=4.0*PHI(I,J+1)/9.0+2.0*PHI(I,J-1)/9.  PHI(I+2,J)/3.0
      GO TO 702
   36 DDF=4.0*PHI(I,J+1)/9.0+2.0*PHI(I,J-1)/9.  PHI(I-2,J)/3.0
      GO TO 702
   37 DDF=4.0*PHI(I,J+1)/9.0+2.0*PHI(I,J-1)/9.  (PHI(I+2,J)+PHI(I-2,J))/
     16.0
  702 GAF=ABS(DDF-PHI(I,J))
      IF (GAF-RES) 701,701,703
  703 RES=GAF
  701 PHI(I,J)=OMEGA*DDF+(1.0-OMEGA)*PHI(I,J)
  718 CONTINUE
      DO 525 I=2,NA,2
  525 PHI(I,J)=(PHI(I+1,J)+PHI(I-1,J))/2.0
      RETURN
      END
C
C
C
      SUBROUTINE HHH
      COMMON X(301),Z(41),PHI(301,41),PHIN(301),JJ(301),GUESS(301),
     1NP(10),GUEST(10),JRITE(301),JLEFT(301),N,L,MM,MESH,JA,JB,JC,JD,
     2IPLOT,DELX,DELPHI,PHIMIN,PHIMAX,TOL,XONE,ZONE,OMEGA,S,ZZERO,RES,
     3NA,NB,KAR,J
      DO 740 I=1,N
      IF (J-1) 106,106,107
  106 IF (I-1) 32,32,108
  108 IF (I-N) 34,33,33
  107 IF (I-1) 28,28,109
  109 IF (I-N) 3,3,24
    3 DDF=(PHI(I+1,J)+PHI(I-1,J)+PHI(I,J+1)+PHI(I,J-1))/4.0
      GO TO 702
   24 DDF=(PHI(I,J+1)+PHI(I,J-1)+2.0*PHI(I-1,J))/4.0
```

```
      GO TO 702
   28 DDF=(PHI(I,J+1)+PHI(I,J-1)+2.0*PHI(I+1,J))/4.0
      GO TO 702
   32 DDF=(PHI(I,J+1)+PHI(I+1,J))/2.0
      GO TO 702
   33 DDF=(PHI(I,J+1)+PHI(I-1,J))/2.0
      GO TO 702
   34 DDF=(PHI(I+1,J)+PHI(I-1,J)+2.0*PHI(I,J+1))/4.0
  702 GAF=ABS(DDF-PHI(I,J))
      IF (GAF-RES) 701,701,703
  703 RES=GAF
  701 PHI(I,J)=OMEGA*DDF+(1.0-OMEGA)*PHI(I,J)
  740 CONTINUE
      RETURN
      END
C
C
C
      SUBROUTINE PPP
      COMMON X(301),Z(41),PHI(301,41),PHIN(301),JJ(301),GUESS(301),
     1NP(10),GUEST(10),JRITE(301),JLEFT(301),N,L,MM,MESH,JA,JB,JC,JD,
     2IPLOT,DELX,DELPHI,PHIMIN,PHIMAX,TOL,XONE,ZONE,OMEGA,S,ZZERO,RES,
     3NA,NB,KAR,J
      DO 742 I=1,N,2
      IF (I-1) 38,38,110
  110 IF (I-N) 40,39,39
   38 DDF=(PHI(I,J+1)+PHI(I,J-2)+2.0*PHI(I+2,J))/4.0
      GO TO 702
   39 DDF=(PHI(I,J+1)+PHI(I,J-2)+2.0*PHI(I-2,J))/4.0
      GO TO 702
   40 DDF=(PHI(I+2,J)+PHI(I-2,J)+PHI(I,J+1)+PHI(I,J-2))/4.0
  702 GAF=ABS(DDF-PHI(I,J))
      IF (GAF-RES) 701,701,703
  703 RES=GAF
  701 PHI(I,J)=OMEGA*DDF+(1.0-OMEGA)*PHI(I,J)
  742 CONTINUE
      DO 530 I=2,NA,2
  530 PHI(I,J)=(PHI(I+1,J)+PHI(I-1,J))/2.0
      RETURN
      END
C
C
C
      SUBROUTINE RRR
      COMMON X(301),Z(41),PHI(301,41),PHIN(301),JJ(301),GUESS(301),
     1NP(10),GUEST(10),JRITE(301),JLEFT(301),N,L,MM,MESH,JA,JB,JC,JD,
     2IPLOT,DELX,DELPHI,PHIMIN,PHIMAX,TOL,XONE,ZONE,OMEGA,S,ZZERO,RES,
     3NA,NB,KAR,J
      IF (KAR-1) 130,130,131
  130 DO 552 I=2,NA,2
  552 PHI(I,J)=0.0
  131 DO 780 I=1,N,4
      IF (I-1) 12,12,135
  135 IF (I-N) 5,22,22
    5 DDF=(PHI(I+4,J)+PHI(I-4,J)+PHI(I,J+1)+PHI(I,J-2))/4.0
      GO TO 702
   12 DDF=(PHI(I,J+1)+PHI(I,J-2)+2.0*PHI(I+4,J))/4.0
      GO TO 702
   22 DDF=(PHI(I,J+1)+PHI(I,J-2)+2.0*PHI(I-4,J))/4.0
```

```
  702 GAF=ABS(DDF-PHI(I,J))
      IF (GAF-RES) 701,701,703
  703 RES=GAF
  701 PHI(I,J)=OMEGA*DDF+(1.0-OMEGA)*PHI(I,J)
  780 CONTINUE
      DO 554 I=3,NB,4
  554 PHI(I,J)=(PHI(I+2,J)+PHI(I-2,J))/2.0
      RETURN
      END
C
      SUBROUTINE CONTWO
      COMMON X(301),Z(41),PHI(301,41),PHIN(301),JJ(301),GUESS(301),
     1NP(10),GUEST(10),JRITE(301),JLEFT(301),N,L,MM,MESH,JA,JB,JC,JD,
     2IPLOT,DELX,DELPHI,PHIMIN,PHIMAX,TOL,XONE,ZONE,OMEGA,S,ZZERO,RES,
     3NA,NB,KAR,J
      DIMENSION T(4,3),XX(2),ZZ(2)
      COMMON /CCPOOL/ XMIN,XMAX,YMIN,YMAX,CCXMIN,CCXMAX,CCYMIN,CCYMAX
      IF (IPLOT-2) 40,41,42
   40 XMIN=-1875.0
      XMAX=23125.0
      YMIN=-4250.0
      YMAX=12250.0
      CCXMIN=100.0
      CCXMAX=1100.0
      CCYMIN=250.0
      CCYMAX=910.0
      CALL CCBGN
      CALL CCGRID (6HNOLBLS)
      XMIN=0.0
      XMAX=20000.0
      YMIN=-0.001
      YMAX=12000.0
      CCXMIN=175.0
      CCXMAX=975.0
      CCYMIN=420.0
      CCYMAX=900.0
      CALL CCBGN
      CALL CCGRID (1,10,6HNOLBLS,1,6)
      WRITE (98,20)
   20 FORMAT (116H0         0.1S          .2S         0.3S          0.4S
     1  0.5S        0.6S          0.7S          .8S          0.9S           S)
      CALL CCALTR (175.0,405.0,0,1)
      CALL CCALTR ( 980.0,420.0,0,1,1H0)
      CALL CCALTR (980.0,500.0,0,1,4H0.1S)
      CALL CCALTR (980.0,580.0,0,1,4H0.2S)
      CALL CCALTR (980.0,660.0,0,1,4H0.3S)
      CALL CCALTR (980.0,740.0,0,1,4H0.4S)
      CALL CCALTR (980.0,820.0,0,1,4H0.5S)
      CALL CCALTR (980.0,900.0,0,1,4H0.6S)
      GO TO 43
   41 XMIN=-1875.0
      XMAX=43125.0
      YMIN=-4250.0
      YMAX=12250.0
      CCXMIN=100.0
      CCXMAX=2100.0
      CCYMIN=250.0
      CCYMAX=910.0
      CALL CCBGN
      CALL CCGRID (6HNOLBLS)
```

```
      XMIN=0.0
      XMAX=40000.0
      YMIN=-0.001
      YMAX=12000.0
      CCXMIN=175.0
      CCXMAX=1775.0
      CCYMIN=420.0
      CCYMAX=900.0
      CALL CCBGN
      CALL CCGRID (1,20,6HNOLBLS,1,6)
      WRITE (98,21)
   21 FORMAT (117H0                          .1S                          0.2S
     1              0.3S                            .4S                          0.5S)
      CALL CCALTR (175.0,405.0,0,1)
      WRITE (98,23)
   23 FORMAT (113H                       0.6S                          0.7S
     1          0.8S                           .9S                               S)
      CALL CCALTR (989.0,405.0,0,1)
      CALL CCALTR (1780.0,420.0,0,1,1H0)
      CALL CCALTR (1780.0,580.0,0,1,4H0.1S)
      CALL CCALTR (1780.0,740.0,0,1,4H0.2S)
      CALL CCALTR (1780.0,900.0,0,1,4H0.3S)
      GO TO 43
   42 XMIN=-1875.0
      XMAX=63125.0
      YMIN=-4250.0
      YMAX=12250.0
      CCXMIN=100.0
      CCXMAX=3100.0
      CCYMIN=250.0
      CCYMAX=910.0
      CALL CCBGN
      CALL CCGRID (6HNOLBLS)
      XMIN=0.0
      XMAX=60000.0
      YMIN=-0.001
      YMAX=12000.0
      CCXMIN=175.0
      CCXMAX=2575.0
      CCYMIN=420.0
      CCYMAX=900.0
      CALL CCBGN
      CALL CCGRID (1,30,6HNOLBLS,1,6)
      WRITE (98,22)
   22 FORMAT (115H0                                        0.1S
     1              .2S                                        0.3S           )
      CALL CCALTR (175.0,405.0,0,1)
      WRITE (98,24)
   24 FORMAT (114H                       0.4S
     1 0.5S                                    .6S                            )
      CALL CCALTR (980.0,405.0,0,1)
      WRITE (98,25)
   25 FORMAT (114H         0.7S                                        0.8S
     1                          0.9S                                        S)
      CALL CCALTR (1778.0,405.0,0,1)
      CALL CCALTR (2580.0,420.0,0,1,1H0)
      CALL CCALTR (2580.0,660.0,0,1,4H0.1S)
      CALL CCALTR (2580.0,900.0,0,1,4H0.2S)
   43 LL=L-1
```

```
      NN=N-1
      DO 1 J=1,LL
      GO TO (604,601,602,601,602,601,602),MESH
  601 IF (J-JA) 603,604,605
  605 IF (J-JB) 604,603,607
  607 IF (J-JC) 603,604,604
  603 KK=2
      GO TO 650
  604 KK=1
      GO TO 650
  602 IF (J-JA) 610,611,615
  615 IF (J-JB) 611,610,616
  616 IF (J-JC) 610,611,617
  617 IF (J-JD) 611,612,612
  610 KK=4
      GO TO 650
  611 KK=2
      GO TO 650
  612 KK=1
  650 DO 2 I=1,NN,KK
      IK=I+KK
      PHILOW=AMIN1(PHI(I,J),PHI(IK,J),PHI(IK,J 1),PHI(I,J+1))
      PHIHI =AMAX1(PHI(I,J),PHI(IK,J),PHI(IK,J 1),PHI(I,J+1))
      IF (PHIHI-PHILOW) 2,2,51
   51 IF (PHILOW-PHIMAX) 53,53,2
   53 IF (PHIHI-PHIMIN) 2,5,5
    5 IF (PHILOW-PHIMIN) 56,54,55
   56 IF (PHILOW-10.0) 101,101,54
  101 TA=PHI(I,J)
      TB=PHI(IK,J)
      TC=PHI(IK,J+1)
      TD=PHI(I,J+1)
      IF (TA-10.0) 102,102,103
  102 IF (TB-10.0) 2,2,105
  105 IF (TC-10.0) 2,2,106
  106 PHILOW=AMIN1(TB,TC)
      GO TO 55
  103 IF (TB-10.0) 107,107,108
  107 IF(TD-10.0) 2,2,109
  109 PHILOW=AMIN1(TA,TD)
      GO TO 55
  108 IF (TC-TD) 110,112,111
  110 IF (TD-10.0) 112,112,113
  113 PHILOW=AMIN1(TA,TB,TD)
      GO TO 55
  111 IF (TC-10.0) 112,112,114
  114 PHILOW=AMIN1(TA,TB,TC)
      GO TO 55
  112 PHILOW=AMIN1(TA,TB)
      GO TO 55
   54 AA=PHIMIN
      GO TO 3
   55 AA= FLOAT(IFIX((PHILOW-PHIMIN)/DELPHI)+1)*DELPHI+PHIMIN
    3 IFLAG=0
      T(1,1)=PHI(I,J)
      T(2,1)=PHI(IK,J)
      T(3,1)=PHI(IK,J+1)
      T(4,1)=PHI(I,J+1)
      T(1,2)=X(I)
      T(2,2)=X(IK)
```

```
      T(3,2)=T(2,2)
      T(4,2)=T(1,2)
      T(1,3)=Z(J)
      T(2,3)=T(1,3)
      T(3,3)=T(1,3)+DELX
      T(4,3)=T(3,3)
    4 K=0
  613 IF (T(1,1)-10.0) 11,11,600
  600 IF (T(2,1)-10.0) 11,11,6
    6 IF(T(1,1)-T(2,1)) 7,11,7
    7 F=(AA-T(1,1))/(T(2,1)-T(1,1))
      IF (F-1.0) 71,71,11
   71 IF(F) 11,11,8
    8 IDIOT=1+IFLAG
      XX(IDIOT)=(1.0-F)*T(1,2)+F*T(2,2)
      ZZ(IDIOT)=(1.0-F)*T(1,3)+F*T(2,3)
   85 IF(IFLAG) 10,10,9
    9 CALL CCPLOT (XX,ZZ,2,6HNOJOIN,1,1)
      XX(1)=XX(2)
      ZZ(1)=ZZ(2)
      GO TO 11
   10 IFLAG=1
   11 K=K+1
      IF(K-4) 13,12,12
   13 TT1=T(1,1)
      TT2=T(1,2)
      TT3=T(1,3)
      DO 131 NA=1,3
      DO 131 NB=1,3
  131 T(NB,NA)=T(NB+1,NA)
      T(4,1)=TT1
      T(4,2)=TT2
      T(4,3)=TT3
      IF (K-2) 1620,1614,1620
 1614 IF (J-JA) 1620,11,1615
 1615 IF (J-JB) 1620,11,1616
 1616 IF (J-JC) 1620,11,1617
 1617 IF (J-JD) 1620,11,1620
 1620 GO TO 613
   12 AA=AA+DELPHI
   14 IF(AA-PHIHI) 15,15,2
   15 IF (AA-PHIMAX) 3,3,2
    2 CONTINUE
    1 CONTINUE
      RETURN
      END
```

```
C NUMERICAL PROGRAM 3
      COMMON X(301),Z(41),PHI(301,41),PHIN(301),JJ(301),GUESS(301),
     1NP(10),GUEST(10),JRITE(301),JLEFT(301),PERM(41),PERK(41),LP(41),
     2GUESR(10),GUESQ(301),N,L,MM,IPLOT,DELX,DELPHI,PHIMIN,PHIMAX,TOL,
     3XONE,ZONE,OMEGA,S,ZZERO,RES,KAR,J,INPUT,JI
 7000 READ 303,TITLE1,TITLE2
      IF (TITLE1) 304,1000,304
  304 READ 300,N,L,MM,MP,IPLOT,INPUT,JI,KART
      READ 301,DELX,DELPHI,PHIMIN,PHIMAX,TOL,XONE,ZONE,OMEGA,S,ZZERO
      READ 301, (PHIN(I),I=1,N)
      READ 302,(JJ(I),I=1,N)
  300 FORMAT (14I5)
  301 FORMAT (7F10.2)
  302 FORMAT (24I3)
  303 FORMAT (2A6)
      MMM=MM+1
      READ 300,(NP(M),M=1,MMM)
      READ 301,(GUEST(M),M=1,MM)
      IF (INPUT-1) 6001,6000,6000
 6000 READ 301, (GUESR(M),M=1,MM)
 6001 DO 305 M=1,MM
      NPR=NP(M)
      NPQ=NP(M+1)
      DO 306 I=NPR,NPQ
      IF (INPUT-1) 306,6306,6306
 6306 GUESQ(I)=GUESR(M)
  306 GUESS(I)=GUEST(M)
  305 CONTINUE
      MMP=MP+1
      READ 300, (LP(M),M=1,MMP)
      READ 301, (PERK(M),M=1,MP)
      DO 1120 M=1,MP
      LPR=LP(M)
      LPQ=LP(M+1)
      DO 1121 J=LPR,LPQ
 1121 PERM(J)=PERK(M)
 1120 CONTINUE
C
      DO 330 I=1,N
      IF (I-1) 331,331,332
  331 X(1)=XONE
      GO TO 330
  332 X(I)=X(I-1)+DELX
  330 CONTINUE
C
      DO 340 J=1,L
      IF (J-1) 341,341,342
  341 Z(1)=ZONE
      GO TO 340
  342 Z(J)=Z(J-1)+DELX
  340 CONTINUE
C
      ZZERA=FLOAT(JJ(1)-1)*DELX
      IF (ZZERA-ZZERO) 376,377,376
  377 SA=FLOAT(N-1)*DELX
      IF (SA-S) 376,320,376
  376 PRINT 378
  378 FORMAT (1H1,18H     CHECK GEOMETRY)
      GO TO 7000
```

```
C
  320 DO 328 I=1,N
      JRITE(I)=JJ(I)-JJ(I+1)
      JLEFT(I)=JJ(I)-JJ(I-1)
      DO 328 J=1,L
      IF (J-JJ(I)) 325,326,327
  327 PHI(I,J)=0.0
      GO TO 328
  326 PHI(I,J)=PHIN(I)
      GO TO 328
  325 IF (INPUT-1) 6400,6401,6401
 6401 IF (J-JI) 6402,6403,6403
 6402 PHI(I,J)=GUESS(I)
      GO TO 328
 6403 PHI(I,J)=GUESQ(I)
      GO TO 328
 6400 PHI(I,J)=GUESS(I)
  328 CONTINUE
C
      DO 206 KAR=1,KART
      RES=0.0
   40 CALL MESH1A
  205 IF (RES-TOL) 400,206,206
  206 CONTINUE
C
  400 PRINT 401,KAR,RES
  401 FORMAT (1H1,I10,F10.5)
C
      PRINT 403,TITLE1,TITLE2
  403 FORMAT (1H1,24H1      NUMERICAL PROBLEM 2A6//12X,4HX(I)//)
      PRINT 404,(X(I),I=1,N)
      PRINT 405
  405 FORMAT (1H1,12X,4HZ(J)//)
      PRINT 404,(Z(J),J=1,L)
  404 FORMAT (10F12.4)
      PRINT 415
  415 FORMAT (1H1,10X,8HPHI(I,J)//)
      DO 406 I=1,N
      PRINT 407,I
  407 FORMAT (1H0,12X,2HI=,I3//)
  406 PRINT 408, (PHI(I,J),J=1,L)
  408 FORMAT (10F12.4)
  414 CALL CONTHR
      CALL CCNEXT
      GO TO 7000
 1000 CALL CCEND
      STOP
      END
C
C
C
C
C
      SUBROUTINE MESH1A
      COMMON X(301),Z(41),PHI(301,41),PHIN(301),JJ(301),GUESS(301),
     1NP(10),GUEST(10),JRITE(301),JLEFT(301),PERM(41),PERK(41),LP(41),
     2GUESR(10),GUESQ(301),N,L,MM,IPLOT,DELX,DELPHI,PHIMIN,PHIMAX,TOL,
     3XONE,ZONE,OMEGA,S,ZZERO,RES,KAR,J,INPUT,JI
      DO 701 K=1,L
      J=L+1-K
```

```
      DO 701 I=1,N
      IF (I-1) 41,41,42
   41 IF (J-1) 32,32,43
   43 IF(J-JJ(I)) 44,25,26
   44 IF (JRITE(I)-1) 28,28,180
   42 IF (I-N) 46,47,47
   46 IF (J-1) 34,34,48
   48 IF (J-JJ(I)) 49,25,26
   49 IF (JLEFT(I)-1) 50,50,181
   50 IF (JRITE(I)-1) 3,3,182
   47 IF (J-1) 33,33,51
   51 IF (J-JJ(I)) 52,25,26
   52 IF (JLEFT(I)-1) 24,24,183
  180 IF (J-JJ(I+1)) 28,28,29
  183 IF (J-JJ(I-1)) 24,24,29
  182 IF (J-JJ(I+1)) 3,3,193
  181 IF (JRITE(I)-1) 185,185,186
  185 IF (J-JJ(I-1)) 3,3,192
  186 IF (JJ(I-1)-JJ(I+1)) 188,187,190
  187 IF (J-JJ(I-1)) 3,3,29
  188 IF (J-JJ(I-1)) 3,3,189
  189 IF (J-JJ(I+1)) 192,192,29
  190 IF (J-JJ(I+1)) 3,3,191
  191 IF (J-JJ(I-1)) 193,193,29
  193 JJA=JJ(I)-JJ(I+1)
      JJB=JJ(I)-J
      DELTA=DELX*FLOAT(JJB/JJA)
      PHIT=PHIN(I)-FLOAT(JJB/JJA)*(PHIN(I)-PHIN(I+1))
      GO TO 31
  192 JJC=JJ(I)-JJ(I-1)
      JJD=JJ(I)-J
      DELTA=DELX*FLOAT(JJD/JJC)
      PHIT=PHIN(I)-FLOAT(JJD/JJC)*(PHIN(I)-PHIN(I-1))
      GO TO 30
    3 DDF=(PERM(J)*(PHI(I+1,J)+PHI(I-1,J)+PHI(I,J+1))+PERM(J-1)*PHI(I,
     1J-1))/(3.0*PERM(J)+PERM(J-1))
      GO TO 702
   24 DDF=(PERM(J)*(PHI(I,J+1)+PHI(I-1,J)*2.0) PERM(J-1)*PHI(I,J-1))
     1/(3.0*PERM(J)+PERM(J-1))
      GO TO 702
   25 DDF=PHIN(I)
      GO TO 702
   26 DDF=0.0
      GO TO 702
   28 DDF=(PERM(J)*(PHI(I,J+1)+PHI(I+1,J)*2.0) PERM(J-1)*PHI(I,J-1))
     1/(3.0*PERM(J)+PERM(J-1))
      GO TO 702
   29 DDF=(PERM(J)*PHI(I,J+1)+PERM(J-1)*PHI(I,J-1))/(PERM(J)+PERM(J-1))
      GO TO 702
   30 DDF=(PERM(J)*(PHI(I+1,J)+DELX/DELTA*PHIT)+((DELTA+DELX)/(2.0*DELX
     1))*(PERM(J)*PHI(I,J+1)+PERM(J-1)*PHI(I,J-1)))/(PERM(J)*(DELX/DELTA
     2+1.00)+((DELTA+DELX)/(2.0*DELX))*(PERM(J)+PERM(J-1)))
      GO TO 702
   31 DDF=(PERM(J)*(PHI(I-1,J)+DELX/DELTA*PHIT)+((DELTA+DELX)/(2.0*DELX
     1))*(PERM(J)*PHI(I,J+1)+PERM(J-1)*PHI(I,J-1)))/(PERM(J)*(DELX/DELTA
     2+1.0)+((DELTA+DELX)/(2.0*DELX))*(PERM(J)+PERM(J-1)))
      GO TO 702
   32 DDF=(PHI(I,J+1)+PHI(I+1,J))/2.0
      GO TO 702
```

```
   33 DDF=(PHI(I,J+1)+PHI(I-1,J))/2.0
      GO TO 702
   34 DDF=(PHI(I+1,J)+PHI(I-1,J)+2.0*PHI(I,J+1))/4.0
  702 GAF=ABS(DDF-PHI(I,J))
      IF (GAF-RES) 701,701,703
  703 RES=GAF
  701 PHI(I,J)=OMEGA*DDF+(1.0-OMEGA)*PHI(I,J)
      RETURN
      END
C
C
C
      SUBROUTINE CONTHR
      COMMON X(301),Z(41),PHI(301,41),PHIN(301),JJ(301),GUESS(301),
     1NP(10),GUEST(10),JRITE(301),JLEFT(301),PERM(41),PERK(41),LP(41),
     2GUESR(10),GUESQ(301),N,L,MM,IPLOT,DELX,DELPHI,PHIMIN,PHIMAX,TOL,
     3XONE,ZONE,OMEGA,S,ZZERO,RES,KAR,J,INPUT,JI
      DIMENSION T(4,3),XX(2),ZZ(2)
      COMMON /CCPOOL/ XMIN,XMAX,YMIN,YMAX,CCXMIN,CCXMAX,CCYMIN,CCYMAX
      IF (IPLOT-2) 40,41,42
   40 XMIN=-1875.0
      XMAX=23125.0
      YMIN=-4250.0
      YMAX=12250.0
      CCXMIN=100.0
      CCXMAX=1100.0
      CCYMIN=250.0
      CCYMAX=910.0
      CALL CCBGN
      CALL CCGRID (6HNOLBLS)
      XMIN=0.0
      XMAX=20000.0
      YMIN=-0.001
      YMAX=12000.0
      CCXMIN=175.0
      CCXMAX=975.0
      CCYMIN=420.0
      CCYMAX=900.0
      CALL CCBGN
      CALL CCGRID (1,10,6HNOLBLS,1,6)
      WRITE (98,20)
   20 FORMAT (116H0         0.1S          .2S         0.3S          0.4S
     1  0.5S         0.6S          0.7S          .8S          0.9S           S)
      CALL CCALTR (175.0,405.0,0,1)
      CALL CCALTR ( 980.0,420.0,0,1,1H0)
      CALL CCALTR (980.0,500.0,0,1,4H0.1S)
      CALL CCALTR (980.0,580.0,0,1,4H0.2S)
      CALL CCALTR (980.0,660.0,0,1,4H0.3S)
      CALL CCALTR (980.0,740.0,0,1,4H0.4S)
      CALL CCALTR (980.0,820.0,0,1,4H0.5S)
      CALL CCALTR (980.0,900.0,0,1,4H0.6S)
      GO TO 43
   41 XMIN=-1875.0
      XMAX=43125.0
      YMIN=-4250.0
      YMAX=12250.0
      CCXMIN=100.0
      CCXMAX=2100.0
      CCYMIN=250.0
      CCYMAX=910.0
```

```
      CALL CCBGN
      CALL CCGRID (6HNOLBLS)
      XMIN=0.0
      XMAX=40000.0
      YMIN=-0.001
      YMAX=12000.0
      CCXMIN=175.0
      CCXMAX=1775.0
      CCYMIN=420.0
      CCYMAX=900.0
      CALL CCBGN
      CALL CCGRID (1,20,6HNOLBLS,1,6)
      WRITE (98,21)
   21 FORMAT (117H0                          .1S                          0.2S
     1              0.3S                          .4S                          0.5S)
      CALL CCALTR (175.0,405.0,0,1)
      WRITE (98,23)
   23 FORMAT (113H                       0.6S                          0.7S
     1           0.8S                          .9S                               S)
      CALL CCALTR (989.0,405.0,0,1)
      CALL CCALTR (1780.0,420.0,0,1,1H0)
      CALL CCALTR (1780.0,580.0,0,1,4H0.1S)
      CALL CCALTR (1780.0,740.0,0,1,4H0.2S)
      CALL CCALTR (1780.0,900.0,0,1,4H0.3S)
      GO TO 43
   42 XMIN=-1875.0
      XMAX=63125.0
      YMIN=-4250.0
      YMAX=12250.0
      CCXMIN=100.0
      CCXMAX=3100.0
      CCYMIN=250.0
      CCYMAX=910.0
      CALL CCBGN
      CALL CCGRID (6HNOLBLS)
      XMIN=0.0
      XMAX=60000.0
      YMIN=-0.001
      YMAX=12000.0
      CCXMIN=175.0
      CCXMAX=2575.0
      CCYMIN=420.0
      CCYMAX=900.0
      CALL CCBGN
      CALL CCGRID (1,30,6HNOLBLS,1,6)
      WRITE (98,22)
   22 FORMAT (115H0                                        0.1S
     1              .2S                                        0.3S           )
      CALL CCALTR (175.0,405.0,0,1)
      WRITE (98,24)
   24 FORMAT (114H                       0.4S
     1 0.5S                                .6S                          )
      CALL CCALTR (980.0,405.0,0,1)
      WRITE (98,25)
   25 FORMAT (114H         0.7S                                        0.8S
     1                          0.9S                                     S)
      CALL CCALTR (1778.0,405.0,0,1)
      CALL CCALTR (2580.0,420.0,0,1,1H0)
      CALL CCALTR (2580.0,660.0,0,1,4H0.1S)
```

```
      CALL CCALTR (2580.0,900.0,0,1,4H0.2S)
   43 LL=L-1
      NN=N-1
      DO 1 J=1,LL
      DO 2 I=1,NN
      PHILOW=AMIN1(PHI(I,J),PHI(I+1,J),PHI(I+1,J+1),PHI(I,J+1))
      PHIHI =AMAX1(PHI(I,J),PHI(I+1,J),PHI(I+1,J+1),PHI(I,J+1))
      IF (PHIHI-PHILOW) 2,2,51
   51 IF (PHILOW-PHIMAX) 53,53,2
   53 IF (PHIHI-PHIMIN) 2,5,5
    5 IF (PHILOW-PHIMIN) 56,54,55
   56 IF (PHILOW-10.0) 101,101,54
  101 TA=PHI(I,J)
      TB=PHI(I+1,J)
      TC =PHI(I+1,J+1)
      TD=PHI(I,J+1)
      IF (TA-10.0) 102,102,103
  102 IF (TB-10.0) 2,2,105
  105 IF (TC-10.0) 2,2,106
  106 PHILOW=AMIN1(TB,TC)
      GO TO 55
  103 IF (TB-10.0) 107,107,108
  107 IF(TD-10.0) 2,2,109
  109 PHILOW=AMIN1(TA,TD)
      GO TO 55
  108 IF (TC-TD) 110,112,111
  110 IF (TD-10.0) 112,112,113
  113 PHILOW=AMIN1(TA,TB,TD)
      GO TO 55
  111 IF (TC-10.0) 112,112,114
  114 PHILOW=AMIN1(TA,TB,TC)
      GO TO 55
  112 PHILOW=AMIN1(TA,TB)
      GO TO 55
   54 AA=PHIMIN
      GO TO 3
   55 AA= FLOAT(IFIX((PHILOW-PHIMIN)/DELPHI)+1)*DELPHI+PHIMIN
    3 IFLAG=0
      T(1,1)=PHI(I,J)
      T(2,1)=PHI(I+1,J)
      T(3,1)=PHI(I+1,J+1)
      T(4,1)=PHI(I,J+1)
      T(1,2)=X(I)
      T(2,2)=T(1,2)+DELX
      T(3,2)=T(2,2)
      T(4,2)=T(1,2)
      T(1,3)=Z(J)
      T(2,3)=T(1,3)
      T(3,3)=T(1,3)+DELX
      T(4,3)=T(3,3)
    4 K=0
  613 IF (T(1,1)-10.0) 11,11,600
  600 IF (T(2,1)-10.0) 11,11,6
    6 IF(T(1,1)-T(2,1)) 7,11,7
    7 F=(AA-T(1,1))/(T(2,1)-T(1,1))
      IF (F-1.0) 71,71,11
   71 IF(F) 11,11,8
    8 IDIOT=1+IFLAG
      XX(IDIOT)=(1.0-F)*T(1,2)+F*T(2,2)
      ZZ(IDIOT)=(1.0-F)*T(1,3)+F*T(2,3)
```

```
 85 IF(IFLAG) 10,10,9
  9 CALL CCPLOT (XX,ZZ,2,6HNOJOIN,1,1)
    XX(1)=XX(2)
    ZZ(1)=ZZ(2)
    GO TO 11
 10 IFLAG=1
 11 K=K+1
    IF(K-4) 13,12,12
 13 TT1=T(1,1)
    TT2=T(1,2)
    TT3=T(1,3)
    DO 131 NA=1,3
    DO 131 NB=1,3
131 T(NB,NA)=T(NB+1,NA)
    T(4,1)=TT1
    T(4,2)=TT2
    T(4,3)=TT3
    GO TO 613
 12 AA=AA+DELPHI
 14 IF(AA-PHIHI) 15,15,2
 15 IF (AA-PHIMAX) 3,3,2
  2 CONTINUE
  1 CONTINUE
    RETURN
    END
```

```
C NUMERICAL PROGRAM 4
      COMMON X(151),Z(41),PHI(151,41),PHIN(151),JJ(151),GUESS(151),
     1NP(10),GUEST(10),JRITE(151),JLEFT(151),PERM(151,41),PERK(41),
     2LP(41),GUESR(10),GUESQ(151),MA(41),MC(10),N,L,MM,
     3IPLOT,DELX,DELPHI,PHIMIN,PHIMAX,TOL,XONE,ZONE,OMEGA,S,ZZERO,RES,
     4KAR,J,INPUT,JI,INPERM,MB,MD
 7000 READ 7001,TITLE1,TITLE2
 7001 FORMAT (2A6)
      IF (TITLE1) 7300,1000,7300
 7300 READ 300,N,L,MM,MP,IPLOT,INPUT,JI,INPERM,KART
      READ 301,DELX,DELPHI,PHIMIN,PHIMAX,TOL,XONE,ZONE,OMEGA,S,ZZERO
      READ 301, (PHIN(I),I=1,N)
      READ 302,(JJ(I),I=1,N)
  300 FORMAT (14I5)
  301 FORMAT (7F10.2)
  302 FORMAT (24I3)
      MMM=MM+1
      READ 300,(NP(M),M=1,MMM)
      READ 301,(GUEST(M),M=1,MM)
      IF (INPUT-1) 6001,6000,6000
 6000 READ 301, (GUESR(M),M=1,MM)
 6001 DO 305 M=1,MM
      NPR=NP(M)
      NPQ=NP(M+1)
      DO 306 I=NPR,NPQ
      IF (INPUT-1) 306,6306,6306
 6306 GUESQ(I)=GUESR(M)
  306 GUESS(I)=GUEST(M)
  305 CONTINUE
      IF (INPERM-1) 6010,6011,6011
 6010 MMP=MP+1
      READ 300, (LP(M),M=1,MMP)
      READ 301, (PERK(M),M=1,MP)
      DO 1120 M=1,MP
      LPR=LP(M)
      LPQ=LP(M+1)
      DO 1121 J=LPR,LPQ
      DO 1121 I=1,N
 1121 PERM(I,J)=PERK(M)
 1120 CONTINUE
      GO TO 6012
 6011 READ 300, (MA(J),J=1,L)
      DO 6022 J=1,L
      MB=MA(J)+1
      MD=MA(J)
      READ 300, (MC(M),M=1,MB)
      READ 301, (PERK(M),M=1,MD)
      DO 6021 M=1,MD
      MCR=MC(M)
      MCQ=MC(M+1)
      DO 6020 I=MCR,MCQ
 6020 PERM(I,J)=PERK(M)
 6021 CONTINUE
 6022 CONTINUE
C
 6012 DO 330 I=1,N
      IF (I-1) 331,331,332
  331 X(1)=XONE
      GO TO 330
```

```
  332 X(I)=X(I-1)+DELX
  330 CONTINUE
C
      DO 340 J=1,L
      IF (J-1) 341,341,342
  341 Z(1)=ZONE
      GO TO 340
  342 Z(J)=Z(J-1)+DELX
  340 CONTINUE
C
      ZZERA=FLOAT(JJ(1)-1)*DELX
      IF (ZZERA-ZZERO) 376,377,376
  377 SA=FLOAT(N-1)*DELX
      IF (SA-S) 376,320,376
  376 PRINT 378
  378 FORMAT (1H1,18H     CHECK GEOMETRY)
      GO TO 7000
C
  320 DO 328 I=1,N
      JRITE(I)=JJ(I)-JJ(I+1)
      JLEFT(I)=JJ(I)-JJ(I-1)
      DO 328 J=1,L
      IF (J-JJ(I)) 325,326,327
  327 PHI(I,J)=0.0
      GO TO 328
  326 PHI(I,J)=PHIN(I)
      GO TO 328
  325 IF (INPUT-1) 6400,6401,6401
 6401 IF (J-JI)  6402,6403,6403
 6402 PHI(I,J)=GUESS(I)
      GO TO 328
 6403 PHI(I,J)=GUESQ(I)
      GO TO 328
 6400 PHI(I,J)=GUESS(I)
  328 CONTINUE
C
      DO 206 KAR=1,KART
      RES=0.0
   40 CALL MESH1B
  205 IF (RES-TOL) 400,206,206
  206 CONTINUE
C
  400 PRINT 401,KAR,RES
  401 FORMAT (1H1,I10,F10.5)
C
      PRINT 403,TITLE1,TITLE2
  403 FORMAT (1H1,24H1      NUMERICAL PROBLEM 2A6//12X,4HX(I)//)
      PRINT 404,(X(I),I=1,N)
      PRINT 405
  405 FORMAT (1H1,12X,4HZ(J)//)
      PRINT 404,(Z(J),J=1,L)
  404 FORMAT (10F12.4)
      PRINT 415
  415 FORMAT (1H1,10X,8HPHI(I,J)//)
      DO 406 I=1,N
      PRINT 407,I
  407 FORMAT (1H0,12X,2HI=,I3//)
  406 PRINT 408, (PHI(I,J),J=1,L)
  408 FORMAT (10F12.4)
  414 CALL CONFOR
```

```
      CALL CCNEXT
      GO TO 7000
 1000 CALL CCEND
      STOP
      END
C
C
C
C
C
      SUBROUTINE MESH1B
      COMMON X(151),Z(41),PHI(151,41),PHIN(151),JJ(151),GUESS(151),
     1NP(10),GUEST(10),JRITE(151),JLEFT(151),PERM(151,41),PERK(41),
     2LP(41),GUESR(10),GUESQ(151),MA(41),MC(10),N,L,MM,
     3IPLOT,DELX,DELPHI,PHIMIN,PHIMAX,TOL,XONE,ZONE,OMEGA,S,ZZERO,RES,
     4KAR,J,INPUT,JI,INPERM,MB,MD
      DO 701 K=1,L
      J=L+1-K
      DO 701 I=1,N
      IF (I-1) 41,41,42
   41 IF (J-1) 32,32,43
   43 IF (J-JJ(I)) 44,25,26
   44 IF (JRITE(I)-1) 28,28,180
   42 IF (I-N) 46,47,47
   46 IF (J-1) 34,34,48
   48 IF (J-JJ(I)) 49,25,26
   49 IF (JLEFT(I)-1) 50,50,181
   50 IF (JRITE(I)-1) 3,3,182
   47 IF (J-1) 33,33,51
   51 IF (J-JJ(I)) 52,25,26
   52 IF (JLEFT(I)-1) 24,24,183
  180 IF (J-JJ(I+1)) 28,28,29
  183 IF (J-JJ(I-1)) 24,24,29
  182 IF (J-JJ(I+1)) 3,3,193
  181 IF (JRITE(I)-1) 185,185,186
  185 IF (J-JJ(I-1)) 3,3,192
  186 IF (JJ(I-1)-JJ(I+1)) 188,187,190
  187 IF (J-JJ(I-1)) 3,3,29
  188 IF (J-JJ(I-1)) 3,3,189
  189 IF (J-JJ(I+1)) 192,192,29
  190 IF (J-JJ(I+1)) 3,3,191
  191 IF (J-JJ(I-1)) 193,193,29
  193 JJA=JJ(I)-JJ(I+1)
      JJB=JJ(I)-J
      DELTA=DELX*FLOAT(JJB/JJA)
      PHIT=PHIN(I)-FLOAT(JJB/JJA)*(PHIN(I)-PHIN(I+1))
      GO TO 31
  192 JJC=JJ(I)-JJ(I-1)
      JJD=JJ(I)-J
      DELTA=DELX*FLOAT(JJD/JJC)
      PHIT=PHIN(I)-FLOAT(JJD/JJC)*(PHIN(I)-PHIN(I-1))
      GO TO 30
    3 DDF=(PERM(I,J)*PHI(I+1,J)+PERM(I-1,J)*PHI(I-1,J)+PERM(I,J)*PHI(I,
     1J+1)+PERM(I,J-1)*PHI(I,J-1))/(2.0*PERM(I,J)+PERM(I-1,J)+PERM
     2(I,J-1))
      GO TO 702
   24 DDF=(PERM(I-1,J)*2.0*PHI(I-1,J)+PERM(I,J)*PHI(I,J+1)+
     2PERM(I,J-1)*PHI(I,J-1))/(PERM(I,J)+2.0*PERM(I-1,J)+PERM(I,J-1))
      GO TO 702
```

```
   25 DDF=PHIN(I)
      GO TO 702
   26 DDF=0.0
      GO TO 702
   28 DDF=(2.0*PERM(I,J)*PHI(I+1,J)+PERM(I,J)*PHI(I,J+1)+PERM(I,J-1)*PHI
     1(I,J-1))/(3.0*PERM(I,J)+PERM(I,J-1))
      GO TO 702
   29 DDF=(PERM(I,J)*PHI(I,J+1)+PERM(I,J-1)*PHI(I,J-1))/(PERM(I,J)+
     1PERM(I,J-1))
      GO TO 702
   30 DDF=(PERM(I,J)*PHI(I+1,J)+DELX/DELTA*PHIT)+((DELTA+DELX)/(2.0*
     1DELX))*(PERM(I,J)*PHI(I,J+1)+PERM(I,J-1)*PHI(I,J-1)))/(PERM(I,J)
     2*(DELX/DELTA+1.0)+((DELTA+DELX)/(2.0*DELX))*(PERM(I,J)+PERM(I,J-1
     3)))
      GO TO 702
   31 DDF=(PERM(I-1,J)*PHI(I-1,J)+PERM(I,J)*PHIT*DELX/DELTA+((DELTA+DELX
     1)/(2.0*DELX))*(PERM(I,J)*PHI(I,J+1)+PERM(I,J-1)*PHI(I,J-1)))/(PERM
     2(I,J)*DELX/DELTA+PERM(I-1,J)+((DELTA+DELX)/(2.0*DELX))*(PERM(I,J)
     3+PERM(I,J-1)))
      GO TO 702
   32 DDF=(PHI(I,J+1)+PHI(I+1,J))/2.0
      GO TO 702
   33 DDF=(PERM(I,J)*PHI(I,J+1)+PERM(I-1,J)*PHI(I-1,J))/(PERM(I,J)+
     1PERM(I-1,J))
      GO TO 702
   34 DDF=(PERM(I,J)*PHI(I+1,J)+PERM(I-1,J)*PHI(I-1,J)+2.0*PERM(I,J)*
     1PHI(I,J+1))/(3.0*PERM(I,J)+PERM(I 1,J))
  702 GAF=ABS(DDF-PHI(I,J))
      IF (GAF-RES) 701,701,703
  703 RES=GAF
  701 PHI(I,J)=OMEGA*DDF+(1.0-OMEGA)*PHI(I,J)
      RETURN
      END
C
C
C
C
C
      SUBROUTINE CONFOR
      COMMON X(151),Z(41),PHI(151,41),PHIN(151),JJ(151),GUESS(151),
     1NP(10),GUEST(10),JRITE(151),JLEFT(151),PERM(151,41),PERK(41),
     2LP(41),GUESR(10),GUESQ(151),MA(41),MC(10),N,L,MM,
     3IPLOT,DELX,DELPHI,PHIMIN,PHIMAX,TOL,XONE,ZONE,OMEGA,S,ZZERO,RES,
     4KAR,J,INPUT,JI,INPERM,MB,MD
      DIMENSION T(4,3),XX(4),ZZ(4)
      COMMON /CCPOOL/ XMIN,XMAX,YMIN,YMAX,CCXMIN,CCXMAX,CCYMIN,CCYMAX
      IF (IPLOT-2) 40,41,42
   40 XMIN=-1875.0
      XMAX=23125.0
      YMIN=-4250.0
      YMAX=12250.0
      CCXMIN=100.0
      CCXMAX=1100.0
      CCYMIN=250.0
      CCYMAX=910.0
      CALL CCBGN
      CALL CCGRID (6HNOLBLS)
      XMIN=0.0
      XMAX=20000.0
      YMIN=-0.001
```

```
      YMAX=12000.0
      CCXMIN=175.0
      CCXMAX=975.0
      CCYMIN=420.0
      CCYMAX=900.0
      CALL CCBGN
      CALL CCGRID (1,10,6HNOLBLS,1,6)
      WRITE (98,20)
   20 FORMAT (116H0         0.1S          .2S         0.3S         0.4S
     1  0.5S        0.6S         0.7S          .8S         0.9S          S)
      CALL CCALTR (175.0,405.0,0,1)
      CALL CCALTR ( 980.0,420.0,0,1,1H0)
      CALL CCALTR (980.0,500.0,0,1,4H0.1S)
      CALL CCALTR (980.0,580.0,0,1,4H0.2S)
      CALL CCALTR (980.0,660.0,0,1,4H0.3S)
      CALL CCALTR (980.0,740.0,0,1,4H0.4S)
      CALL CCALTR (980.0,820.0,0,1,4H0.5S)
      CALL CCALTR (980.0,900.0,0,1,4H0.6S)
      GO TO 43
   41 XMIN=-1875.0
      XMAX=43125.0
      YMIN=-4250.0
      YMAX=12250.0
      CCXMIN=100.0
      CCXMAX=2100.0
      CCYMIN=250.0
      CCYMAX=910.0
      CALL CCBGN
      CALL CCGRID (6HNOLBLS)
      XMIN=0.0
      XMAX=40000.0
      YMIN=-0.001
      YMAX=12000.0
      CCXMIN=175.0
      CCXMAX=1775.0
      CCYMIN=420.0
      CCYMAX=900.0
      CALL CCBGN
      CALL CCGRID (1,20,6HNOLBLS,1,6)
      WRITE (98,21)
   21 FORMAT (117H0                          .1S                        0.2S
     1              0.3S                          .4S                          0.5S)
      CALL CCALTR (175.0,405.0,0,1)
      WRITE (98,23)
   23 FORMAT (113H                     0.6S                          0.7S
     1           0.8S                          .9S                           S)
      CALL CCALTR (989.0,405.0,0,1)
      CALL CCALTR (1780.0,420.0,0,1,1H0)
      CALL CCALTR (1780.0,580.0,0,1,4H0.1S)
      CALL CCALTR (1780.0,740.0,0,1,4H0.2S)
      CALL CCALTR (1780.0,900.0,0,1,4H0.3S)
      GO TO 43
   42 XMIN=-1875.0
      XMAX=63125.0
      YMIN=-4250.0
      YMAX=12250.0
      CCXMIN=100.0
      CCXMAX=3100.0
      CCYMIN=250.0
```

```
      CCYMAX=910.0
      CALL CCBGN
      CALL CCGRID (6HNOLBLS)
      XMIN=0.0
      XMAX=60000.0
      YMIN=-0.001
      YMAX=12000.0
      CCXMIN=175.0
      CCXMAX=2575.0
      CCYMIN=420.0
      CCYMAX=900.0
      CALL CCBGN
      CALL CCGRID (1,30,6HNOLBLS,1,6)
      WRITE (98,22)
   22 FORMAT (115H0                                        0.1S
     1              .2S                                      0.3S           )
      CALL CCALTR (175.0,405.0,0,1)
      WRITE (98,24)
   24 FORMAT (114H                       0.4S
     1 0.5S                                    .6S                          )
      CALL CCALTR (980.0,405.0,0,1)
      WRITE (98,25)
   25 FORMAT (114H         0.7S                                          0.8S
     1                       0.9S                                           S)
      CALL CCALTR (1778.0,405.0,0,1)
      CALL CCALTR (2580.0,420.0,0,1,1H0)
      CALL CCALTR (2580.0,660.0,0,1,4H0.1S)
      CALL CCALTR (2580.0,900.0,0,1,4H0.2S)
   43 LL=L-1
      NN=N-1
      DO 1 J=1,LL
      DO 2 I=1,NN
      PHILOW=AMIN1(PHI(I,J),PHI(I+1,J),PHI(I+1,J+1),PHI(I,J+1))
      PHIHI =AMAX1(PHI(I,J),PHI(I+1,J),PHI(I+1,J+1),PHI(I,J+1))
      IF (PHIHI-PHILOW) 2,2,51
   51 IF (PHILOW-PHIMAX) 53,53,2
   53 IF (PHIHI-PHIMIN) 2,5,5
    5 IF (PHILOW-PHIMIN) 56,54,55
   56 IF (PHILOW-10.0) 101,101,54
  101 TA=PHI(I,J)
      TB=PHI(I+1,J)
      TC=PHI(I+1,J+1)
      TD=PHI(I,J+1)
      IF (TA-10.0) 102,102,103
  105 IF (TC-10.0) 2,2,106
  106 PHILOW=AMIN1(TB,TC)
  102 IF (TB-10.0) 2,2,105
      GO TO 55
  103 IF (TB-10.0) 107,107,108
  107 IF(TD-10.0) 2,2,109
  109 PHILOW=AMIN1(TA,TD)
      GO TO 55
  108 IF (TC-TD) 110,112,111
  110 IF (TD-10.0) 112,112,113
  113 PHILOW=AMIN1(TA,TB,TD)
      GO TO 55
  111 IF (TC-10.0) 112,112,114
  114 PHILOW=AMIN1(TA,TB,TC)
      GO TO 55
  112 PHILOW=AMIN1(TA,TB)
```

```
      GO TO 55
   54 AA=PHIMIN
      GO TO 3
   55 AA= FLOAT(IFIX((PHILOW-PHIMIN)/DELPHI)+1)*DELPHI+PHIMIN
    3 IFLAG=0
      T(1,1)=PHI(I,J)
      T(2,1)=PHI(I+1,J)
      T(3,1)=PHI(I+1,J+1)
      T(4,1)=PHI(I,J+1)
      T(1,2)=X(I)
      T(2,2)=T(1,2)+DELX
      T(3,2)=T(2,2)
      T(4,2)=T(1,2)
      T(1,3)=Z(J)
      T(2,3)=T(1,3)
      T(3,3)=T(1,3)+DELX
      T(4,3)=T(3,3)
    4 K=0
  613 IF (T(1,1)-10.0) 11,11,600
  600 IF (T(2,1)-10.0) 11,11,6
    6 IF(T(1,1)-T(2,1)) 7,11,7
    7 F=(AA-T(1,1))/(T(2,1)-T(1,1))
      IF (F-1.0) 71,71,11
   71 IF(F) 11,11,8
    8 IDIOT=1+IFLAG
      XX(IDIOT)=(1.0-F)*T(1,2)+F*T(2,2)
      ZZ(IDIOT)=(1.0-F)*T(1,3)+F*T(2,3)
   85 IF(IFLAG) 10,10,9
    9 CALL CCPLOT (XX,ZZ,2,6HNOJOIN,1,1)
      XX(1)=XX(2)
      ZZ(1)=ZZ(2)
      GO TO 11
   10 IFLAG=1
   11 K=K+1
      IF(K-4) 13,12,12
   13 TT1=T(1,1)
      TT2=T(1,2)
      TT3=T(1,3)
      DO 131 NA=1,3
      DO 131 NB=1,3
  131 T(NB,NA)=T(NB+1,NA)
      T(4,1)=TT1
      T(4,2)=TT2
      T(4,3)=TT3
      GO TO 613
   12 AA=AA+DELPHI
   14 IF(AA-PHIHI) 15,15,2
   15 IF (AA-PHIMAX) 3,3,2
    2 CONTINUE
    1 CONTINUE
      RETURN
      END
```

```
C NUMERICAL PROGRAM 5
      COMMON X(101),Z(31),PHI(101,31),PHIN(101),JJ(101),GUESS(101),
     1NP(10),GUEST(10),JRITE(101),JLEFT(101),PERMH(101,31),PERMV(101,31)
     2,PERKH(31),PERKV(31),LP(31),GUESR(10),GUESQ(101),MA(31),MC(10),
     3N,L,MM,DELX,DELPHI,PHIMIN,PHIMAX,TOL,XONE,ZONE,OMEGA,S,
     4ZZERO,RES,KAR,J,INPUT,JI,INPERM,MB,MD,DELZ,ALPHA,ALFA,SXPL,SZPL
     5,SX,SZ
 7000 READ 7001,TITLE1,TITLE2
 7001 FORMAT (2A6)
      IF (TITLE1) 7300,1000,7300
 7300 READ 300,N,L,MM,MP,INPUT,JI,INPERM,KART
      READ 301,DELX,DELZ,DELPHI,PHIMIN,PHIMAX,TOL,XONE,ZONE,OMEGA,S,
     1ZZERO,SXPL,SZPL,SX,SZ
      READ 301, (PHIN(I),I=1,N)
      READ 302,(JJ(I),I=1,N)
  300 FORMAT (14I5)
  301 FORMAT (7F10.2)
  302 FORMAT (24I3)
      MMM=MM+1
      READ 300,(NP(M),M=1,MMM)
      READ 301,(GUEST(M),M=1,MM)
      IF (INPUT-1) 6001,6000,6000
 6000 READ 301, (GUESR(M),M=1,MM)
 6001 DO 305 M=1,MM
      NPR=NP(M)
      NPQ=NP(M+1)
      DO 306 I=NPR,NPQ
      IF (INPUT-1) 306,6306,6306
 6306 GUESQ(I)=GUESR(M)
  306 GUESS(I)=GUEST(M)
  305 CONTINUE
      IF (INPERM-1) 6010,6011,6011
 6010 MMP=MP+1
      READ 300, (LP(M),M=1,MMP)
      READ 301, (PERKH(M),M=1,MP)
      READ 301, (PERKV(M),M=1,MP)
      DO 1120 M=1,MP
      LPR=LP(M)
      LPQ=LP(M+1)
      DO 1121 J=LPR,LPQ
      DO 1121 I=1,N
      PERMH(I,J)=PERKH(M)
 1121 PERMV(I,J)=PERKV(M)
 1120 CONTINUE
      GO TO 6012
 6011 READ 300, (MA(J),J=1,L)
      DO 6022 J=1,L
      MB=MA(J)+1
      MD=MA(J)
      READ 300, (MC(M),M=1,MB)
      READ 301, (PERKH(M),M=1,MD)
      READ 301, (PERKV(M),M=1,MD)
      DO 6021 M=1,MD
      MCR=MC(M)
      MCQ=MC(M+1)
      DO 6020 I=MCR,MCQ
      PERMH(I,J)=PERKH(M)
 6020 PERMV(I,J)=PERKV(M)
 6021 CONTINUE
```

```
 6022 CONTINUE
C
 6012 DO 330 I=1,N
      IF (I-1) 331,331,332
  331 X(1)=XONE
      GO TO 330
  332 X(I)=X(I-1)+DELX
  330 CONTINUE
C
      DO 340 J=1,L
      IF (J-1) 341,341,342
  341 Z(1)=ZONE
      GO TO 340
  342 Z(J)=Z(J-1)+DELZ
  340 CONTINUE
C
      ZZERA=FLOAT(JJ(1)-1)*DELZ
      IF (ZZERA-ZZERO) 376,377,376
  377 SA=FLOAT(N-1)*DELX
      IF (SA-S) 376,320,376
  376 PRINT 378
  378 FORMAT (1H1,18H     CHECK GEOMETRY)
      GO TO 7000
C
  320 DO 328 I=1,N
      JRITE(I)=JJ(I)-JJ(I+1)
      JLEFT(I)=JJ(I)-JJ(I-1)
      DO 328 J=1,L
      IF (J-JJ(I)) 325,326,327
  327 PHI(I,J)=0.0
      GO TO 328
  326 PHI(I,J)=PHIN(I)
      GO TO 328
  325 IF (INPUT-1) 6400,6401,6401
 6401 IF (J-JI)  6402,6403,6403
 6402 PHI(I,J)=GUESS(I)
      GO TO 328
 6403 PHI(I,J)=GUESQ(I)
      GO TO 328
 6400 PHI(I,J)=GUESS(I)
  328 CONTINUE
C
      ALPHA=DELX/DELZ
      ALFA=ALPHA**2
C
      DO 206 KAR=1,KART
      RES=0.0
   40 CALL MESH1C
  205 IF (RES-TOL) 400,206,206
  206 CONTINUE
C
  400 PRINT 401,KAR,RES
  401 FORMAT (1H1,I10,F10.5)
C
      PRINT 403,TITLE1,TITLE2
  403 FORMAT (1H1,24H1      NUMERICAL PROBLEM 2A6//12X,4HX(I)//)
      PRINT 404,(X(I),I=1,N)
      PRINT 405
  405 FORMAT (1H1,12X,4HZ(J)//)
      PRINT 404,(Z(J),J=1,L)
```

```
  404 FORMAT (10F12.4)
      PRINT 415
  415 FORMAT (1H1,10X,8HPHI(I,J)//)
      DO 406 I=1,N
      PRINT 407,I
  407 FORMAT (1H0,12X,2HI=,I3//)
  406 PRINT 408, (PHI(I,J),J=1,L)
  408 FORMAT (10F12.4)
  414 CALL CONFIV
      CALL CCNEXT
      GO TO 7000
 1000 CALL CCEND
      STOP
      END
C
C
C
C
C
      SUBROUTINE MESH1C
      COMMON X(101),Z(31),PHI(101,31),PHIN(101),JJ(101),GUESS(101),
     1NP(10),GUEST(10),JRITE(101),JLEFT(101),PERMH(101,31),PERMV(101,31)
     2,PERKH(31),PERKV(31),LP(31),GUESR(10),GUESQ(101),MA(31),MC(10),
     3N,L,MM,DELX,DELPHI,PHIMIN,PHIMAX,TOL,XONE,ZONE,OMEGA,S,
     4ZZERO,RES,KAR,J,INPUT,JI,INPERM,MB,MD,DELZ,ALPHA,ALFA,SXPL,SZPL
     5,SX,SZ
      DO 701 K=1,L
      J=L+1-K
      DO 701 I=1,N
      IF (I-1) 41,41,42
   41 IF (J-1) 32,32,43
   43 IF (J-JJ(I)) 44,25,26
   44 IF (JRITE(I)-1) 28,28,180
   42 IF (I-N) 46,47,47
   46 IF (J-1) 34,34,48
   48 IF (J-JJ(I)) 49,25,26
   49 IF (JLEFT(I)-1) 50,50,181
   50 IF (JRITE(I)-1) 3,3,182
   47 IF (J-1) 33,33,51
   51 IF (J-JJ(I)) 52,25,26
   52 IF (JLEFT(I)-1) 24,24,183
  180 IF (J-JJ(I+1)) 28,28,29
  183 IF (J-JJ(I-1)) 24,24,29
  182 IF (J-JJ(I+1)) 3,3,193
  181 IF (JRITE(I)-1) 185,185,186
  185 IF (J-JJ(I-1)) 3,3,192
  186 IF (JJ(I-1)-JJ(I+1)) 188,187,190
  187 IF (J-JJ(I-1)) 3,3,29
  188 IF (J-JJ(I-1)) 3,3,189
  189 IF (J-JJ(I+1)) 192,192,29
  190 IF (J-JJ(I+1)) 3,3,191
  191 IF (J-JJ(I-1)) 193,193,29
  193 JJA=JJ(I)-JJ(I+1)
      JJB=JJ(I)-J
      DELTA=DELX*FLOAT(JJB/JJA)
      PHIT=PHIN(I)-FLOAT(JJB/JJA)*(PHIN(I)-PHIN(I+1))
      GO TO 31
  192 JJC=JJ(I)-JJ(I-1)
      JJD=JJ(I)-J
```

```
      DELTA=DELX*FLOAT(JJD/JJC)
      PHIT=PHIN(I)-FLOAT(JJD/JJC)*(PHIN(I)-PHIN(I-1))
      GO TO 30
    3 DDF=(PERMH(I,J)*PHI(I+1,J)+PERMH(I-1,J)*PHI(I-1,J)+ALFA*PERMV(I,J)
     1*PHI(I,J+1)+ALFA*PERMV(I,J-1)*PHI(I,J-1))/(PERMH(I,J)+PERMH(I-1,J)
     2+ALFA*(PERMV(I,J-1)+PERMV(I,J)))
      GO TO 702
   24 DDF=(PERMH(I-1,J)*2.0*PHI(I-1,J)+ALFA*PERMV(I,J)*PHI(I,J+1)+ALFA*
     2PERMV(I,J-1)*PHI(I,J-1))/(2.0*PERMH(I-1,J)+ALFA*(PERMV(I,J-1)
     3+PERMV(I,J)))
      GO TO 702
   25 DDF=PHIN(I)
      GO TO 702
   26 DDF=0.0
      GO TO 702
   28 DDF=(2.0*PERMH(I,J)*PHI(I+1,J)+ALFA*PERMV(I,J)*PHI(I,J+1)+ALFA*
     1PERMV(I,J-1)*PHI(I,J-1))/(2.0*PERMH(I,J) ALFA*(PERMV(I,J-1)+
     2PERMV(I,J)))
      GO TO 702
   29 DDF=(PERMV(I,J)*PHI(I,J+1)+PERMV(I,J-1)*PHI(I,J-1))/(PERMV(I,J)
     1PERMV(I,J-1))
      GO TO 702
   30 DDF=(PERMH(I,J)*(PHI(I+1,J)*DELZ/DELX+PHIT*DELZ/DELTA)+((DELTA+
     1DELX)/(2.0*DELZ))*(PERMV(I,J)*PHI(I,J+1)+PERMV(I,J-1)*PHI(I,J-1)))
     2/(PERMH(I,J)*(DELZ/DELTA+DELZ/DELX)+((DELTA+DELX)/(2.0*DELZ))*
     3(PERMV(I,J)+PERMV(I,J-1)))
      GO TO 702
   31 DDF=(PERMH(I,J)*PHIT*DELZ/DELTA+PERMH(I-1,J)*PHI(I-1,J)*DELZ/DELX
     1+((DELTA+DELX)/(2.0*DELZ))*(PERMV(I,J)*PHI(I,J+1)+PERMV(I,J-1)*PHI
     2(I,J-1)))/(PERMH(I,J)*DELZ/DELTA+PERMH(I-1,J)*DELZ/DELX+((DELTA
     3+DELX)/(2.0*DELZ))*(PERMV(I,J)+PERMV(I,J-1)))
      GO TO 702
   32 DDF=(ALFA*PERMV(I,J)*PHI(I,J+1)+PERMH(I,J)*PHI(I+1,J))/(ALFA*
     1PERMV(I,J)+PERMH(I,J))
      GO TO 702
   33 DDF=(ALFA*PERMV(I,J)*PHI(I,J+1)+PERMH(I-1,J)*PHI(I-1,J))/(ALFA*
     1PERMV(I,J)+PERMH(I-1,J))
      GO TO 702
   34 DDF=(PERMH(I,J)*PHI(I+1,J)+PERMH(I-1,J)*PHI(I-1,J)+2.0*ALFA*
     1PERMV(I,J)*PHI(I,J+1))/(2.0*ALFA*PERMV(I,J)+PERMH(I-1,J)+PERMH(I,J
     2))
  702 GAF=ABS(DDF-PHI(I,J))
      IF (GAF-RES) 701,701,703
  703 RES=GAF
  701 PHI(I,J)=OMEGA*DDF+(1.0-OMEGA)*PHI(I,J)
      RETURN
      END
C
C
C
C
C
      SUBROUTINE CONFIV
      COMMON X(101),Z(31),PHI(101,31),PHIN(101),JJ(101),GUESS(101),
     1NP(10),GUEST(10),JRITE(101),JLEFT(101),PERMH(101,31),PERMV(101,31)
     2,PERKH(31),PERKV(31),LP(31),GUESR(10),GUESQ(101),MA(31),MC(10),
     3N,L,MM,DELX,DELPHI,PHIMIN,PHIMAX,TOL,XONE,ZONE,OMEGA,S,
     4ZZERO,RES,KAR,J,INPUT,JI,INPERM,MB,MD,DELZ,ALPHA,ALFA,SXPL,SZPL
     5,SX,SZ
      DIMENSION T(4,3),XX(4),ZZ(4)
```

```
      COMMON /CCPOOL/ XMIN,XMAX,YMIN,YMAX,CCXMIN,CCXMAX,CCYMIN,CCYMAX
      XMIN=0.0
      XMAX=SX
      YMIN=-0.001
      YMAX=SZ
      CCXMIN=175.0
      CCXMAX=SXPL
      CCYMIN=420.0
      CCYMAX=SZPL
      CALL CCBGN
      CALL CCGRID (6HNOLBLS)
      LL=L-1
      NN=N-1
      DO 1 J=1,LL
      DO 2 I=1,NN
      PHILOW=AMIN1(PHI(I,J),PHI(I+1,J),PHI(I+1,J+1),PHI(I,J+1))
      PHIHI =AMAX1(PHI(I,J),PHI(I+1,J),PHI(I+1,J+1),PHI(I,J+1))
      IF (PHIHI-PHILOW) 2,2,51
   51 IF (PHILOW-PHIMAX) 53,53,2
   53 IF (PHIHI-PHIMIN) 2,5,5
    5 IF (PHILOW-PHIMIN) 56,54,55
   56 IF (PHILOW-10.0) 101,101,54
  101 TA=PHI(I,J)
      TB=PHI(I+1,J)
      TC=PHI(I+1,J+1)
      TD=PHI(I,J+1)
      IF (TA-10.0) 102,102,103
  102 IF (TB-10.0) 2,2,105
  105 IF (TC-10.0) 2,2,106
  106 PHILOW=AMIN1(TB,TC)
      GO TO 55
  103 IF (TB-10.0) 107,107,108
  107 IF(TD-10.0) 2,2,109
  109 PHILOW=AMIN1(TA,TD)
      GO TO 55
  108 IF (TC-TD) 110,112,111
  110 IF (TD-10.0) 112,112,113
  113 PHILOW=AMIN1(TA,TB,TD)
      GO TO 55
  111 IF (TC-10.0) 112,112,114
  114 PHILOW=AMIN1(TA,TB,TC)
      GO TO 55
  112 PHILOW=AMIN1(TA,TB)
      GO TO 55
   54 AA=PHIMIN
      GO TO 3
   55 AA= FLOAT(IFIX((PHILOW-PHIMIN)/DELPHI)+1)*DELPHI+PHIMIN
    3 IFLAG=0
      T(1,1)=PHI(I,J)
      T(2,1)=PHI(I+1,J)
      T(3,1)=PHI(I+1,J+1)
      T(4,1)=PHI(I,J+1)
      T(1,2)=X(I)
      T(2,2)=T(1,2)+DELX
      T(3,2)=T(2,2)
      T(4,2)=T(1,2)
      T(1,3)=Z(J)
      T(2,3)=T(1,3)
      T(3,3)=T(1,3)+DELZ
```

```
      T(4,3)=T(3,3)
    4 K=0
  613 IF (T(1,1)-10.0) 11,11,600
  600 IF (T(2,1)-10.0) 11,11,6
    6 IF(T(1,1)-T(2,1)) 7,11,7
    7 F=(AA-T(1,1))/(T(2,1)-T(1,1))
      IF (F-1.0) 71,71,11
   71 IF(F) 11,11,8
    8 IDIOT=1+IFLAG
      XX(IDIOT)=(1.0-F)*T(1,2)+F*T(2,2)
      ZZ(IDIOT)=(1.0-F)*T(1,3)+F*T(2,3)
   85 IF(IFLAG) 10,10,9
    9 CALL CCPLOT (XX,ZZ,2,6HNOJOIN,1,1)
      XX(1)=XX(2)
      ZZ(1)=ZZ(2)
      GO TO 11
   10 IFLAG=1
   11 K=K+1
      IF(K-4) 13,12,12
   13 TT1=T(1,1)
      TT2=T(1,2)
      TT3=T(1,3)
      DO 131 NA=1,3
      DO 131 NB=1,3
  131 T(NB,NA)=T(NB+1,NA)
      T(4,1)=TT1
      T(4,2)=TT2
      T(4,3)=TT3
      GO TO 613
   12 AA=AA+DELPHI
   14 IF(AA-PHIHI) 15,15,2
   15 IF (AA-PHIMAX) 3,3,2
    2 CONTINUE
    1 CONTINUE
      RETURN
      END
```

```
C NUMERICAL PROGRAM 6
      COMMON X(25),Y(25),Z(12),PHI(25,25,12),PERM(25,25,12),PHIN(25,
     125),JJ(25,25),GUESI(25),GUESK(25),IPERM(12),PERL2(25),PERL3(25),
     2MA(25),NA(25),MB(12),NB(12),PERL4(12),PERL5(12),KPLOT(25),IPLOT
     3(25),JPLOT(12),RES,TOL,OMEGA,N,M,L,ALPHA,ALFA,PHIMAX,PHIMIN,
     4SX,SY,SZ,SXPL,SYPL,SZPL,DELPHI,I,J,K,DELX,DELZ
 7000 READ 103,TITLE1,TITLE2
      IF (TITLE1) 7001,1000,7001
 7001 READ 100,N,M,L,MAY,KART
      READ 101,DELX,DELZ,TOL,OMEGA,SX,SY,SZ,ALPHA,PHIMIN,PHIMAX,
     1SXPL,SYPL,SZPL,DELPHI
      READ 101,((PHIN(I,K),I=1,N),K=1,M)
      READ 102, (KPLOT(K),K=1,M)
      READ 102, (IPLOT(I),I=1,N)
      READ 102, (JPLOT(J), J=1,L)
      READ 102,((JJ(I,K),I=1,N),K=1,M)
      READ 102,(IPERM(J),J=1,L)
  100 FORMAT (14I5)
  101 FORMAT (7F10.2)
  102 FORMAT (24I3)
  103 FORMAT (2A6)
      IF (MAY) 105,105,106
  105 READ 101,(GUESI(I),I=1,N)
      GO TO 107
  106 READ 101,(GUESK(K),K=1,M)
C
  107 DO 129 J=1,L
      IF (IPERM(J)-2) 108,109,110
  110 IF (IPERM(J)-4) 115,116,119
  108 READ 101,PERL1
      DO 111 I=1,N
      DO 111 K=1,M
  111 PERM(I,K,J)=PERL1
      GO TO 129
  109 READ 101, (PERL2(I),I=1,N)
      DO 112 I=1,N
      DO 112 K=1,M
  112 PERM(I,K,J)=PERL2(I)
      GO TO 129
  115 READ 101,(PERL3(K),K=1,M)
      DO 113 K=1,M
      DO 113 I=1,N
  113 PERM(I,K,J)=PERL3(K)
      GO TO 129
  116 READ 100, (MA(I),I=1,N)
      DO 118 I=1,N
      MC=MA(I)+1
      READ 100, (MB(MK),MK=1,MC)
      MD=MA(I)
      READ 101, (PERL4(ME),ME=1,MD)
      DO 118 ME=1,MD
      MG=MB(ME)
      MH=MB(ME+1)
      DO 117 K=MG,MH
  117 PERM(I,K,J)=PERL4(ME)
  118 CONTINUE
      GO TO 129
  119 READ 100, (NA(K),K=1,M)
      DO 128 K=1,M
      NC=NA(K)+1
```

```
      READ 100, (NB(NK),NK=1,NC)
      ND=NA(K)
      READ 101, (PERL5(NE),NE=1,ND)
      DO 128 NE=1,ND
      NG=NB(NE)
      NH=NB(NE+1)
      DO 127 I=NG,NH
  127 PERM(I,K,J)=PERL5(NE)
  128 CONTINUE
  129 CONTINUE
C
      DO 132 I=1,N
      IF (I-1) 130,130,131
  130 X(I)=0.0
      GO TO 132
  131 X(I)=X(I-1)+DELX
  132 CONTINUE
      SXX=ABS(X(N)-SX)
      IF (SXX-10.0) 133,140,140
C
  133 DO 138 K=1,M
      IF (K-1) 134,134,135
  134 Y(K)=0.0
      GO TO 138
  135 Y(K)=Y(K-1)+DELX
  138 CONTINUE
      SYY=ABS(Y(M)-SY)
      IF (SYY-10.0) 139,140,140
C
  139 DO 141 J=1,L
      IF (J-1) 142,142,143
  142 Z(J)=0.0
      GO TO 141
  143 Z(J)=Z(J-1)+DELZ
  141 CONTINUE
      SZZ=ABS(Z(L)-SZ)
      IF (SZZ-10.0) 145,140,140
C
  140 PRINT 144
  144 FORMAT (1H1,18H     CHECK GEOMETRY)
      GO TO 7000
C
  145 DO 151 J=1,L
      DO 151 I=1,N
      DO 151 K=1,M
      IF (J-JJ(I,K)) 146,147,148
  148 PHI(I,K,J)=0.
      GO TO 151
  147 PHI(I,K,J)=PHIN(I,K)
      GO TO 151
  146 IF (MAY) 149,149,150
  149 PHI(I,K,J)=GUESI(I)
      GO TO 151
  150 PHI(I,K,J)=GUESK(K)
  151 CONTINUE
C
      ALFA=ALPHA**2
C
      DO 160 KAR=1,KART
```

```
      RES=0.0
      CALL MESH8
      IF (RES-TOL) 161,160,16
  160 CONTINUE
C
  161 PRINT 401,KAR,RES
  401 FORMAT (1H1,I10,F10.5)
C
      PRINT 403,TITLE1,TITLE2
  403 FORMAT (1H1,24H1     NUMERICAL PROBLEM 2A6//12X,4HX(I)//)
      PRINT 404,(X(I),I=1,N)
      PRINT 420
  420 FORMAT (1H1,12X,4HY(K)//)
      PRINT 404,(Y(K),K=1,M)
      PRINT 405
  405 FORMAT (1H1,12X,4HZ(J)//)
      PRINT 404,(Z(J),J=1,L)
  404 FORMAT (10F12.4)
      PRINT 415
  415 FORMAT (1H1,10X,10HPHI(I,K,J)//)
      DO 425 J=1,L
      PRINT 427,J
  427 FORMAT (1H0,12X,2HJ=,I2//)
      DO 406 I=1,N
      PRINT 407,I
  407 FORMAT (1H0,12X,2HI=,I2//)
  406 PRINT 408, (PHI(I,K,J),K=1,M)
  408 FORMAT (10F12.4)
  425 CONTINUE
      DO 501 K=1,M
      IF (KPLOT(K)) 500,500,501
  500 CALL CONSKX
      CALL CCNEXT
  501 CONTINUE
      DO 502 I=1,N
      IF (IPLOT(I)) 503,503,502
  503 CALL CONSIX
      CALL CCNEXT
  502 CONTINUE
      DO 504 J=1,L
      IF (JPLOT(J)) 505,505,504
  505 CALL CONSJX
      CALL CCNEXT
  504 CONTINUE
      GO TO 7000
 1000 CALL CCEND
      STOP
      END
C
C
C
C
C
      SUBROUTINE MESH8
      COMMON X(25),Y(25),Z(12),PHI(25,25,12),PERM(25,25,12),PHIN(25,
     125),JJ(25,25),GUESI(25),GUESK(25),IPERM(12),PERL2(25),PERL3(25),
     2MA(25),NA(25),MB(12),NB(12),PERL4(12),PERL5(12),KPLOT(25),IPLOT
     3(25),JPLOT(12),RES,TOL,OMEGA,N,M,L,ALPHA,ALFA,PHIMAX,PHIMIN,
     4SX,SY,SZ,SXPL,SYPL,SZPL,DELPHI,I,J,K,DELX,DELZ
      DO 200 JTOP=1,L
```

```
      J=L+1-JTOP
      DO 200 I=1,N
      DO 200 K=1,M
      IF (J-JJ(I,K)) 210,2,1
  210 IF (I-1) 211,211,220
  211 IF (K-1) 212,212,213
  212 IF (J-1) 13,13,8
  213 IF (K-M) 215,214,214
  214 IF (J-1) 16,16,11
  215 IF (J-1) 216,216,217
  216 IF (JJ(I,K-1)-1)  13,13,218
  218 IF (JJ(I,K+1)-1)  16,16,17
  217 IF (JJ(I,K-1)-1)  8,8,219
  219 IF (JJ(I,K+1)-1)  11,11,6
  220 IF (I-N) 230,221,221
  221 IF (K-1) 222,222,223
  222 IF (J-1) 14,14,9
  223 IF (K-M) 225,224,224
  224 IF (J-1) 15,15,10
  225 IF (J-1) 226,226,227
  226 IF (JJ(I,K-1)-1)  14,14,228
  228 IF (JJ(I,K+1)-1)  15,15,18
  227 IF (JJ(I,K-1)-1)  9,9,229
  229 IF (JJ(I,K+1)-1)  10,10,7
  230 IF (K-1) 231,231,236
  231 IF (J-1) 232,232,234
  232 IF (JJ(I-1,K)-1)  13,13,233
  233 IF (JJ(I+1,K)-1)  14,14,19
  234 IF (JJ(I-1,K)-1)  8,8,235
  235 IF (JJ(I+1,K)-1)  9,9,4
  236 IF (K-M) 242,237,237
  237 IF (J-1) 238,238,240
  238 IF (JJ(I-1,K)-1)  16,16,239
  239 IF (JJ(I+1,K)-1)  15,15,20
  240 IF (JJ(I-1,K)-1)  11,11,241
  241 IF (JJ(I+1,K)-1)  10,10,5
  242 IF (J-1) 243,243,253
  243 IF (JJ(I-1,K)-1)  244,244,246
  244 IF (JJ(I,K-1)-1)  13,13,245
  245 IF (JJ(I,K+1)-1)  16,16,17
  246 IF (JJ(I+1,K)-1)  247,247,249
  247 IF (JJ(I,K-1)-1)  14,14,248
  248 IF (JJ(I,K+1)-1)  15,15,18
  249 IF (JJ(I,K-1)-1)  19,19,250
  250 IF (JJ(I,K+1)-1)  20,20,12
  253 IF (JJ(I-1,K)-1)  254,254,256
  254 IF (JJ(I,K-1)-1)  8,8,255
  255 IF (JJ(I,K+1)-1)  11,11,6
  256 IF (JJ(I+1,K)-1)  257,257,259
  257 IF (JJ(I,K-1)-1)  9,9,258
  258 IF (JJ(I,K+1)-1)  10,10,7
  259 IF (JJ(I,K-1)-1)  4,4,260
  260 IF (JJ(I,K+1)-1)  5,5,3
    1 DDF=0.0
      GO TO 201
    2 DDF=PHIN(I,K)
      GO TO 201
    3 DDF=(PERM(I,K,J)*(PHI(I+1,K,J)+PHI(I,K+1,J)+ALFA*PHI(I,K,J+1))
     1+PERM(I-1,K,J)*PHI(I-1,K,J)+PERM(I,K-1,J)*PHI(I,K-1,J)+ALFA*
```

```
     2PERM(I,K,J-1)*PHI(I,K,J-1))/((2.0+ALFA)*PERM(I,K,J)+PERM(I-1,K,J)
     3+PERM(I,K-1,J)+ALFA*PERM(I,K,J-1))
      GO TO 201
    4 DDF=(PERM(I,K,J)*(PHI(I+1,K,J)+2.0*PHI(I,K+1,J)+ALFA*PHI(I,
     1K,J+1))+PERM(I-1,K,J)*PHI(I-1,K,J)+ALFA*PERM(I,K,J-1)*PHI
     2(I,K,J-1))/((3.0+ALFA)*PERM(I,K,J)+PERM(I-1,K,J)+ALFA*PERM(I,K,
     3J-1))
      GO TO 201
    5 DDF=(PERM(I,K,J)*(PHI(I+1,K,J)+ALFA*PHI(I,K,J+1))
     1+PERM(I-1,K,J)*PHI(I-1,K,J)+2.0*PERM(I,K 1,J)*PHI(I,K-1,J)+ALFA*
     2PERM(I,K,J-1)*PHI(I,K,J-1))/((1.0+ALFA)*PERM(I,K,J)+PERM(I-1,K,
     3J)+2.0*PERM(I,K-1,J)+ALFA*PERM(I,K,J-1))
      GO TO 201
    6 DDF=(PERM(I,K,J)*(2.0*PHI(I+1,K,J)+PHI(I,K+1,J)+ALFA*PHI(I,K,J+1))
     1+PERM(I,K-1,J)*PHI(I,K-1,J)+ALFA
     2*PERM(I,K,J-1)*PHI(I,K,J-1))/((3.0+ALFA)*PERM(I,K,J)
     3+PERM(I,K-1,J)+ALFA*PERM(I,K,J-1))
      GO TO 201
    7 DDF=(PERM(I,K,J)*(PHI(I,K+1,J)+ALFA*PHI(I,K,J+1))
     1+2.0*PERM(I-1,K,J)*PHI(I-1,K,J)+PERM(I,K 1,J)*PHI(I,K-1,J)+ALFA*
     2PERM(I,K,J-1)*PHI(I,K,J-1))/((1.0+ALFA)*PERM(I,K,J)+2.0*PERM(I-1,K
     3,J)+PERM(I,K-1,J)+ALFA*PERM(I,K,J 1))
      GO TO 201
    8 DDF=(PERM(I,K,J)*(2.0*PHI(I+1,K,J)+2.0*PHI(I,K+1,J)+ALFA*
     1PHI(I,K,J+1))+ALFA*PERM(I,K,J-1)*PHI(I,K,J-1))/((4.0+ALFA)
     2*PERM(I,K,J)+ALFA*PERM(I,K,J-1))
      GO TO 201
    9 DDF=(PERM(I,K,J)*(2.0*PHI(I,K+1,J)+ALFA*PHI(I,K,J+1))
     1+2.0*PERM(I-1,K,J)*PHI(I-1,K,J)+ALFA*
     2PERM(I,K,J-1)*PHI(I,K,J-1))/((2.0+ALFA)*PERM(I,K,J)+2.0*PERM(I-1,K
     3,J)+ALFA*PERM(I,K,J-1))
      GO TO 201
   10 DDF=(PERM(I,K,J)*ALFA*PHI(I,K,J+1)
     1+2.0*PERM(I-1,K,J)*PHI(I-1,K,J)+2.0*PERM(I,K-1,J)*PHI(I,K-1,J)+
     2ALFA*PERM(I,K,J-1)*PHI(I,K,J-1))/(ALFA*PERM(I,K,J)+2.0*PERM(I-1,K,
     3J)+2.0*PERM(I,K-1,J)+ALFA*PERM(I,K,J-1))
      GO TO 201
   11 DDF=(PERM(I,K,J)*(2.0*PHI(I+1,K,J)+ALFA*PHI(I,K,J+1))
     1+2.0*PERM(I,K-1,J)*PHI(I,K-1,J)+ALFA*
     2PERM(I,K,J-1)*PHI(I,K,J-1))/((2.0+ALFA)*PERM(I,K,J)+2.0*PERM(I,K-1
     3,J)+ALFA*PERM(I,K,J-1))
      GO TO 201
   12 DDF=(PERM(I,K,J)*(PHI(I+1,K,J)+PHI(I,K+1,J)+2.0*ALFA*PHI(I,K,
     1J+1))+PERM(I-1,K,J)*PHI(I-1,K,J)+PERM(I,K-1,J)*PHI(I,K-1,J))
     2/((2.0+2.0*ALFA)*PERM(I,K,J)+PERM(I-1,K,J)
     3+PERM(I,K-1,J))
      GO TO 201
   13 DDF=(PERM(I,K,J)*2.0*(PHI(I+1,K,J)+PHI(I,K+1,J)+ALFA*PHI(I,K,
     1J+1)))/((4.0+2.0*ALFA)*PERM(I,K,J))
      GO TO 201
   14 DDF=(PERM(I,K,J)*2.0*(PHI(I,K+1,J)+ALFA*PHI(I,K,J+1))
     1+2.0*PERM(I-1,K,J)*PHI(I-1,K,J))/((2.0+2.0*ALFA)
     2*PERM(I,K,J)+2.0*PERM(I-1,K,J))
      GO TO 201
   15 DDF=(2.0*PERM(I,K,J)*ALFA*PHI(I,K,J+1)
     1+2.0*PERM(I-1,K,J)*PHI(I-1,K,J)+2.0*PERM(I,K-1,J)*PHI(I,K-1,J))/
     2(2.0*ALFA*PERM(I,K,J)+2.0*PERM(I-1,K,J)+2.0*PERM(I,K-1,J))
      GO TO 201
   16 DDF=(PERM(I,K,J)*2.0*(PHI(I+1,K,J)+ALFA*PHI(I,K,J+1))
     1+2.0*PERM(I,K-1,J)*PHI(I,K-1,J))/((2.0+2.0*ALFA)
```

```
     2*PERM(I,K,J)+2.0*PERM(I,K-1,J))
      GO TO 201
   17 DDF=(PERM(I,K,J)*(2.0*PHI(I+1,K,J)+PHI(I,K+1,J)+2.0*ALFA*PHI(I,K,
     1J+1))+PERM(I,K-1,J)*PHI(I,K-1,J))/((3.0+2.0*ALFA)*PERM(I,K,J)
     2+PERM(I,K-1,J))
      GO TO 201
   18 DDF=(PERM(I,K,J)*(PHI(I,K+1,J)+2.0*ALFA*PHI(I,K,J+1))
     1+2.0*PERM(I-1,K,J)*PHI(I-1,K,J)+PERM(I,K 1,J)*PHI(I,K-1,J))
     2/((1.0+2.0*ALFA)*PERM(I,K,J)+2.0*PERM(I-1,K,J)+PERM(I,K-1,J))
      GO TO 201
   19 DDF=(PERM(I,K,J)*(PHI(I+1,K,J)+2.0*PHI(I,K+1,J)+ALFA*2.0*PHI(I,K,
     1J+1))+PERM(I-1,K,J)*PHI(I-1,K,J))/((3.0+2.0*ALFA)*PERM(I,K,J)
     2+PERM(I-1,K,J))
      GO TO 201
   20 DDF=(PERM(I,K,J)*(PHI(I+1,K,J)+2.0*ALFA*PHI(I,K,J+1))
     1+PERM(I-1,K,J)*PHI(I-1,K,J)+2.0*PERM(I,K 1,J)*PHI(I,K-1,J))/
     2((1.0+2.0*ALFA)*PERM(I,K,J)+PERM(I-1,K,J)+2.0*PERM(I,K-1,J))
  201 GAF=ABS(DDF-PHI(I,K,J))
      IF (GAF-RES) 200,200,202
  202 RES=GAF
  200 PHI(I,K,J)=OMEGA*DDF+(1.0-OMEGA)*PHI(I,K,J)
      RETURN
      END
C
C
C
C
C
      SUBROUTINE CONSKX
      COMMON X(25),Y(25),Z(12),PHI(25,25,12),PERM(25,25,12),PHIN(25,
     125),JJ(25,25),GUESI(25),GUESK(25),IPERM(12),PERL2(25),PERL3(25),
     2MA(25),NA(25),MB(12),NB(12),PERL4(12),PERL5(12),KPLOT(25),IPLOT
     3(25),JPLOT(12),RES,TOL,OMEGA,N,M,L,ALPHA,ALFA,PHIMAX,PHIMIN,
     4SX,SY,SZ,SXPL,SYPL,SZPL,DELPHI,I,J,K,DELX,DELZ
      DIMENSION T(4,3),XX(2),ZZ(2)
      COMMON /CCPOOL/ XMIN,XMAX,YMIN,YMAX,CCXMIN,CCXMAX,CCYMIN,CCYMAX
      XMIN=0.0
      XMAX=SX
      YMIN=0.0
      YMAX=SZ
      CCXMIN=100.0
      CCXMAX=SXPL
      CCYMIN=100.0
      CCYMAX=SZPL
      CALL CCBGN
      CALL CCGRID (6HNOLBLS)
      LL=L-1
      NN=N-1
      DO 1 J=1,LL
      DO 2 I=1,NN
      PHILOW=AMIN1 (PHI(I,K,J),PHI(I+1,K,J),PHI(I+1,K,J+1),PHI(I,K,J+1))
      PHIHI= AMAX1 (PHI(I,K,J),PHI(I+1,K,J),PHI(I+1,K,J+1),PHI(I,K,J+1))
      IF (PHIHI-PHILOW) 2,2,51
   51 IF (PHILOW-PHIMAX) 53,53,2
   53 IF (PHIHI-PHIMIN) 2,5,5
    5 IF (PHILOW-PHIMIN) 56,54,55
   56 IF (PHILOW-10.0) 101,101,54
  101 TA=PHI(I,K,J)
      TB=PHI(I+1,K,J)
```

```
      TC=PHI(I+1,K,J+1)
      TD=PHI(I,K,J+1)
      IF (TA-10.0) 102,102,103
  102 IF (TB-10.0) 2,2,105
  105 IF (TC-10.0) 2,2,106
  106 PHILOW=AMIN1(TB,TC)
      GO TO 55
  103 IF (TB-10.0) 107,107,108
  107 IF(TD-10.0) 2,2,109
  109 PHILOW=AMIN1(TA,TD)
      GO TO 55
  108 IF (TC-TD) 110,112,111
  110 IF (TD-10.0) 112,112,113
  113 PHILOW=AMIN1(TA,TB,TD)
      GO TO 55
  111 IF (TC-10.0) 112,112,114
  114 PHILOW=AMIN1(TA,TB,TC)
      GO TO 55
  112 PHILOW=AMIN1(TA,TB)
      GO TO 55
   54 AA=PHIMIN
      GO TO 3
   55 AA= FLOAT(IFIX((PHILOW-PHIMIN)/DELPHI)+1)*DELPHI+PHIMIN
    3 IFLAG=0
      T(1,1)=PHI(I,K,J)
      T(2,1)=PHI(I+1,K,J)
      T(3,1)=PHI(I+1,K,J+1)
      T(4,1)=PHI(I,K,J+1)
      T(1,2)=FLOAT(I-1)*DELX
      T(2,2)=T(1,2)+DELX
      T(3,2)=T(2,2)
      T(4,2)=T(1,2)
      T(1,3)=FLOAT(J-1)*DELZ
      T(2,3)=T(1,3)
      T(3,3)=T(1,3)+DELZ
      T(4,3)=T(3,3)
    4 KAT=0
  613 IF (T(1,1)-10.0) 11,11,600
  600 IF (T(2,1)-10.0) 11,11,6
    6 IF(T(1,1)-T(2,1)) 7,11,7
    7 F=(AA-T(1,1))/(T(2,1)-T(1,1))
      IF (F-1.0) 71,71,11
   71 IF(F) 11,11,8
    8 IDIOT=1+IFLAG
      XX(IDIOT)=(1.0-F)*T(1,2)+F*T(2,2)
      ZZ(IDIOT)=(1.0-F)*T(1,3)+F*T(2,3)
   85 IF(IFLAG) 10,10,9
    9 CALL CCPLOT(XX,ZZ,2,6HNOJOIN,1,1)
      XX(1)=XX(2)
      ZZ(1)=ZZ(2)
      GO TO 11
   10 IFLAG=1
   11 KAT=KAT+1
      IF (KAT-4) 13,12,12
   13 TT1=T(1,1)
      TT2=T(1,2)
      TT3=T(1,3)
      DO 131 KA=1,3
      DO 131 KB=1,3
  131 T(KB,KA)=T(KB+1,KA)
```

```
      T(4,1)=TT1
      T(4,2)=TT2
      T(4,3)=TT3
      GO TO 613
   12 AA=AA+DELPHI
   14 IF(AA-PHIHI) 15,15,2
   15 IF (AA-PHIMAX) 3,3,2
    2 CONTINUE
    1 CONTINUE
      RETURN
      END
C
C
C
C
C
      SUBROUTINE CONSIX
      COMMON X(25),Y(25),Z(12),PHI(25,25,12),PERM(25,25,12),PHIN(25,
     125),JJ(25,25),GUESI(25),GUESK(25),IPERM(12),PERL2(25),PERL3(25),
     2MA(25),NA(25),MB(12),NB(12),PERL4(12),PERL5(12),KPLOT(25),IPLOT
     3(25),JPLOT(12),RES,TOL,OMEGA,N,M,L,ALPHA,ALFA,PHIMAX,PHIMIN,
     4SX,SY,SZ,SXPL,SYPL,SZPL,DELPHI,I,J,K,DELX,DELZ
      DIMENSION T(4,3),XX(2),ZZ(2)
      COMMON /CCPOOL/ XMIN,XMAX,YMIN,YMAX,CCXMIN,CCXMAX,CCYMIN,CCYMAX
      XMIN=0.0
      XMAX=SY
      YMIN=0.0
      YMAX=SZ
      CCXMIN=100.0
      CCXMAX=SYPL
      CCYMIN=100.0
      CCYMAX=SZPL
      CALL CCBGN
      CALL CCGRID (6HNOLBLS)
      LL=L-1
      MM=M-1
      DO 1 J=1,LL
      DO 2 K=1,MM
      PHILOW=AMIN1 (PHI(I,K,J),PHI(I,K+1,J),PHI(I,K+1,J+1),PHI(I,K,J+1))
      PHIHI =AMAX1 (PHI(I,K,J),PHI(I,K+1,J),PHI(I,K+1,J+1),PHI(I,K,J+1))
      IF (PHIHI-PHILOW) 2,2,51
   51 IF (PHILOW-PHIMAX) 53,53,2
   53 IF (PHIHI-PHIMIN) 2,5,5
    5 IF (PHILOW-PHIMIN) 56,54,55
   56 IF (PHILOW-10.0) 101,101,54
  101 TA=PHI(I,K,J)
      TB=PHI(I,K+1,J)
      TC=PHI(I,K+1,J+1)
      TD=PHI(I,K,J+1)
      IF (TA-10.0) 102,102,103
  102 IF (TB-10.0) 2,2,105
  105 IF (TC-10.0) 2,2,106
  106 PHILOW=AMIN1(TB,TC)
      GO TO 55
  103 IF (TB-10.0) 107,107,108
  107 IF(TD-10.0) 2,2,109
  109 PHILOW=AMIN1(TA,TD)
      GO TO 55
  108 IF (TC-TD) 110,112,111
```

```
  110 IF (TD-10.0) 112,112,113
  113 PHILOW=AMIN1(TA,TB,TD)
      GO TO 55
  111 IF (TC-10.0) 112,112,114
  114 PHILOW=AMIN1(TA,TB,TC)
      GO TO 55
  112 PHILOW=AMIN1(TA,TB)
      GO TO 55
   54 AA=PHIMIN
      GO TO 3
   55 AA= FLOAT(IFIX((PHILOW-PHIMIN)/DELPHI)+1)*DELPHI+PHIMIN
    3 IFLAG=0
      T(1,1)=PHI(I,K,J)
      T(2,1)=PHI(I,K+1,J)
      T(3,1)=PHI(I,K+1,J+1)
      T(4,1)=PHI(I,K,J+1)
      T(1,2)=FLOAT(K-1)*DELX
      T(2,2)=T(1,2)+DELX
      T(3,2)=T(2,2)
      T(4,2)=T(1,2)
      T(1,3)=FLOAT(J-1)*DELZ
      T(2,3)=T(1,3)
      T(3,3)=T(1,3)+DELZ
      T(4,3)=T(3,3)
    4 KAT=0
  613 IF (T(1,1)-10.0) 11,11,600
  600 IF (T(2,1)-10.0) 11,11,6
    6 IF(T(1,1)-T(2,1)) 7,11,7
    7 F=(AA-T(1,1))/(T(2,1)-T(1,1))
      IF (F-1.0) 71,71,11
   71 IF(F) 11,11,8
    8 IDIOT=1+IFLAG
      XX(IDIOT)=(1.0-F)*T(1,2)+F*T(2,2)
      ZZ(IDIOT)=(1.0-F)*T(1,3)+F*T(2,3)
   85 IF(IFLAG) 10,10,9
    9 CALL CCPLOT(XX,ZZ,2,6HNOJOIN,1,1)
      XX(1)=XX(2)
      ZZ(1)=ZZ(2)
      GO TO 11
   10 IFLAG=1
   11 KAT=KAT+1
      IF (KAT-4) 13,12,12
   13 TT1=T(1,1)
      TT2=T(1,2)
      TT3=T(1,3)
      DO 131 KA=1,3
      DO 131 KB=1,3
  131 T(KB,KA)=T(KB+1,KA)
      T(4,1)=TT1
      T(4,2)=TT2
      T(4,3)=TT3
      GO TO 613
   12 AA=AA+DELPHI
   14 IF(AA-PHIHI) 15,15,2
   15 IF (AA-PHIMAX) 3,3,2
    2 CONTINUE
    1 CONTINUE
      RETURN
      END
C
```

```
C
C
C
C
C
C
      SUBROUTINE CONSJX
      COMMON X(25),Y(25),Z(12),PHI(25,25,12),PERM(25,25,12),PHIN(25,
     125),JJ(25,25),GUESI(25),GUESK(25),IPERM(12),PERL2(25),PERL3(25),
     2MA(25),NA(25),MB(12),NB(12),PERL4(12),PERL5(12),KPLOT(25),IPLOT
     3(25),JPLOT(12),RES,TOL,OMEGA,N,M,L,ALPHA,ALFA,PHIMAX,PHIMIN,
     4SX,SY,SZ,SXPL,SYPL,SZPL,DELPHI,I,J,K,DELX,DELZ
      DIMENSION T(4,3),XX(2),ZZ(2)
      COMMON /CCPOOL/ XMIN,XMAX,YMIN,YMAX,CCXMIN,CCXMAX,CCYMIN,CCYMAX
      XMIN=0.0
      XMAX=SX
      YMIN=0.0
      YMAX=SY
      CCXMIN=100.0
      CCXMAX=SXPL
      CCYMIN=100.0
      CCYMAX=SYPL
      CALL CCBGN
      CALL CCGRID (6HNOLBLS)
      MM=M-1
      NN=N-1
      DO 1 K=1,MM
      DO 2 I=1,NN
      PHILOW=AMIN1 (PHI(I,K,J),PHI(I+1,K,J),PHI(I+1,K+1,J),PHI(I,K+1,J))
      PHIHI= AMAX1 (PHI(I,K,J),PHI(I+1,K,J),PHI(I+1,K+1,J),PHI(I,K+1,J))
      IF (PHIHI-PHILOW) 2,2,51
   51 IF (PHILOW-PHIMAX) 53,53,2
   53 IF (PHIHI-PHIMIN) 2,5,5
    5 IF (PHILOW-PHIMIN) 56,54,55
   56 IF (PHILOW-10.0) 101,101,54
  101 TA=PHI(I,K,J)
      TB=PHI(I+1,K,J)
      TC=PHI(I+1,K+1,J)
      TD=PHI(I,K+1,J)
      IF (TA-10.0) 102,102,103
  102 IF (TB-10.0) 2,2,105
  105 IF (TC-10.0) 2,2,106
  106 PHILOW=AMIN1(TB,TC)
      GO TO 55
  103 IF (TB-10.0) 107,107,108
  107 IF(TD-10.0) 2,2,109
  109 PHILOW=AMIN1(TA,TD)
      GO TO 55
  108 IF (TC-TD) 110,112,111
  110 IF (TD-10.0) 112,112,113
  113 PHILOW=AMIN1(TA,TB,TD)
      GO TO 55
  111 IF (TC-10.0) 112,112,114
  114 PHILOW=AMIN1(TA,TB,TC)
      GO TO 55
  112 PHILOW=AMIN1(TA,TB)
      GO TO 55
   54 AA=PHIMIN
      GO TO 3
```

```
 55 AA= FLOAT(IFIX((PHILOW-PHIMIN)/DELPHI)+1)*DELPHI+PHIMIN
  3 IFLAG=0
    T(1,1)=PHI(I,K,J)
    T(2,1)=PHI(I+1,K,J)
    T(3,1)=PHI(I+1,K+1,J)
    T(4,1)=PHI(I,K+1,J)
    T(1,2)=FLOAT(I-1)*DELX
    T(2,2)=T(1,2)+DELX
    T(3,2)=T(2,2)
    T(4,2)=T(1,2)
    T(1,3)=FLOAT(K-1)*DELX
    T(2,3)=T(1,3)
    T(3,3)=T(1,3)+DELX
    T(4,3)=T(3,3)
  4 KAT=0
613 IF (T(1,1)-10.0) 11,11,600
600 IF (T(2,1)-10.0) 11,11,6
  6 IF(T(1,1)-T(2,1)) 7,11,7
  7 F=(AA-T(1,1))/(T(2,1)-T(1,1))
    IF (F-1.0) 71,71,11
 71 IF(F) 11,11,8
  8 IDIOT=1+IFLAG
    XX(IDIOT)=(1.0-F)*T(1,2)+F*T(2,2)
    ZZ(IDIOT)=(1.0-F)*T(1,3)+F*T(2,3)
 85 IF(IFLAG) 10,10,9
  9 CALL CCPLOT(XX,ZZ,2,6HNOJOIN,1,1)
    XX(1)=XX(2)
    ZZ(1)=ZZ(2)
    GO TO 11
 10 IFLAG=1
 11 KAT=KAT+1
    IF (KAT-4) 13,12,12
 13 TT1=T(1,1)
    TT2=T(1,2)
    TT3=T(1,3)
    DO 131 KA=1,3
    DO 131 KB=1,3
131 T(KB,KA)=T(KB+1,KA)
    T(4,1)=TT1
    T(4,2)=TT2
    T(4,3)=TT3
    GO TO 613
 12 AA=AA+DELPHI
 14 IF(AA-PHIHI) 15,15,2
 15 IF (AA-PHIMAX) 3,3,2
  2 CONTINUE
  1 CONTINUE
    RETURN
    END
```

SCIENTIFIC SERIES

No. 1 Hydrogeology of the Moncton Map-Area, New Brunswick. P.A. Carr, 1968.

A report evaluating the results of the groundwater investigation begun in 1960 in the Moncton Map-Area. The qualitative and quantitative aspects of groundwater are integrated in the report to produce a description of the groundwater flow system.

No. 2 Hydrochemical Interpretation of Groundwater Movement in the Red River Valley, Manitoba. J.E. Charron.

(IN PRESS)

A report on the results of a geological study of the Red River Valley carried out over five field seasons. The writer has concentrated mainly on the hydrochemical aspect of the groundwater to define groundwater movement in the Red River Valley.